1987

Borehole Friction Assessment and Application to Oilfield Casing Design in Directional Wells.

Eric Edgar Maidla
Louisiana State University and Agricultural & Mechanical College

Order Number 8811422

Borehole friction assessment and application to oilfield casing design in directional wells

Maidla, Eric Edgar, Ph.D.

The Louisiana State University and Agricultural and Mechanical Col., 1987

U·M·I
300 N. Zeeb Rd.
Ann Arbor, MI 48106

BOREHOLE FRICTION ASSESSMENT AND APPLICATION TO OILFIELD CASING DESIGN IN DIRECTIONAL WELLS

A dissertation

Submitted to the Graduate Faculty of the
Louisiana State University
and Agricultural and Mechanical College
in partial fulfillment
of the requirements for the degree of
Doctor of philosophy

in

The department of Petroleum Engineering

by

Eric Edgar Maidla
B.S., Escola de Engenharia Maua, 1981
M.S., Louisiana State University, 1985

(December 1987)

ACKNOWLEDGMENTS

The author wishes to thank his major professor Dr. Andrzej Wojtanowicz, assistant professor of the Department of Petroleum Engineering, for his guidance, assistance and friendly non-research advice providing a pleasant and productive experience.

The author is grateful to the following professors for their participation: Dr. Julius Langlinais, of the Department of Petroleum Engineering, Dr. Robert Desbrandes, of the Department of Petroleum Engineering, Dr. Adam T. Bourgoyne, Jr., of the Department of Petroleum Engineering, Dr. John Brewer III, of the Department of Mechanical Engineering, Dr. David Thompson, of the Department of Mechanical Engineering, Professor Andrew J. McPhate, of the Department of Mechanical Engineering, Dr. Mehdy Sabbaghian, of the Department of Mechanical Engineering. The author also thanks Mr. Orville Allen Kelly, from the LSU Petroleum Engineering Research and Technology Transfer Laboratory, for his assistance and helpful suggestions.

The assistance of Dr. Emma Brossard, former director of the Center for Latin American Affairs and former director of the Center for Energy Studies, throughout his stay at Louisiana State University, is greatly appreciated.

The author is very grateful to Standard Oil Production Company - Lafayette District, Exxon Company USA - New Orleans, Shell Offshore Inc. - New Orleans and Tenneco Oil Company - Lafayette for help in recording the field data, and TOTCO, Martin-Decker, NCI Dillon, Ray Oil Tool Company and NL Baroid for their assistance and equipment support.

The financial assistance provided by the Conselho Nacional de Desenvolvimento Cientifico e Tecnologico - CNPq/Brazil, the Center for Latin American Affairs, the Center for Energy Studies, the Mineral Mining Institute and the Petroleum Engineering Department is gratefully appreciated.

The author also thanks the Society of Petroleum Engineers for granting permission to use reprints of our published papers.

He also thanks his parents Beryl and Edgar and other relatives for their encouragement.

Most importantly the author thanks his wife Lydia for her assistance, tolerance and love throughout this work.

TABLE OF CONTENTS

LIST OF TABLES

LIST OF FIGURES

ABSTRACT

The phenomenon of mechanical friction in the oil well borehole was investigated. Immediate application of such a study is to improve casing design in directional wells. An additional application is the prediction of reciprocating loads in directional wells for cementing purposes, that is recognized to be an effective method to avoid cement channeling through efficient mud displacement.

Field studies on the borehole friction coefficient revealed its insensitivity to depth, various well trajectories, size of pipe and its surface configuration, leading to the conclusion that one value of the borehole friction factor can represent a single well. Also there was good agreement between 2-D and 3-D model predictions for drag-weight ratios above 25%, and spatial irregularities retained at minimun above the kick-off point.

The prediction of surface axial loads at the planning stage of the well using the 2-D model was also investigated. It showed that surface running loads can be planned for in advance as long as surface irregularities are kept within reasonable limits, and a good estimate of the borehole friction factor is made. Minimum design factors for the borehole friction factor and predicted running loads are estimated for this research. The results suggest the

inclusion to the design process of casing strings in directional wells.

Laboratory experiments were also conducted on an instrument with dynamic filtration and friction factor evaluation capabilities, using 6 in. rock cores. Seven water base and three oil base drilling fluids were used. The results showed that most of the friction factor values fell within the range of 0.2 to 0.3, and for most cases these values were insensitive to lubricant addition. It was found that its effect can be significant in areas of low contact pressures and high filtration rates. Such conditions are associated with the long slant hole section of directional wells.

A new method for casing design in directional wells was developed. The method is based on determination of maximum axial pulling loads. The criteria of minimum cost of casing string is used for selection of the combination casing string. The calculation procedure is based on the dynamic programming technique.

INTRODUCTION

This research began in 1985 when I first faced a problem of the price-weight conflict that occurs when minimizing a cost of the combination casing string for a given set of mechanical loads. At this early stage, only vertical wells were considered. The next step was to extend the optimization procedure to the design of casing strings for directional wells. It was found that existing casing design methods considered only static loads. Thus disregarding both the spatial profile of a directional well and the possibility of pipe motion (running loads).

One possible reason for disregarding the running loads was that, to date, no research effort has been made to evaluate a borehole friction factor between the casing string and the open borehole. Therefore any improvement in this area was bound to by determination of this coefficient. Designing casing for running loads can aid the primary cementing job through casing reciprocation without compromising its mechanical integrity. The mathematical model can be used to monitor casing drag in order to take corrective actions such as circulating or

rotating with casing tongs before the casing string becomes stuck off bottom.

In order to determine the borehole friction factor, a method was developed that required field measurements of hook loads recorded during actual casing runs in directional wells. Since the hook-load recording equipment used on drilling rigs proved not to be sensitive enough for such measurements, I assembled a hook-load sensing system by borrowing a precision equipment from the rig instrumentation companies. I calibrated the instruments and I used them during my research trips to drilling locations. All the field data collected are my own measurements. The first description of the field method is presented in Appendix B. This paper was later revised in order to: (1) include the experience gained in several other field trips, (2) consider other technological alternatives to accurately record hook loads such as the load pin and the hydraulic sensor, and, (3) improve the mathematical model by adding the hydrodynamic viscous drag effect, and by considering direction changes and surface contact effects. Chapter I is a revised version of the Appendix B. It presents the most complete description of the 2-D model for axial load predictions as well as it introduces the drag-weight ratio concept.

In this research, the 2-D model was initially derived and used in calculations because of its simplicity and because it was considered the only option at the planning stage of the well. The actual wells, however, deviate from the vertical plane and the 2-D model overestimates the borehole friction coefficient. Therefore a 3-D model was developed that included direction changes and contact surface effects. Chapter II describes the 3-D model, repeats the 2-D model formulas, and compares both models using numerical simulation and field data.

Despite the 2-D and 3-D models discrepancies, the question still remained how much error one could make by designing loads using the planned trajectory. This was done in Chapter III by comparing hook load predictions made using the planned trajectory with actual hook load data measured in the field. The good results obtained with such predictions suggested the inclusion of the 2-D method for running loads prediction to the casing design process.

In addition to the field experiments, Chapter IV reports on friction coefficients. Such research was performed in the laboratory using specially designed apparatus which measured a friction coefficient between rock and steel surfaces in the presence of drilling mud and the filter cake. The effects of different mud

systems, lithologies and lubricant additions were investigated. Also the values of friction coefficient were compared with the field values of the borehole friction factor.

Finally Chapter V presents the new method for casing design in directional wells. The method is based on the optimization theory to find the minimum cost of a casing string. In this method the axial loads of a casing string are calculated using the borehole friction factor values and a 2-D mathematical model.

CHAPTER I

A FIELD METHOD FOR ASSESSING BOREHOLE FRICTION FOR DIRECTIONAL WELL CASING

ABSTRACT

A field procedure to evaluate the borehole friction factor between a pipe string and a borehole was developed. The primary concern of this research was to investigate and mathematically describe the drag associated with casing runs in directional wells through the use of the two-dimensional approach. The borehole friction factor was found, through an iterative procedure, by matching the calculated hook load to the measured one at the surface. The borehole friction factor was calculated as the unique value for the match.

This study shows the necessary precision requirements for the hook load measurement instrumentation and presents three different types of equipment that meet accuracy demands. The significance of the mechanical friction effect on hook load was also addressed, by introducing the drag-weight ratio concept. It was found that to assure accuracy of the method, the minimum required value of the drag-weight ratio should be 25%.

The statistical analysis revealed that one single value of the borehole friction factor can represent the well.

It was concluded in the study that the model can be used for prediction of tensional load of a casing string in a directional well.

INTRODUCTION

Unlike vertical wells, the mechanical friction represents an important interaction between a borehole and a pipe string in directional wells. To date, only the drillstring friction was studied using field measurements of torque and drag [1].

Recently, the casing string friction was introduced into the casing design procedure for directional wells [2]. In this procedure, calculations of the maximum axial stresses were based on the presumption that the casing string might be pulled on in order to adjust its position or to reciprocate it during cementing operations. The importance of reciprocating casing strings for a better cement bond is widely recognized [3].

The present methods for casing design in directional wells disregard the effect of friction and simply do not consider any possibility of upward pipe movement. In the actual field operations however, the reciprocation of the casing string is often required. Then, an attempt is made to pull on casing without any knowledge of the drag opposing the upward pipe motion. Such an approach may result either in unsuccessful reciprocation, when the maximum pulling load has been underestimated, or it may cause casing damage.

As suggested by other authors [1], friction between borehole and casing is represented by the borehole friction factor which is relatively constant along a borehole. The borehole friction factor is a simplification of what is believed to be a complex mechanism of mechanical interaction between a tubular string and a borehole. It disregards the effects of lithology stratification, and the irregularities of the borehole size.

The borehole friction factor is defined as [4]:

$$\mu_B = \frac{\left| F_H \cdot Q_V \pm F_D \right|}{\int^D q_D(\ell) \cdot d\ell} \tag{1}$$

(see end of chapter for nomenclature)

Unfortunately, equation (1) cannot be solved explicitly because the normal force results from the axial load immediately below it integrated along the curved path. Instead, a computer and a recursive procedure have to be used to calculate the borehole friction factor.

DESCRIPTION OF THE MODEL

The calculations proceed from the bottom of the casing string upward. The same procedure is used for the casing being pulled out of a well as well as being run into the well. Calculations are performed at each survey point. If the casing bottom falls in between two survey points, linear interpolation is used to assign survey values to it. The simplified flowchart of the computer program is shown in Fig. 1.

The following effects are considered in the model:

- o Buoyancy
- o Well inclination changes
- o Hydrodynamic friction

The effects disregarded by the model include:

- o Well direction changes
- o Pipe-borehole contact surface effect on drag
- o Torsion, stabbing and spring effects
- o Differential sticking
- o Irregular size of an open hole

The stepwise procedure was used for calculating tensional loads. Each step represented a borehole section between two consecutive stations of the directional survey. Before proceeding to the next step, there were three possible situations to consider:

1. Build-up:

   Inclination increases with increasing depth

2. Drop-off:

   Inclination decreases with increasing depth

3. Slant hole:

   Inclination remains constant with increasing depth

1. Build-up

The borehole friction is controlled by the direction and the value of the normal force. Forces acting on a small casing element in the well are shown in Fig. 2. Here, three positions of casing in the borehole are possible - Fig. 3. For the uppermost position while pulling casing out of a well the tensional load at the upper station "i-1" is

$$F_{A_{i-1}} = A_1 \cdot F_{A_i} + \frac{q.R}{1+\mu_B^2} \cdot [(\mu_B^2-1)(\sin\alpha_{i-1}-A_1\sin\alpha_i) - 2\mu_B (\cos\alpha_{i-1}-A_1\cos\alpha_i)] \quad (2)$$

where:

$$F_{A_1} = 0$$

$$A_1 = \exp [\mu_B (\alpha_i-\alpha_{i-1})]$$

$$R = \frac{\ell_i-\ell_{i-1}}{\alpha_i-\alpha_{i-1}} \quad (3)$$

For the intermediate position while pulling-on casing string

$$F_{A_{i-1}} = F_{A_i} + q.R (\sin\alpha_i-\sin\alpha_{i-1}) \quad (4)$$

and for the bottom position, the tensional load equation is:

$$F_{A_{i-1}} = A_2 \cdot F_{A_i} + \frac{q.R}{1+\mu_B^2} \cdot [(\mu_B^2-1)(\sin\alpha_{i-1}-A_2\sin\alpha_i) + 2\mu_B (\cos\alpha_{i-1}-A_2\cos\alpha_i)] \quad (5)$$

where:

$$A_2 = \exp [\mu_B (\alpha_{i-1}-\alpha_i)]$$

2. Drop-off

For the drop-off portion of a borehole, tensional load is controlled only by the type of operation i.e. pulling-out or running-in. The forces acting on a small casing element are shown in Fig. 4. For pulling-out operation, the tensional load is

$$F_{A_{i-1}} = A_2 \cdot F_{A_i} - \frac{q.R}{1+\mu_B^2} \cdot [(\mu_B^2-1)(\sin\alpha_{i-1} - A_2\sin\alpha_i) + 2\mu_B (\cos\alpha_{i-1} - A_2\cos\alpha_i)] \quad (6)$$

and for the running-in operation:

$$F_{A_{i-1}} = A_1 \cdot F_{A_i} - \frac{q.R}{1+\mu_B^2} \cdot [(\mu_B^2-1)(\sin\alpha_{i-1} - A_1\sin\alpha_i) - 2\mu_B (\cos\alpha_{i-1} - A_1\cos\alpha_i) \quad (7)$$

3. Slant hole

For the slant hole portion of a borehole, the forces acting on a small casing element are shown in Fig. 5. The tensional load, while pulling-out, is:

$$F_{A_{i-1}} = F_{A_i} + q\ (\ell_i - \ell_{i-1})(\mu_B \sin\alpha_i + \cos\alpha_i) \quad (8)$$

and while running in

$$F_{A_{i-1}} = F_{A_i} + q\ (\ell_i - \ell_{i-1})(\cos\alpha_i - \mu_B \sin\alpha_i) \quad (9)$$

Using equations (2) through (9) it is possible to calculate a hook load for a given friction factor value, as:

$$F_H = F_{A_1} \pm \frac{\pi}{4} \sum_{m=1}^{M} \left(\frac{dp}{dl}\right)_m \cdot L_m \cdot d_m^2 \quad (10)$$

FIELD PROCEDURE

Experimental data were collected during casing installations in several wells located offshore Louisiana and Texas. Experience gained from these field tests gave rise to the development of a field procedure for recording hook loads.

The following information is needed in order to evaluate a borehole friction factor:

- o Casing string geometry (external and internal diameters, unit weight of pipe, casing string length).
- o Previous casing geometry and setting depth (internal diameter and casing string length).
- o Drilling fluid properties (density, consistency index, flow-behavior index).
- o Borehole geometry and well trajectory (bit diameter, directional survey).
- o Hook loads and corresponding casing shoe depths.

With the exception of hook loads, the rest of the data is readily available from drilling reports. Therefore the main problem here is that of recording, and precision of the hook load measurements. Our experience shows that for casing and drill string runs; (1) A hook load error of 1000 lbf is acceptable; (2) The ratio between the borehole drag and the buoyant string weight (drag-weight ratio) should remain above 25% as explained later in this report; (3) The average value of the stabilized portion of the hook load record should be considered for a single casing joint run; (4) A hook load recording rate should be about 1 sec^{-1} for the casing running speed around 2 ft/s; (5) In the case of pulling out casing, when casing motion is slow, the sampling rate can be

decreased to 0.4 sec^{-1}.

In the light of the above requirements the common rig weight indicators proved to be inadequate instruments for the method. Their accuracy deteriorates in time. When first installed on the rig floor, and calibrated, they are reported by manufacturers to have the necessary accuracy of ±1000 lbf and readability of ±5000 lbf. Throughout their use, however, they are rarely calibrated and checked for such an accuracy. Furthermore, their analog display makes it hard to sample manually at a reasonable rate. The small hydraulic diaphragm sensors that are commonly attached to the dead line, should not be used for this method since their response is nonlinear for the wide range of hook loads of interest. This fact is presently recognized by the manufacturing companies of this equipment.

Three types of sensors, Fig. 6, were used in this research that can provide accuracies within 1000 lbf (if calibrated immediately before the running casing installation): hydraulic sensor, load pin and tensiometer.

The portable hydraulic sensor was connected to the hydraulic line from the dead line anchor signal to the driller's console. In response to the dead line tension the anchor would slightly rotate and its movement was stopped by the hydraulic sensor. The hydraulic signal produced by this sensor was proportional to the hook load for a given number of strings through the blocks, a given diameter of the deadline anchor, length of the pivoting arm and a given area of the sensor device. The hydraulic signal was converted to an electrical signal that was further digitized and displayed.

The load pin sensor was installed by replacing the pin connecting the hydraulic load cell (on the deadline anchor) to the rig. The

shearing stress proportional to the hook load values was measured by the strain gauges. The electrical signal was digitized and displayed.

The tensiometer was installed at the dead line and it sensed its deflection by means of three roller bearing sheaves. The middle sheave was pivoted and rested against a load cell containing strain gauges. The deflection compressive load was proportional to the tension in the cable. The electronic signal was digitized and stored. The ideal setup for data processing in this method would be to record the electrical signal with a computer so the hook load vs. time record can be stored and later correlated with depth. This correlation is usually obtained by counting pipe joints and then referring to the tally sheet for their unique lengths so the depth vs. hook load record can be made. If the automatic depth counter is available the depth-time-hook load record can be stored by the computer.

It was found necessary to check upon the accuracy obtained with each sensor. The accuracy depended upon the calibration and maintenance of the components involved in the whole measuring setup. Specific calibration details are not addressed here because different type of equipment had its own peculiarities. It was found that one "point checkup" for the whole system is necessary. Its procedure is as follows: While circulating on bottom (before running casing), stop the pump, rotate for a while and then measure the hook load with the same equipment that will be used to record the casing hook load. The measured load should equal the calculated vertical projected buoyant weight of the pipe.

If the hole conditions are good the possibility of picking up the casing string should be studied at predetermined depths. The picking up

procedure used in this research was as follows: casing was slowly picked up until hook loads stabilized - normally between 10 to 30 ft above slips. These points were used to calculate a friction factor while pulling casing out. The values of the borehole friction factor calculated from pulling tests, provided an ultimate verification of the procedure. Ideally, of course, they should be equal to those calculated from the running-in data. The discrepancy between the two was a measure of the effect of some other factors such as incorrect measurements or additional drag components disregarded by the model.

In order to avoid casing damage while pulling out, it is recommended that the hook load does not exceed 70% of the weakest pipe strength.

VERIFICATION AND ERROR ANALYSIS

One case history will be used to exemplify the field procedure to evaluate the borehole friction factor. The same well was used in another study [4] and therefore has already been described. It was an S-shaped well drilled to 11270 ft with a maximum inclination of 39.2° and build up rate averaging 2.2°/100 ft, Fig. 7 and 8. Table 1 provides data concerning casing geometry, drilling fluid properties, previous casing setting depth and borehole geometry. In this study only the last casing run was considered.

The hook load was recorded using a hydraulic sensor hooked up to a computer. This portable unit was calibrated using a dead weight testor just before taking it to the drilling rig. Prior to the casing run the equipment was calibrated and the hook load was recorded every second and stored on magnetic tape. After the casing run was over the equipment was re-checked for possible calibration deviation which did not occur.

During the casing string installation each pipe was counted and notes were taken on any unusual event that occurred. In this particular casing run, for instance, about 30 ft of casing were pulled out of the hole at depths 4897 ft and 4924 ft to keep the casing moving until more casing was available on the rig floor. The whole operation was only observed and recorded without any interference with the routine casing string installation.

The hook load versus time records were plotted on two 120-in. long strips of paper similar to a logging plot. An example of one casing joint run is shown in Fig. 9. For each casing joint run, the average hook load value was determined from the stabilized portion of hook load values. Then, the instantaneous casing depth was tied in. Also calculated was the average velocity of a casing string. Finally, the computer program was used to calculate a borehole friction factor for the casing joint.

A plot of friction factor versus depth is shown in Fig. 10. Similar plots were obtained for many other field measurements [4]. The results indicated that: (1) The mean borehole friction factor seemed insensitive to depth; (2) At each depth, the data scatter was very symmetrical; (3) The data scatter rapidly decreased with increasing depth.

The depth insensitivity of the borehole friction factor implied a reason for expecting that one value of this factor would fully represent the pipe-borehole friction factor for a particular well. The correlation-regression analysis was used to verify this concept. In particular the coefficient of determination, r^2, was calculated to be 0.077. Also the least-squares straight line fit was made using the data in Fig. 10 and the regression coefficient, b, was calculated to be

8×10^{-6} ft^{-1}. Both coefficients were very small. Furthermore, the coefficient of determination and the regression coefficient were statistically tested for the possibility of being zero. The coefficient of determination was tested by using the null-hypothesis for the correlation coefficient, r, as

$$H_o: \rho=0 \; ; \quad H_a: \rho \neq 0$$

and the test statistics value was

$$t = \frac{r\sqrt{n-2}}{\sqrt{1-r^2}} = 1.64 \qquad (11)$$

where ρ is the population correlation coefficient.

The null-hypothesis for the coefficient was also tested

$$H_o: \beta=0 \; ; \quad H_a: = \beta \neq 0$$

$$t = \frac{b.\sqrt{Sxx\ (n-2)}}{\sqrt{Syy-b\ Sxy}} = 1.64 \qquad (12)$$

where β is the population regression coefficient and

$$Sxx = \Sigma D^2-(\Sigma D)^2/n = 111373312$$

$$Sxy = \Sigma D.\mu_B-(\Sigma D)(\Sigma \mu_B)/n = 871$$

$$Syy = \Sigma \mu_B{}^2-(\Sigma \mu_B)^2/n = 0.08823$$

At 10% significant level the critical value from student t-distribution table was

$$t_{\Omega/2,n-2} = t_{5,32} = 1.69$$

As t was smaller than $t_{5,32}$ the null hypothesis were not rejected. Therefore it was concluded that the available field data provided no significant reason for disbelief that the borehole friction factor was depth independent and had one constant value. This leads to the

possibility of predicting casing running loads using the average borehole friction factor value.

The symmetry of the scatter suggested a random nature of data dispersion with no other controlling factors. Thus the hypothesis was formulated that the borehole friction factor values were a random sample from a normal distribution. This hypothesis was tested using the Shapiro-Wilk W-statistics [6] that confirmed normality at a 95% confidence level. It was then concluded that the available field data did not provide evidence of any other factors at work than those included in the mathematical model.

The convergence of the experimental data with increasing depth suggested that the borehole friction factor could be more precisely determined in deep sections of a directional well. Consequently, the error of the method seemed directly correlated with the depth of the running pipe or, more precisely, the length of pipe already in the well. The error analysis was performed using all available data from four directional wells analyzed in the early research [4]. The measured depths for each well were divided into four portions. For each portion, the following magnitudes were calculated: (1) average depth; (2) average borehole friction factor, and (3) standard deviation. For each part, the relative error δ was calculated at a confidence level of 95% using the formula:

$$\delta = \frac{|t_{5/2,n-1} \cdot s|}{|\bar{\mu}_B \cdot \sqrt{n}|} \qquad (13)$$

The results are shown in Table 2. Indeed, a rapid improvement of accuracy with measured depth can be observed.

Further experimental evidence, however, excluded the measured depth as being a single factor affecting accuracy of the borehole friction factor determination. This analysis included effects of direction, inclination and the length of the slant portion of the four directional wells identified in the previous work [4]. Eventually one dimensionless magnitude was identified that implied effects of various factors on the method's accuracy; that was the ratio of the borehole drag to the pipe buoyant weight.

Using all the data, the average borehole friction factor was calculated and used by the computer program to estimate the amount of drag for depths corresponding to the average values for each of the four sections. Also the buoyant string weight with no drag was calculated for each average depth. The ratio of these two values was called drag-weight ratio and was assigned to any instantaneous depth of a casing str' g. The procedure was repeated for another three casing runs and the one wireline run.

The plot of the relative error versus the drag-weight ratio is shown in Fig 11. It can be noticed that, for a drag-weight ratio above 25% there is a significant reduction in the relative error. This occurs as a result of drag becoming a significant part of the measured hook load, which is the only parameter measured. The drag-weight ratio value of 25% indicates the depth below which more reliable values of the borehole friction factor can be obtained.

Final verification of the method was performed by predicting the actual hook loads.

The computer program was used to calculate the running-in and the pulling-out loads, as shown in Fig 12. Only the average value of the borehole friction factor calculated from the running-in record was used for prediction. Also plotted was the actual hook load data. There was very good agreement between measured and predicted hook load values for running-in casing but some discrepancy occurred for the pulling-out values. This same discrepancy has been observed in another casing run [4]. A possible explanation of this discrepancy was the stabbing effect when the casing shoe worked against the borehole wall while running-in. Such an effect is not present while pulling casing out of a well. Assuming that stabbing effect was at work we could quantify its magnitude by subtracting the predicted hook load from the measured pulling-out hook load. In this example, the load reduction due to stabbing was 8000 lbf (5.5%) at 4897 ft and 10000 lbf (5.7%) at 5924 ft.

In addition, the predicted value of the hook load associated with the casing setting depth of 11270 ft provided an unexpected explanation for the unsuccessful attempt to reciprocate casing that was performed at the drilling rig. In this attempt, the maximum pull of 334,000 lbf was used in order to pick up the whole casing string which had been erroneously set one joint too deep. Our prediction indicates that the minimum pull value should have been 350,000 lbf.

CONCLUSIONS

- There is a single value of an average borehole friction factor which represents mechanical drag associated with axial pipe movement.
- The borehole friction factor can be accurately measured in the field using the method presented here. To use the method the hook load instrumentation has to be upgraded to meet precision requirements specified in this paper.
- The accurate and reliable values of the borehole friction factor can be obtained when the drag-weight ratio exceeds 25%.
- The mathematical model described here, enables calculation of the axial stresses occurring in the moving pipe in a directional well, given the borehole friction factor value. Hence the method, presented in this paper, provides experimental evidence necessary for casing design in directional well.

NOMENCLATURE

b	=	Sample regression coefficient
D	=	Measured depth, ft
d	=	External diameter of the pipe, in.
F_A	=	Axial load, lbf
F_D	=	Hydrodynamic viscous drag, lbf
F_H	=	Hook load, lbf
L	=	Pipe section length (same external diameter), ft
ℓ	=	Length of pipe, ft
M	=	Number of pipe sections in the borehole
n	=	Number of running in measured hook loads
$dp/d\ell$	=	Pressure gradient due to flow friction
Q_v	=	Vertical projected buoyant weight at pipe
q	=	Unit buoyant weight of pipe
q_D	=	Unit drag or rate of drag change, lbf/ft
R	=	Radius of curvature
r	=	Sample correlation coefficient
r^2	=	Sample coefficient of determination
s	=	Sample standard deviation
t	=	Value of student t-distribution
α	=	Inclination angle, rad
δ	=	Uncertainty
ρ	=	Population correlation coefficient
μ_B	=	Borehole friction factor
β	=	Population regression coefficient
χ^2	=	Chi-square distribution value
Ω	=	Significance level

ACKNOWLEDGMENTS

The authors would like to thank Standard Oil Production Company-Lafayette District for help in recording field data and TOTCO for their assistance and equipment support. Special thanks to Ann Lewis for her help in preparing the manuscript.

REFERENCES

1. Johancsik, C.A., et al., "Torque and Drag in Directional Wells - Prediction and Measurement", JPT, June 1984, pp 987-992.

2. Wojtanowicz, A.K., Maidla, E.E., "Minimum Cost Casing Design for Vertical and Directional Wells", SPE #14499, 1985.

3. Crook, R.J., et al., "Deviated Wellbore Cementing: Part 2-Solutions", JPT, August 1987, pp 964-966.

4. Maidla, E.E. Wojtanowicz, A.K., "Field Comparison of 2-D and 3-D Methods for the Borehole Friction Evaluation in Directional Wells", SPE #16663, 1987.

5. Dowdy, S. Wearden, S., "Statistics for Research", John Wiley & Sons, New York, 1983.

6. Shapiro, S.S. and M.B. Wilk, "An Analysis of Variance Test for Normality (Complete Samples)", Biometrika, 1965, Vol. 52, pp. 591-611.

APPENDIX

Derivation of the Main Formulas

1. Build-up section

1.1 Pulling-out casing:

The forces acting on a small casing element in the build-up section are shown in Fig. 2. At equilibrium, the following differential equation results:

$$\frac{dF_A}{d\alpha} = -\mu_B \left|R.q.\sin\alpha - F_A\right| - R.q.\cos\alpha \qquad (A1)$$

boundary conditions:

$$F_A\,(\alpha_i) = F_{A_i}$$

$$F_A\,(\alpha_{i-1}) = F_{A_{i-1}} \qquad (A2)$$

Solving eq. (A1) using boundary conditions (A2), and also considering the situations depicted in Fig. 3, results in equations (2), (4) and (5).

1.2 Running-in situation:

In a similar way (Fig. 2), at equilibrium:

$$\frac{dF_A}{d\alpha} = \mu_B \left|R.q.\sin\alpha - F_A\right| - R.q.\cos\alpha \qquad (A3)$$

Equations (A3) and (A1) yield the same results but for different scenarios (Fig. 3). This is due to the sign convention used. The main text clearly explains which situation each equation pertains.

2. Drop-off section

2.1 Pulling-out casing:

The forces acting on a small casing element in the drop-off section is shown in Fig. 4. At equilibrium:

$$\frac{dF_A}{d\alpha} = \mu_B \ (R.q.\sin\alpha+F_A)+R.q.\cos\alpha \qquad (A4)$$

Using the boundary conditions (A2), the solution is equation (6).

2.2 Running-in casing:

In a similar way (Fig. 4), at equilibrium:

$$\frac{dF_A}{d\alpha} = -\mu_B \ (R.q.\sin\alpha+F_A)+R.q.\cos\alpha \qquad (A5)$$

Using boundary conditions (A2), the solution is equation (7).

3. Slant section

3.1 Pulling-out casing:

The forces acting on a small casing element in the slant hole portion are shown in Fig. 5. At equilibrium:

$$\frac{dF_A}{dD} = q.\mu_B.\sin\alpha+q.\cos\alpha \qquad (A6)$$

boundary conditions:

$$F_A \ (D_i) = F_{A_i}$$

$$F_A \ (D_{i-1}) = F_{A_{i-1}} \qquad (A7)$$

Using these boundary conditions, the solution is equation (8).

3.2 Running-in casing:

In a similar way (Fig. 5), at equilibrium:

$$\frac{dF_A}{dD} = -q.\mu_B.\sin\alpha+q.\cos\alpha \qquad (A8)$$

Using boundary condition (A7) the solution is equation (9).

TABLE 1

WELL # 1 - CASING

COMPARISON OF THE MODELS USING FIELD DATA

DATA USED: .MUD DENSITY: 10.80 LBF/GAL
.CONSISTENCY INDEX: 124.9 EQCP
.FLOW-BEHAVIOR INDEX: 0.781
.BIT DIAMETER: 9.875 IN
.PREVIOUS CASING DIAMETER: 10.750 IN
.PREVIOUS CASING DEPTH: 3210. FT
.STRING BREAK DOWN:

DEPTH (FT)	OD (IN)	ID (IN)	WEIGHT (LB/FT)	REMARK
5390.	7.625	6.875	29.70	LTC
10267.	7.625	6.640	33.70	LTC
11232.	7.625	6.500	39.00	LTC

RESULTS:

INPUT DATA				BOR. FRIC. FACTOR
CASING SHOE DEPTH (FT)	MEASURED HOOK LOAD (LBF)	MODE	PIPE VELOC. (FT/S)	2-D MODEL
4579.	108800.	IN	1.7	0.38
4619.	109000.	IN	2.0	0.37
4659.	108400.	IN	2.0	0.42
4699.	114000.	IN	0.5	0.32
4897.	113100.	IN	2.1	0.36
4897.	144100.	UP	1.0	0.26
5135.	113500.	IN	2.0	0.45
5175.	114000.	IN	1.5	0.48
5294.	114200.	IN	2.0	0.48
5371.	115100.	IN	2.0	0.48
5407.	113900.	IN	2.0	0.53
5605.	115300.	IN	2.0	0.55
5882.	128400.	IN	0.1	0.43
5924.	130000.	IN	0.1	0.41
5924.	174900.	UP	0.7	0.30
5924.	127000.	IN	0.5	0.44
5964.	125900.	IN	2.0	0.39
6385.	133800.	IN	0.5	0.41
6912.	135800.	IN	0.6	0.47
7079.	134100.	IN	2.2	0.44
7157.	136800.	IN	0.7	0.49

TABLE 2

Relative Error of the μ_B Determination (δ)

(95% Confidence Level)

*Well #	Sample Size	Aver. Depth (ft)	**Aver. μ_B	Standard Deviat.	Student	Relative Error (%)
1 CASING	8	4882	0.407	0.0586	2.365	12.04
	8	5808	0.456	0.0585	2.365	10.73
	8	7357	0.446	0.0247	2.365	4.63
	8	9367	0.452	0.0200	2.262	3.17
1 WIREL.	5	10240	0.326	0.0037	2.776	3.15
2 CASING	38	3739	0.450	0.0851	2.2027	6.22
	38	5492	0.481	0.0454	2.2027	3.10
	38	7180	0.448	0.0310	2.2027	2.28
	37	8837	0.447	0.0188	2.0290	1.40
3 CASING	14	6019	1.278	0.3011	2.160	13.60
	14	8119	0.968	0.1772	2.160	10.57
	14	10099	1.187	0.0668	2.160	3.25
	15	10850	1.113	0.0853	2.145	4.24

*For well description see paper SPE 16663

**2-D Model was used

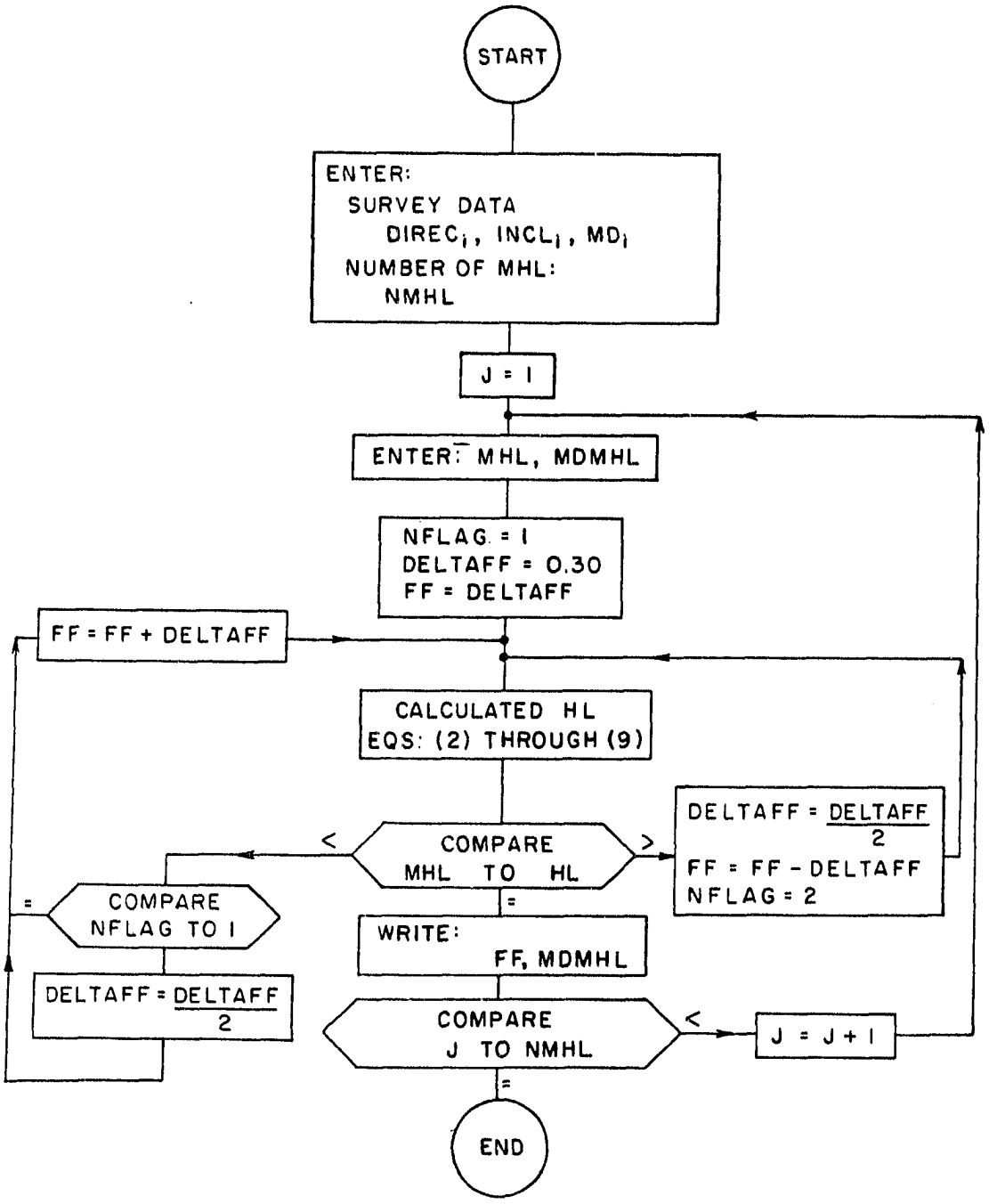

Fig. 1 - Flow diagram of the friction factor computation procedure.

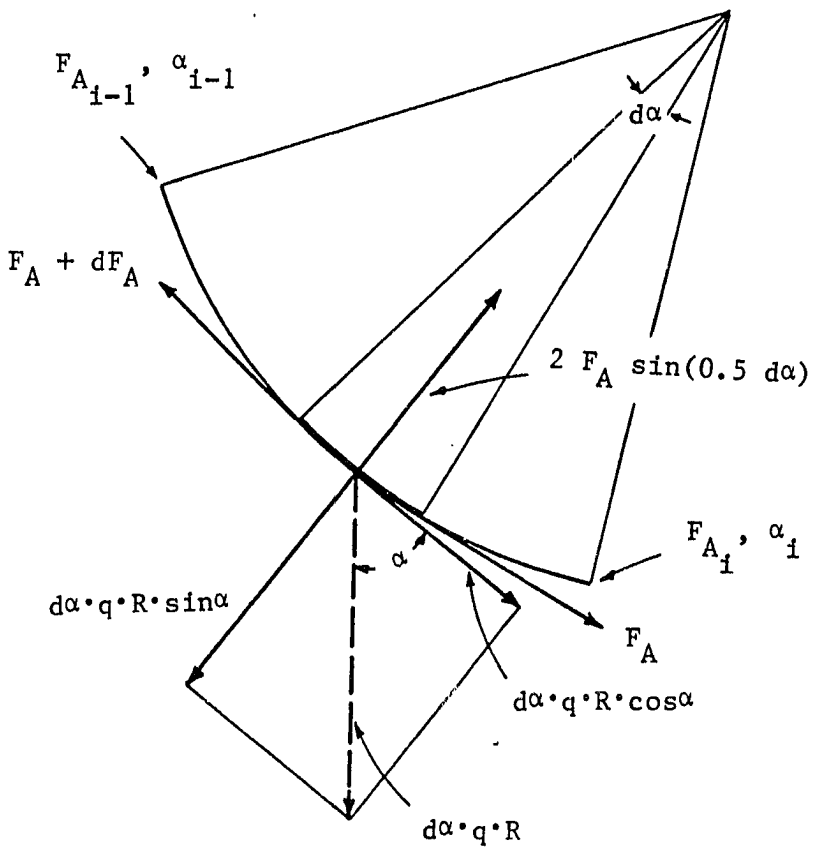

Fig. 2 - Forces acting on a small casing element within buildup section

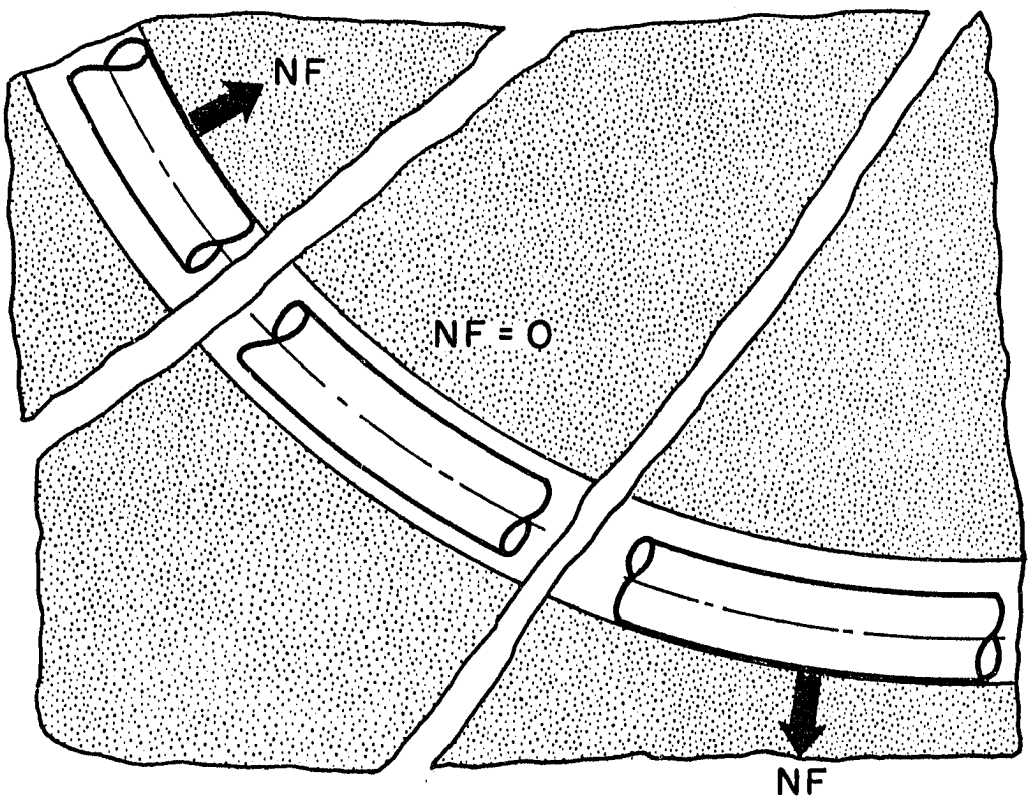

Fig. 3 - Possible directions of the normal force in a buildup section.

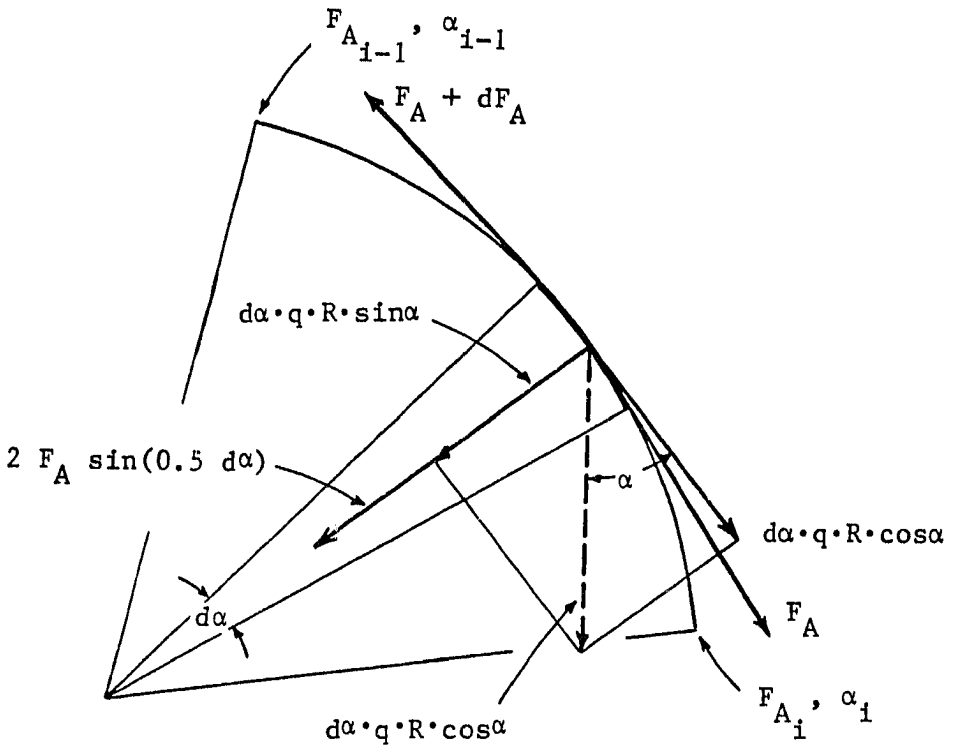

Fig. 4 - Forces acting on a small casing element within drop-off section.

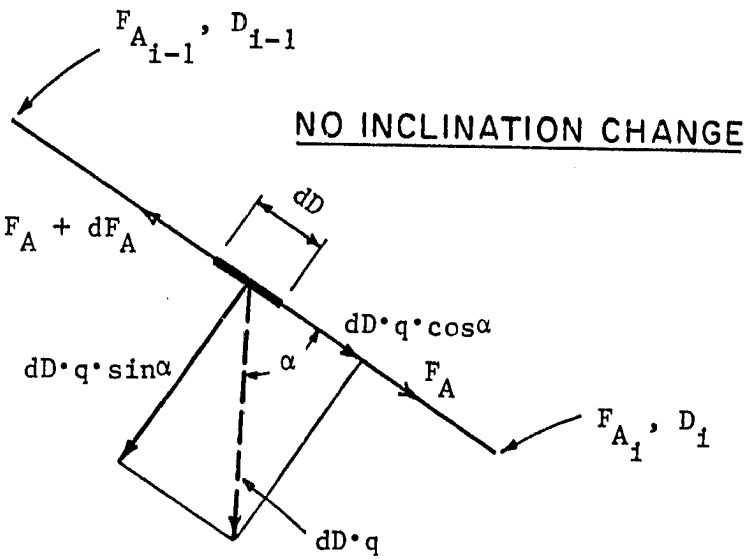

Fig. 5 - Forces acting on a small casing element within slant section.

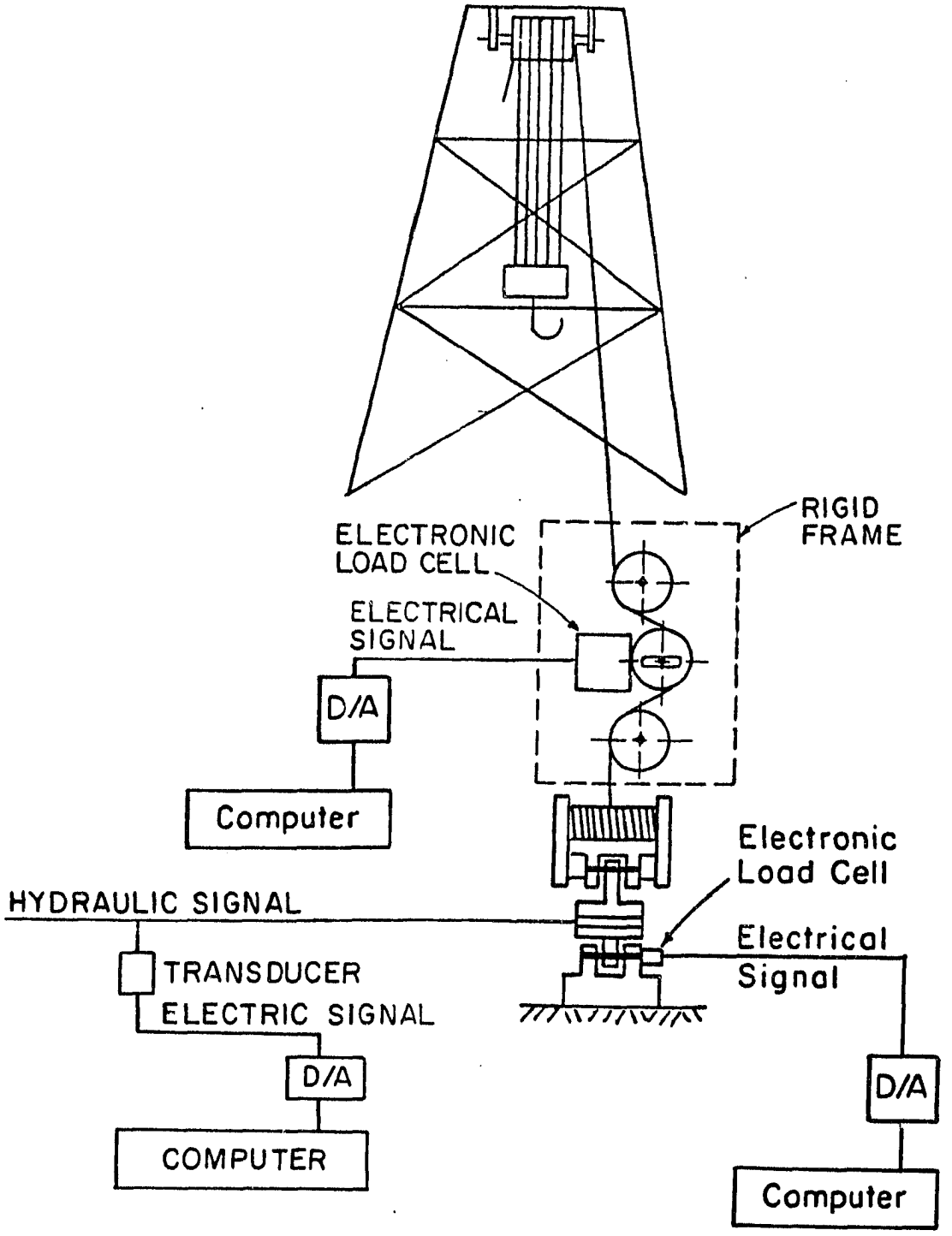

Fig. 6 - Schematics of the hook load recording process.

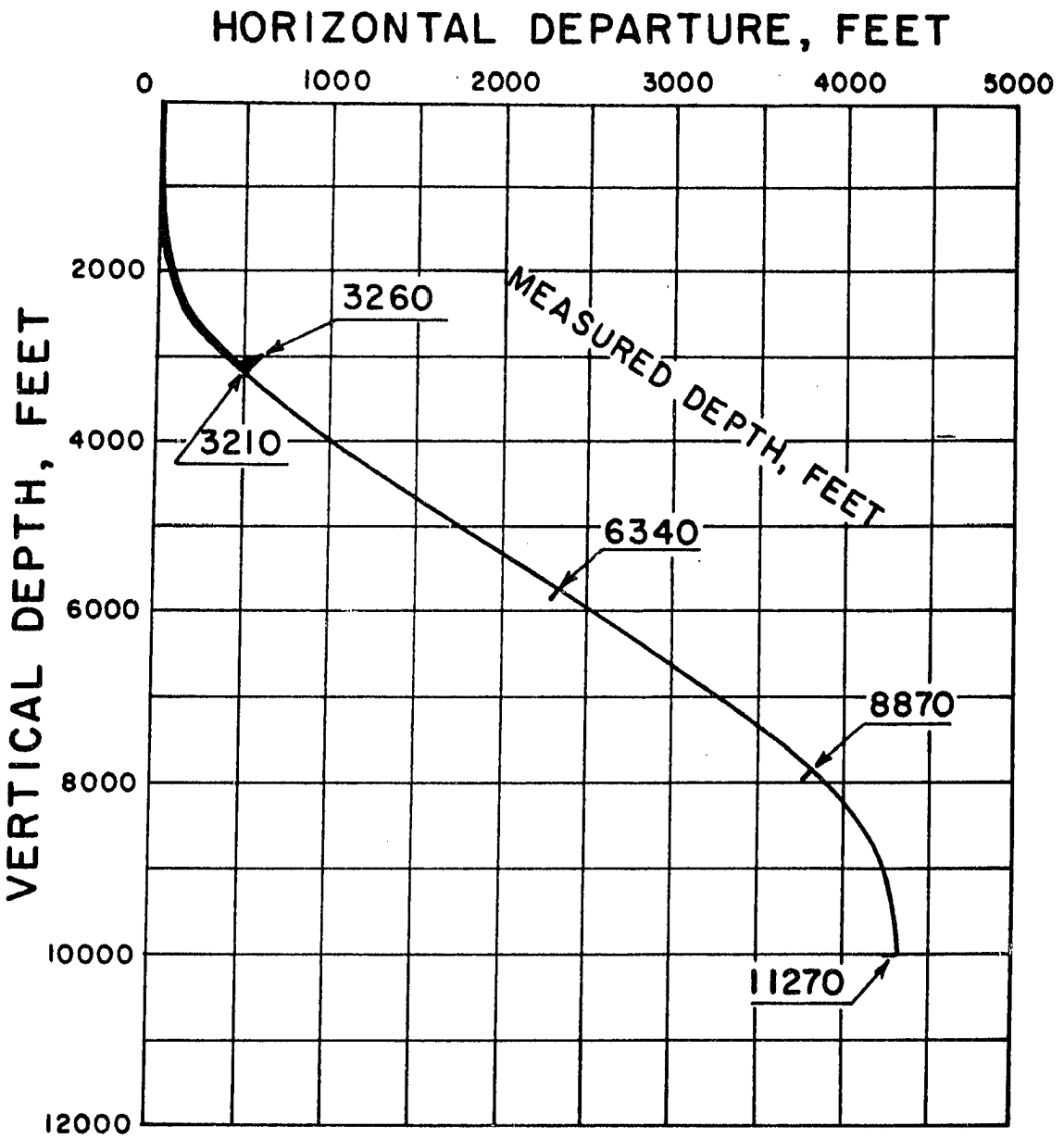

Fig. 7 - Vertical projection of Well 1.

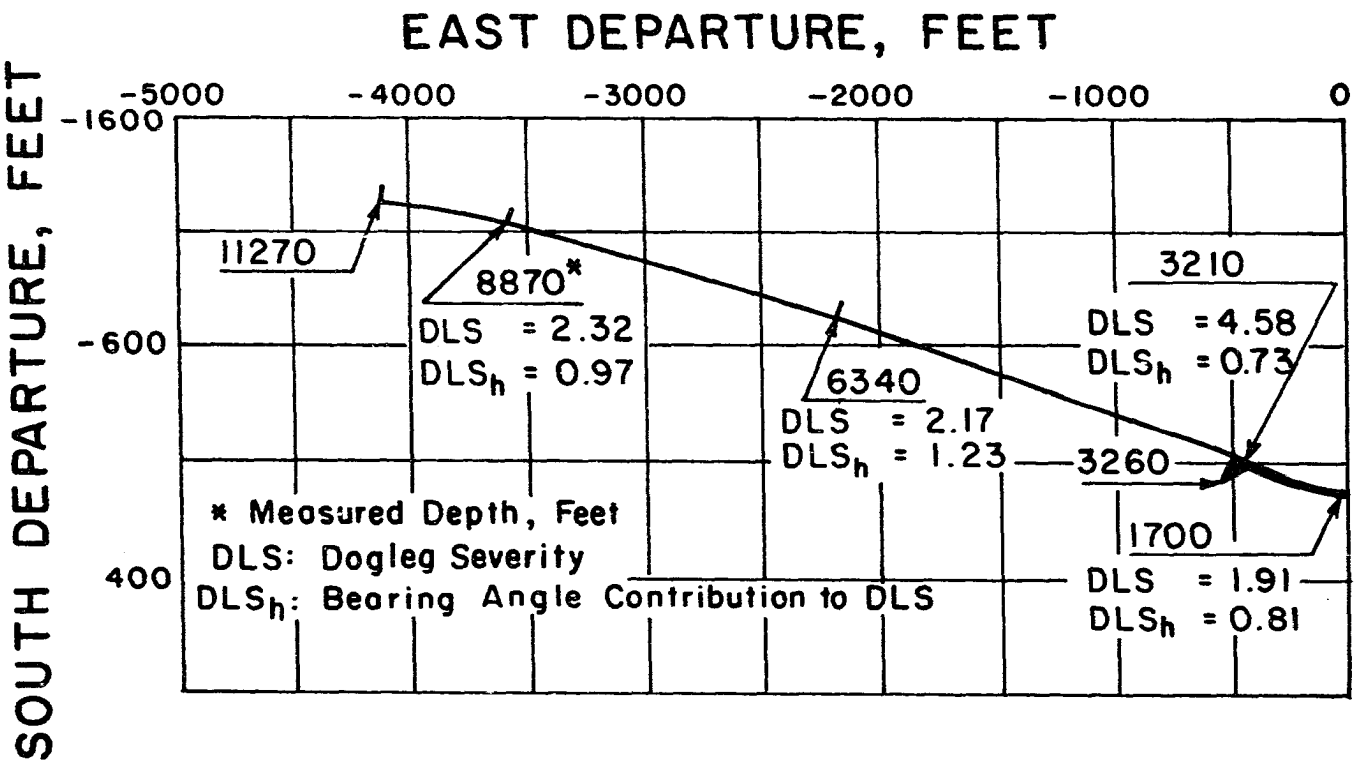

Fig. 8 - Horizontal projection of Well 1.

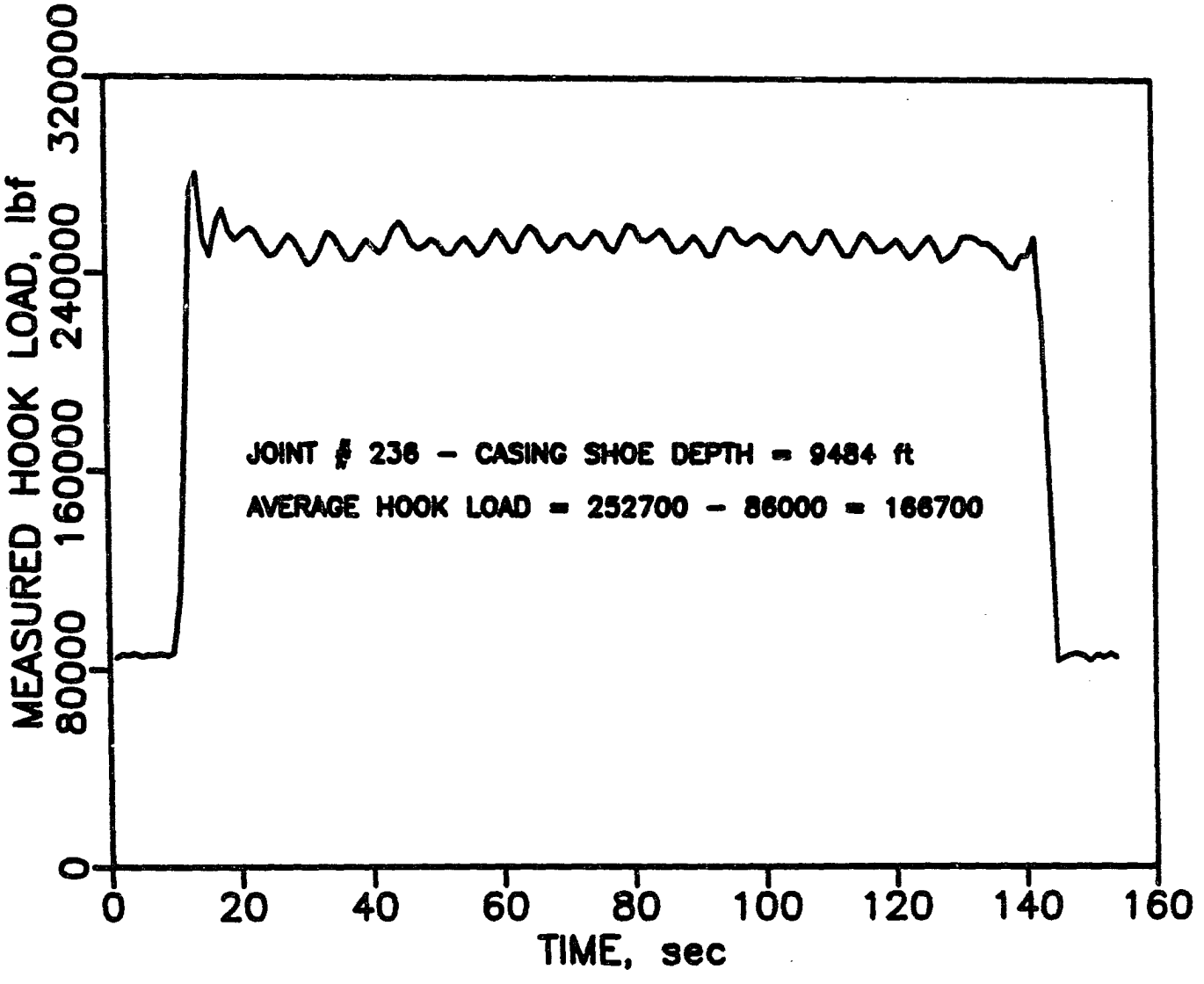

Fig. 9 - Hook load record while running one casing pipe.

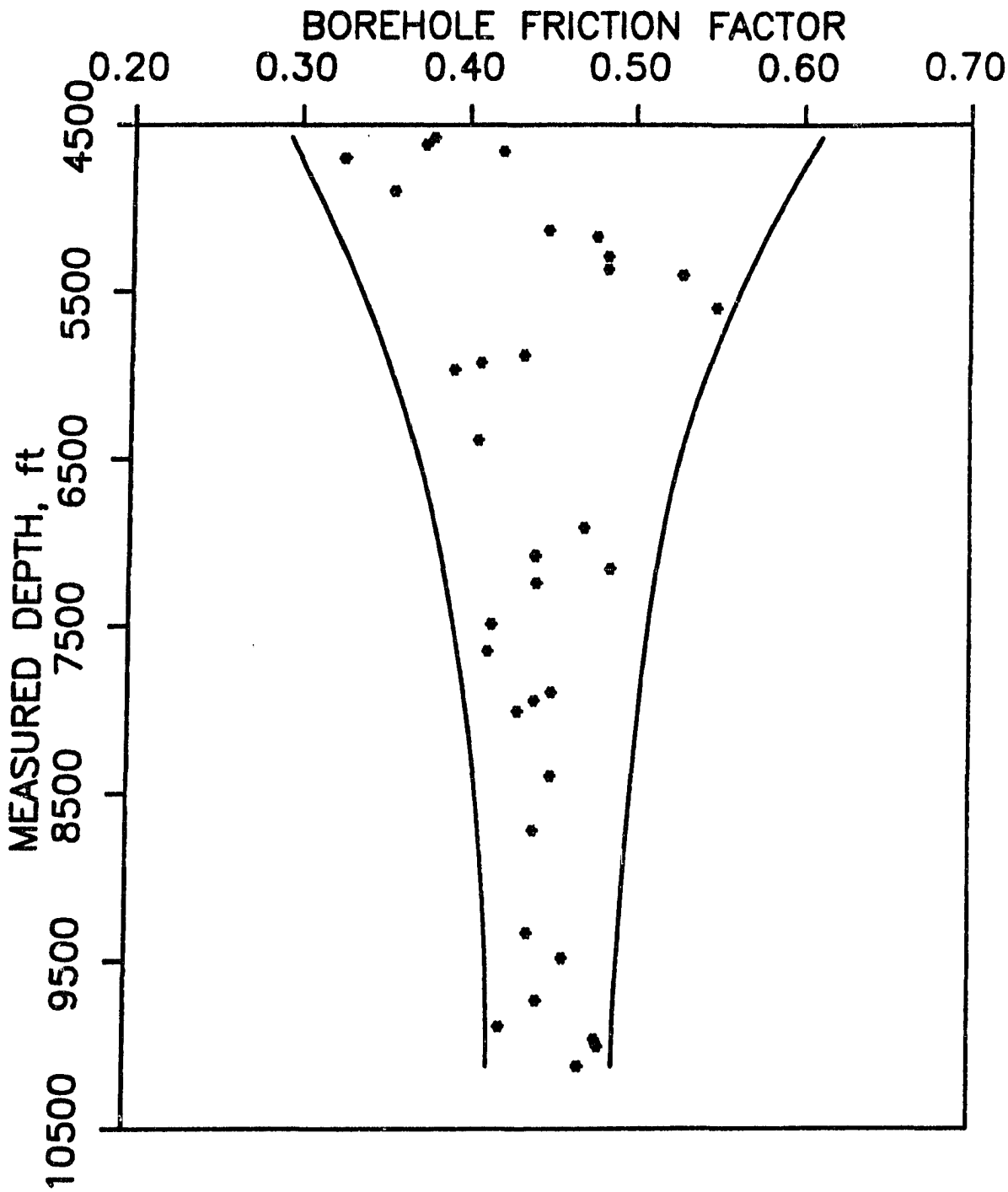

Fig. 10 - Stabilization of the borehole friction factor.

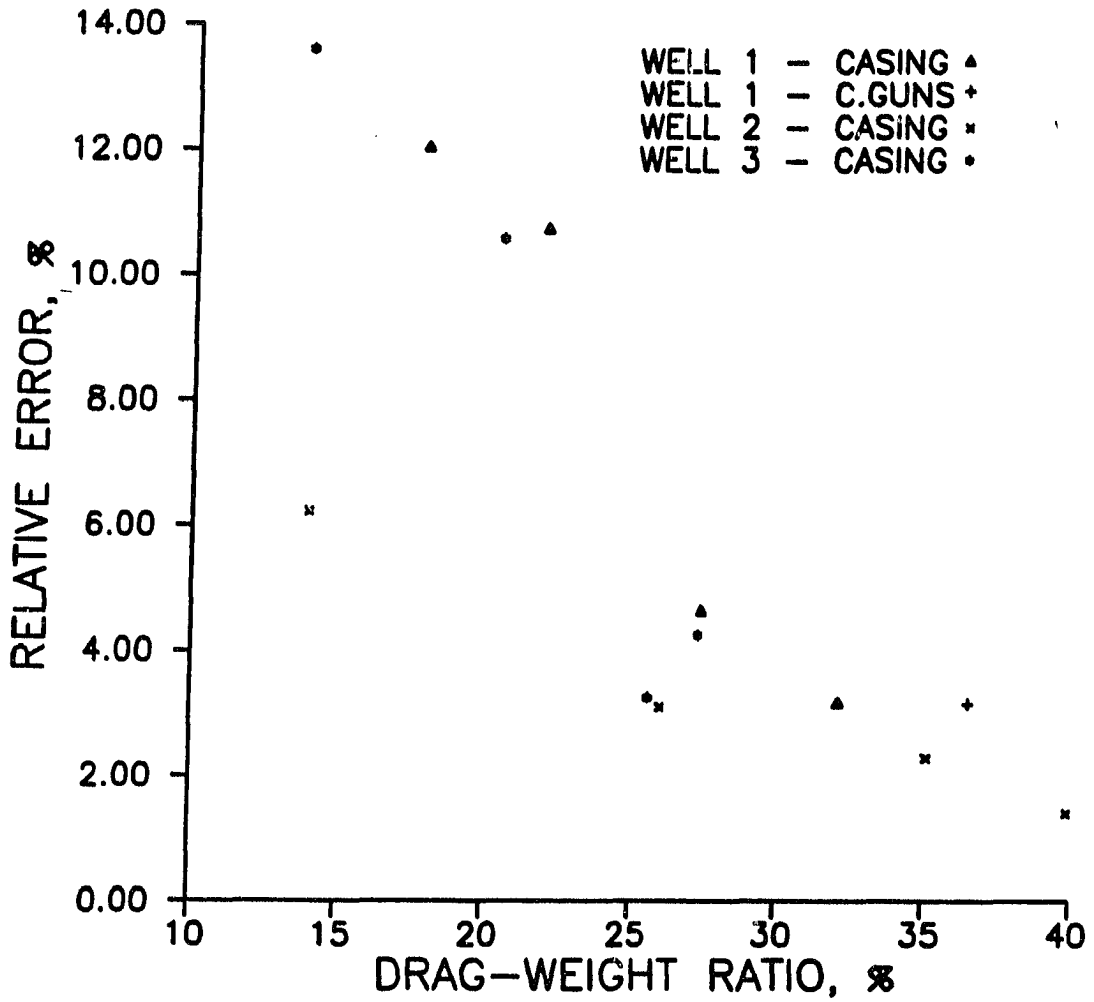

Fig. 11 - Borehole friction factor computation accuracy for several different casing and core gun runs.

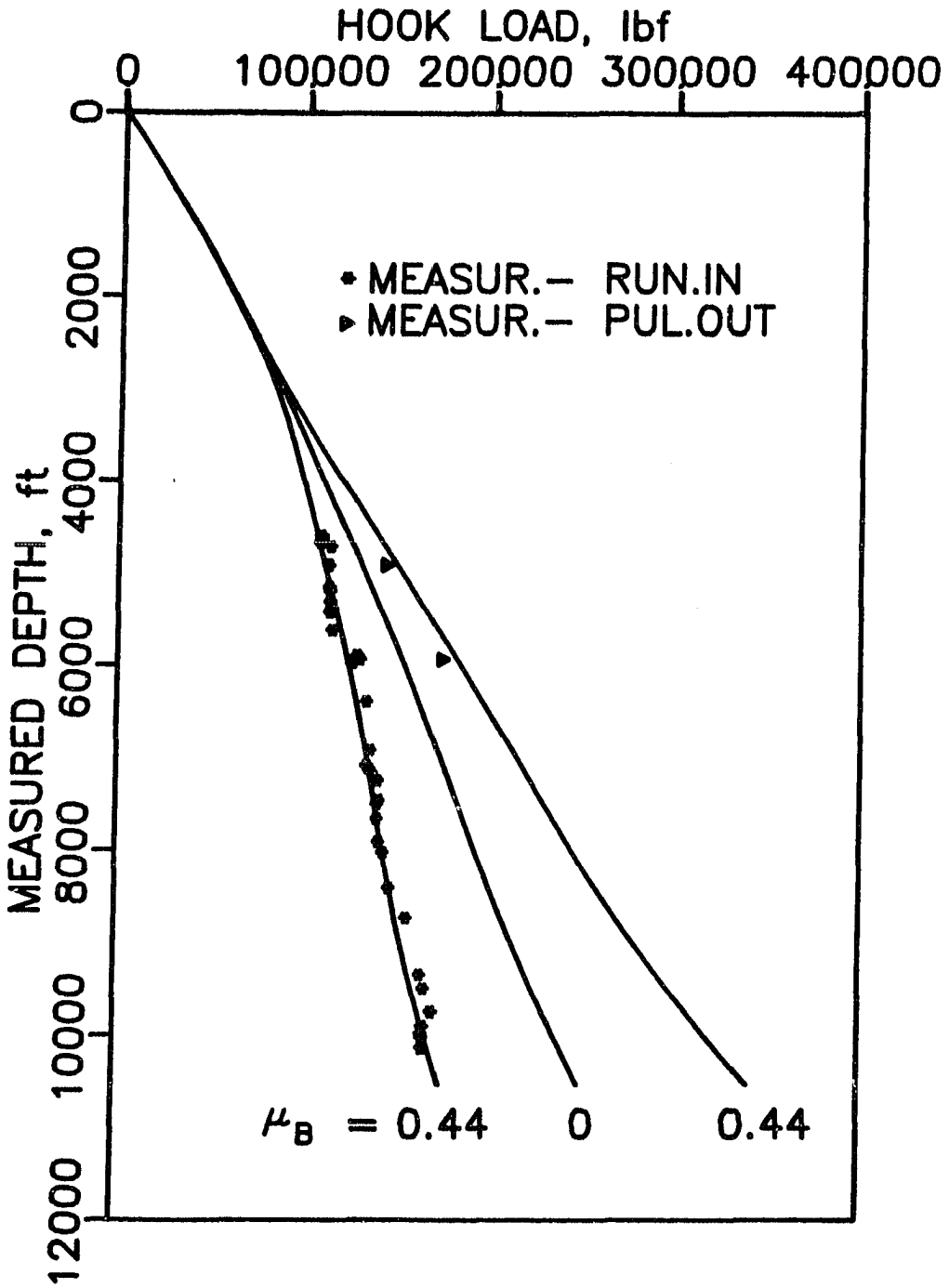

Fig. 12 - Well 1: Measured and predicted hook loads for the casing run.

CHAPTER II

FIELD COMPARISON OF 2-D AND 3-D METHODS FOR THE BOREHOLE FRICTION EVALUATION IN DIRECTIONAL WELLS

Reprint:

Maidla, E. E., Wojtanowicz, A. K.,

"Field Comparison of 2-D and 3-D Methods for the Borehole Friction Evaluation in Directional Wells",

SPE 16663, Sep., 1987.

ABSTRACT

The two new general procedures for the borehole drag prediction, based on the borehole friction factor concept were compared. The procedures employed iteration over the directional survey stations, numerical integration between the stations and mathematical models of the axial loads within a moving pipe in the borehole. The models considered several new effects such as hydrodynamic viscous drag, contact surface, and the bearing angle component of dogleg severity.

The study addressed the extent and conditions under which the two-dimensional and the three-dimensional procedures diverged significantly. The method was based on the computer calculated values of the borehole friction factor from the measured hook loads. The field data used included four casing runs from the offshore locations in the Gulf Coast area. In addition, the systematic theoretical study was performed with over 100 computer-simulated directional wells.

The study revealed a good agreement between 2-D and 3-D procedures for most common drilling conditions. The 2-D model's accuracy was mostly affected by the bearing angle component of shallow doglegs. In addition, the reliability of the borehole friction factor field

assessment was mainly controlled by the inclination angle and the length of the slant hole section of a well.

INTRODUCTION

The complex spatial configuration of directional wells engender an additional axial load (drag) when pipe or bottom hole tools are run in the boreholes. Traditionally, the frictional effects were not computed but were accounted for by the design factors. Such an approach resulted in the overestimated design and high operational uncertainty. The example here might be reluctance of many operators to reciprocate casing strings, despite a beneficial effect of this operation on the cement bond.

The knowledge of the frictional loads will improve the design criteria, and will help to optimize the design for the minimum cost.

In their interesting study, Johancsik et al., [1], developed a simplified model to predict torque and drag for the drillstring. They also used the model to find the sliding friction coefficient. The model was tested in three directional wells with a significant length of the cased hole section (70%, 83%, and 99%). No distinction

was made between cased hole friction and the open borehole friction. Also, the hydrodynamic effects were not considered which, for the drillstring movement, might have been an adequate simplification.

Sheppard, et al. [2] investigated the advantages of planning an undersection trajectory (steady buildup) to reduce torque and drag. In the one field case studied, they evaluated friction factor values of 0.36 only within the shallow depth interval 1900 to 2400 ft.

Bratovich, et al, [3] investigated problems of running logging tools in high-angle wells. The field tests and the laboratory tests were performed. For the open hole, they reported a friction factor value 0.36 for the stand-off tool, and 0.40 for the wireline. The open hole tests were conducted in lignosulfonate water-base muds with densities varying between 9.7 to 12.5 lbm/gal.

To date, very few tests have been performed with the actual field data. The concept, that a single value of the friction factor represents borehole conditions has not been verified. Furthermore the existing models are not general since they were developed for a specific pipe type and size. The casing problems

concerning borehole friction have not been addressed yet.

This study is a continuation of the research that began by considering the borehole drag impact on the casing string loads and its effect on the casing design criteria [4]. Later, the concept of the borehole friction factor and the field method for its determination, based on the two-dimensional model, were developed [5]. Most of the early findings were in good agreement with this research. However, the excessively high values of the calculated friction factors [5] indicated effects of some unexplained forces not included in the original two-dimensional model.

The concept of the borehole friction factor implies its value being constant throughout the depth of the well and independent from the wellbore trajectory (inclination, bearing angles, doglegs). It represents the mechanical frictional interaction between the pipe surface and the borehole surface and it shall only depend upon: drilling fluid lubricity, mud cake lubricating properties, lithology, casing coupling size relative to borehole size, pipe surface configuration (centralizers, coating) and the borehole surface configuration (washouts, keyseats, ledges, etc).

The definition of the borehole friction factor is

$$\mu_B = \frac{|F_H - Q_V \pm F_D|}{\int_0^D q_D(\ell)d\ell} \qquad (1)$$

The minus and the plus signs are for the pulling-out and the running-in situations, respectively.

The hydrodynamic viscous drag term F_D represented one of the unexplained forces disregarded in the previous work [5]. Other potential contributors to the error made by the two-dimensional treatment included spatial belt friction effects due to the bit walk and doglegs. As a result the new 3-D model was developed which accounted for the above effects and for the effect of the contact surface between pipe and borehole.

The main objective of this study was to verify the integrity of Equ. (1), and to define an applicability of the 2-D and 3-D treatments.

METHOD

The calculations of the borehole friction factor were performed by the two computer programs. Each program consisted of a mathematical model of borehole drag (2-D

or 3-D), and the iterative procedure for calculating hook load.

The input data included: drilling mud properties, casing string composition, borehole profile (directional survey), borehole geometry, series of measured hook loads while running (pulling) casing, casing string velocity, and the measured depth of the casing shoe.

The calculation procedure started by assuming some value of the borehole friction factor and recurrently calculating the axial load from the casing shoe upwards until the calculated hook load was determined. If the calculated hook load did not match the measured value, the new value was assumed and the procedure was repeated until the hook loads match occurred. The match indicated the correct last assumed value of the borehole friction factor.

In this method, the borehole friction factor is not a measured magnitude but it is calculated from the hook load measurements. Therefore a major error can be made due to incorrect axial load predictions by the mathematical model. Consequently, it is important to account for all possible phenomena which affect the borehole drag. Eventually, the model can be simplified by ignoring those

effects which show a small impact on the borehole friction factor value.

The approach used in this study was based both on the computer-simulated conditions and the actual field data. The simulation approach was used to systematically investigate effects of spatial parameters such as bit walk, bearing angle, inclination angle and dogleg severity, including their extreme values which were not readily available from the field records.

The collected field data were used for an empirical verification of the borehole friction factor concept and applicability of the 2-D and 3-D models to its determination. Unlike the simulation study, the field verification method was based on the actual directional surveys and on the on-site record of the hook loads. To increase precision, the hook loads were measured with the portable equipment bypassing the existing rig instrumentation. The portable unit was assembled to the deadline anchor hydraulic signal, and consisted of a hydraulic load cell, transmitter, digitizer, and recorder which stored the data on magnetic tape. The equipment's accuracy was 1000 lbf and the sampling rate at which the data was recorded on the tape was 1 sec. Before and after every rig trip, the equipment was calibrated and its readings were checked for accuracy.

The other field data regarding drilling mud properties, borehole geometry, current depth of the casing shoe, and velocity of the pipe movement were collected or directly measured on the drilling locations.

The method used for the analysis of the field data was similar to the simulation study. The calculated values of the borehole friction factors were examined for their dependence upon depth, well trajectory, doglegs, and their statistical scatter. In all calculations, friction in the cased upper section of the borehole was modelled by using sliding friction coefficient for steel surfaces 0.25.

BOREHOLE DRAG MODELS

The predicted hook load was calculated from the equation:

$$F_H = F_A \pm \frac{\pi}{4} \sum_{m=1}^{M} \left(\frac{dp}{d\ell} \right)_m L_m d_m^2 \qquad (2)$$

In Equ. (2), the plus sign is used for upward pipe movement and the minus sign for downward motion. The second term in this equation accounts for hydrodynamic friction effects and is the same for all models. The relevant calculations are shown in Appendix A.

3-D Model

The model is based on the analytical description of the well profile. It was derived by analyzing forces acting on a small casing element as shown in Fig. 1. In this study, the minimum curvature method was used to interpolate a curve between two directional survey points. In fact, the equations of the model are general and can be used with any other interpolating scheme.

The model considers the following effects:

* Spatial changes of the well direction as measured by rates of buildup, drop-off, bit walk, as well as dogleg severity and horizontal component of the dogleg severity;
* Buoyancy effect;
* One value of the borehole friction factor for a well;
* Hydrodynamic friction effects calculated as the surge or swab pressures;
* Effect of the pipe-borehole contact surface on the drag;
* Torsion and spring effects are ignored.

The axial load equation is:

$$\frac{dF_A}{d\ell} = q_u(\ell) \pm \mu_B \, C_s(\ell) \, q_N(\ell) \qquad (3)$$

and

$$q_N(\ell) = \sqrt{[q_b(\ell)]^2 + [q_p(\ell) + \frac{F_A(\ell)}{R(\ell)}]^2} \qquad (4)$$

where

$$q_u(\ell) = \vec{q} \cdot \vec{u}(\ell)$$

$$q_b(\ell) = \vec{q} \cdot \vec{b}(\ell) \qquad (5)$$

$$q_p(\ell) = \vec{q} \cdot \vec{p}(\ell)$$

$$R = \frac{\ell_i - \ell_{i-1}}{\arccos[\cos(\Theta_i - \Theta_{i-1}) \cdot \sin\alpha_i \cdot \sin\alpha_{i-1} + \cos\alpha_i \cdot \cos\alpha_{i-1}]} \qquad (6)$$

In the Equ. (3), the positive sign applies to the upward pipe movement and the negative sign is for the downward movement. Equations (5) describe projections of the distributed pipe weight on the trihedron [11] axis associated with any given point of the well trajectory.

The correction factor, C_s, represents an effect of the contact surface between the pipe and the borehole.

Its derivation is presented in Appendix B. The correction factor values vary between 1 and $4/\pi$ and are dependent upon the contact surface angle γ as shown by the equation:

$$C_s(\ell) = \frac{2}{\pi}\,\gamma(\ell)\,\left(\frac{4}{\pi} - 1\right) + 1 \qquad (7)$$

In all cases studied here, the correction factor was always very close to unity. Therefore it can simply be ignored in most engineering calculations.

Equation (3) does not include torsion effects which might contribute to the normal force. Since an analytical solution to equation (3) is not generally possible, numerical integration must be used. Our calculations indicated that, when using the classic Runge-Kutta method, only three steps are necessary to perform the integration.

2-D Model

This model ignores bearing angle changes and the shape of the contact surface between pipe and the borehole. In all other aspects its construction is similar to that of the 3-D model. However, in the two-dimensional space, the dot product expressions (5) simplify and become the explicit algebraic functions. Therefore, the iterative formula for the

axial load becomes

$$F_{A_{i-1}} = A \cdot F_{A_i} + C_1 \cdot \frac{q\,R}{1+\mu_B^2}\left[(\mu_B^2-1)(\sin\alpha_{i-1}-A\sin\alpha_i)\right.$$

$$\left. + 2C_2\mu_B(\cos\alpha_{i-1} - A\cos\alpha_i)\right] \qquad (8)$$

where:

$$A = \exp\left[\mu_B C_2(\alpha_{i-1}-\alpha_i)\right] \qquad (9)$$

when pulling pipe out of the well, and

$$A = \exp\left[\mu_B C_2(\alpha_i-\alpha_{i-1})\right] \qquad (10)$$

when running pipe into the well.

The constants C_1 , C_2 are the sign convention constants dependent upon direction of the normal force - Table 1.

Also, for the two-dimensional borehole, the radius of curvature expression (6) simplifies to

$$R = \frac{\ell_i-\ell_{i-1}}{\alpha_i-\alpha_{i-1}} \qquad (11)$$

It should be emphasized that, though simplified, the two-dimensional model has a strong practical appeal. From the engineering standpoint, such a model is the only solution to the problem of predicting axial loads during the well planning stage. At this stage the casing string design can be achieved only by

considering a simplified two- dimensional profile of the planned well.

THEORETICAL STUDY

The main objective of this study was to compare the two borehole drag models using wide range of the directional well configurations and to determine conditions under which the models' results became significantly different. The practical purpose was to find an error, in terms of the borehole friction factor value, associated with using 2-dimensional model instead of a 3-dimensional. Since the available field data did not represent variety of configurations necessary for such a study, the directional surveys were simulated by the computer. More than 100 directional wells were generated. Drilling mud properties, casing specification and the bit size were chosen to be the same as in the case history of Well 1. The final vertical depth was simulated at approximately 8000 ft. The kick- off point was set at 2000 ft and the directional survey base of 100 ft was selected.

Computer-generated plots of the bit walk and inclination patterns were also used to provide better understanding and visual control of the well paths. The

examples of such plots are shown in Figs. 2 and 3 for a buildup rate of 2 deg/100 ft and the inclination of 30 deg.

Initially, a buildup rate of 2 deg/100 ft was assumed with the bit walk varying between 0 and 2.4 deg/100 ft. Also, an inclination of the slant (sailing) portion varied from 10 deg to 60 deg . For each well, the reference hook load was calculated using the 3-D model and value of the borehole friction factor 0.4. The reference hook load was then used by the 2-D model to evaluate a new value of the borehole friction factor. Such a procedure provided an easy way to compare, in dimensionless terms, results between wells of different configurations. In addition, the significance of the hydrodynamic effects was evaluated by running the 3-D program with and without hydrodynamic component.

The comparison between 3-D and 2-D models are summarized in Figs. 4 and 5. The 2-D model overestimated borehole friction factor by up to 25% for severe doglegs, large bit walks and small slant angles. The sensitivity of the 2-D model to bearing angle changes is caused by the spatial component of the capstan effect which is not considered in this model.

The effect of the hydrodynamic friction is shown in Table 2. The error introduced by ignoring this effect

was as much as 50-60% for a wide range of the well buildup rates from 0.5 to 2 deg/100 ft at small inclination angle of 10 deg . Moreover, the hydrodynamic effect became less important with increasing inclination angle and for the slant holes inclined more than 60 deg its contribution to the calculated value of the borehole friction factor was smaller than 17%. The reason was that in the high- inclination holes a sliding friction dominated all other effects, particularly the effect of the swab and surge pressures which, by their nature, were independent from the inclination angle.

In the second part of the theoretical study we examined the effect of doglegs on the borehole drag models response. A single dogleg was introduced at the end of the buildup section of the simulated wells. The dogleg was entirely confined in the bearing angle change with no effect on the inclination. Such a configuration represented the worst possible case for the two-dimensional treatment since inclination was entirely unaffected by the dogleg and the 2-D model could not respond to its value. No bit walk was assumed to eliminate other spatial effects. Buildup rate of 0.5 deg/100 ft and the slant hole inclination of 20 deg were constant while dogleg severity (due to bearing angle changes) varied from 0 to 10 deg/100 ft.

The comparison is shown in Fig 5. The 2-D model responded with a maximum deviation of 34% for the dogleg severity 10 deg/100 ft thus demonstrating its sensitivity to bearing angle doglegs.

FIELD STUDY

There were four field case histories considered here. All located offshore Louisiana Gulf Coast as shown in Fig. 6. The drilling fluids used in all cases were the dispersed water-base mud systems with the similar mud densities.

Well Description and Data Acquisition Technique

Well 1 was an S-shaped well drilled to 11270 ft -Figs. 7, 8, and Tables 4-6. Its maximum inclination was 39.20 deg at the measured depth of 5032 ft and its build-up rate averaged 2.2 deg/100ft. After the well had been conditioned for the casing run, further side wall cores were requested from the geology department. During that run, the cable tension of the side core barrel was recorded manually using the logging unit equipment available on the platform. The depth was measured by the use of a calibrated wheel. During the wiper trip before the casing run the pulling out hook load for the drillstring

was measured manually using our portable unit. The casing run was also recorded using the unit - Table 4. The measured hook load vs. time was plotted on two 120 in. strips of paper in the form of logs, and the average hook loads and velocities were determined for 36 joints of casing. Then the depths were correlated with the hook loads by using the tally sheet with the recorded time. During the casing run, the casing string was picked up at 4897 and 5924 ft and the two pulling hook loads were recorded. The casing was equipped with rigid-type centralizers.

Well 2 was a build-and-hold type well drilled to 9610 ft - Figs. 11, 12 and Tables 7, 8. Its maximum inclination was 48.3 deg at the measured depth of 5043 ft and its build up rate averaged 3.3 deg/100ft. The rig instrumentation was used for the hook load measurements. It was equipped with a load pin and three strain gauges. The hook loads were recorded manually from a monitor in the mud logging unit. Prior to the measurements, the load sensor was calibrated. The equipment's accuracy was 1000 lbf. During the wiper trip the hook load was recorded while pulling out the drillstring-Table 8. Total of 252 joints of casing were run in approximately 10 hours and 151 average hook loads were recorded for the deeper joints. Table 7 shows the selected data recorded. The pick-up attempt (only pipe stretching) was made once

at the total depth with the maximum pull 265,000 lbf. Forty bow-type centralizers were installed on every joint on the lower sections of the casing string.

Well 3 was a build-and-hold type well drilled to 11538 ft - Figs. 15, 16 and Table 9. Its maximum inclination was 16.35 deg at the measured depth of 10200 ft, and its build-up rate averaged 0.5 deg/100ft. The rig instrumentation was similar to that of the portable unit. It consisted of a 100,000 lbf capacity tensiometer placed at the dead line. The electronic signal from the load cell, equipped with strain gauges, was digitized and stored on a computer hard disk. The hook load and depth were recorded every second. During the casing run the casing string was picked up three times. The hook load was recorded for 60 joint runs. Table 8 contains some of the data recorded. After the last joint was run, the casing string pick-up was attempted (only pipe stretching) to 356,000 lbf to try and reciprocate the casing string while cementing. Thirty bow-type centralizers were used on every joint on the lower section of the casing string.

Well 4 was a build-and-hold type well drilled to 8967 ft - Figs 18, 19 and Table 10. Its maximum inclination was 52.25 deg at a measured depth of 6810 ft and its build-up rate averaged 2.8 deg/100ft. Due to the

malfunction of the portable unit, only one hook load reading was obtained during the last joint run, using the weight indicator at the driller's console. The resolution of the equipment was 5000 lbf and there was no record of any previous calibration. After the last joint was run, the casing string was picked-up at 270,000 lbf (only pipe stretching). Rigid-type centralizers were used.

Results and Discussion

The results are presented in Tables 3-10 and in Figs. 9, 10, 11, 14, 17. The data provided information on the average values of the borehole friction factor, its insensitivity to the spatial geometry of directional wells as well as the reliability of the two-dimensional approach. Though the presented results are organized on the well-by- well basis, they will be discussed by topic rather than by the field case.

1. Borehole friction factor values

Similar borehole friction factors values were obtained for the similar mud programs, as shown in Table 3:

* For all casing runs, the average borehole

friction factor calculated from running-in hook loads were greater than those from pulling hook loads.

* The average borehole friction factor values calculated for the upward motion, in the high inclination wells (Wells 1 and 2) fell within range from 0.21 to 0.30.
* The average borehole friction factors for wells 1, 2 and 4, calculated for running-in conditions were from 0.38 to 0.43.

Therefore, it was concluded that some effects present while running-in casing were not active while pulling out. These effects were disregarded by both models. One of the effects absent in the models was the effect of torsion (spring or unbending effect). The discrepancy between pulling and running values of the borehole friction factor cannot, however, be explained by this effect, because of its presence disregarding direction of the pipe movement. Some possible explanation was that ledges, washouts or bridges caused by slaughing borehole walls would work against the downward movement of the pipe. These effects constituted phenomenon which might be called "borehole conditions" which was not associated with mechanical friction. Though there is no phenomenological description of these effects, their contribution to axial

loads can be numerically estimated from pulling and running loads difference.

2. Accuracy of the two-dimensional approach

The values of the borehole friction factor based on the 2-D model showed a good agreement with those from the 3-D model in Wells 1 and 2. In the remaining two wells, however, the 2-D approach overestimated the borehole friction factor by 24-45%.

To improve the analysis, the overall dogleg severity and the horizontal component of the dogleg severity were calculated. The horizontal dogleg was an indication of the bearing angle change contribution to the overall dogleg severity.

The analysis revealed that the distortion of the 2-D calculations was controlled mainly by the horizontal components of shallow doglegs. For example, in Well 3 the shallow depth dogleg was composed mainly of the bearing angle change and it significantly contributed to the hook load. This effect was disregarded by the 2-D model which caused an overestimation of the borehole friction factor. Situation in Well 4 was similar with several shallow doglegs affected mainly by the bearing angle. In Well 2, however, the large horizontal dogleg

was located deep in the well and did not affect 2-D model accuracy. The depth, the magnitude and quantity of horizontal doglegs were considered important factors in the 2-D model applications. It is believed that their contribution was caused by the capstan effect which, in turn, depended upon the pipe length below the dogleg.

Directional survey of Well 1 did not show any significant horizontal doglegs so the 2-D and 3-D calculations agreed very well.

Apparently, the 2-D model discrepancies in assessing the borehole friction factor were greatly affected by spatial irregularities within the shallow borehole section above the kick-off point. The same irregularities in the lower, directional portion of the well had negligible effect on the hook load. It seems that the main problem in directional drilling as far as casing design is concerned, is associated with the dogleg severity in the vertical hole portion of the well.

3. Borehole friction factor vs depth

The results from Wells 1, 2 and 3 proved no correlation between the calculated value of the

borehole friction factor and depth as indicated by the small values of the coefficients of determination and the regression coefficients in Table 3, at the level of confidence 95%. Stability of the method was further supported by the low values of standard deviations. Moreover, the inherent scatter of the calculated values was largely reduced at greater depths as shown in Fig. 13, for Well 2. This plot shows a convergence of the borehole friction factor values with increasing depth. Similar plots were obtained for Wells 1 and 3.

4. Effect of well trajectories

The insensitivity of the borehole friction factor to the well trajectory was demonstrated by similar values obtained for different wells having various trajectories (see well descriptions and Table 3). However, more field data from the same area, and with the same drilling mud, is required to come to more definite conclusion.

5. Effect of the type of string in the well

In Wells 1 and 2 the hook load was recorded for the casing, the drill string and for the wireline tool runs. Each type of string was characterized by different

surface configurations and external diameters. Analysis of the results indicated insensitivity of the borehole friction factor, calculated from the pulling out loads to these differences as shown in Table 3.

6. Hook load error effect

The theoretical effect of the measured hook load on the calculated value of the borehole friction factor is shown in Fig. 21. It can be noticed that, for low inclination wells, small changes in the recorded hook loads may significantly affect the calculated values of the borehole friction factor. Thus the reliability of the method increases in more deviated holes. Also, the importance of accurately measured hook loads is further emphasized.

The above statement was further verified by the field results obtained in Wells 1 and 3. In these wells, the borehole friction factor calculated from the running-in loads was used to predict the pulling loads - Figs. 10, 17. In both wells, the predicted loads were about 7% higher than the recorded ones. This relatively small hook load difference was associated with some changes in the borehole friction values calculated from pulling and

running conditions: for Well 1 (inclination 39 deg), from 0.27 to 0.43; and for Well 3 (inclination 16 deg), from 0.44 to 0.83. Therefore, the same relative change in the hook load implied much smaller change of the borehole friction factor in the high-inclination Well 1 than in the low inclination Well 3.

CONCLUSIONS

All the findings of this research can be summarized as follows:

1. The borehole friction factor appeared fairly insensitive to measured depth, various well trajectories, size of pipe and its surface. The borehole friction factor values, for most cases were 0.21-0.30 for pulling conditions, and 0.27-0.43 for running conditions. The latter were always 10-37% larger due to non-frictional phenomena resisting downward pipe movement in the open hole. These effects have not been yet modelled.

2. The two-dimensional approach tended to overestimate values of the borehole friction factor. When used for the running axial loads calculations, at the well planning stage, it

will underestimate predicted axial loads. The 2-D model cannot be used for field assessment of the borehole friction factor unless the directional survey shows no shallow doglegs with a significant value of their bearing angle component.

3. Two factors positively affect the borehole friction assessment accuracy; the overall inclination, and the measured depth. Therefore the measurements taken at shallow depths in slightly deviated holes should not be used for prediction in deeper and more inclined wells.

4. The further investigations should provide more field information from various areas and drilling muds. Also a laboratory study on the mud cake effect on the pipe-borehole friction seems a logical next step in this research.

ACKNOWLEDGMENTS

The authors would like to thank Standard Oil Production Company-Lafayette District, Exxon Company USA-New Orleans, Mobil Oil Exploration and Production

Southeast Inc.-New Orleans, for help in recording the field data.

Grateful appreciation is given to TOTCO, Martin-Decker, NCI Dillon, Ray Oil Tool Company for their assistance and equipment support.

NOMENCLATURE

b = Unit vector in the binormal direction

C_c = Mud clinging constant

C_s = Contact surface correction factor

D = Measured depth, ft

Δd = External diameter of the pipe, in

d_B = Borehole diameter, in

d = Pipe deformation due to borehole reaction, in.

E = Modulus of elasticity, lbf/in^2

F_A = Axial load, lbf

F_D = Hydrodynamic viscous drag, lbf

F_H = Hook load, lbf

f = Flow friction factor

K = Consistency index, $dyne.s^n/100\ cm^2$

L = Pipe section length (same external diameter), ft

ℓ = Length of pipe, ft

M = Number of sections of different external diameters

N = Number of surveyed points

N_{Re} = Reynolds number

n = Flow-behavior index

p = Pressure, psi

dp/dt = Pressure gradient due to flow friction, psi/ft

$\mathbf{p}$ = Unit vector in the principal normal direction

Q = Buoyant weight, lbf

Q_v = Vertical projected buoyant weight of pipe, lbf

q = Unit buoyant weight of pipe, lbf/ft

q_b = Unit buoyant weight projection on the binormal direction, lbf/ft

q_D = Unit drag or rate of drag change, lbf/ft

q_N = Unit buoyant weight projection on the principal normal direction, lbf/ft

q_u = Unit buoyant weight projection on the tangent direction, lbf/ft

R = Radius of curvature, ft

t = Pipe wall thickness, in

$\mathbf{u}$ = Unit vector in the tangent direction

v_p = Pipe velocity, ft/s

v_{ae} = Equivalent displacement velocity, ft/s

X = X-coordinate of intersection point, in

Y = Y-coordinate of intersection point, in

α = Inclination angle, rad

$\bar{\alpha}$ = Average inclination between two surveyed points, rad

β = Overall angle change, rad

γ = Contact angle, rad

δ = Pipe-borehole ratio

Θ = Bearing angle, rad

ρ = Mud density /gal

μ_B = Borehole friction coefficient

REFERENCES

1. Johancsik, C. A., et. al., "Torque And Drag In Directional Wells - Prediction And Measurement", SPE 11380, 1983.

2. Sheppard, M. C., "Designing Well Paths To Reduce Drag And Torque", SPE 15463, 1986.

3. Bratovich, et al., "Improved Techniques For Logging High-Angle Wells", SPE 6818, 1977.

4. Wojtanowicz, A. K., Maidla, E. E., "Minimum Cost Casing Design for Vertical and Directional Wells", SPE 14499, 1985.

5. Maidla, E. E., Wojtanowicz, A. K.," Field Method of Assessing Borehole Friction For Directional Well Casing", SPE 15696, 1987.

6. Fontenot, J. E., Clark, R. K., "An Improved Method for Calculating Swab and Surge Pressures and Circulating Pressure in a Drilling Well",

SPEJ, Oct 1974, p. 451-62.

7. Burkhardt, J. A., "Wellbore Pressure Surges Produced by Pipe Movement", JPT, June 1961, p. 595-605; Trans., AIME, 222.

8. Taylor, H. L., Mason, C. M., "A Systematic Approach to Well Surveying Calculations", SPE 3362, 1971. .po 69 9. Bol, G. M., Effect of Mud Composition On Wear And Friction of Casing and Tool Joints, SPE Drilling Engineering, Oct. 1986, pp 369-376.

10. Bourgoyne, Jr., A. T., et al., Applied Drilling Engineering, SPE Texbook series, Vol. 2 Society of Petroleum Engineers, Richardson, TX, 1986 pp. 167, 153.

11. Kreyszig E., Advanced Engineering Mathematics, John Wiley and Sons, New York, 1983, p 375-376.

12. Craig Jr., J. T., Randal, B. V., "Directional Survey Calculation", Petroleum Engineering, March 1976. p. 38-54.

13. "The Rheology of Oil-Well Drilling Fluids" API Bul. 13D, American Petroleum Institute, Dallas,

TX, Aug. 1980 p.23.

APPENDIX A

Hydrodynamic Effects

The hydrodynamic effects are considered by calculating surge or swab pressures associated with drilling mud flow, caused by pipe movement in the borehole. The pipe is assumed close-ended. The calculation procedure is based on the theory of viscous drag for Power - Law fluids in boreholes [6] [7] [10] [13]. The inertial forces and transient effects are ignored. The calculation procedure includes:

1. Calculation of the mud clinging constant for the laminar flow [6],

$$C_c = \frac{\delta^2 - 2\delta^2 \ln\delta - 1}{2(1-\delta^2)\ln\delta} \qquad (12)$$

and for the turbulent flow [10],

$$C_c = \frac{\sqrt{\frac{\delta^4+\delta}{1+\delta}} - \delta^2}{1-\delta^2} \qquad (13)$$

where δ represents a ratio of the pipe diameter to the borehole diameter

2. Calculation of the equivalent displacement velocity [7],

$$v_{ae} = v_p \left(\frac{\delta^2}{1-\delta} + C_c \right) \qquad (14)$$

and the Reynolds number,

$$N_{Re} = 10.9 \cdot 10^4 \frac{\rho \, v_{ae}^{2-n}}{K} \left(\frac{d_B - d}{48} \cdot \frac{n}{2n+1} \right)^n \qquad (15)$$

3. Calculation of the critical values of the Reynolds number [13],

$$N_{Re1} = 3470 - 1370 \, n \qquad (16)$$

$$N_{Re2} = 4270 - 1370 \, n \qquad (17)$$

4. Decision whether flow pattern is laminar, transitional, or turbulent based on the logical elimination;

5. Calculation of the friction factor by solving the Dodge and Metzner equation

$$\sqrt{\frac{1}{f}} = \frac{4}{n^{0.75}} \log \left(N_{Re} \, f^{1-0.5n} \right) - \frac{0.395}{n^{1.2}} \qquad (18)$$

6. Calculation of the frictional pressure losses for the laminar flow

$$\frac{dp}{d\ell} = \frac{K}{14.4 \cdot 10^4 (d_B - d)} \left(\frac{48}{d_B - d} \cdot \frac{2n+1}{n} \right)^n \qquad (19)$$

or for the turbulent flow

$$\frac{dp}{d\ell} = \frac{f \, v_{ae}^2 \, \rho}{21.1 (d_B - d)} \qquad (20)$$

For the transitional flow both laminar and turbulent pressure losses are calculated and the larger value is chosen.

APPENDIX B

Effect of the Contact Surface

Consider a cylinder, size d, sliding in a pipe of the same size. When applying a normal force F_n, the resulting drag F_D can be found by integrating the small pressure area elements along the surface of contact. The result is

$$F_D = \frac{4}{\pi} \mu_B F_N \qquad (21)$$

In this scenario, the value of correction factor is $4/\pi$, which means that the actual drag is $4/\pi$ times larger than that for the flat contact surface. In our case, the pipe diameter is smaller than the borehole diameter. Thus

$$\frac{dF_D}{d\ell} = q_D = C_s \mu_B q_N \qquad (22)$$

The contact surface correction factor C_s in equ. (22), depends upon the contact angle γ.

The following simplifying assumptions are used to estimate the contact surface angle:

* Pipe deformation is elastic.
* The contact surface assumes a shape of the borehole.
* There is a linear relation between contact surface corrections factor and the contact angle.
* The contact surface is defined as shown in Fig. 20 i.e. it is controlled by the length of an arc between interception points of the two circles.

Initially, the circles are internally tangent then the smaller circle is shifted by the value

of pipe deformation Δd .

The approximate pipe deformation in the direction of the applied normal force is

$$\Delta d = \frac{\pi}{24E} q_N \frac{d}{t} \qquad (23)$$

The distributed normal force is given by Equ. (4). Let us consider Cartesian plane x-y normal to the pipe at point ℓ . The point (0.0) is assumed at the borehole centerline. The intersection points coordinates are

$$Y = 0.25 \left| \frac{d^2 - d_B^2 + (d_B - d + 2\Delta d)^2}{d_B - d + 2\Delta d} \right| \qquad (24)$$

$$X = 0.5 \sqrt{d^2 - 4Y^2} \qquad (25)$$

Finally, the contact angle is

$$\gamma = \left| \arctan \left(\frac{2X}{2Y - d_B + d} \right) \right| \qquad (26)$$

Appendix C

Unit Buoyant Weight Projections Equations using the Minimum Curvature Method to Interpolate the Trajectory Between Two Survey Points

The nomenclature referring exclusively to the minimum curvature method is identical to the one used by Taylor and Mason [8].

$$q_u(\ell) = \left| d\ell.Q\ [AZ.\sin\lambda + VZ.\cos\lambda] \right| \qquad (C1)$$

$$q_b(\ell) = d\ell.Q\ (AX.VY - VX.AY) \qquad (C2)$$

$$q_p(\ell) = Q\ [AZ.\cos\lambda - VZ.\sin\lambda] \qquad (C3)$$

where:

$$\lambda = \frac{(\ell_i - \ell_{i-1} - \ell).\beta}{\ell_i - \ell_{i-1}}$$

$$VX = \sin\alpha_{i-1}\ \cos\Theta_{i-1}$$

$$VY = \sin\alpha_{i-1}\ \sin\Theta_{i-1}$$

$$VZ = \cos\alpha_{i-1}$$

$$UX = \sin\alpha_i\ \ \sin\Theta_i$$

$$UZ = \cos\alpha_i$$

$$\beta = \arccos\ [UX.VX + UY.VY + UZ.VZ]$$

$$AX = \frac{UX - VX.\cos\beta}{\sin\beta}$$

$$AY = \frac{UY - VY.\cos\beta}{\sin\beta}$$

$$AZ = \frac{UZ - VZ.\cos\beta}{\sin\beta}$$

TABLE I

SIGN CONVENTION IN EQUATION 8

Borehole Section	Operation	Pipe Position	C_1	C_2
Build-up	Pulling	Upper	+1	-1
		Lower	+1	+1
	Running	Upper	+1	+1
		Lower	+1	-1
Drop-off	Pulling	Lower	-1	+1
	Running	Lower	-1	-1

TABLE 2
STUDY OF THE HYDRODYNAMIC FRICTION EFFECT

BOREHOLE FRICTION FACTOR USING 3-D MODEL WITHOUT HYDRODYNAMICS CONSIDERED*			
BIT WALK (DEG/100FT)	INCLINATION (DEG)		
	10	20	30
0	0.599	0.524	0.506
.4	0.599	0.524	0.506
.8	0.594	0.523	0.505
1.2	0.588	0.521	0.505
1.6	0.581	0.518	0.504
2.0	0.574	0.516	0.503
2.4	0.568	0.513	0.502

*3-D Model Value = 0.40

TABLE 3

FIELD STUDY SUMMARY AND STATISTICS

Well No.	Remarks	Model	$\bar{\mu}_B$ Run. In	$\bar{\mu}_B$ Pul.Out	Coef. of Def.	Reg.Coef. 10^6 Ft^{-1}	Stand. Dev.
1	Casing	3-D	0.43	0.27	0.036	5	0.045
		2-D	0.44	0.28	0.078	7	0.045
	Drill-string	3-D	–	0.21	–	–	–
		2-D	–	0.24	–	–	–
	Core Guns	3-D	0.27	0.30	–	–	–
		2-D	0.29	0.33	–	–	–
2	Casing	3-D	0.43	–	0.007	2	0.050
		2-D	0.46	–	0.006	-2	0.051
	Drill-string	3-D	–	0.25	–	–	–
		2-D	–	0.28	–	–	–
3	Casing	3-D	0.83	0.44	0.016	12	0.183
		2-D	1.14	0.64	0.025	-17	0.214
4	Casing	3-D	0.38	–	–	–	–
		2-D	0.47	–	–	–	–

TABLE 4

WELL # 1 - CASING

COMPARISON OF THE MODELS USING FIELD DATA

DATA USED: .MUD DENSITY: 10.80 LBF/GAL
.CONSISTENCY INDEX: 124.9 EQCP
.FLOW-BEHAVIOR INDEX: 0.781
.BIT DIAMETER: 9.875 IN
.PREVIOUS CASING DIAMETER: 10.750 IN
.PREVIOUS CASING DEPTH: 3210. FT
.STRING BREAK DOWN:

DEPTH (FT)	OD (IN)	ID (IN)	WEIGHT (LB/FT)	REMARK
5390.	7.625	6.875	29.70	LTC
10267.	7.625	6.640	33.70	LTC
11232.	7.625	6.500	39.00	LTC

RESULTS:

INPUT DATA				BOR. FRIC. FACTOR	
CASING SHOE DEPTH (FT)	MEASURED HOOK LOAD (LBF)	MODE	PIPE VELOC. (FT/S)	3-D MODEL	2-D MODEL
4579.	108800.	IN	1.7	0.36	0.38
4619.	109000.	IN	2.0	0.36	0.37
4659.	108400.	IN	2.0	0.41	0.42
4699.	114000.	IN	0.5	0.31	0.32
4897.	113100.	IN	2.1	0.34	0.36
4897.	144100.	UP	1.0	0.25	0.26
5135.	113500.	IN	2.0	0.44	0.45
5175.	114000.	IN	1.5	0.47	0.48
5294.	114200.	IN	2.0	0.47	0.48
5371.	115100.	IN	2.0	0.47	0.48
5407.	113900.	IN	2.0	0.52	0.53
5605.	115300.	IN	2.0	0.54	0.55
5882.	128400.	IN	0.1	0.42	0.43
5924.	130000.	IN	0.1	0.40	0.41
5924.	174900.	UP	0.7	0.29	0.30
5924.	127000.	IN	0.5	0.43	0.44
5964.	125900.	IN	2.0	0.38	0.39
6385.	133800.	IN	0.5	0.39	0.41
6912.	135800.	IN	0.6	0.46	0.47
7079.	134100.	IN	2.2	0.43	0.44
7157.	136800.	IN	0.7	0.47	0.49

EQCP = $DYNE.S^N/100.CM^2$

TABLE 5

WELL # 1 - DRILLSTRING

COMPARISON OF THE MODELS USING FIELD DATA

DATA USED: .MUD DENSITY: 10.80 LBF/GAL
.CONSISTENCY INDEX: 124.9 EQCP
.FLOW-BEHAVIOR INDEX: 0.781
.BIT DIAMETER: 9.875 IN
.PREVIOUS CASING DIAMETER: 10.750 IN
.PREVIOUS CASING DEPTH: 3210. FT
.STRING BREAK DOWN

DEPTH (FT)	OD (IN)	ID (IN)	WEIGHT (LB/FT)	REMARK
9646.	5.000	4.276	21.40	PIPE
11166.	5.000	3.000	49.30	HWPIPE
11270.	7.000	2.813	110.00	BHA

RESULTS:

INPUT DATA				BOR. FRIC. FACTOR	
CASING SHOE DEPTH (FT)	MEASURED HOOK LOAD (LBF)	MODE	PIPE VELOC. (FT/S)	3-D MODEL	2-D MODEL
11250.	269000.	UP	4.0	0.21	0.24

EQCP = $DYNE.S^N/100.CM^2$

TABLE 6

WELL # 1 - CORE GUNS

COMPARISON OF THE MODELS USING FIELD DATA

DATA USED: .MUD DENSITY: 10.80 LBF/GAL
.CONSISTENCY INDEX: 124.9 EQCP
.FLOW-BEHAVIOR INDEX: 0.781
.BIT DIAMETER: 9.875 IN
.PREVIOUS CASING DIAMETER: 10.750 IN
.PREVIOUS CASING DEPTH: 0. FT
.STRING BREAK DOWN:

DEPTH (FT)	OD (IN)	ID (IN)	WEIGHT (LB/FT)	REMARK
10600.	0.500	0.0	0.35	CABLE
10630.	3.000	0.0	16.67	C.GUNS

RESULTS:

INPUT DATA				BOR. FRIC. FACTOR	
CASING SHOE DEPTH (FT)	MEASURED HOOK LOAD (LBF)	MODE	CABLE VELOC. (FT/S)	3-D MODEL	2-D MODEL
10070.	4200.	UP	0.7	0.30	0.32
10200.	4400.	UP	0.7	0.32	0.35
10260.	2400.	IN	0.7	0.23	0.24
10260.	4100.	UP	0.7	0.25	0.28
10270.	2200.	IN	0.7	0.32	0.34
10270.	4400.	UP	0.7	0.31	0.34
10350.	4500.	UP	0.7	0.32	0.35

EQCP = $DYNE.S^N/100.CM^2$

TABLE 7

WELL # 2 - CASING

COMPARISON OF THE MODELS USING FIELD DATA

DATA USED: .MUD DENSITY: 10.70 LBF/GAL
.CONSISTENCY INDEX: 300.9 EQCP
.FLOW-BEHAVIOR INDEX: 0.619
.BIT DIAMETER: 9.875 IN
.PREVIOUS CASING DIAMETER: 10.750 IN
.PREVIOUS CASING DEPTH: 2000. FT
.STRING BREAK DOWN:

DEPTH (FT)	OD (IN)	ID (IN)	WEIGHT (LB/FT)	REMARK
315.	7.000	6.276	26.00	LTC
5005.	7.000	6.366	23.00	LTC
5912.	7.000	6.366	23.00	LTC
9610.	7.000	6.276	26.00	LTC

RESULTS:

INPUT DATA				BOR. FRIC. FACTOR	
CASING SHOE DEPTH (FT)	MEASURED HOOK LOAD (LBF)	MODE	PIPE VELOC. (FT/S)	3-D MODEL	2-D MODEL
2981.	60500.	IN	2.0	0.26	0.31
3140.	61500.	IN	2.0	0.43	0.49
3576.	67000.	IN	2.0	0.34	0.38
4060.	69500.	IN	2.0	0.43	0.48
4144.	69000.	IN	2.0	0.48	0.53
4515.	73500.	IN	2.0	0.38	0.41
4686.	72500.	IN	2.0	0.45	0.48
4905.	72500.	IN	2.0	0.47	0.51
5197.	74000.	IN	2.0	0.45	0.48
5719.	77000.	IN	2.0	0.42	0.45
5895.	75500.	IN	2.0	0.47	0.49
6108.	78000.	IN	2.0	0.43	0.45
6286.	75500.	IN	2.0	0.49	0.52
6628.	81000.	IN	2.0	0.41	0.43
6801.	78000.	IN	2.0	0.47	0.50
7024.	80500.	IN	2.0	0.44	0.46
7202.	85000.	IN	2.0	0.38	0.40
7556.	85000.	IN	2.0	0.41	0.43
7732.	85000.	IN	2.0	0.42	0.45
7909.	86000.	IN	2.0	0.42	0.44
8081.	87500.	IN	2.0	0.41	0.44
8258.	88000.	IN	2.0	0.42	0.44
8432.	88000.	IN	2.0	0.43	0.46
8592.	91500.	IN	2.0	0.41	0.43
8808.	92000.	IN	2.0	0.42	0.44
8985.	91000.	IN	2.0	0.44	0.47
9161.	91000.	IN	2.0	0.46	0.48
9205.	92500.	IN	2.0	0.44	0.47

EQCP = $DYNE.S^N/100.CM^2$

TABLE 8

WELL # 2 - DRILLSTRING

COMPARISON OF THE MODELS USING FIELD DATA

DATA USED: .MUD DENSITY: 10.70 LBF/GAL
.CONSISTENCY INDEX: 300.9 EQCP
.FLOW-BEHAVIOR INDEX: 0.619
.BIT DIAMETER: 9.875 IN
.PREVIOUS CASING DIAMETER: 10.750 IN
.PREVIOUS CASING DEPTH: 2000. FT
.STRING BREAK DOWN:

DEPTH (FT)	OD (IN)	ID (IN)	WEIGHT (LB/FT)	REMARK
4103.	4.500	3.640	22.10	PIPE
9337.	4.500	3.826	18.40	PIPE
9610.	7.000	2.813	110.00	BHA

RESULTS:

INPUT DATA				BOR. FRIC. FACTOR	
CASING SHOE DEPTH (FT)	MEASURED HOOK LOAD (LBF)	MODE	PIPE VELOC. (FT/S)	3-D MODEL	2-D MODEL
9610.	194000.	UP	2.0	0.25	0.28

EQCP = $DYNE.S^N/100.CM^2$

TABLE 9

WELL # 3 - CASING

COMPARISON OF THE MODELS USING FIELD DATA

DATA USED: .MUD DENSITY: 9.30 LBF/GAL
.CONSISTENCY INDEX: 125.7 EQCP
.FLOW-BEHAVIOR INDEX: 0.688
.BIT DIAMETER: 9.500 IN
.PREVIOUS CASING DIAMETER: 10.750 IN
.PREVIOUS CASING DEPTH: 3800. FT
.STRING BREAK DOWN:

DEPTH (FT)	OD (IN)	ID (IN)	WEIGHT (LB/FT)	REMARK
11538.	7.625	6.875	29.70	LTC

RESULTS:

INPUT DATA				BOR. FRIC. FACTOR	
CASING SHOE DEPTH (FT)	MEASURED HOOK LOAD (LBF)	MODE	PIPE VELOC. (FT/S)	3-D MODEL	2-D MODEL
5922.	132000.	IN	2.0	1.03	1.47
6004.	135000.	IN	2.0	0.76	1.16
6174.	137000.	IN	2.0	0.91	1.30
6257.	140000.	IN	2.0	0.69	1.05
6300.	139000.	IN	2.0	0.93	1.31
6717.	148000.	IN	2.0	0.72	1.04
7093.	154000.	IN	2.0	0.75	1.05
7799.	166000.	IN	2.0	0.72	1.00
7927.	174000.	IN	2.0	0.39	0.63
9400.	192000.	IN	2.0	0.68	0.93
9400.	277000.	UP	2.0	0.38	0.58
9442.	192000.	IN	2.0	0.70	0.96
9656.	192000.	IN	2.0	0.81	1.08
9741.	195000.	IN	2.0	0.75	1.01
9741.	294000.	UP	2.0	0.49	0.70
9828.	192000.	IN	2.0	0.89	1.17
9911.	192000.	IN	2.0	0.93	1.21
10039.	195000.	IN	2.0	0.88	1.16
10039.	302000.	UP	2.0	0.45	0.65
10079.	194000.	IN	2.0	0.93	1.22
10209.	194000.	IN	2.0	0.98	1.27
10380.	198000.	IN	2.0	0.93	1.20
10508.	203000.	IN	2.0	0.83	1.09
10593.	203000.	IN	2.0	0.86	1.13
10674.	203000.	IN	2.0	0.89	1.16
10761.	206000.	IN	2.0	0.84	1.10
10845.	206000.	IN	2.0	0.87	1.13
10974.	211000.	IN	2.0	0.79	1.04
11101.	209000.	IN	2.0	0.88	1.14
11189.	213000.	IN	2.0	0.81	1.06

EQCP = $DYNE.S^N/100.CM^2$

TABLE 10

WELL # 4 - CASING

COMPARISON OF THE MODELS USING FIELD DATA

DATA USED: .MUD DENSITY: 10.20 LBF/GAL
.CONSISTENCY INDEX: 143.4 EQCP
.FLOW-BEHAVIOR INDEX: 0.726
.BIT DIAMETER: 9.875 IN
.PREVIOUS CASING DIAMETER: 10.750 IN
.PREVIOUS CASING DEPTH: 3334. FT
.STRING BREAK DOWN:

DEPTH (FT)	OD (IN)	ID (IN)	WEIGHT (LB/FT)	REMARK
8967.	7.625	6.625	39.00	LTC

RESULTS:

INPUT DATA				BOR. FRIC. FACTOR	
CASING SHOE DEPTH (FT)	MEASURED HOOK LOAD (LBF)	MODE	PIPE VELOC. (FT/S)	3-D MODEL	2-D MODEL
8967.	160000.	IN	2.0	0.38	0.40

EQCP = $DYNE.S^N/100.CM^2$

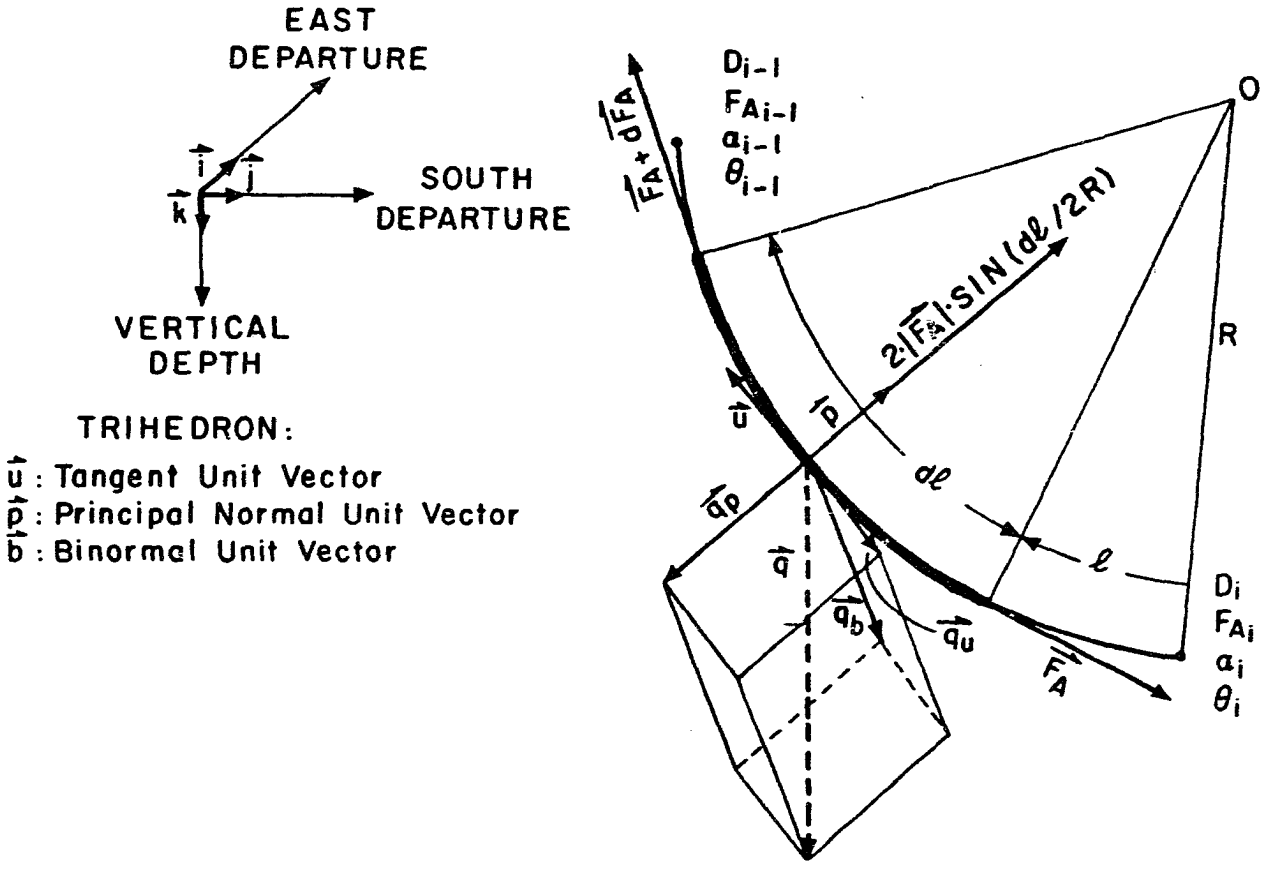

1. Forces Acting on a Small Casing Element Within the Build-up Section.

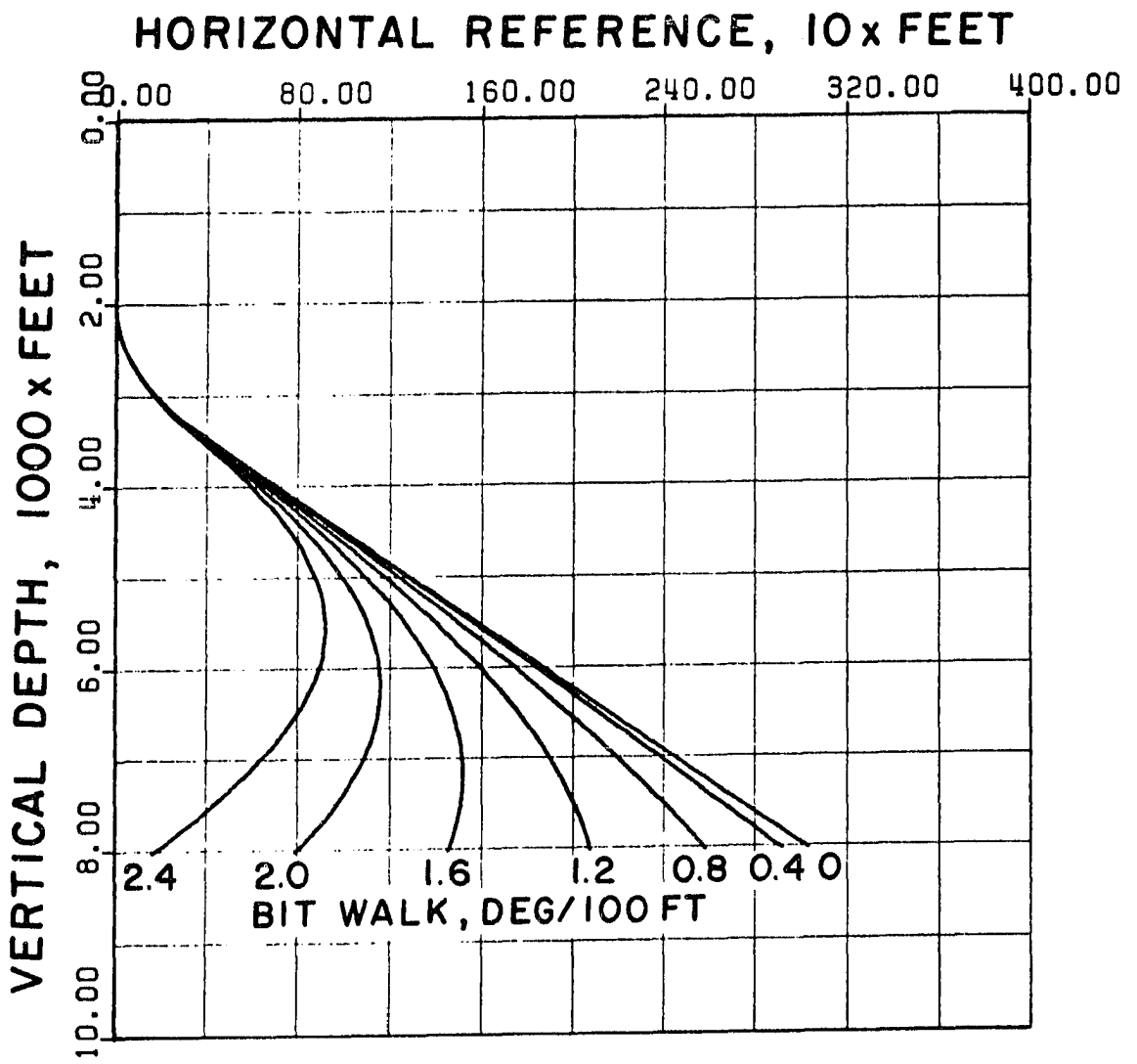

2. Vertical Section of the Computer-Generated Well Trajectories.

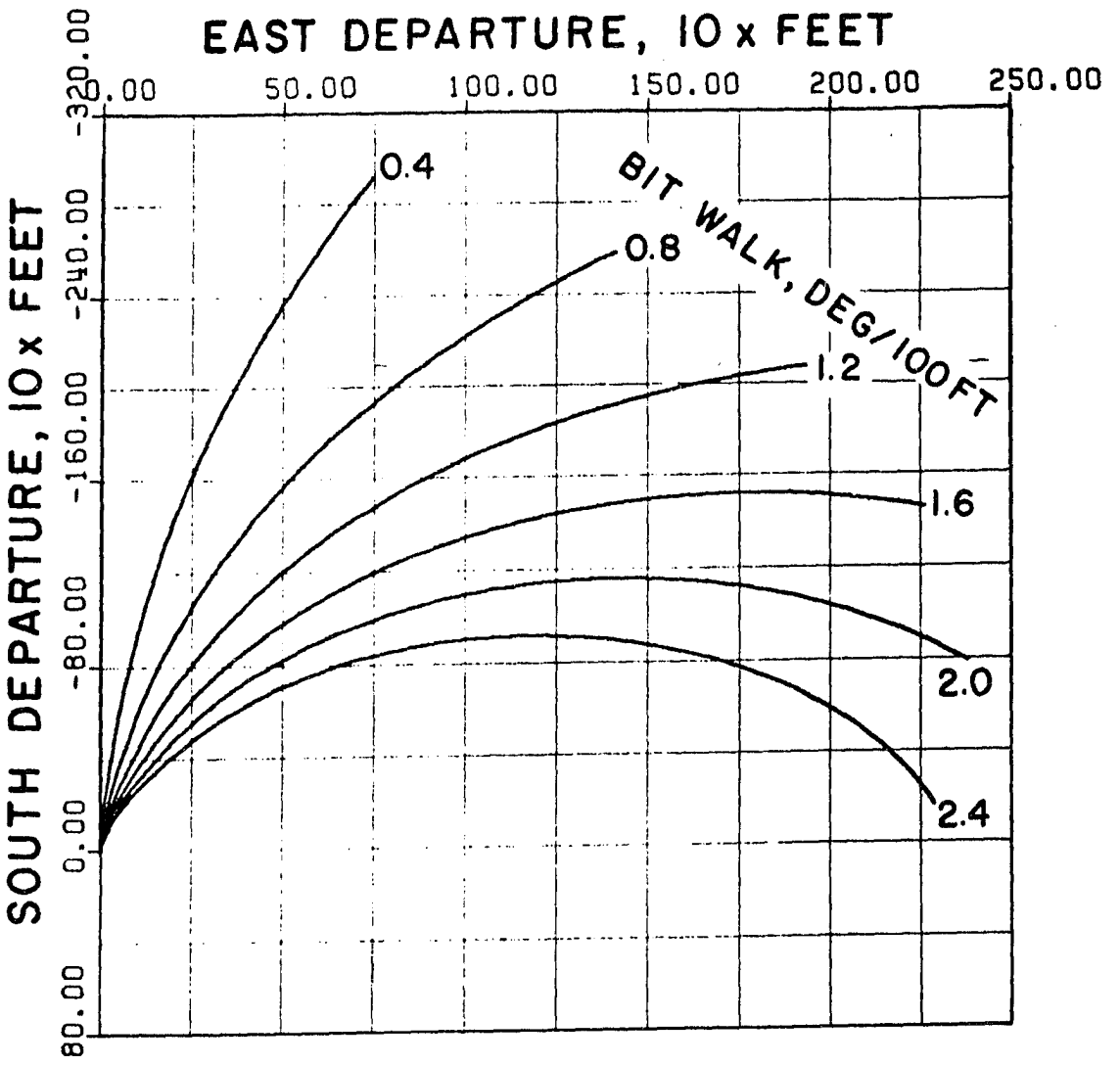

3. Horizontal Section of the Computer Generated Well Trajectories.

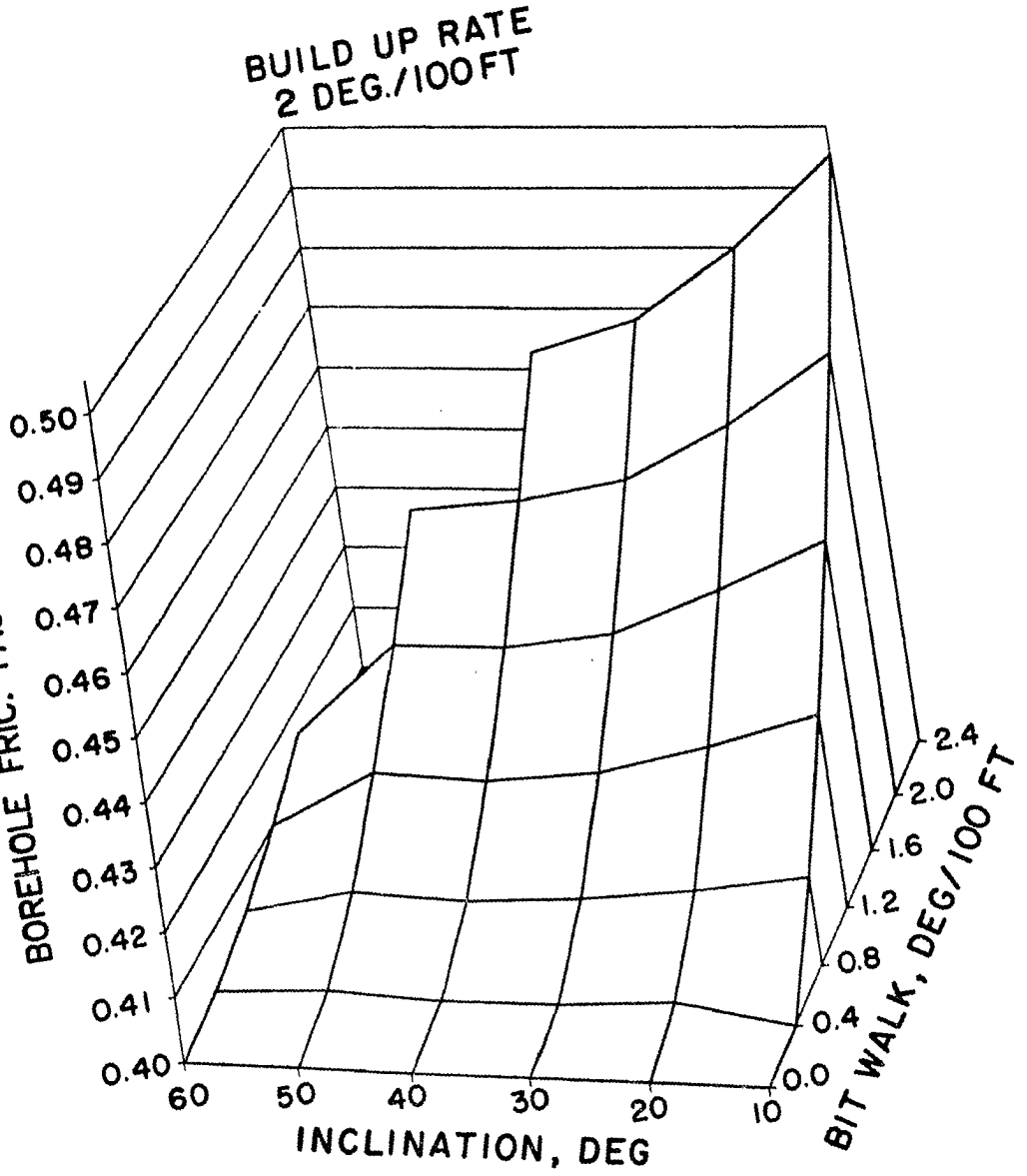

4. Sensitivity of the 2-D Model to Bitwalk Rates and Slant Hole Inclinations.

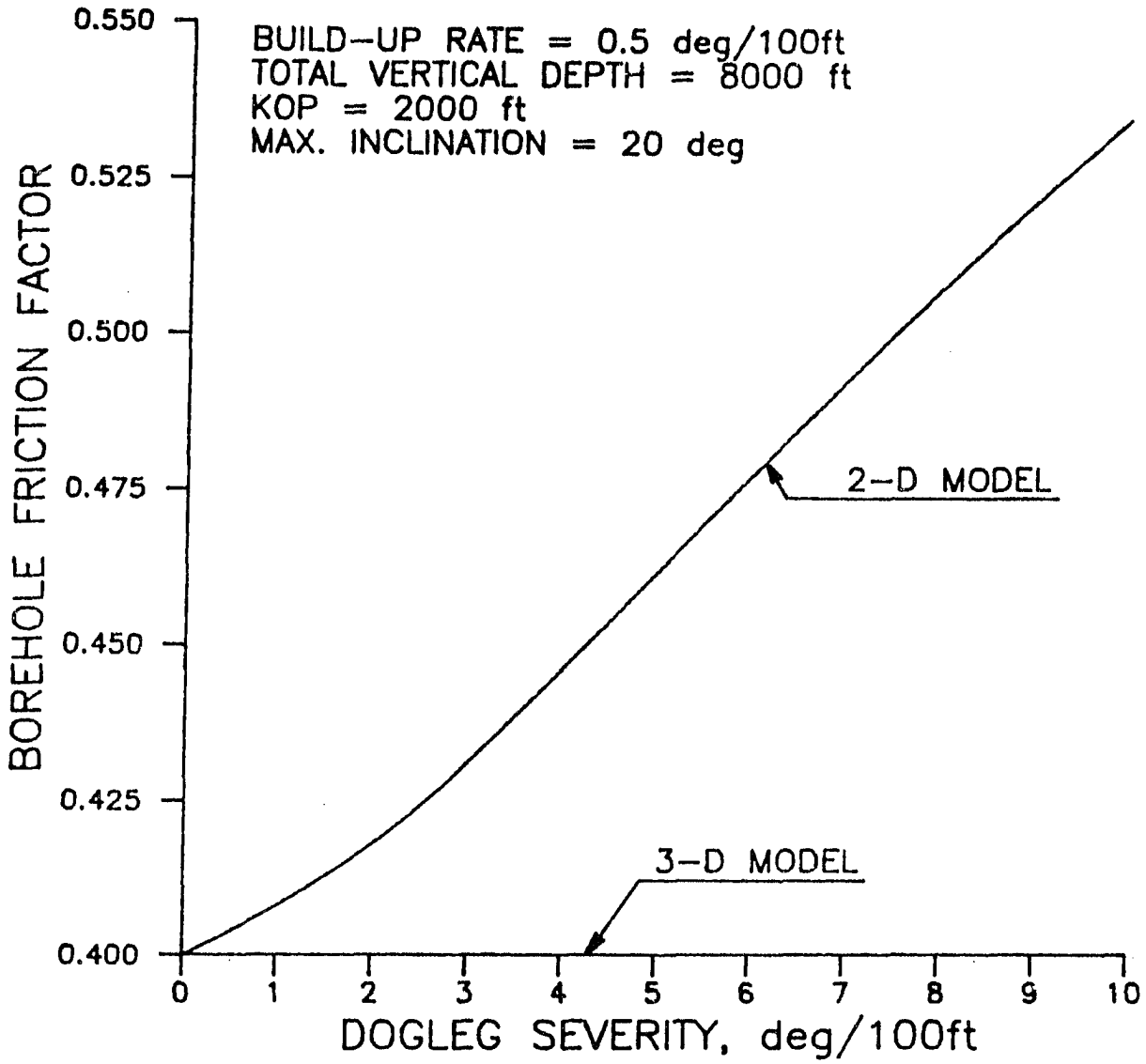

5. Sensitivity of the 2-D Model to Horizontal Doglegs.

6. Rig Locations Used in Field Study.

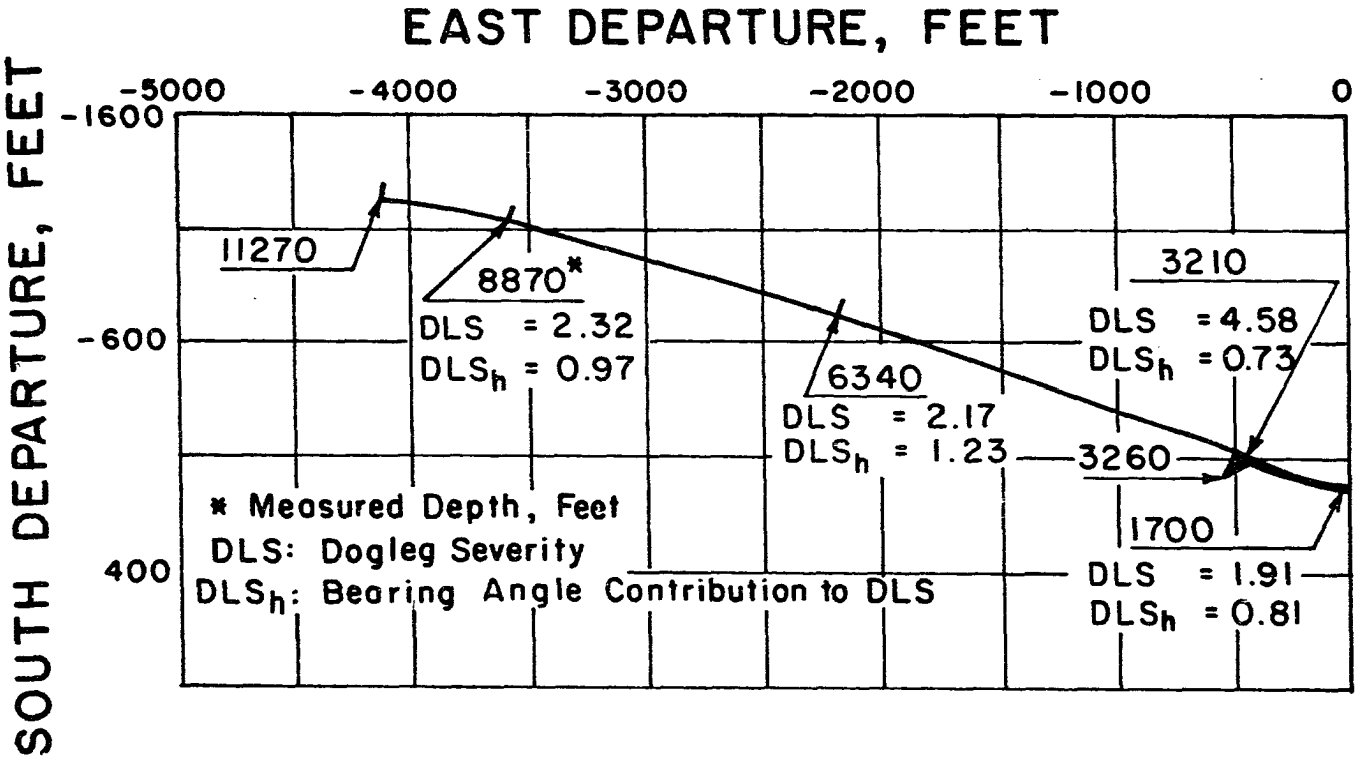

7. Well 1 - Horizontal Section and Directional Survey Data.

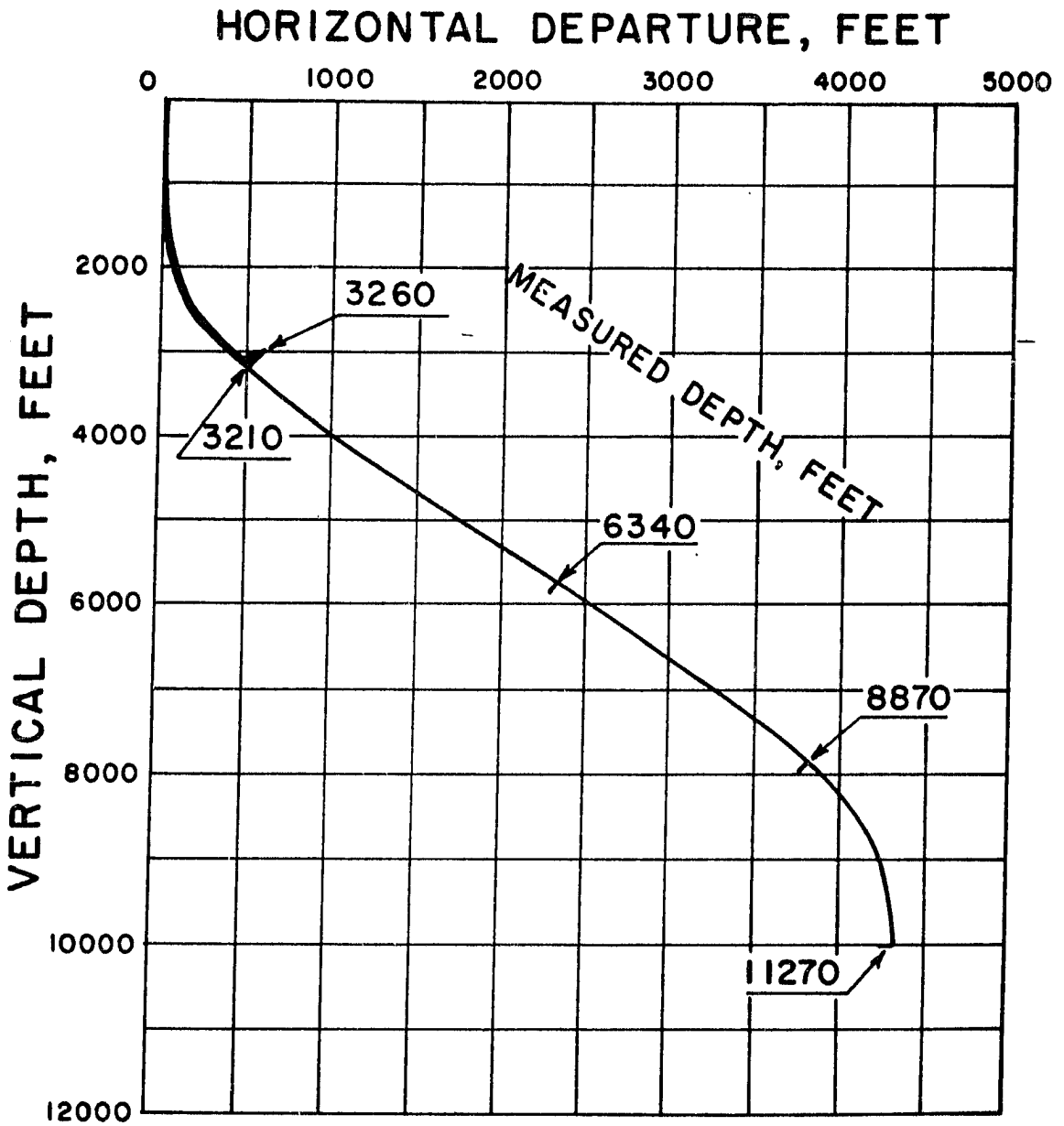

8. Well 1 - Vertical Section and Measured Depths.

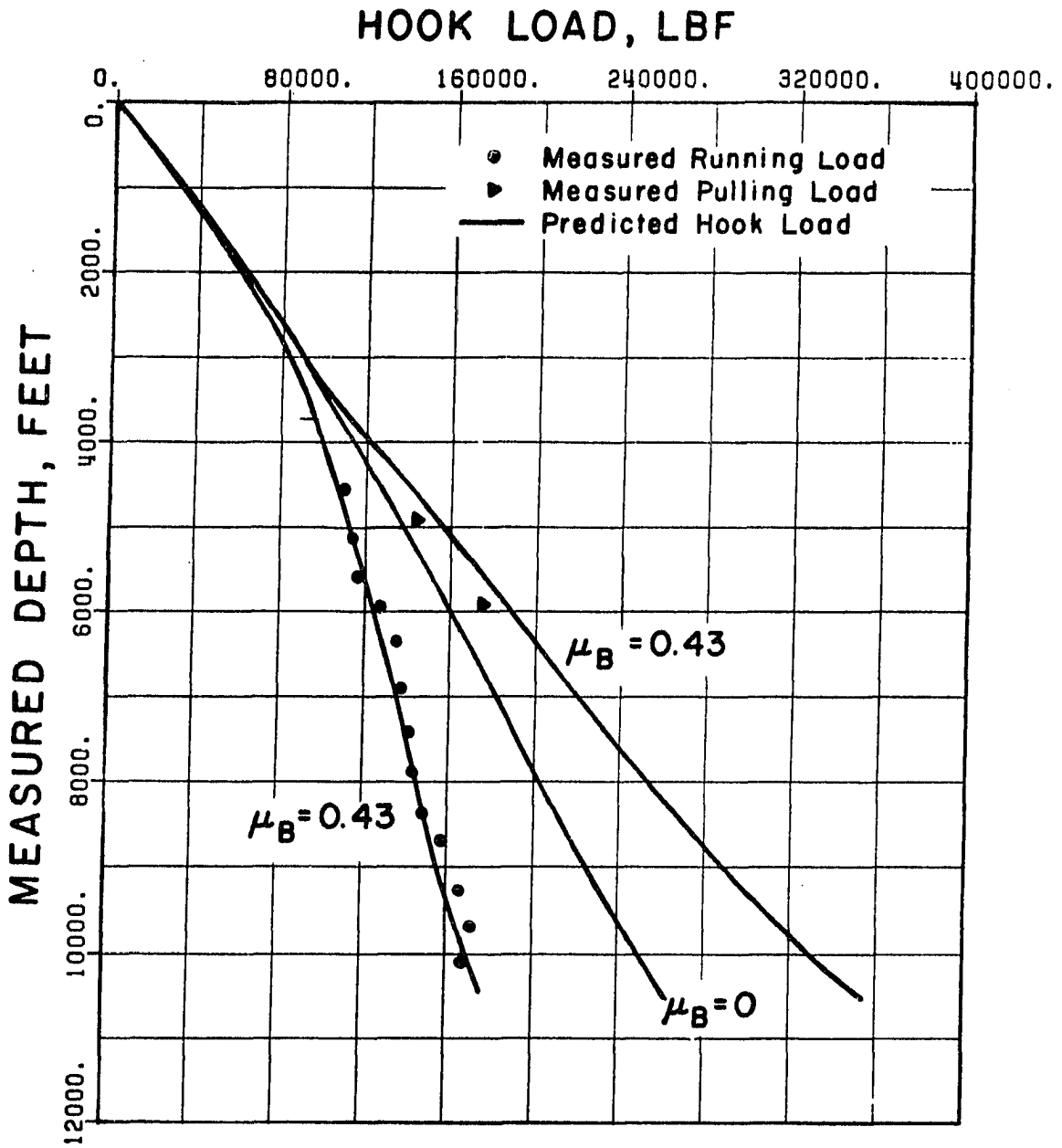

9. Well 1 - Measured and Predicted Hook Loads for the Casing Run.

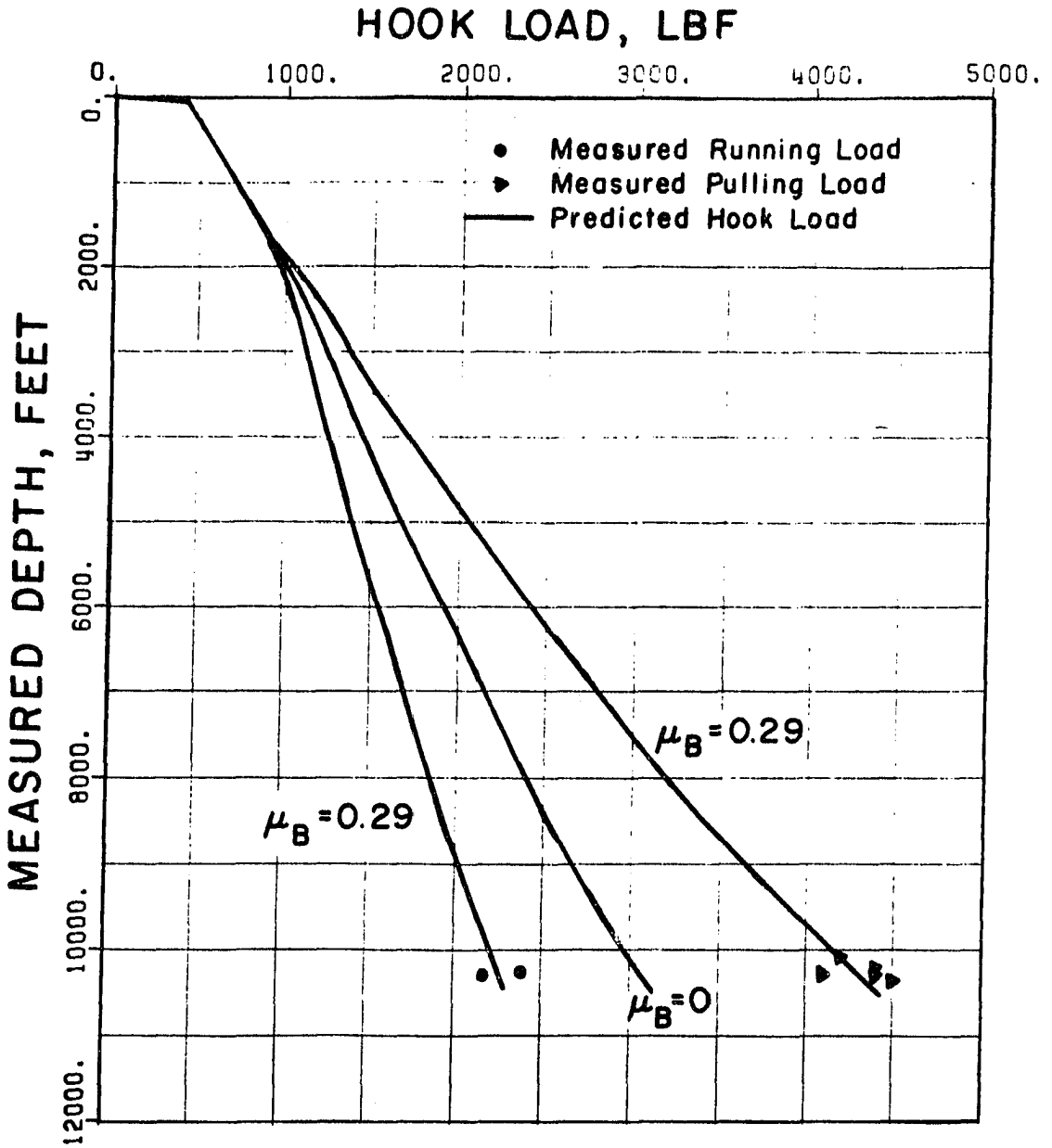

10.Well 1 - Measured and Predicted Hook Loads for the Core Guns Run.

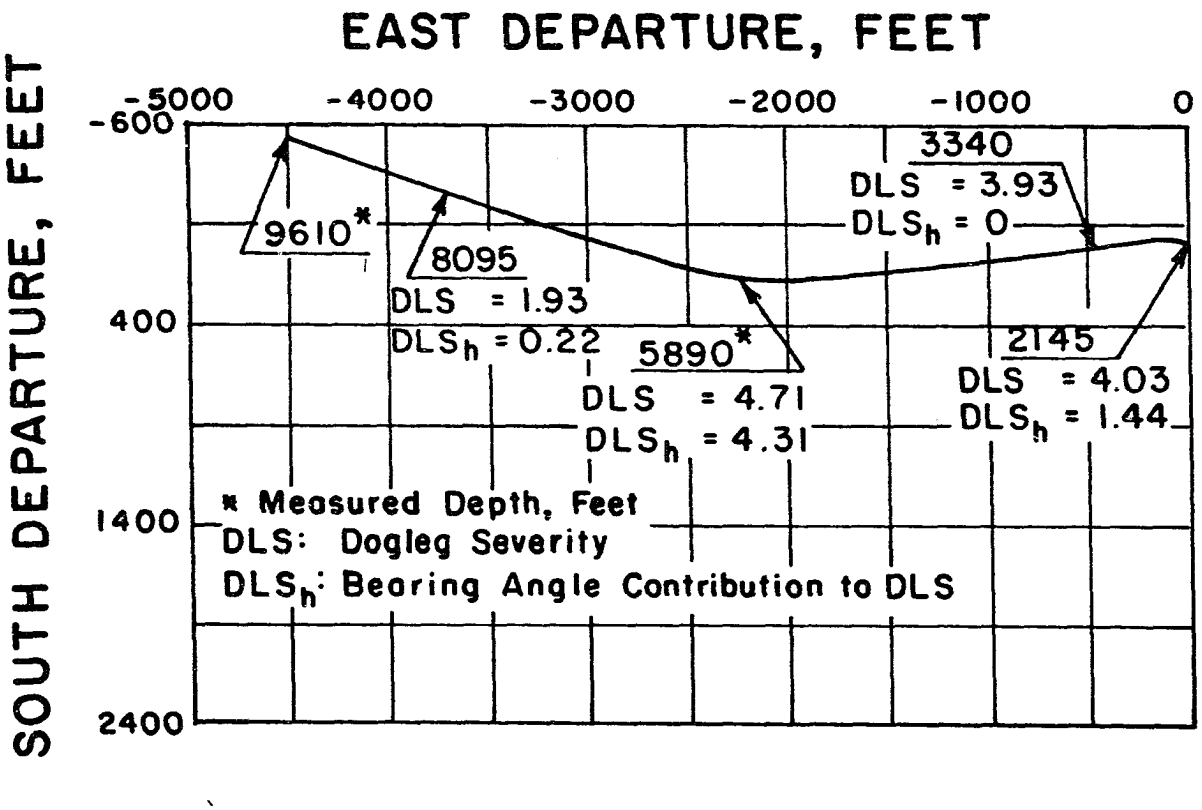

11.Well 2 - Horizontal Section and Directional Survey Data.

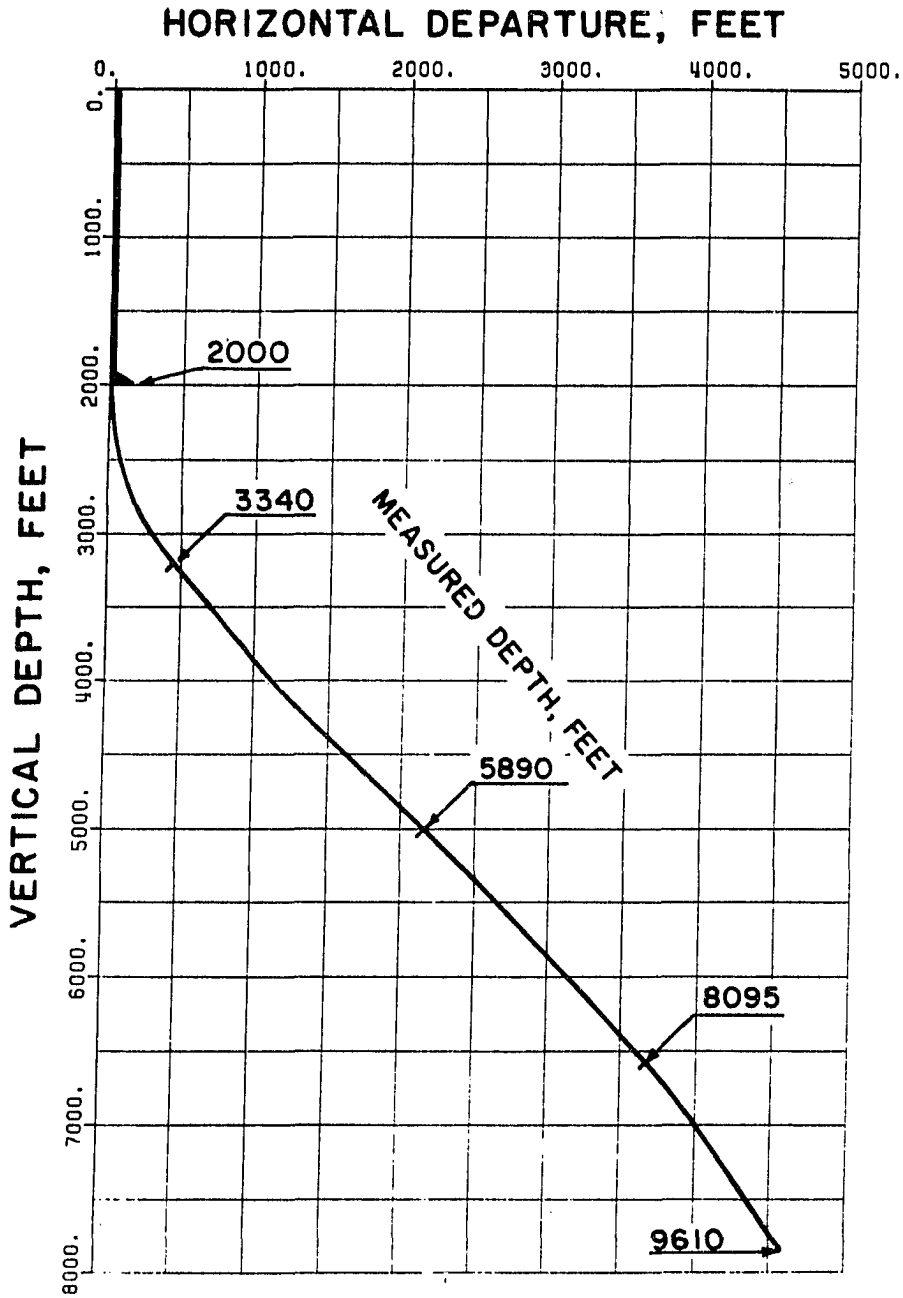

12.Well 2 - Vertical Section and Measured Depths.

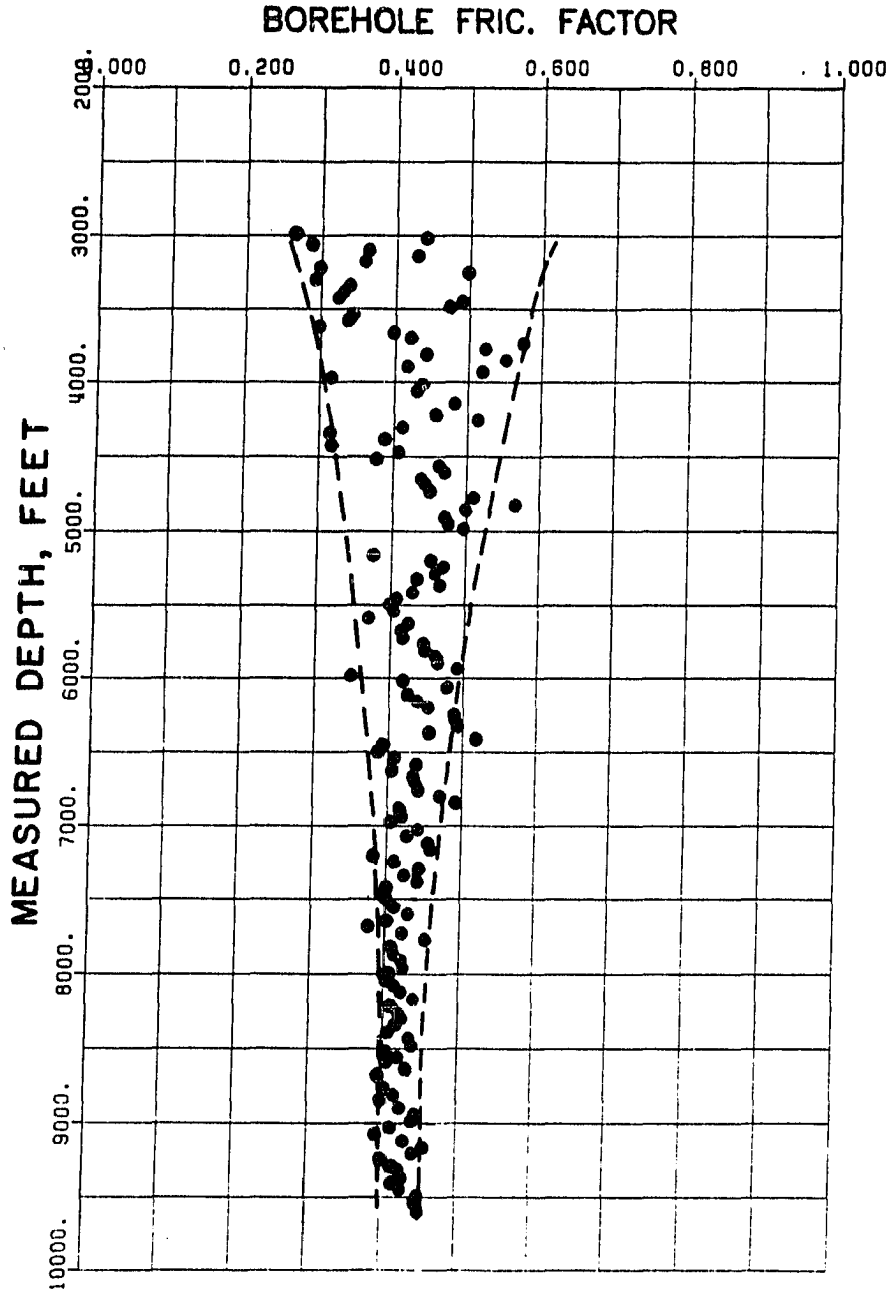

13.Well 2 - Stability of the Borehole Friction Factor.

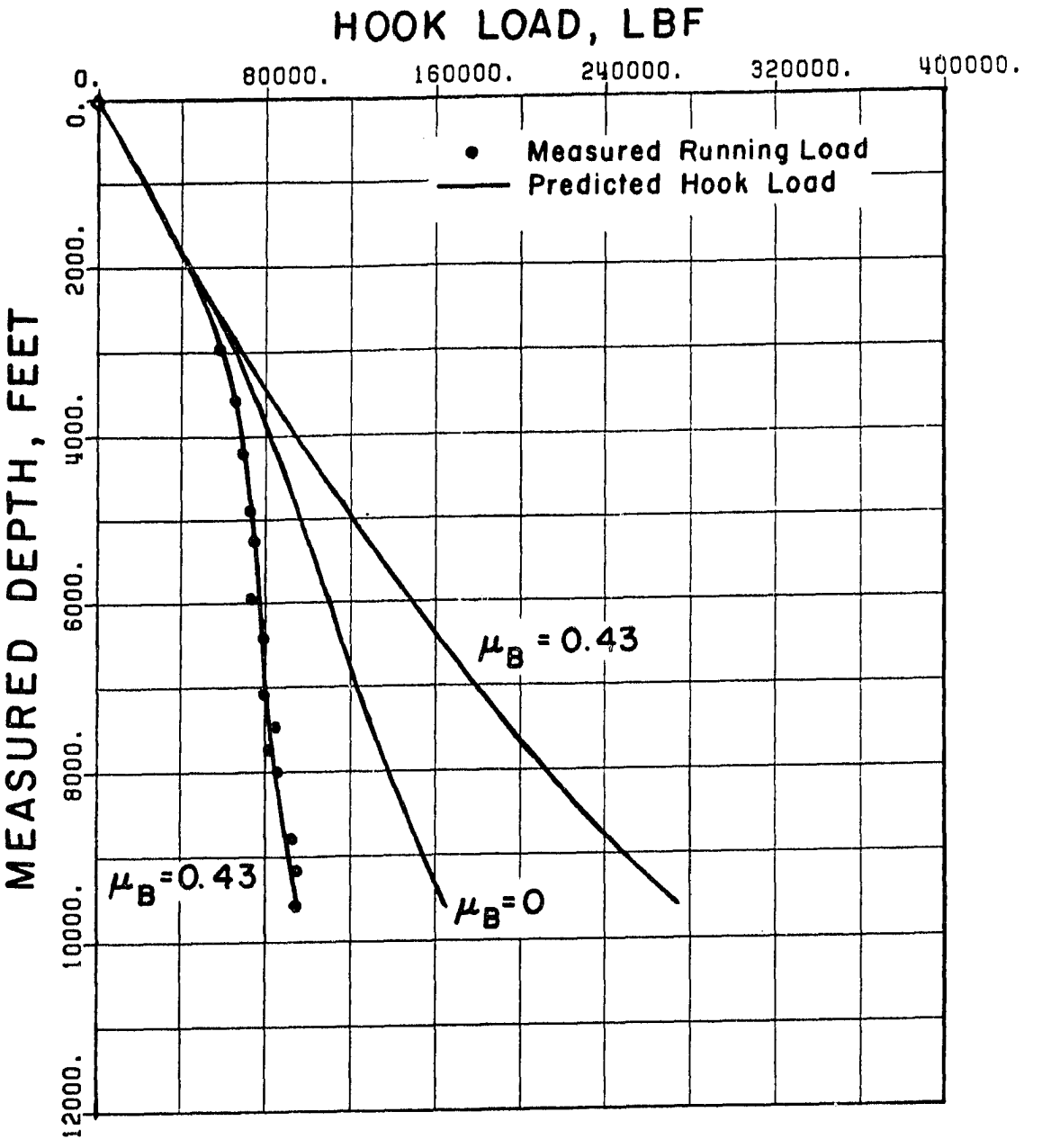

14.Well 2 - Measured and Predicted Hook Loads for the Casing Run.

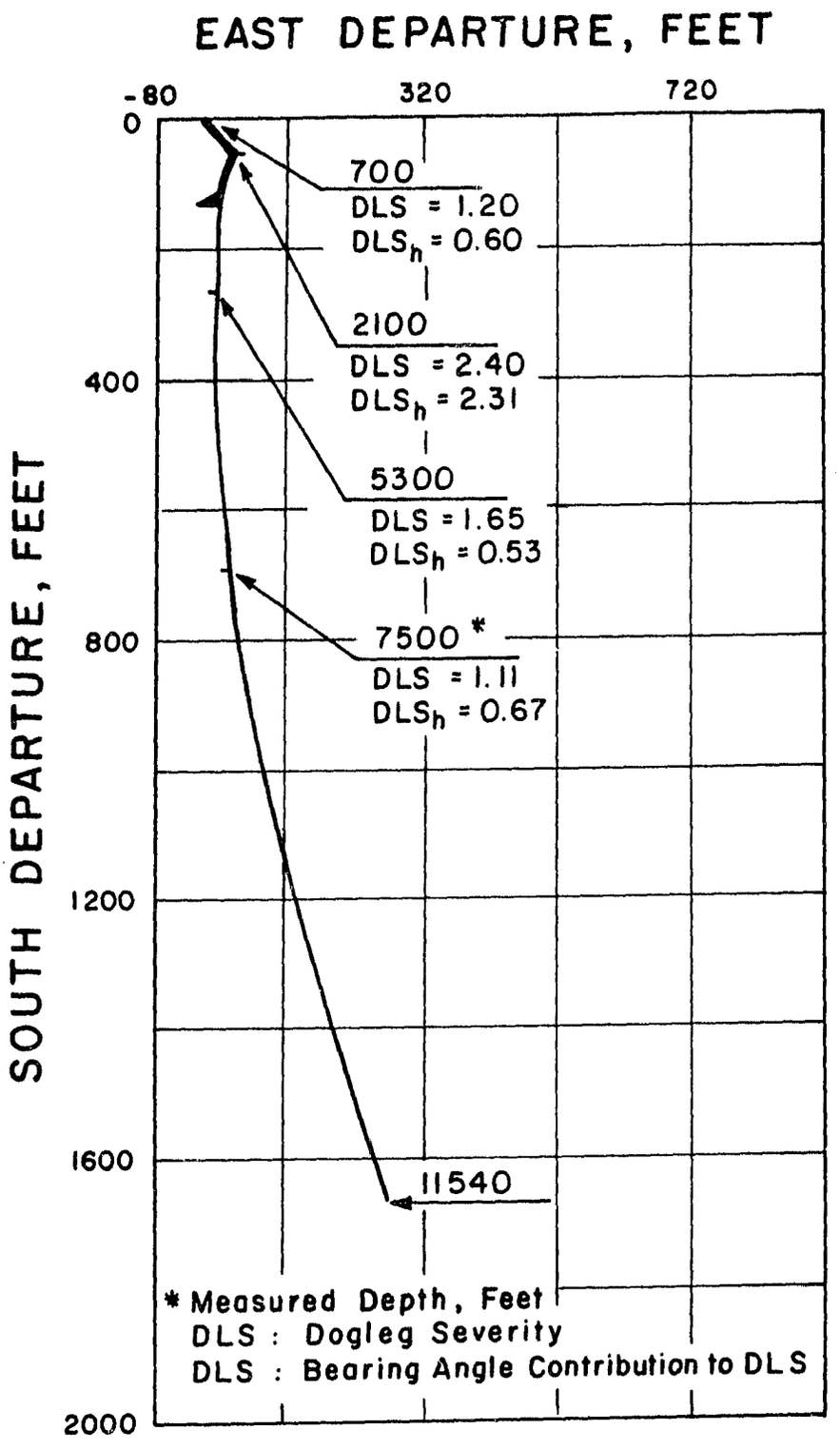

15.Well 3 - Horizontal Section and Directional Survey Data.

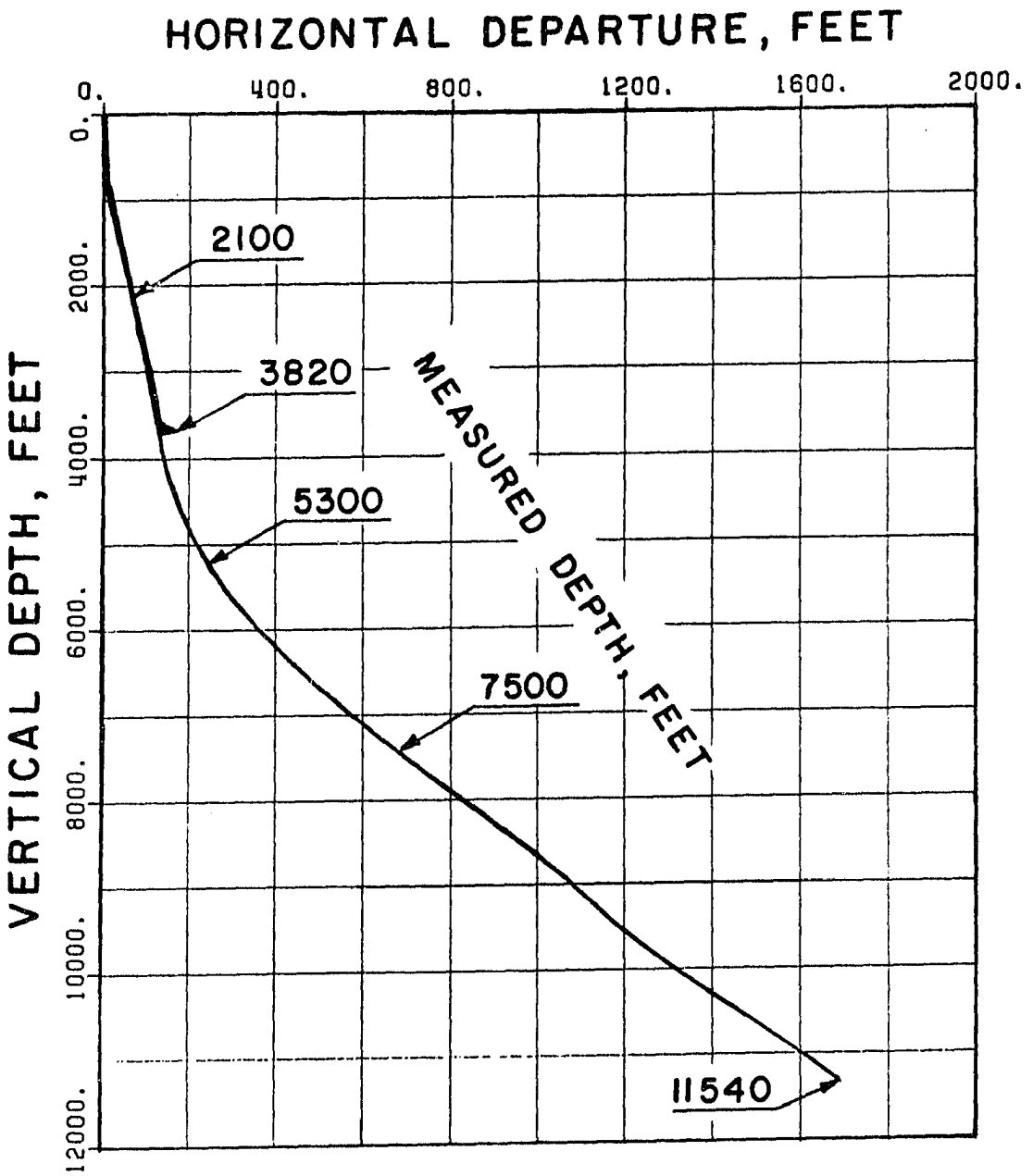

16.Well 3 - Vertical Section and Measured Depths.

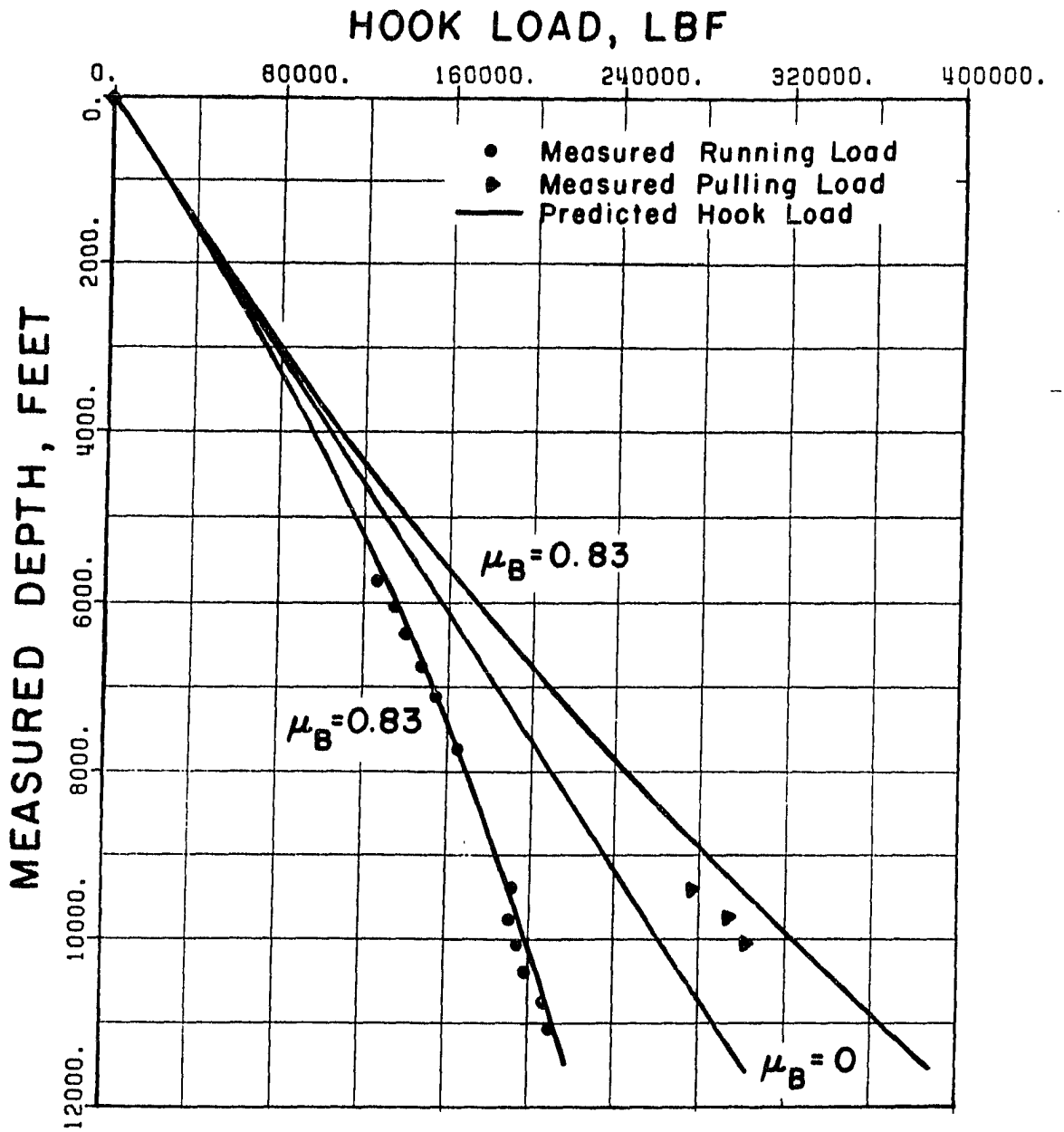

17.Well 3 - Measured and Predicted Hook Loads for the Casing Run.

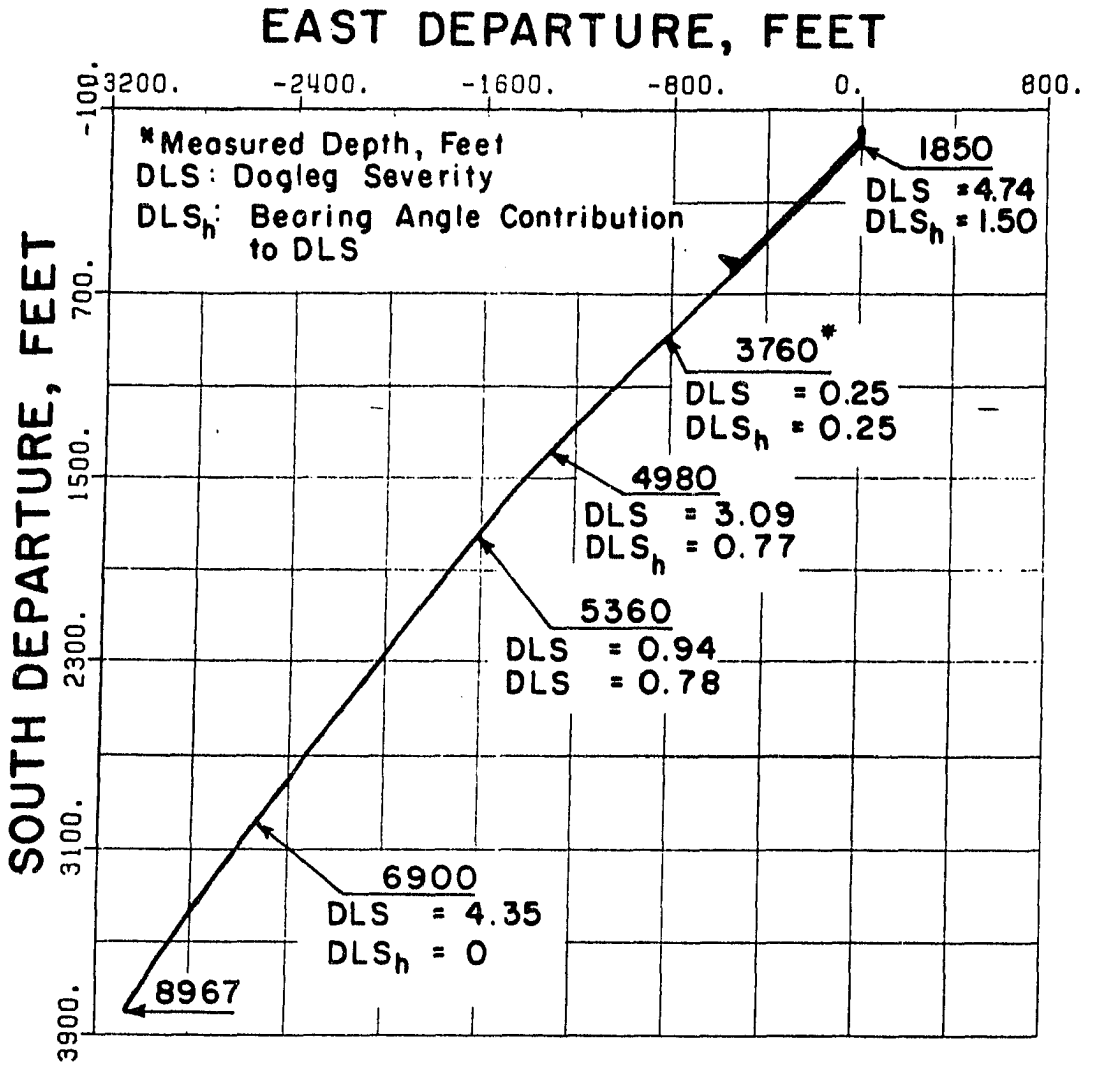

18.Well 4 - Horizontal Section and Directional Survey Data.

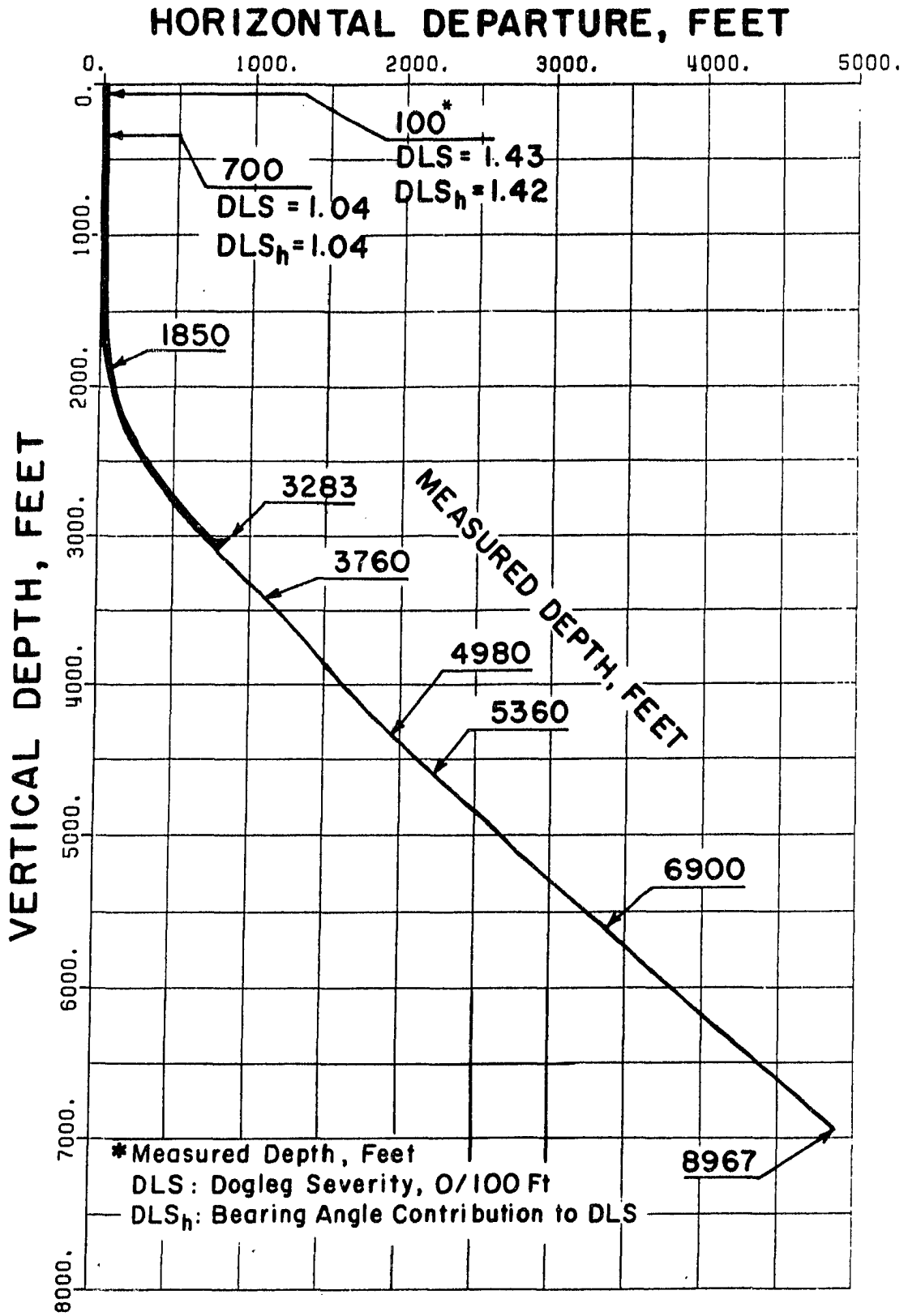

19.Well 4 - Vertical Section, Measured Depths and Directional Survey Data.

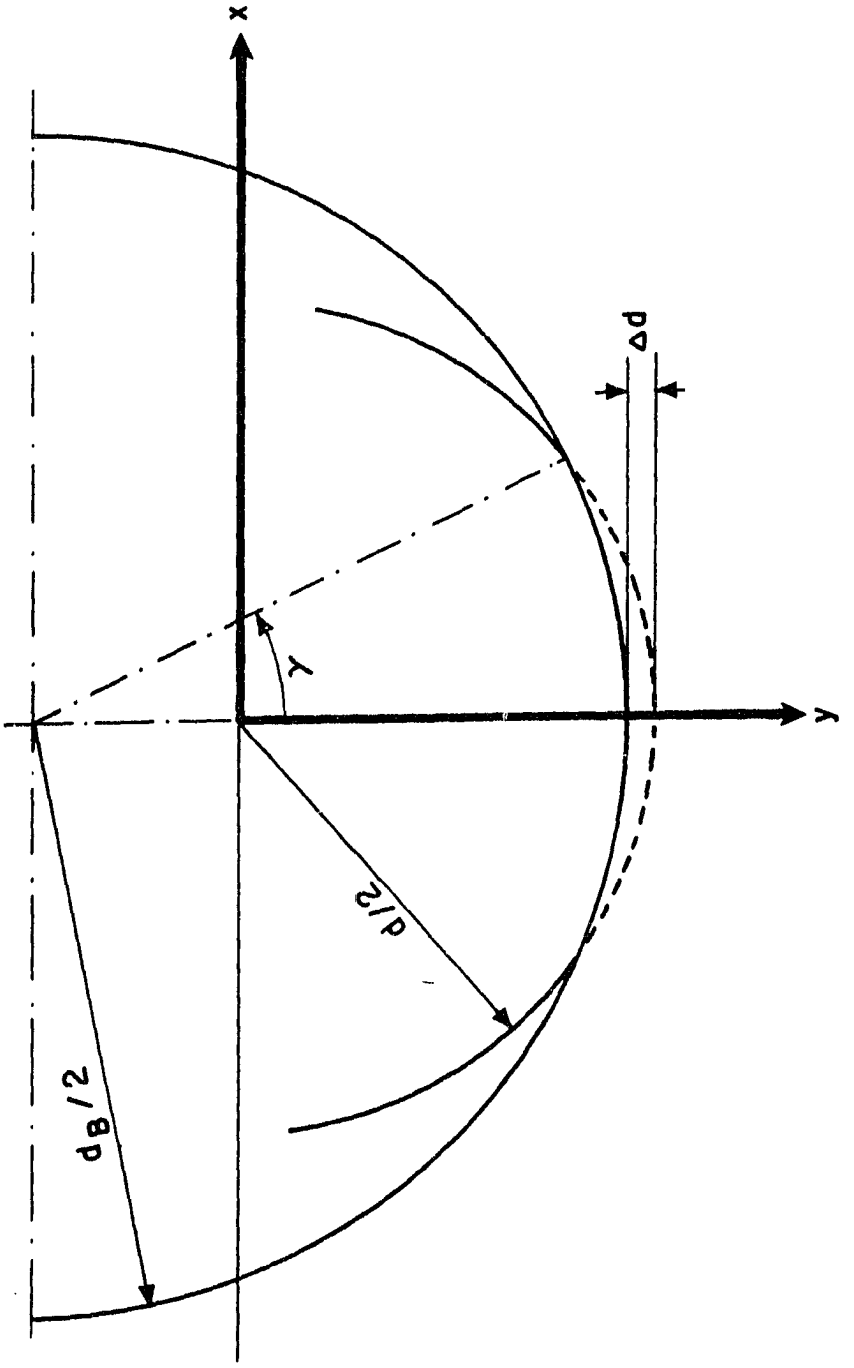

20. Surface of Contact Between Borehole and Pipe.

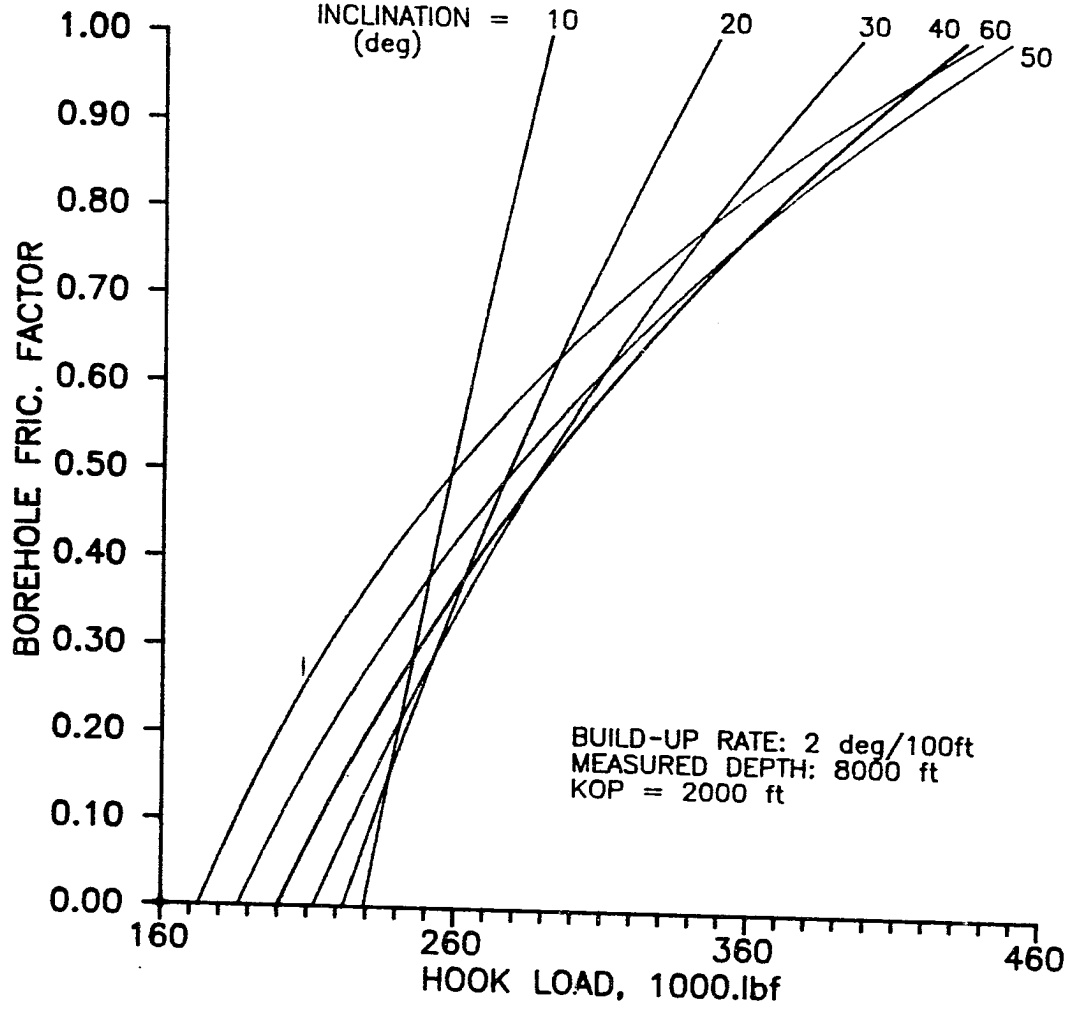

21. Sensitivity of Borehole Friction Factor to Hook Loads and Well Inclinations.

CHAPTER III

PREDICTION OF CASING HOOK LOADS FOR PLANNED WELLS

INTRODUCTION

The surface running loads of a casing string are predicted using the planned trajectory of the directional well. The results are compared with actual field data recorded offshore Louisiana for four casing runs described in detail in a previous publication [1].

Keller, et al. [2], and Crook, et al. [3], investigated the primary cementing problems in a deviated-wellbore. Using water-base drilling fluids they demonstrated the settling of solids at the bottom of the annulus of a laboratory deviated wellbore. This phenomenon was reported not to occur above a threshold value of mud yield point that varied according to the deviation angle of the well. Nevertheless, for drilling fluids in which settling did occur, pipe rotation and reciprocation significantly improved displacement efficiency of the cement slurry. The authors reported this finding as "potentially significant" as large size drilled cuttings will most probably settle in spite of the settling of mud solids. Current technology of

the wellbore cementing does not encourage rotation of an entire string of casing in deviated wells. Reciprocation, however, has already been attempted.

Previous research by the authors [4] suggested the inclusion of the pipe pulling loads to the casing design process to account for additional axial loads produced during the reciprocation prior to cementing. Also the pulling loads may be considered at any depth as an emergency measure to retrieve the casing string from the wellbore. The final maximum axial running loads acting along the casing string was determined using a method that utilized the mathematical modeling of the forces acting on small casing elements and the knowledge of the borehole friction factor.

Further improvements in the mathematical model and extensive research on the evaluation of the borehole friction factor [1,5] made it possible to finally investigate quantitatively the surface load prediction and its accuracy.

The objective off this research is to compare casing running hook loads measured in the field, with the predicted surface running loads calculated from the planned two-dimentional trajectory of a directional well. The original planned trajectory of a well is normally restricted

to a vertical plane containing both surface and target locations. At the planning stage, no direction changes are foreseen and therefore the two-dimensional model for running loads prediction is the only applicable one to be used, instead of a three-dimensional model. The borehole friction factor used at the planning stage is obtained from field measurements from offset wells in the same area, explained in the previous publications [1,5].

PREDICTION METHOD

Field data was collected from four directional wells offshore Louisiana. These wells have been described in detail in a previous publication [1]. The drilling fluids used in all cases were a lignosulfonate water-base mud system with the similar mud densities. All trajectories were planned on a vertical plane and their detailed description is shown in Table 1.

For each well a range of hook loads was predicted both for running-in and for pulling-out scenarios. These predicted hook loads were calculated using the 2-D model [1,5] of the tensional loads in casing string. The effect of the hydrodynamic viscous drag was included in the model.

For all cases the predicted hook load range were calculated using borehole friction factors of 0.30 and 0.40.

These values were selected since the borehole friction factor while pulling out casing reported for two casing runs [1] had values of 0.27 and 0.44. Also based on previous experience [1], the velocity of the pipe was selected to be 2.0 ft/s while running in and 0.75 ft/s while pulling out. In addition, static tensional loads were calculated (borehole friction factor of zero and zero velocity). The static loads represent the conventional method for casing design. They also help to identity the total amount of drag (mechanical drag and viscous drag) at every depth in the wellbore.

The predicted loads were plotted together with the measured loads. The plots are shown in Figs 1-4. All plots have the same format. The two first curves to the left represent prediction loads while running in casing and were constructed using a borehole friction factor value of 0.4 and 0.3. The center load line represents the conventional prediction loads (static loads) in which borehole friction factor and velocity are zero. The last two curves on the right represent prediction loads while pulling out casing and were constructed using a borehole friction factor value of 0.3 and 0.4, and a pulling out velocity of 0.75 ft/s.

RESULTS AND DISCUSSION

The analysis will be handled on a well by well basis. Then the most important observations will be discussed.

Well 1

The predicted and measured hook loads are shown in Fig 1. The field data matches both running in and pulling out hook loads values. There is a slight overestimation of hook load values while running in casing but nevertheless 50% of the data points fell within the predicted range with maximum error of 6.3% leaving no room for any further discussion.

Well 2

The only hook loads were measured for this well while running in casing. An unsuccessful reciprocation was attempted with the casing shoe on bottom with maximum pull of 265,000 lbf. With few exceptions the data does not fall exactly within the prediction range but an overall trend is clearly noticeable. The measured hook loads are smaller and parallel to the prediction line, with maximum deviation of 10.5%.

This well has already been studied regarding its actual three-dimensional configuration [1] in which the same data matched the 3-D prediction curve very well for a borehole friction coefficient of 0.43. The previous research predicted casing running loads using the actual well trajectory and a 3-D model that accounts for spatial irregularities, as opposed to this research that uses only data considered at the planning-stage of the well. Apparently, the spatial irregularities contributed to the overestimation of predicted hook loads.

The pull out tentative on bottom equaled the upper range of the prediction values for that depth and therefore the prediction value is incorrect to some extent. Although the amount of error will never be known, since the pipe wasn't actually moved, by analyzing the 3-D prediction graph [1] in the previous research at least 274000 lbf would have been necessary to overcome spatial irregularities and a slightly higher value of the borehole friction factor. Thus the minimum error in underestimation of pulling load is of the order of 10%.

Well 3

Apparently, for this well, there was not a good match. The running in loads are overestimated by as much as 15% and pulling out loads are about 10% underestimated.

The main source of error was caused by the spatial configuration (this well deviated significantly from what was planned), shown in Fig. 5. The amount and magnitude of the shallow-depth doglegs significantly distorted the predicted surface loads based on 2-D calculations. The main mechanism involved here was the capstan effect that takes place on curved paths.

Additional error is explained base on the previous research [5] that demonstrated the importance of using hook load values for which the ratio of drag to buoyant weight (drag-weight ratio) falls above 25%. For the drag-weight ratio smaller than 25% there was considerable error in evaluating the borehole friction factor. The same logic was used here but instead of borehole friction factor evaluation, hook load predictions were of interest. In this well the predicted maximum value of the drag-weight ratio, while pulling out the pipe, was only 10%, as opposed to 24% for Well 1 and 35% for Well 2, which further confirms the possibility of inaccuracies to occur. The main source of error is low value of drag so the role of other factors opposing pipe movement becomes significant. These factors include: stabbing of the casing shoe against the formation while running the casing string into the well, keyseats, ledges and other borehole problems.

The above mechanisms were acting simultaneously and they caused a 10% overall underestimation of predicted pulling loads.

Well 4

In this well there is a good match of predicted running loads with the single measurement made at total depth. The drag weight ratio was 33% and the well was drilled close to the planned trajectory. Analysis of the well path reveals some significant doglegs occurring only deep in the well. It is expected that these doglegs will have negligible contribution to hook loads with little error in prediction. Unfortunately no more measurements are available from this well due to malfunction of the portable unit as explained in [1].

Spatial Configuration Effect

When planning for upward pipe movement, the final element needed in the prediction process is some knowledge of the degree of underestimation of surface pulling loads desired. In the actual planning of reciprocation, the predicted pull has to be calculated from the known borehole friction factor value increased by the design factor which will provide for the spatial irregularities in the borehole path. This was done by comparing the maximum pulling out

load predicted during the planning stage, using the 2-D model [1], a borehole friction factor of 0.40 and a velocity of 0.75 ft/s, with the maximum pulling out load predicted using the 3-D model [1], with same velocity and borehole friction factor. Thus the minimum design factor calculated in such a way only accounts for undesired spatial irregularities, and represents only this research.

The ratio between the predicted load using 3-D and 2-D models (as described above) for the four casing runs studied was 1.055, 1.081, 1.069 and 1.033 for wells 1 through 4 respectively. Based on this research data an 8% safety margin would be suggested as a minimum design factor to account for the spatial shape of a directional well.

DISCUSSION AND CONCLUSIONS

1. The inclusion of the borehole friction factor gives far more realistic evaluation of tensional loads both for running-in and pulling-out. The error made due to uncertainty in friction factor coefficient values (0.3-0.4) is much smaller then that made by using conventional (static) approach.

2. Systematic error were observed for running-in and pulling-out hook loads prediction values. They were mainly

due to spatial irregularities and measurement uncertainties. Their values varied from 0 to 16% and in average were about 9%.

3. Prediction of casing running loads should consider the dominating mechanism that can be spatial irregularities, uncertainties in drag prediction mainly if drag-weight ratios are below 25%, and noise due to borehole conditions.

4. The borehole friction factor used for prediction at the planning-stage of the well should be increase by a design factor that will depend upon the expected drag-weight ratios for the well. In this research a 1.05 design factor for drag-weight ratios above 25% is adequate.

5. The predicted tensional loads at the planning-stage of the well should be increased by a design factor to account for spatial irregularities. In this research a design factor of 1.08 is adequate.

6. This research is limited in covering only casing hook load predictions. This was made to enable comparisons between measured data and predicted values. If the prediction curves are used for designing casing, the assumption is that these loads will be the maximum ones for any section of pipe within the casing. In fact the profile of tensional loads will be changed since the most likely

scenario is running-in and reciprocating at total depth only. This will change the casing design method.

REFERENCES

1. Maidla, E. E., Wojtanowicz, A. K., "Field Comparison of 2-D and 3-D Methods for the Borehole Friction Evaluation in Directional Wells", SPE 16663, 1987.

2. Keller, S. R., et al., "Deviated Wellbore Cementing: Part 1 - Problems", JPT (Aug. 1987), pp. 955-960.

3. Crook, R. J., et al., "Deviated Wellbore Cementing: Part 2 - Solutions", JPT (Aug. 1987), pp. 961-966.

4. Wojtanowicz, A. K., Maidla, E. E., "Minimum Cost Casing Design in Vertical and Directional Wells", SPE 14499, 1985.

5. Maidla, E. E., Wojtanowicz, A. K., "A Field Method of Assessing Borehole Friction for Directional Well Casing", SPE 15696, 1987.

6. Johancsik, C. A., et al., "Torque and Drag in Directional Wells - Prediction and Measurement", SPE 11380, 1983.

7. Sheppard, M. C., "Designing Well Paths to Reduce Drag and Torque", SPE 15463, 1986.

8. Bratovick, et al.,"Improved Techniques for Logging High Angle Wells", SPE 6818, 1977.

TABLE 1

PLANNED TRAJECTORIES

	KICK OFF POINT (ft)	BUILD UP RATE (deg/ 100ft)	END OF BUILD (ft)	INCLIN. ANGLE (deg)	DROP OFF POINT (ft)	DROP OFF RATE (deg/ 100ft)	END OF DROP (ft)	INCLIN. ANGLE (deg)	TOTAL MEASU. DEPTH (ft)
WELL 1	1600	2	3434	36.67	8249	1.50	10694	0	11278
WELL 2	2050	3	3533	44.50	5945	0.63	6345	42	10144
WELL 3	6268	1.5	7668	21.00	N/A	N/A	N/A	N/A	11645
WELL 4	1603	3	3170	47.00	N/A	N/A	N/A	N/A	8966

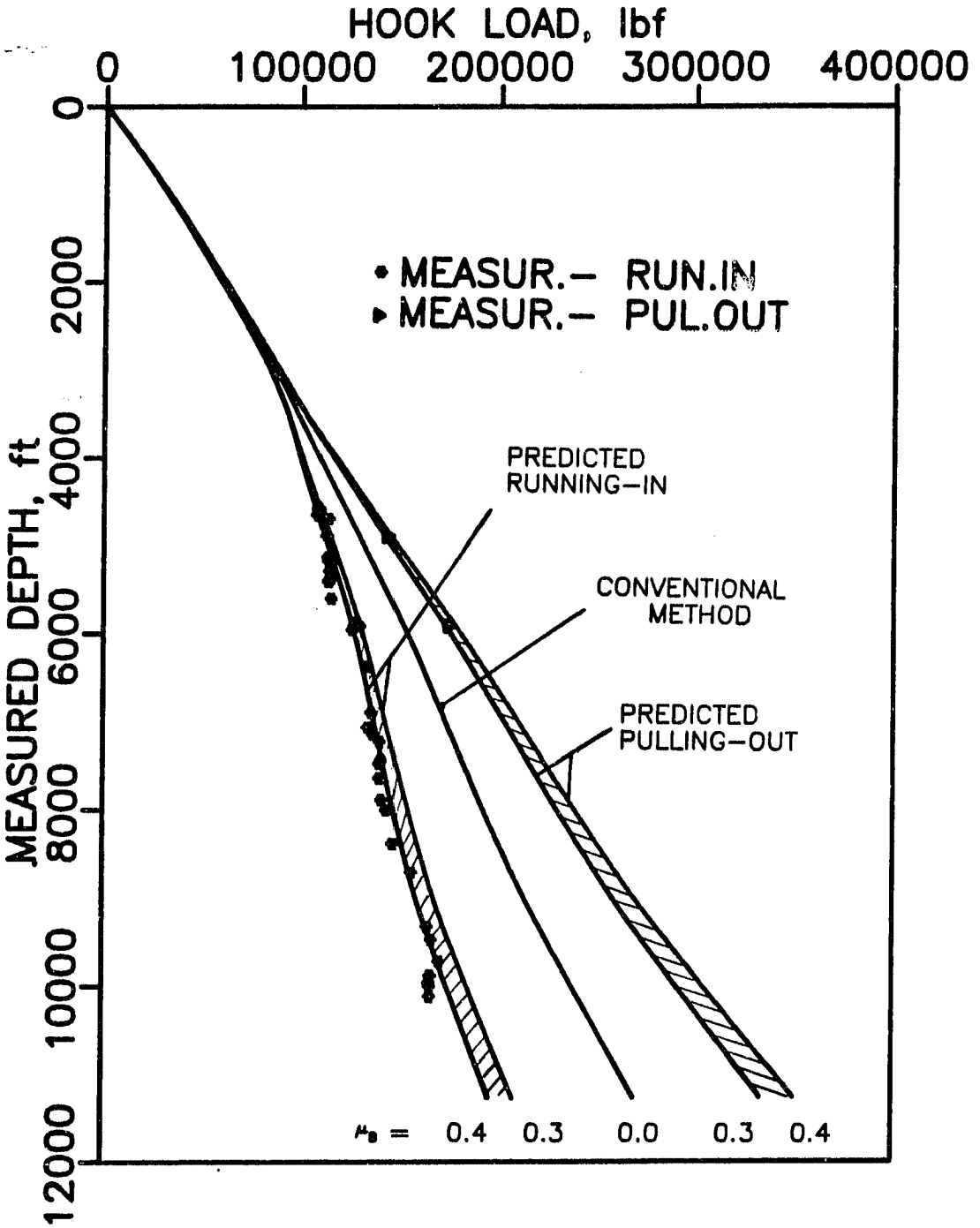

Fig. 1 - Well 1: Predicted range and measured hook loads for the casing run.

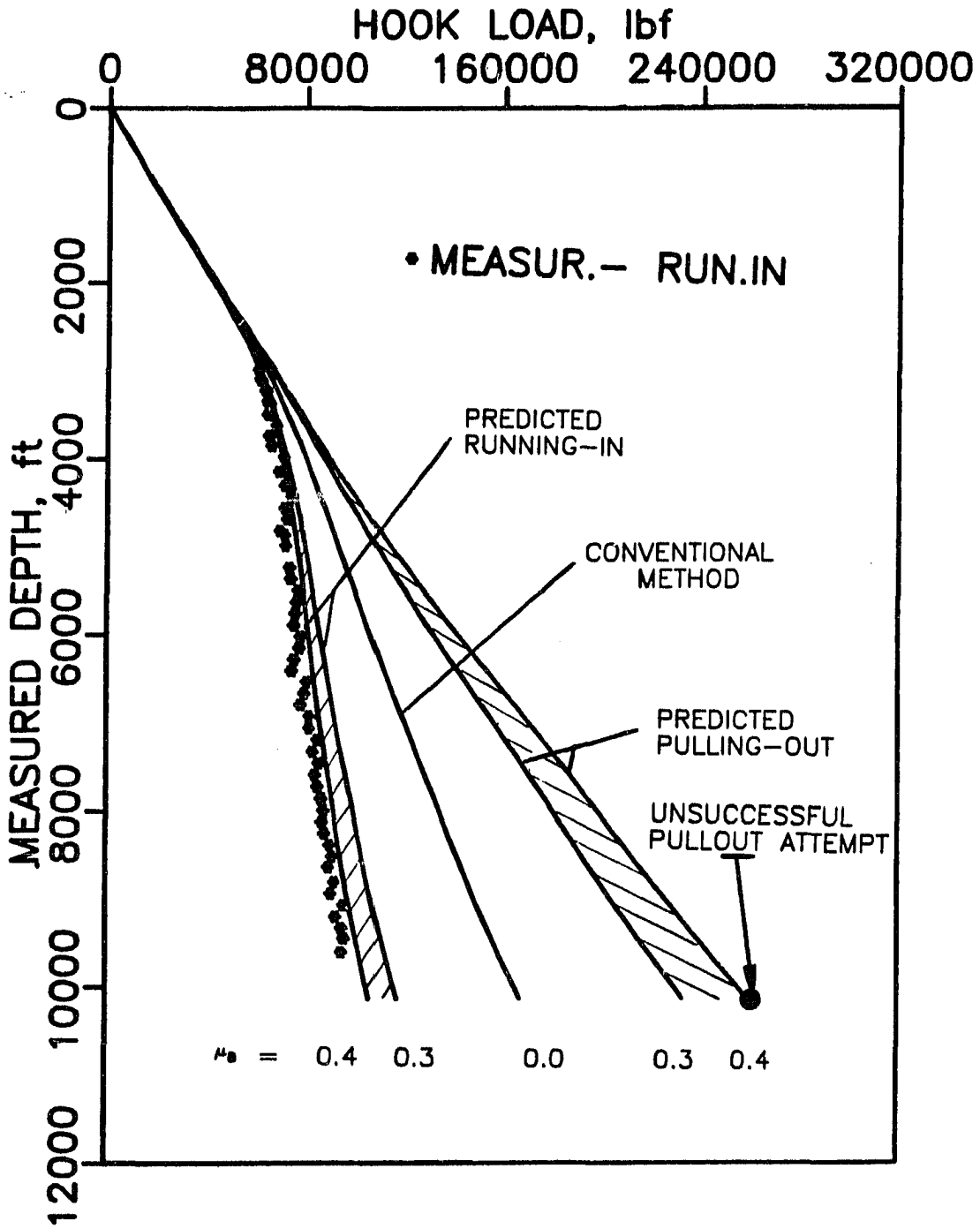

Fig. 2 - Well 2: Predicted range and measured hook loads for the casing run.

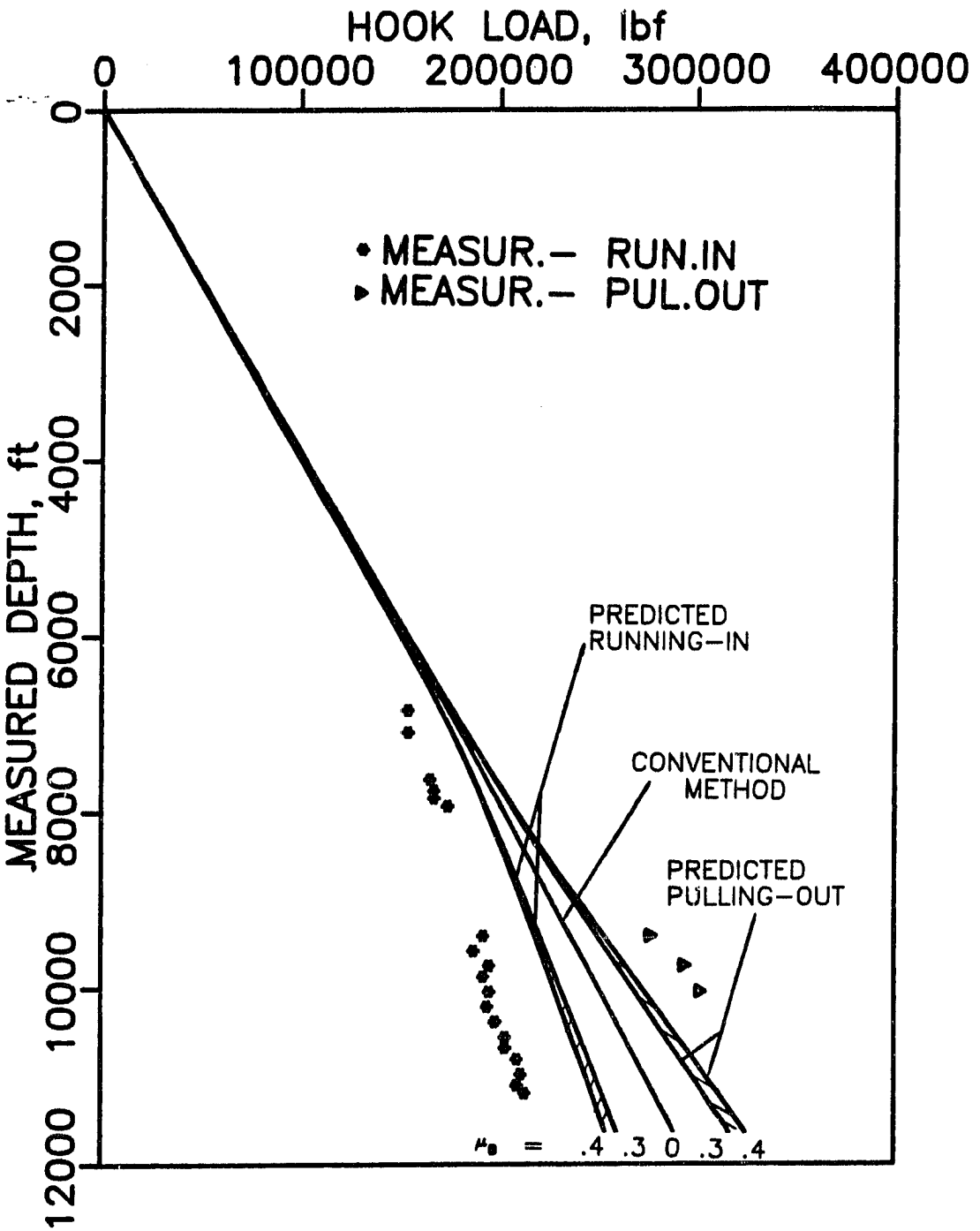

Fig. 3 - Well 3: Predicted range and measured hook loads for the casing run.

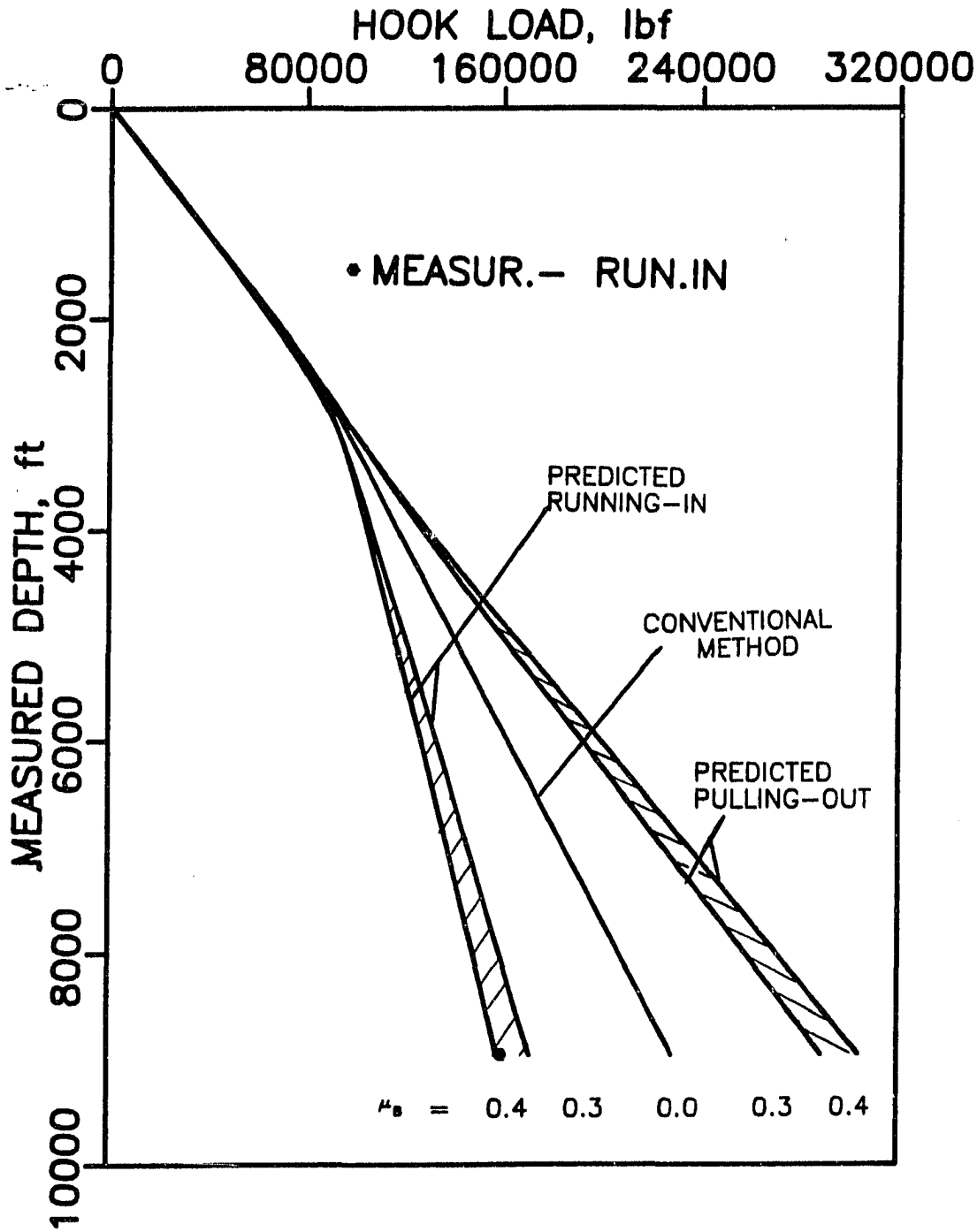

Fig. 4 - Well 4: Predicted range and measured hook loads for the casing run.

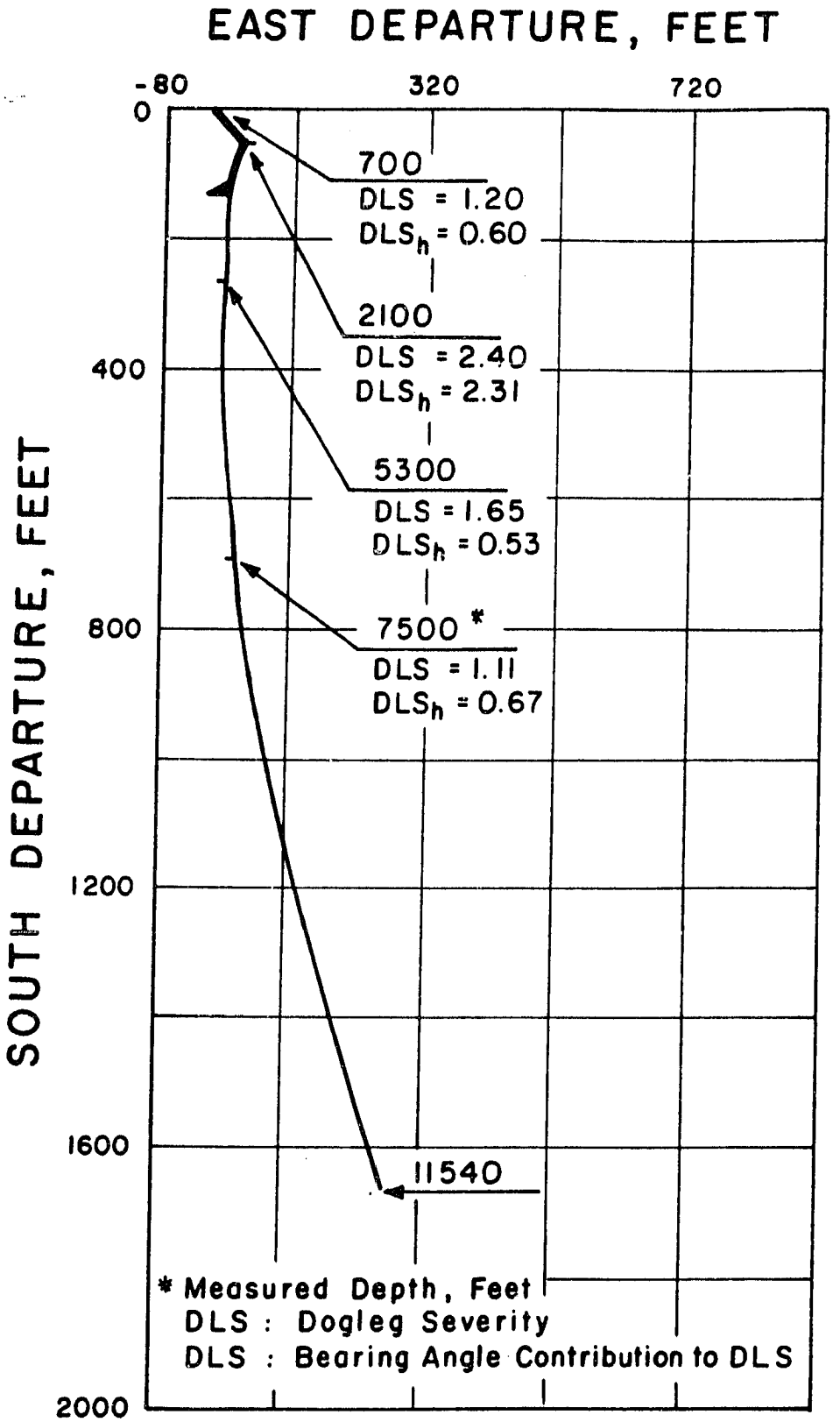

Fig. 5 - Well 3: Horizontal section and directional survey data.

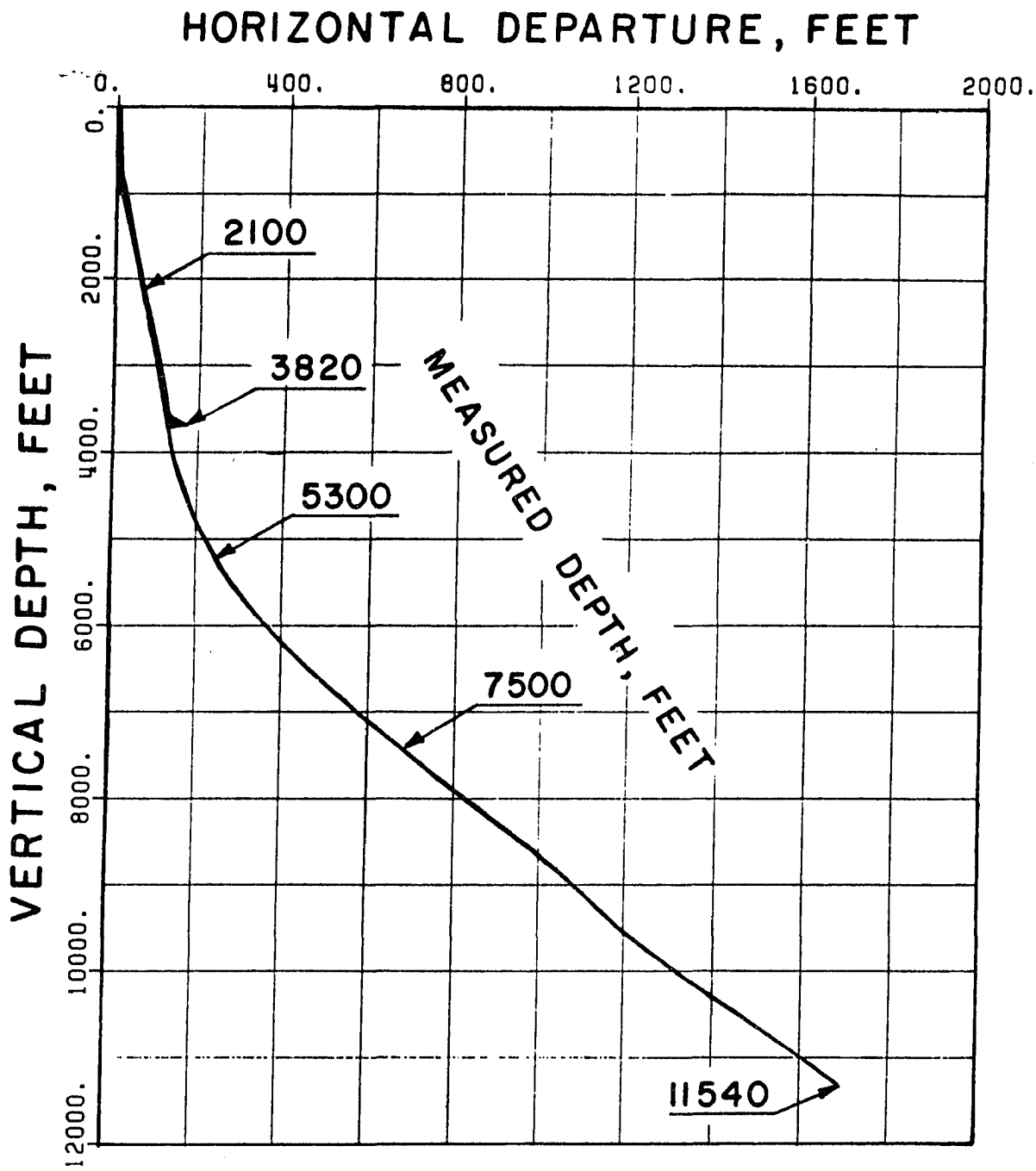

Fig. 6 - Well 3: Vertical section and measured depths.

CHAPTER IV

BOREHOLE FRICTION FACTOR STUDY USING LABORATORY-SIMULATED DYNAMIC FILTRATION CAKE APPARATUS

INTRODUCTION

Drag can become a significant portion of the hook load while moving strings of pipe in a directional well. If ignored, it could cause operational problems during drilling or casing string runs. The commonly known parameters to affect drag are: well trajectory, type of drilling fluid, pipe geometry, the friction factor coefficient for cased and open hole, and the borehole conditions.

Among the parameters mentioned the unknown include: friction factor coefficient and the borehole conditions (washouts, keyseats, ledges etc).

The friction resulting from rock and pipe interaction in the open hole is a complex tribological process that might be affected by temperature, pressure, mud and mud cake compositions, chemical composition of both pipe and rock surface, geometry and contact loads.

The individual effects of these factors on friction are difficult to measure. Some of these factors are represented

by lubricity of drilling mud. A small scale laboratory instrument has been recommended by API [1], that measures a lubricity coefficient to evaluate the mud composition effect on friction. Mondshine [2] defines this lubricity coefficient as being "the coefficient of friction of a Tinken ring rotating in the drilling mud at 60 rpm against a metal surface at 720 psi".

Bol [3] measured the API lubricity for several drilling fluids. For water-base-muds (WBM) he reported a range of values between 0.10 to 0.15, for WBM with lubricant 0.09 to 0.14 and for oil-base-muds (OBM) 0.03 to 0.07. He confronted these values with field data and large-scale apparatus experimental data. His field results using WBM showed friction factors within the range of 0.19 to 0.36 with no improvement due to lubricant addition. While the small-scale laboratory tests with the same drilling fluids showed values 10 times lower. Bol further measured friction factor coefficients using a full-scale tester using an actual casing and tool joint and reported friction factor values of 0.15 for OBM, between 0.35 to 0.50 for unweighted WBM and 0.25 to 0.30 for weighted ones. He also reported that lubricant addition reduced friction for WBM with densities below 10.8 lb/gal, however, did not affect friction for WBM having densities above 12.5 lb/gal. He also reported a solids bailing up phenomenon for lubricant addition in excess of 2 % by volume because mud solids became oil-wet.

He reported that polymeric mud additives, diesel, glass beads, and salts have no effect on friction. He also reported that at early times during an experiment friction factor's were higher than the final stabilized ones. The conclusion was that small-scale tests were nonrepresentative for casing and tool joint friction.

White and Dawson [4] used a large-scale apparatus to determine friction and wear between casing and tool joint. They reported friction coefficient values between 0.05 to 0.26 for WBM and 0.02 to 0.06 for OBM. The typical field values of friction coefficient for WBM fell in between 0.20 and 0.35. The authors explained their lower laboratory values by showing that hydrodynamic lubrication (that occurs when opposing surfaces in relative tangential motion are fully separated by fluid film) was occurring in their experiments. They concluded that boundary lubrication regime (opposing surfaces barely separated by the fluid film) is dominant in the well. They reported that casing wear was significantly higher in OBM than in WBM.

Johancsik, et al. [5], reported friction coefficients between 0.25 to 0.40 for drillstring and mostly cased hole in seawater-base mud. Sheppard, et al. [6]. reported field values of 0.36 for WBM. Bratovich [7] reported friction factor values between 0.36 and 0.40 for logging tools and

wireline in open hole laboratory tests with lignosulfonate WBM.

Brett, et al. [8] used a 3-D model (hydrodynamic drag not considered) to calculate borehole friction factors for both casing and drillstrings for several wells worldwide. He reported values between 0.17 to 0.34. He successfully predicted reciprocating loads and reported friction factor values of 0.22 for drillstring in partially cased holes and 0.25 for casing while reciprocating. His idea of monitoring casing drag to take possible corrective actions during the casing run(such as circulating or rotation with casing tongs) before the casing becomes stuck off bottom is in very good agreement with concepts of this research.

Alford [9] studied the lubricant effect on mud lubricity using a large scale tester consisting of a vertical metal shaft that is rotated against the center hole of a berea sandstone cylinder under mud circulating conditions and atmospheric pressure. He concluded that lubricant efficiency is dependent on mud type and time. Unfortunately he did not convert torque measurements to friction coefficients and therefore no comparison can be made.

This research was undertaken to evaluate the friction factor using a medium-scale laboratory apparatus to simulate

some of the factors affecting the borehole friction factor. An attempt was made to simulate friction between rock and pipe string and between rock with the mud cake and a pipe string. The results were then compared with the field data collected during actual pipe runs. Also the measurements made with the small-scale API lubricity tester were used for comparison.

EXPERIMENT DESIGN

One of the practical objectives of this research regards modeling of casing running loads in the open hole section of directional wells. Therefore the analysis of the experiment was concentrated on determining the main factors that can affect the friction factor coefficient while sliding casing against the formation.

The in-situ conditions that can be expected while running a casing string are:

. Impermeable formation with drilling fluid or drilling fluid with sediment solids (inclined hole) within the contact surface.

. Permeable formation with drilling fluid and filtration cake within the contact surface.

. Permeable formation and inclined hole with sediment, cake and drilling fluid within the surface of contact.

Furthermore, the external casing configuration suggests two running modes while sliding pipe. At the joint edge it is possible to expect some wedging that might remove some mud cake from the permeable formations. For the rest of the pipe the mud cake removal might depend on the existing distributed normal forces and the effective area of contact.

An estimation of the distributed normal forces can be made by considering a 7-in. casing (26 lb/ft) in a borehole of variable inclination from 0 to 90 deg. The distributed normal force is expressed as:

$$q_N = q \sin\alpha \qquad (1)$$

and it would vary from 0 to 26 lb/ft. An estimation of the surface of contact depends upon the pipe length being in contact with the borehole as well as the crossection perimeter of contact. Although the pipe geometry is fairly well known, the borehole geometry is not. A perfect cylindrical hole seems quite unrealistic; therefore sensitivity analysis seems the most practical way to get an idea of what might be the pressures involved.

Lets consider the following equation for pressures:

$$P = \frac{q \sin\alpha}{12 \pi d C_1 C_2} = K \sin\alpha \qquad (2)$$

where C1 and C2 are percentages of length contact and crossection perimeter contact and 12 is a conversion factor. Arbitrarily assuming C1 = 50% , C2 = 5% , q = 26 lb/ft and d = 7 in. results in K = 3.9 psi. Arbitrarily assuming C1 = 10% , C2 = 2% , q = 26 lb/ft and d = 7 in. results in K = 49.3 psi. The values of K represented the maximum contact pressure value for each arbitrary set of conditions. Similar study was carried out for the build up section portion:

$$P = \frac{2\ F \sin(0.5\ \dot{\alpha}\ \ell)}{12\ \ell\ \pi\ d\ C_1\ C_2} \qquad (3)$$

where F is the axial load at the end of the build up section.

Arbitrarily assuming F = 100,000 lb , $\dot{\alpha}$ = 0.03 deg/ft, ℓ = 1000 ft, d = 7 in., C1 = 60% and C2 = 5% results P = 6.5 psi. Changing C1 = 10% and C2 = 2% results in P = 98 psi. These values are greatly dependent upon the build up rate and the axial forces below the build up section besides C1 and C2.

In order to study the effect of mud cake on borehole friction the maximum pressure in the experiment was from 1.3 to 3.4 psi, which corresponds to the conditions in the slant

portion of a directional wellbore. Under these pressure conditions the mud cake effect was pronounced. Also, the final stabilized values after mud cake was removed, was determined.

For the experiment setup there was no need of performing tests on vertical cores since spatial position is not known to effect friction factors and furthermore directional wells are slanted anyway, and therefore flat round 6 in. cores were used in the horizontal position. The experimental setup is shown in Fig.1-4.

The equipment was built to handle a variety of core trickinesses, building mud cake under dynamic filtration conditions at differential pressures of up to 400 psi. All experiments, reported here, involving filtration were carried out at 100 psi pressures.

The filtration part of the experiment and the friction experiment were entirely different setups. At first filtration took place under dynamic filtration conditions and 100 psi pressure. After releasing the pressure and removing the filtration pressure chamber lid, the chamber was placed in another position, Fig.2, and the friction experiment took place at atmospheric pressure.

Mud cakes were generated using two different time periods. The 30 min mud cake build up time was used to simulate long filtration periods that take place in the borehole before running casing. The 2-min. cake build up time simulated an actual average time between two casing joint runs. The pumping flow rate of 8.5 gal/hr was selected so the shearing rate above the cake was similar to that encountered in the wellbore (170 1/sec).

The lithology effect was checked upon by using limestone and berea sandstone cores. The cores slabs were cut from a cylinder core 1 ft long by 6 in, in diameter, using only water to cool the cutting blade. The cores were then dried at 300 F for a 24 hour period and then cooled to room temperature. At the center of each core a small hole of about 0.07 in. deep was made in a cone chapped manner. This helped stabilizing the end of the rotating shaft and prevented vibrations. Close to the shaft end, a key was placed to transmit torque to the rotating steel disc (4.49 x 1.57 in) or steel cylinder (4.49 x 3.66 in). This allowed torque transmission from the shaft to the disc with free axial movement. Several weights were placed on the disc or cylinder to provide a normal force which amounted up to 17.7 lb. A constant rotating speed of 50 rpm was selected, that yielded an average surface velocity of 1 ft/s. This velocity agrees very well with the average casing running-in speeds 1.5-2 ft/s and pulling-out speeds 0.7 ft/s.

The sturdy setup was necessary to minimize shaft vibration. This problem was further mitigated using neoprene seats. The two sliding surfaces were precisely levelled using a horizontal adjustment screws located under the four legs.

A 1/8 hp DC motor with a gear box (max 250 rpm) was used to produce constant rotation with stabilized torque. Initial tests without the gear box (max 2500rpm) showed much variation in angular velocity that were totally eliminated with the new setup. A control unit attached to the DC motor provided constant rpm's for any given torque on the shaft, while accurately monitoring torque that was further recorded on an analog strip-chart. The torque measurements on these charts were later converted to friction factors using the equation derived in appendix A.

EQUIPMENT CALIBRATION

Before any experiments were made all measurements were checked and calibrated.

The strip-chart recorder operation was continuously controlled with the variable external voltage supply of known intensity that in turn was checked against a calibrated multimeter tester of 0.04% + 2 basic DC accuracy.

The accuracy of torque reading was checked upon by using the setup shown in Fig.3. A pulley of known dimensions was attached to the main shaft with some string wrapped around it. The string went through another free rotating pulley installed on the main frame. The string was loaded with known weights which gave a precise determination of torque. This torque was compared to the analog strip-chart readings. More than ten measurements were performed for each set of weights and the largest standard deviation to mean value ratio observed was 1.0% (that corresponded to friction factor values around 0.1 - when using a normal force on the disc of about 17.6 lb; for corresponding friction factor values above 0.2 this ratio was less than 0.5%). All readings were corrected for calibration results that are shown on all the strip-chart figures in this report.

An experimental run was performed on sandstone using water as a lubricant. The result is shown in Fig. 5. They fall within the range from initial value 0.7 to the final value 0.25. This range corresponds to the published data on friction coefficients between steel and wet sandstone from 0.29 to 0.94 [10].

RESULTS

Seven samples of water-base mud (WBM) and three samples of oil-base mud (OBM) were collected at rig sites in

Louisiana. Their description is given in Tables 1 and 2. Original mud samples from the field, provided broad representation of actual field condition (aging, cutting removal, chemical treatment) and were therefore suitable for the experiment. The results of 64 experiments are summarized in Table 3.

Oil Base Muds

All three mud samples were diesel OBM. The typical behavior of friction factors with time, using the cylinder on the rock surface with drilling fluid only (no filtration), is shown in Fig.6 and an actual example is shown in Fig.7.

No mud cake was generated in these experiments because the filtration chamber did not allow for simultaneous high pressure-high temperature filtration and no cake could have been produced under atmospheric conditions. For all OBM there was deposition of solids on the rock surface during cylinder rotation directly between the two containing surfaces, Fig. 8. This phenomenon is believed to occur due to destabilization of the oil mud system within the high shear rate area of the cylinder interface. The result is sedimentation of solids which eventually build up a cake. The reasoning is that the fluid movement and consequently the shearing action in the very small space between steel

and rock surfaces promoted a coalescences of water droplets which destabilized the mud system.

This reasoning was further supported by the other experiments with OBM using the disc instead of the cylinder on the rock surface. The typical behavior plot is shown in Fig.9, and an actual example is shown in Fig.10. Notice that both graphs show first a decrease in the friction factor that later stabilize at higher values. This behavior was common for all muds tested with the disc as reported in Table 3. The reason for discrepancy between cylinder and disc response is the non-uniform deposition of solids under the disc, Fig. 11. The solids cake at the outer edge was slightly thicker and it decreased towards the center. This happened due to larger velocities (shear rates) under the outer most zone of the disc which enhanced higher rates of water coalescence and caused uneven distribution of solids. As a result the actual contact area was smaller and on the outer portion of the disc that differed from the assumption of full surface working area under which the equations for the torque conversion to friction coefficients were derived thus causing overestimation of friction factor values.

To further confirm the solids build-up nature of the friction in oil-base muds, as opposed to a possible filtration theory, the same experiment was repeated using an aluminum disc instead of the rock as a base surface. Again,

the solids settling occurred exactly the same way as with the rock.

The total number of friction tests with rotating cylinder amounted to seven experiments on sandstone. The resulting values of friction coefficients for OBM was 0.16 to 0.29 averaging 0.24. Also temperature does not seem to affect much the value of friction coefficient. Experiments performed at 170 F showed the average value of the coefficient of friction 0.21 which was similar to the results obtained in room temperature.

Water Base Muds

The seven WBM used in the experiment represented four typical mud systems [12]: lime mud, lightly treated lignosulfonate freshwater mud, seawater gel mud, and four lignosulfonate freshwater muds.

1. Lime Mud Experiments

The typical friction response in the lime mud environment with the 30-min. dynamic filtration cake, is shown schematically in Fig. 12. During the first 40 sec friction was controlled by the mud cake (cake period). Later, the cake is entirely removed and the opposing surfaces in relative tangential motion are partially

separated by a film of drilling fluid (mixed mode lubrication). The initial overshoot and lower stable values for the mud cake period is typical of viscoelastic fluid behavior [14]. Its effect is dependent upon dynamic filtration time (mud cake thickness), and applied pressure. Presented in Fig. 13 is a record of an experiment in which dynamic filtration took place for 30 min. at 100 psi pressure differential (typical for all cake buildups), followed by rotating the disc on the cake surface immersed in drilling fluid. The reason was that without immersion the mud cake tended to become sticky, altering its consistency, which in turn yielded an unrealistic behavior of the friction coefficient. Therefore all experiments were performed under a free level of an original mud.

Once cake was removed from the surface, the steel disc contacted the rock surface, which resulted in a sharp increase followed by a slight decrease in friction factor values until final stabilization, as shown in Fig. 13. The initially higher values have been previously reported [3] and were attributed to a break-in period between both surfaces. Another observation, common in most experiments, was a decrease in data scatter with time, as shown in Fig. 13. This could be explained by adjustment of the two sliding surfaces which is routine in any process of mechanical polish.

For all the strip-chart graphs the sliding distance is shown only for qualitative evaluation. It makes it easier to compare frictional response of disc and cylinder. Since their average effective diameters are different and therefore time comparisons could be misleading.

The effect of contact pressure was investigated by comparing disc and cylinder tests with a 30-min. filtration cake. Fig. 14 is an example for the cylinder run under similar conditions to those for the disc in Fig. 13. The contact pressure increased 2.6 times from disc to cylinder and the mud cake period decreased by 30%. No change in the friction coefficient value was observed which further confirms the consistency of the method.

The experiments also showed that the final stabilized friction factor values were independent from filtration period. This is shown in Fig. 15 for the disc test with no cake. The stabilized friction factor value was 0.26 which favorable compared with 0.28 with cake. Similar example for the cylinder test without cake values is shown in Fig. 16 showing a stabilized value of 0.23 against 0.26 for the disc. Notice that for both cases there was a break-in period characterized by higher initial friction factor values.

The effect of filtration time on the mud cake period was investigated by using 2 min. filtration in comparison to 30-min. filtration. The 2-min. filtration was selected because a casing joint is run every 2 min., on average. Fig. 17 shows the significant decrease in mud cake period from 42 sec (30-min. filtration, Fig. 13) to 7 sec. The final friction factor stabilized value of 0.23 was similar to other values. Therefore it was concluded that the only conceivable effect of filtration is the cake period during which the friction factor value is small and it is controlled by the cake rheology.

In the next series of experiments a lubricant was added to the lime mud. A blend of sulfurized triglyceride and an alkanolamide in a paraffinic hydrocarbon carrier lubricant was added in 2% volume quantities to the lime mud. The typical frictional response is shown in Fig. 18, as well as the actual strip-chart record that is shown in Fig. 19. The lubricant increased the mud cake effect period about 3.5 times partially because of thicker cake (increased from 0.04 to 0.07 in.) as shown in Table 1, and also probably due to the lubricant action itself. The final stabilized value of 0.27 is similar to the friction factor values obtained without the lubricant addition. This agrees with other research [3,9] that report on improvements in friction factor values only for low solid drilling fluids, due to particle interactions with the lubricating film.

Experiments were also performed with the lime mud and lubricant without the filtration period and the resulting strip-chart is shown in Fig. 20. A stabilized value around 0.26 was soon achieved showing no improvements in the friction factor value.

The effect of lithology was investigated by repeating the same experiments with lime mud on limestone cores. The typical behavior and an actual strip-chart example is shown in Figs. 21 and 22 respectively. The initial friction behavior was dominated by the mud cake and was similar to the sandstone experiments. However, for greater time periods, the friction factor stabilized at lower values, as shown in Figs 21 and 22 with the full set of data shown in Table 3.

Experiments with limestone also showed other peculiarities. The wear of the limestone core was about 10 times greater than the sandstone core for the same amount of working time. In addition the intermittent sequence of removal and addition of weights to the cylinder, without removing or disturbing its position on the rock surface, showed continuous decrease in friction factor coefficients stabilizing at successively lower friction factor values, finally reaching a value around 0.02. The polishing effect could have contributed to this significant decrease. Such effect was not observed on sandstone cores that consistently yielded equal stabilized friction factor values for

successive changes of normal pressures. The limestone behavior suggested several stabilized values of friction factor, therefore the value considered had to be related to time or sliding distance.

2. Lightly Treated Lignosulfonate Freshwater Mud

Only three runs were obtained for this mud as the sealing system leaked and the mud sample was lost. The two most important runs for this study are shown in Figs 23 and 24. The first experiment was made with no lubricant addition and the stabilized friction factor value was 0.21. For the second experiment 2% by volume of lubricant was added to the mud resulting in a stabilized friction factor value of 0.12. Ending the experiment, both cylinder and rock surfaces were inspected and a black grease film well adhered to both surfaces was observed. This particular mud had a 9.9 lb/gal density and only 5% solids by volume, further confirming the effectiveness of lubricants at very low solid contents. Another benefit from lubricant addition was the significant decrease observed in the inherent error measurement that was probably due to a better distribution of normal pressures between both surfaces.

3. Seawater Gel Mud

The typical frictional response curve is shown in Fig. 25. This drilling fluid was the one with lowest friction factor values averaging about 0.15. Figs 26 and 27 show examples for unlubricated and lubricated mud respectively.

For mud without lubricant the mud cake effect was significantly greater then other mud systems but this was probably due to higher mud cake thickness (as shown in Table 1) rather than the mud properties. For this mud run no difference was observed between friction factor during the cake period and its stabilized value. Addition of lubricant (Fig. 27) did not change the value of the friction factor but only slightly increased the duration of cake period. The explanation can be sought in cake quality for this mud. Apparently the friction factor with cake is similar to the friction factor on the rock surface.

4. Lignosulfonate Freshwater Muds

The typical frictional response is shown in Fig. 28. The average stabilized values for all four muds was about 0.23, with no distinction attributed to the mud source. Figs 29 and 30 are shown to compare the effect of filtration time on mud cake effect that is very small for 2 min.

filtration periods. Lubricant was added to the mud, Fig. 31, and again its effect was an increase of the mud cake period without changing the final stabilized values for all four muds.

DISCUSSION

The stabilized friction factor values measured on the medium-scale laboratory tester were insensitive to API Lubricity for both oil and water base muds, as shown in Fig. 32. This agrees with the results obtained by Bol [3]. Also the reasoning used by White [4] to explain results of his experiment might well be applied to the API lubricity tester. He explained that hydrodynamic lubrication could take place if the drilling fluid is forced into the metal to metal gap carrying part of the normal load. He checked this in his experiment by installing a pressure tap in his apparatus.

The field values of the borehole friction factor evaluated in the field with the lignosulfonate muds [13] ranged from 0.21 to 0.30 for average slant hole inclinations between 39 and 52 deg. This is in very good agreement with the laboratory results as 80% of the stabilized friction factor values were between 0.2 and 0.3. Other field results published [3,4,5,6,7,8,11] also agree with the laboratory results reported here, indicating consistency of field and laboratory conditions.

Comparing these results with other experiments carried out on large-scale testers [3,4] there doesn't seem to be much difference between open hole stabilized friction values and the ones reported for tool joints on casing.

The extent of the mud cake effect in the actual well might not have been well reproduced in these experiments since the contact area is unknown, but the overshoot of mud cake effect for the sea water gel, even if reduced, might lead to erroneous conclusions when friction factor models are being used to diagnose drilling problems. It might suggest differential sticking problems that in reality are not occurring.

CONCLUSIONS

1. The medium-scale tester successfully simulated field lubricating conditions. The friction factor values of 0.23 for lignosulfonate water base muds was close to those obtained in the field 0.21 to 0.44.
2. Most friction factor values were in between 0.2 and 0.3, oil base muds included.
3. There is a qualitative difference between drag mechanisms of water base and oil base mud systems: for water base mud filtration solids were continuously removed from the moving interface until the steel and rock surfaces were partially separated

by the drilling fluid film; for oil base mud there was solids drop-out between the moving interface due to destabilization of the mud system probably due to the coalescences of the water droplets within the high shear rate area at the cylinder interface.

4. In the water-base muds, the mud cake effect on friction reduces the borehole friction factor. This effect reduced in average the friction factor from 0.23 to 0.17. Its duration (cake period) in average was 2 min. corresponding to a sliding distance of 80 ft.
5. Addition of lubricant to the water-base muds decreased friction in the low solids weighted mud, however the lubricant only increased the cake-period in the high solids drilling fluids with no effect on friction.
6. No correlation was observed between the friction factors from the medium-scale laboratory tester and the API lubricity. The probable reason is that the laboratory tester was working in a boundary lubrication regime (very thin fluid film separating the moving surface) and the API lubricity tester was working in a hydrodynamic lubrication regime (thicker fluid film separating the moving surface).
7. For the oil-base muds, the friction coefficients were equal (around 0.24) to the water-base mud values. This is caused mainly by solid cake

deposition between sliding surfaces. Build up of solid cake while running tools in boreholes filled with oil-base mud has not been reported yet. If this phenomenon actually occurs it may have adverse effect on the quality of cementing operations.

ACKNOWLEDGEMENTS

The equipment support by NL Baroid/NL Industries, Inc. - Lafayette, is greatly appreciated.

NOMENCLATURE

A = Area, sqin

C1 = Percent of length contact

C2 = Percent of crossection perimeter in contact with the borehole

d = Pipe diameter, in

F = Force, lbf

ℓ = Length of pipe, ft

P = Pressure, psi

r = radius, in

T = Torque, lbf.in

$\dot{\alpha}$ = build-up rate, deg/ft

REFERENCES

1. API RP 13B, "API Recommended Practice Standard Procedure for Testing Drilling Fluids, Seventh Edition", p 33, April, 1978.
2. Modshine, T. C., "Drilling-Mud Lubricity: Guide to Reduce Torque and Drag", Oil and Gas Journal, pp 70-77, Dec. 7, 1970.
3. Bol, G. M., "Effect of Mud Composition on Wear and Friction of Casing and Tool Joints", SPEDE, pp 369-376, Oct., 1986.
4. White, J. P., Dawson, R., "Casing Wear: Laboratory Measurements and Field Predictions", SPE 14325, 1985.
5. Johancsik, C. A., et al., "Torque and Drag in Directional Wells - Prediction and Measurement", JPT, PP 987-991, June, 1984.
6. Sheppard, M. C., "Designing Well Paths to Reduce Drag and Torque", SPE 15463, 1986.
7. Bratovich, et al., "Improved Techniques for Logging High-Angle Wells", SPE 6818, 1977.
8. Brett, J. F., et al., "Uses and Limitations of a Drillstring Tension and Torque Model to Monitor Hole Conditions", SPE 16664, Sep. 1987.
9. Alford, S. E., "New Technique Evaluates Drilling Mud Lubricants", World Oil, PP 105-110, July 1976.
10. Mark's Standard Handbook for Mechanical Engineers, McGraw Hill Co., New York, p 3-27,

11. Lesage, M., et al., "Evaluating Drilling Practice in Deviated Wells with Torque and Weight Data", SPE 16114, March, 1987.

12. Ayers, R. C., et al., "The Generic Mud Concept for NPDES Permitting of Offshore Drilling Discharges", JPT, p 476, Mar., 1985.

13. Maidla, E. E., Wojtanowicz, A. K., "Field Comparison of 2-D and 3-D Methods for the Borehole Friction Evaluation in Directional Wells", SPE 16663, Sep., 1987.

14. Prentice, J. H., "Measurements in the Rheology of Foodstuffs", Elsevier Applied Science Publishers, England, pp 32-33, 1984.

15. Tsang-Mui-Chung M., et al., "A Device for Friction Measurements of Grains", Transaction of the ASAE, p 1939, 1984.

Appendix

Friction Factor Equation Derivation

These formulas have been previously derived by Tsang-Mui-Chung, et al [15]. The friction factor equation for both cylinder (4.45 x 3.62 in) and disc (4.45 x 1.57 in) are derived by analysing the forces at equilibrium acting on their surfaces, Fig. 30:

$$dT = dF.r \tag{A1}$$

$$dF = P.dA.\mu \tag{A2}$$

$$P = \frac{W}{A} = \frac{W}{\pi(r_2^2-r_1^2)} \tag{A3}$$

$$dA = r.d\Theta.dr \tag{A4}$$

Combining these equations,

$$dT = \frac{W.r^2.d\Theta.dr.\mu}{\pi(r_2^2-r_1^2)} \tag{A5}$$

and integrating,

$$T = \int_0^{2\pi}\int_{r_1}^{r_2} \frac{W.\mu}{\pi(r_2^2-r_1^2)} \cdot r^2.dr.d\Theta \tag{A6}$$

results:

$$\mu = \frac{T}{W} \cdot \frac{3}{2}\frac{r_2^2-r_1^2}{r_2^3-r_1^3} \tag{A7}$$

TABLE 1

WATER BASE DRILLING FLUIDS USED

DRILLING FLUIDS	BASIC ADITIVES	CODE	DENSITY lb/gal	API LUBRICITY	WATER %V/V	OIL %V/V	CHLORIDES ppm	MBT cc	API FILTRATION ml/30min	PH (FILTRATE)	CAKE THICKN. in.	CAKE SOLIDS %W/W	VISCOSITY cp	YIELD POINT lb/100ft^2	GELS 10s/10min lb/100ft^2
LIGNO-	BENTONITE	A1	17.5	0.165	63	0	5000	4.5	1.2	10.8	0.056	84	57	13	4/6
-SULFONATE	BARITE	A2	17.4	0.145	65	TR	5000	4.5	2.0	9.9	0.063	80	80	20	6/26
FRESHWATER	LIME	A3	17.7	0.130	62	TR	5000	6.0	1.2	10.4	0.047	82	59	16	5/9
	CAUSTIC	A4	17.3	0.130	64	TR	10500	6.0	1.3	11.2	0.039	84	65	19	5/11
MUD	LIGNO- -SULFONATE	A4&L*		0.100					1.3	10.6	0.047	83	55	16	5/10
SEAWATER GEL MUD	BENTONITE	B	14.4	0.075	71	0	120000	4.5	9.5	8.0	0.094	78	41	23	9/47
	BARITE	B&L*		0.040					8.1	9.2	0.070	78	38	22	11/47
	CAUSTIC SODA ASH NEW VIS NEW THIN NEW DRILL SALT														
LIGHTLY TREATED LIGNO- -SULFONATE FRESHWATER MUD	BENTONITE	C	9.9	0.270	95	0	1500	3.0	7.7	8.8	0.047	42	37	19	4/47
	HEMATITE	C&L*		0.060					6.6	8.8	0.047	65	11	8	2/3
	LIGNITE KOH LIME														
LIME MUD	BARITE	D	10.3	0.220	87	0	1800	8.5	5.5	11.7	0.040	52	17	15	4/15
	NAOH	D&L*		0.195					10.0	11.7	0.070	54	18	10	5/17
	KOH LIME LIGNO- -SULFONATE CALEX														

* ADDITION OF 2 VOL % OF A COMMERCIAL LUBRICANT CONTAINING SULFURIZED TRIGLICERINE AND AN ALKANOLAMIDA IN A PARAFFINIC HYDROCARBON CARRIER.

TABLE 2

DIESEL OIL BASE DRILLING FLUIDS USED

CODE	DENS lb/gal	API LUBRICITY RT/170°F	API* FILTRATION ml/30min	HP-HT CAKE THICKNESS in.	CAKE SOLIDS %W/W	OIL %V/V	WATER %V/V	SOLIDS %V/V	OIL WATER RATIO	VISCOSITY** cp	YIELD** POINT lb/100ft^2	GELS** 10s/10min$_2$ lb/100ft^2
Z1	17.9	0.06 / 0.10	4.6	0.180	87	47	15	38	76/24	59	14	7/17
Z2	15.6	0.04 / 0.06	3.6	0.156	84	57	12	31	83/17	33	12	7/14
Z3	12.7	0.01 / 0.03	3.4	0.125	78	60	16	24	79/21	22	6	4/9

* MEASURED AT 150°F AND 400 psi PRESSURE DIFFERENTIAL.

** AFTER MUD REPORTS MEASURED AT 150°F.

TABLE 3

AVERAGE FRICTION FACTOR, AT DIFFERENT TIME PERIODS, READ FROM THE EXPERIMENT CHARTS

Z1/O/S/M/C/RT/NF/NL
- NL: NO LUBRICANT (NL); LUBRICANT (L)
- NF: NO FILTRATION (NF); 30 MIN DYNAMIC FILTRATION (30M)
- RT: ROOM TEMPERATURE (RT); 170°F (170F)
- C: 4.45x3.62in. CYLINDER (C); 4.49x1.58in. DISC (D)
- M: DRILLING FLUID ONLY (M); MUD AND MUD CAKE (MK)
- S: SANDSTONE (S); LIMESTONE (L)
- O: OIL BASE MUD (O); WATER BASE MUD (W)
- Z1/Z2/Z3: DRILLING FLUID IDENTIFICATION

OVRT.....OVERSHOOT
STAB VLUE...STABALIZED VALUE
TOT MIN.....TOTAL TIME OF MUD CAKE EFFECT ONLY (minutes)

DESCRIPTION	STEEL ON CAKE			STEEL ON ROCK						
	OVRT	STAB VLUE	TOT MIN	NEXT 30s	NEXT 1MIN	NEXT 2MIN	NEXT 3MIN	NEXT 4MIN	NEXT 5MIN	STAB VLUE
Z1/O/S/M/C/RT/NF	-	-	-	0.21	0.21	0.24	0.24	0.26	0.26	0.16
Z1/O/S/M/C/RT/NF	-	-	-	0.38	0.26	0.24	0.24	0.25	0.23	0.24
Z1/O/S/M/D/RT/NF	-	-	-	0.20	0.26	0.26	0.31	0.35		0.38
Z1/O/S/M/D/RT/NF	-	-	-	0.22	0.20	0.24	0.28	0.28	0.32	0.40
Z2/O/S/M/C/RT/NF	-	-	-	0.33	0.26	0.27	0.24	0.23	0.23	0.23
Z2/O/S/M/C/RT/NF	-	-	-	0.24	0.23	0.22	0.24	0.24	0.24	0.29
Z2/O/S/M/C/170F/NF	-	-	-	0.21	0.19	0.19	0.19	0.21	0.19	0.21
Z2/O/S/M/D/170F/NF	-	-	-	0.30	0.29	0.30	0.38	0.42		0.41
Z2/O/S/M/D/170F/NF	-	-	-	0.27	0.27	0.28	0.27	0.34	0.39	0.36
Z2/O/S/M/D/RT/NF	-	-	-	0.19	0.18	0.24	0.28	0.29	0.27	0.28
Z2/O/S/M/D/RT/NF	-	-	-	0.21	0.16	0.16	0.19	0.21	0.21	0.21
Z3/O/S/M/C/RT/NF	-	-	-	0.21	0.21	0.24	0.26	0.27		0.27
Z3/O/S/M/C/RT/NF	-	-	-	0.21	0.22	0.26	0.30	0.29	0.26	0.26
Z3/O/S/M/D/170F/NF	-	-	-	0.24	0.22	0.28	0.34	0.35		0.35
Z3/O/S/M/D/RT/NF	-	-	-	0.24	0.16	0.15	0.21	0.24	0.27	0.24
Z3/O/S/M/D/RT/NF	-	-	-	0.21	0.18	0.19	0.23	0.30	0.29	0.29
D/W/S/MK/D/RT/30M/NL	0.15	0.05	0.6	0.22	0.32	0.28	0.30	0.28		0.28
D/W/S/MK/C/RT/30M/NL	0.20	0.15	0.3	0.20	0.26	0.31	0.31			0.31
D/W/S/MK/D/RT/2M/NL	NO	0.15	0.1	0.21	0.26	0.24	0.23			0.23
D/W/S/MK/D/RT/2M/NL	NO	0.20	0.1	0.20	0.25	0.26	0.26	0.25		0.25
D/W/S/M/D/RT/NF/NL	-	-	-	0.25	0.23	0.23	0.24	0.24		0.24
D/W/S/M/D/RT/NF/NL	-	-	-	0.34	0.28	0.26	0.26	0.26		0.26
D/W/S/M/D/RT/NF/NL	-	-	-	0.25	0.28	0.25	0.24	0.25		0.24
D/W/S/M/C/RT/NF/NL	-	-	-	0.35	0.31	0.23	0.23	0.23		0.23
D/W/S/MK/D/RT/30M/L	0.27	0.16	2.7	0.21	0.24	0.24	0.27	0.29	0.28	0.28
D/W/S/MK/D/RT/30M/L	0.24	0.11	2.4	0.16	0.16	0.21	0.26	0.28	0.27	0.27
D/W/S/MK/D/RT/2M/L	NO	0.16	0.2	0.19	0.23	0.30	0.31	0.30		0.28
D/W/S/M/D/RT/NF/L	-	-	-	0.28	0.26	0.27	0.27	0.26		0.26
D/W/S/M/D/RT/NF/L	-	-	-	0.23	0.24	0.24	0.24	0.24		0.24
D/W/L/MK/D/RT/30M/NL	0.40	NO	2.4	0.13	0.20	0.22	0.21			0.21
D/W/L/MK/D/RT/30M/NL	0.31	0.22	1.6	0.31	0.31	0.22	0.19	0.21		0.21
D/W/L/MK/D/RT/2M/NL	NO	0.24	0.5	0.27	0.28	0.25	0.21	0.20		0.20
D/W/L/MK/D/RT/2M/NL	NO	0.25	0.2	0.26	0.27	0.25	0.26	0.27		0.28
D/W/L/MK/D/RT/2M/NL	NO	0.20	0.4	0.24	0.27	0.25	0.23			0.21
D/W/L/MK/D/RT/2M/NL	0.24	0.21	0.6	0.27	0.35	0.31	0.26	0.24		0.23
D/W/L/MK/D/RT/2M/NL	0.21	0.17	0.7	0.20	0.28	0.29	0.21	0.19		0.19
D/W/L/M/D/RT/NF/NL	-	-	-	0.37	0.30	0.23	0.18	0.16		0.16
C/W/S/MK/D/RT/30M/NL	RECORDING FAIL.			0.27	0.28	0.34	0.34	0.32		0.29
C/W/S/M/D/RT/NF/NL	-	-	-	RECORD. FAIL.			0.29	0.30		0.21
C/W/S/M/D/RT/NF/L	-	-	-	0.34	0.30	0.27	0.25	0.22		0.12
B/W/S/MK/D/RT/30M/NL	0.53	0.16	4.7	0.21	0.27	0.19	0.19	0.19	0.18	0.14
B/W/S/M/D/RT/NF/NL	-	-	-	0.24	0.22	0.18	0.14	0.11	0.11	0.11
B/W/S/MK/D/RT/30M/L	0.33	0.13	7.0	0.15	0.17	0.18	0.19	0.17		0.17
B/W/S/MK/D/RT/2M/L	0.16	0.08	0.8	0.15	0.18	0.25	0.25	0.22	0.21	0.21
B/W/S/MK/D/RT/2M/L	NO	0.11	1.4	0.13	0.13	0.15	0.16	0.16		0.16
B/W/S/M/D/RT/NF/L	-	-	-	0.19	0.21	0.21	0.20	0.19	0.18	0.18
A4/W/S/MK/D/RT/30M/NL	0.60	0.19	0.4	0.20	0.23	0.26	0.24	0.24	0.23	0.23
A4/W/S/MK/D/RT/2M/NL	0.40	0.21	0.3	0.20	0.24	0.25	0.26	0.25		0.25
A4/W/S/MK/D/RT/2M/NL	0.38	NO	0.2	0.21	0.23	0.27	0.27	0.24	0.23	0.23
A4/W/S/M/D/RT/NF/NL	-	-	-	0.24	0.27	0.24	0.23	0.23	0.23	0.23
A4/W/S/MK/D/RT/30M/L	0.37	0.26	1.0	0.18	0.21	0.24	0.23	0.23	0.23	0.23
A4/W/S/M/D/RT/NF/L	-	-	-	0.26	0.26	0.26	0.24	0.23	0.23	0.23
A3/W/S/MK/D/RT/30M/NL	0.46	0.26	0.5	0.24	0.23	0.24	0.24	0.25	0.26	0.26
A3/W/S/MK/D/RT/2M/NL	0.27	NO	0.1	0.23	0.25	0.27	0.26	0.27		0.27
A3/W/S/MK/D/RT/2M/NL	0.47	0.25	0.5	0.21	0.21	0.22	0.23			0.23
A3/W/S/M/D/RT/NF/NL	-	-	-	0.27	0.28	0.27	0.26	0.24	0.21	0.21
A2/W/S/MK/D/RT/30M/NL	0.25	0.15	1.2	0.21	0.28	0.27	0.24	0.23	0.21	0.21
A2/W/S/MK/D/RT/2M/NL	0.19	0.15	0.1	0.19	0.21	0.23	0.21	0.21		0.21
A2/W/S/MK/D/RT/2M/NL	0.24	0.18	0.1	0.21	0.25	0.25	0.22	0.21	0.21	0.21
A2/W/S/M/D/RT/NF/NL	-	-	-	0.27	0.29	0.26	0.23	0.20	0.17	0.17
A1/W/S/MK/D/RT/30M/NL	0.44	0.21	1.3	0.23	0.29	0.28	0.27	0.27		0.27
A1/W/S/MK/D/RT/2M/NL	0.48	0.20	0.5	0.21	0.23	0.24	0.24			0.24
A1/W/S/MK/D/RT/2M/NL	0.56	0.18	0.3	0.21	0.25	0.27	0.27	0.25		0.25
A1/W/S/M/D/RT/NF/NL	-	-	-	0.24	0.23	0.23	0.22	0.22		0.22

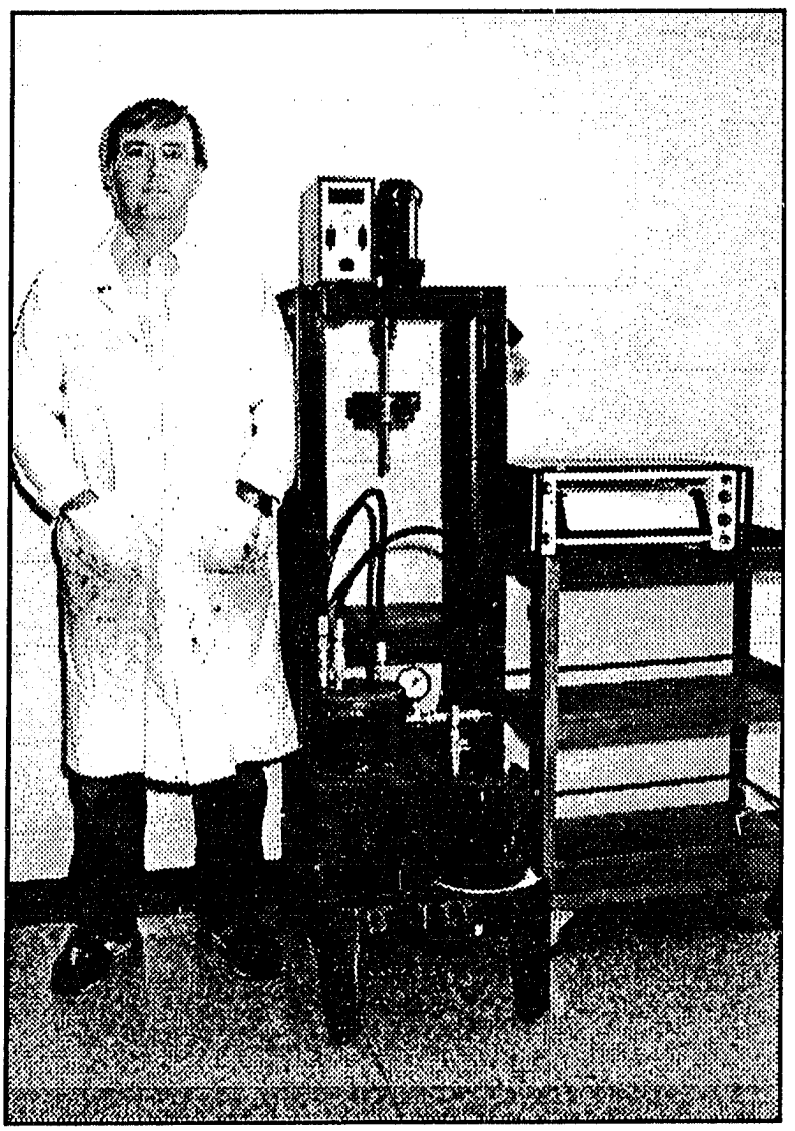

Fig. 1 - Filtration stage of the medium-scale laboratory apparatus.

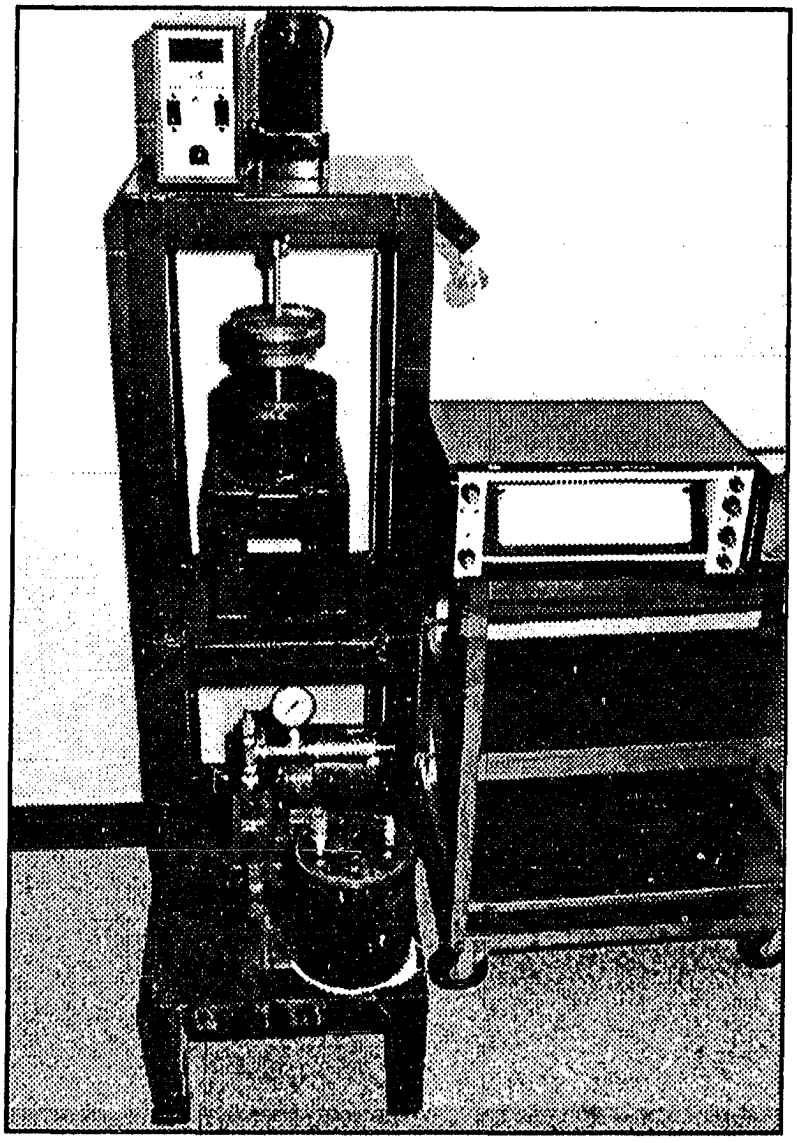

Fig. 2 - Experimental setup for friction factor evaluation using the medium-scale laboratory apparatus.

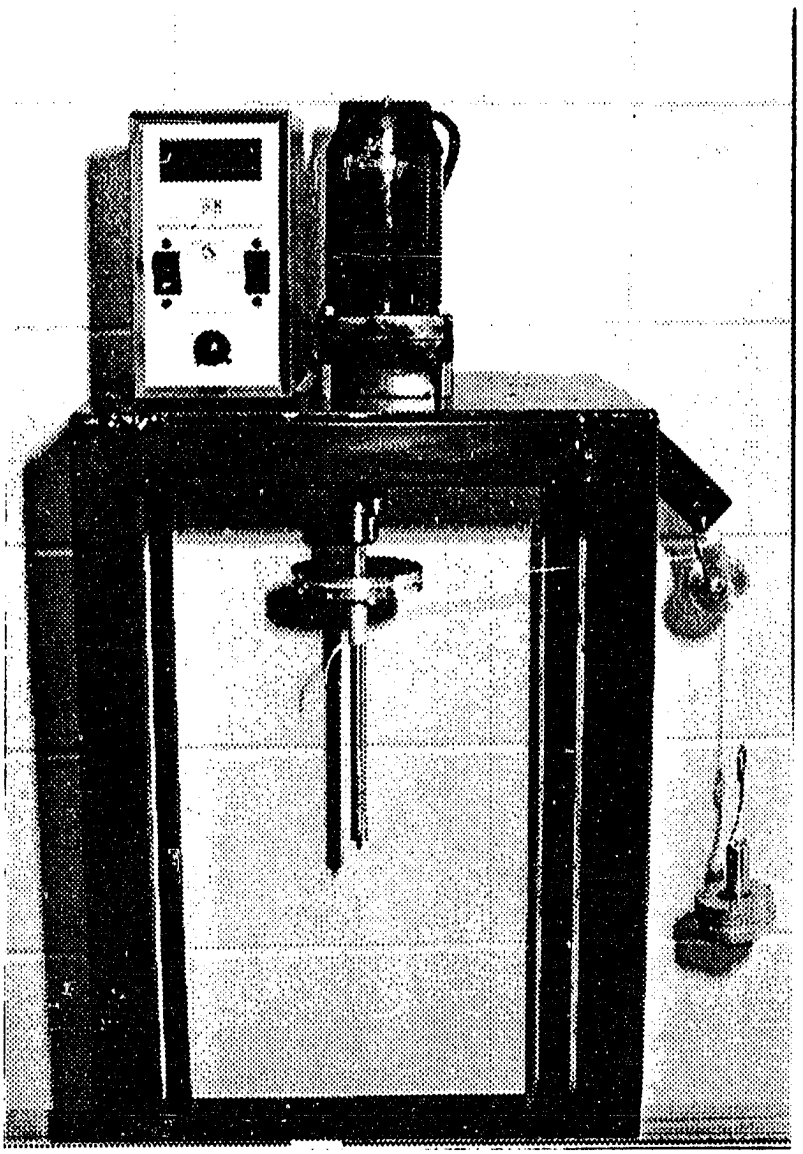

Fig. 3 - Calibration procedure for the medium-scale laboratory apparatus.

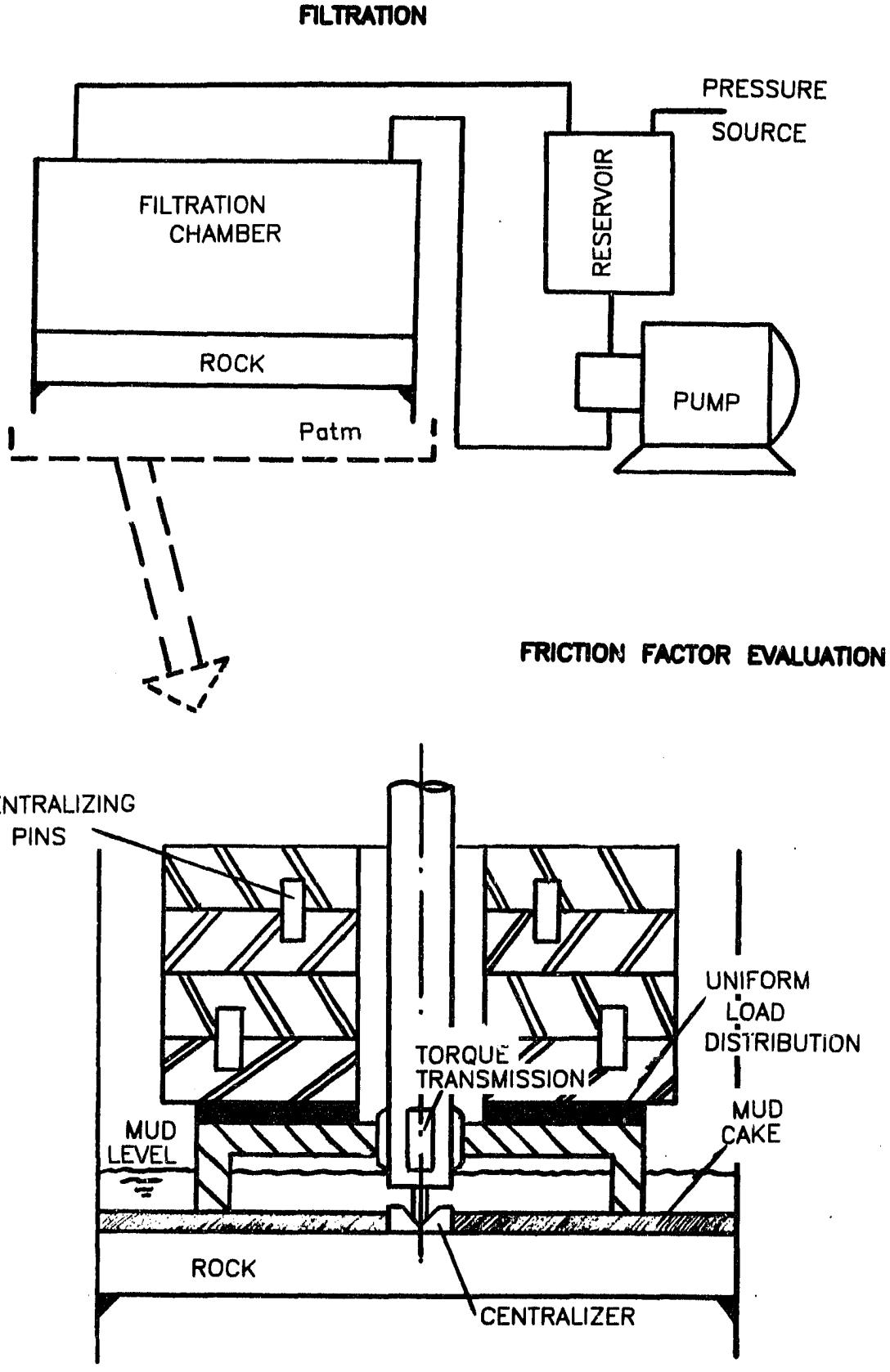

Fig. 4 - Functional diagram for the medium-scale laboratory apparatus.

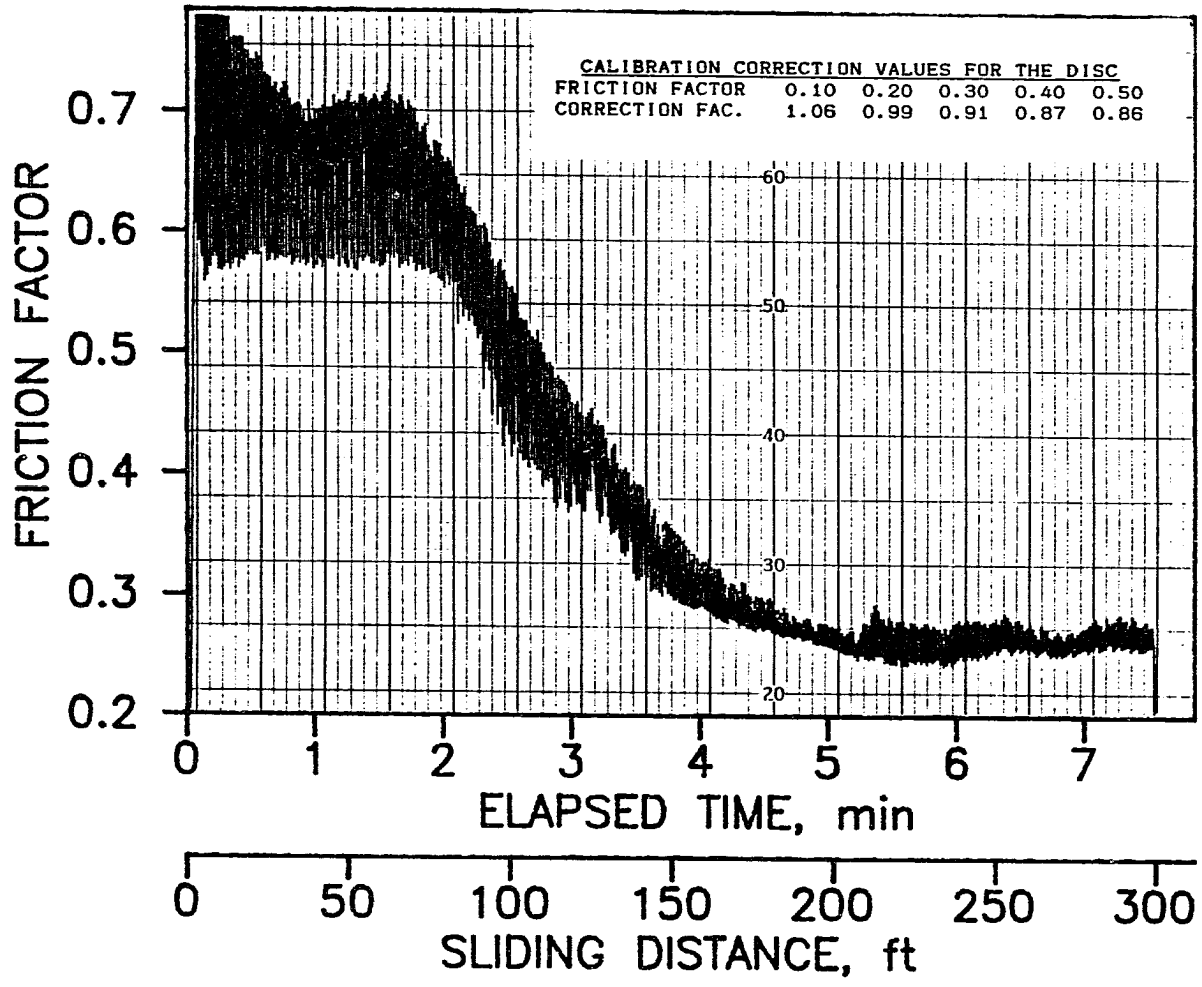

Fig. 5 - Friction factor values using the disc on sandstone and water as a lubricating agent.

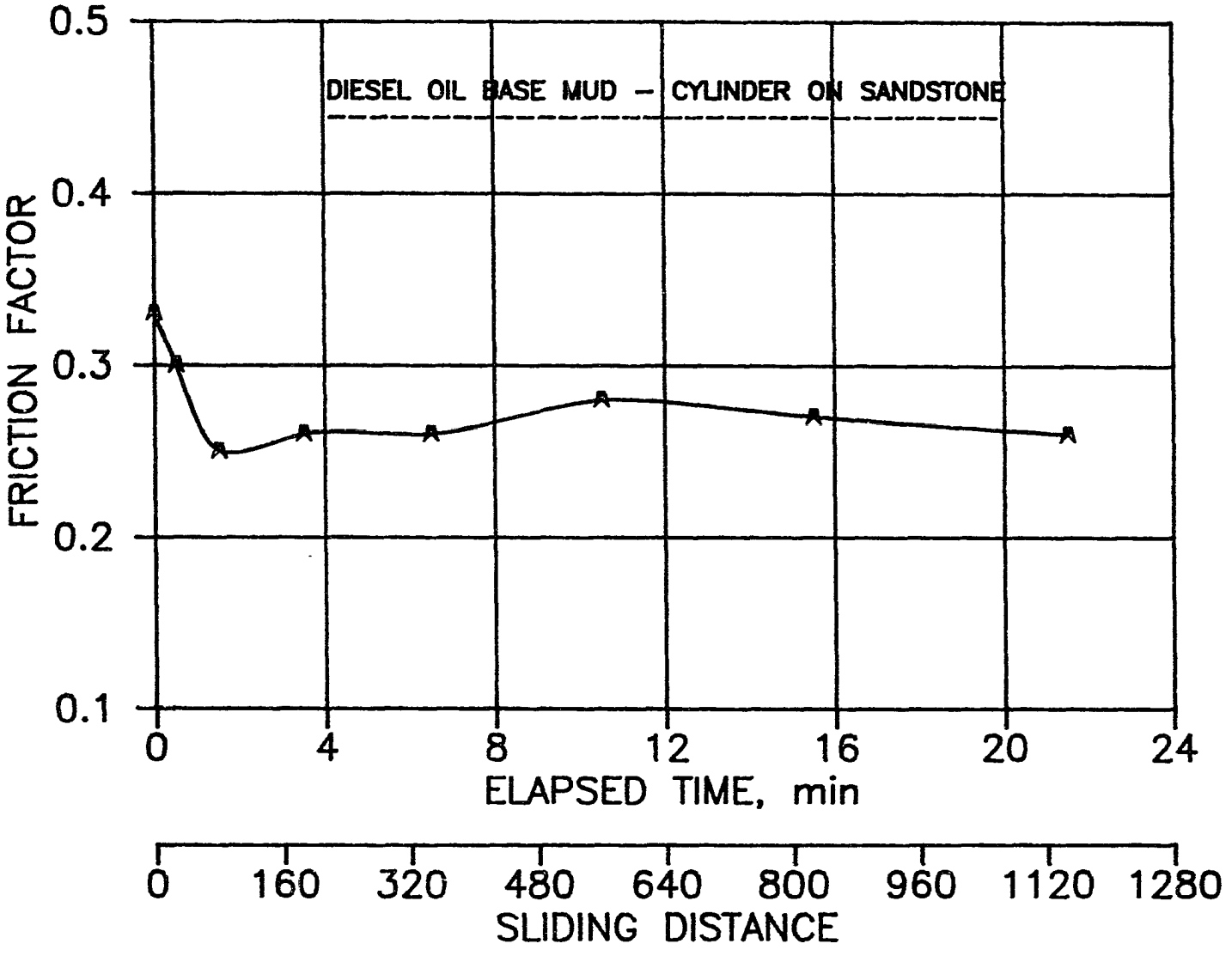

Fig. 6 - Typical frictional response for the cylinder in diesel oil base muds.

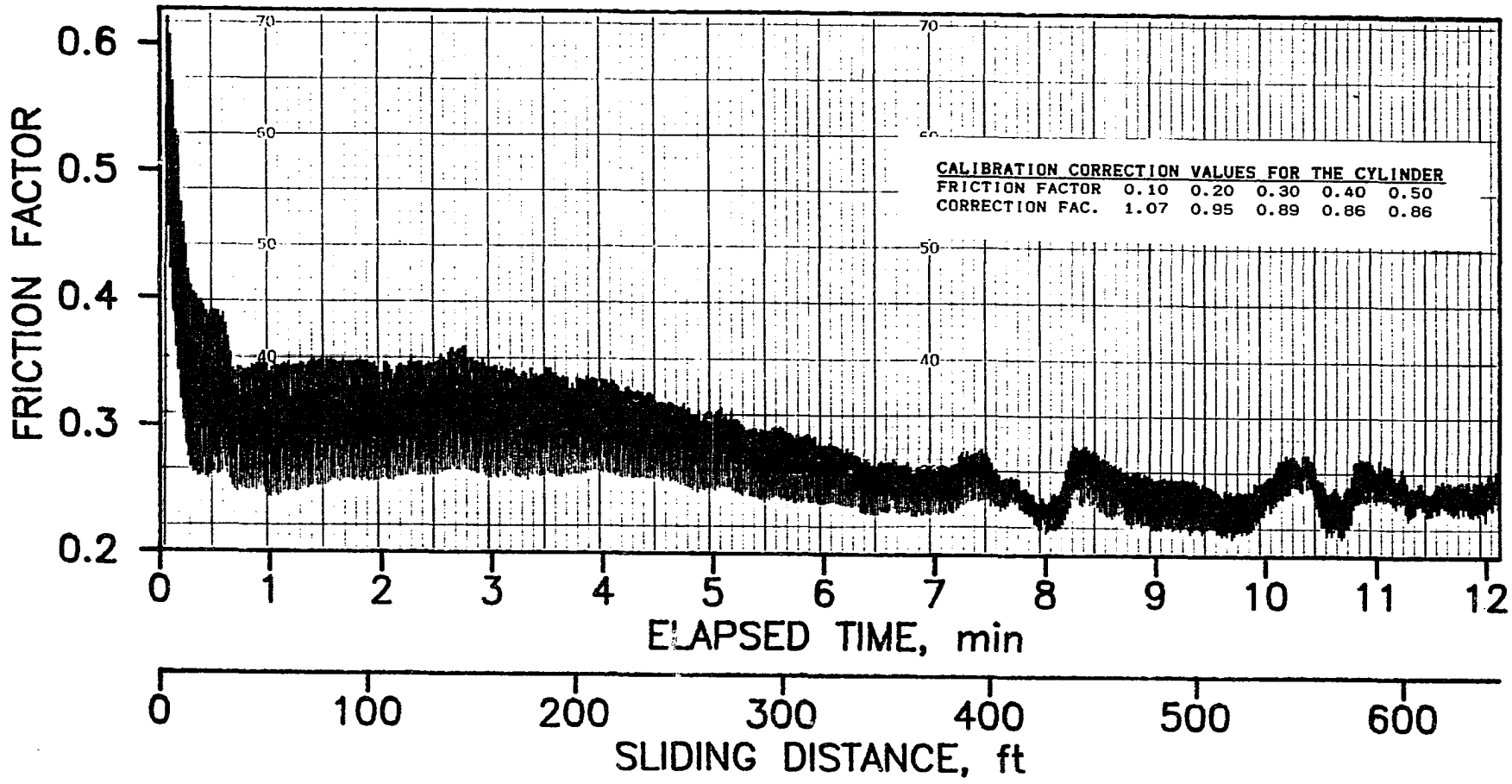

Fig. 7 - Experiment record for an oil base mud, on sandstone, using the cylinder - Z2/O/S/M/C/RT/NF.

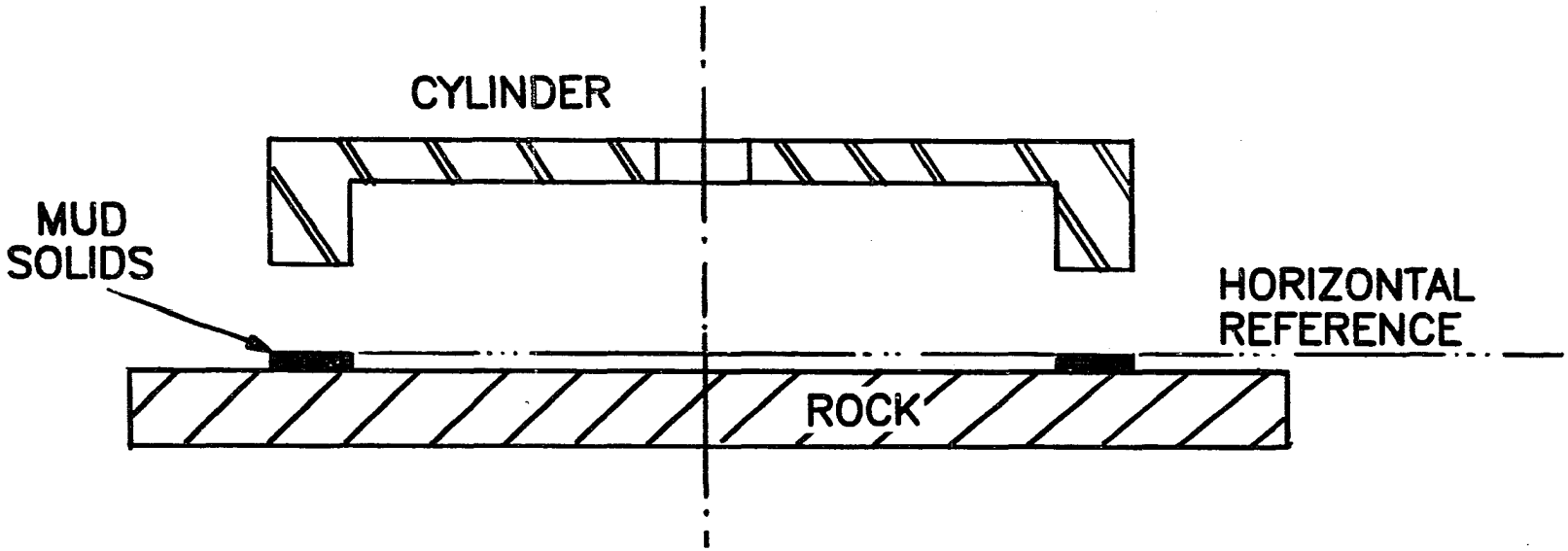

Fig. 8 - Schematics of solids deposition using oil base muds and the cylinder.

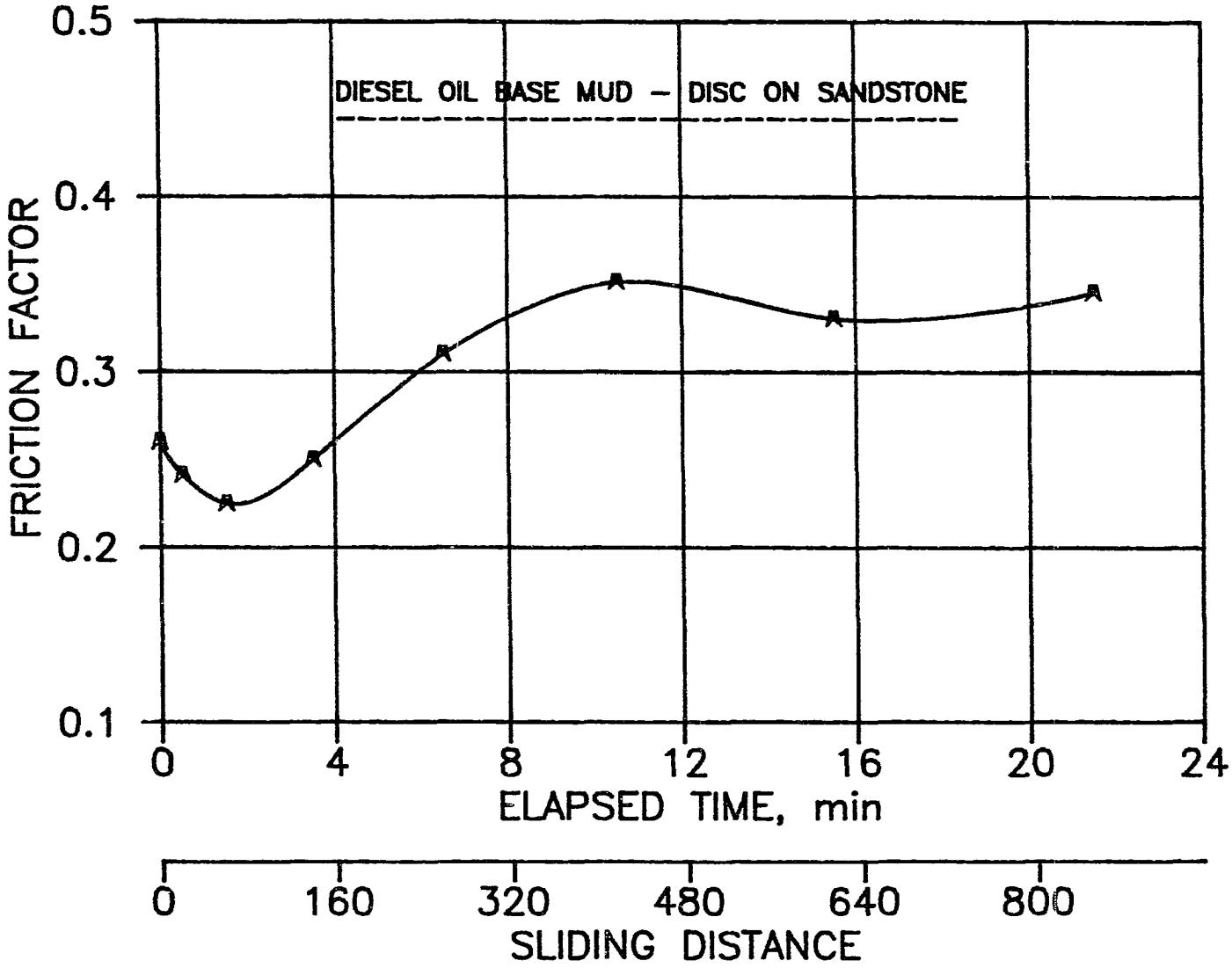

Fig. 9 - Typical frictional response for the disc in diesel oil base muds.

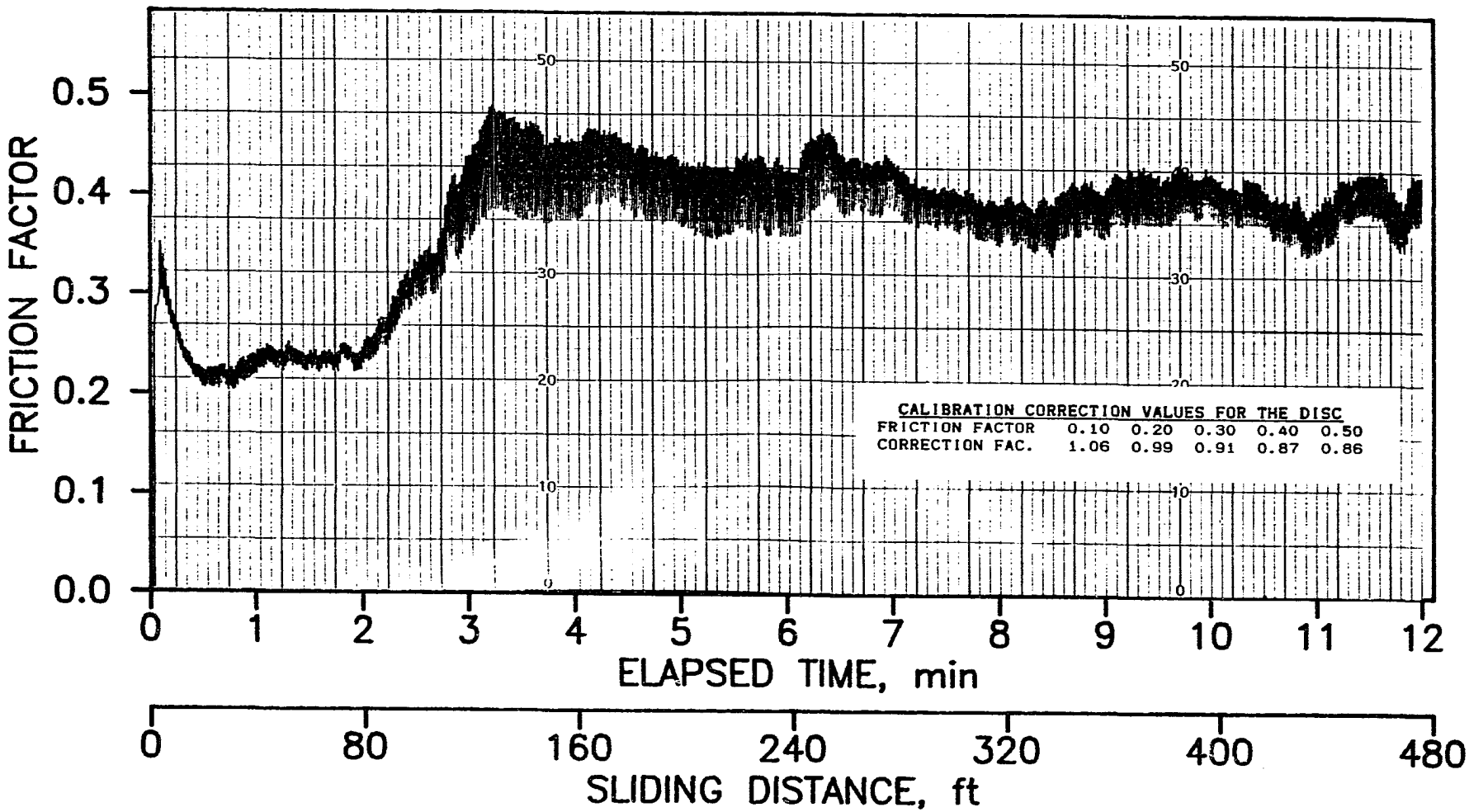

Fig. 10 - Experiment record for an oil base mud, on sandstone, using the disc - Z3/O/S/M/D/170F/NF.

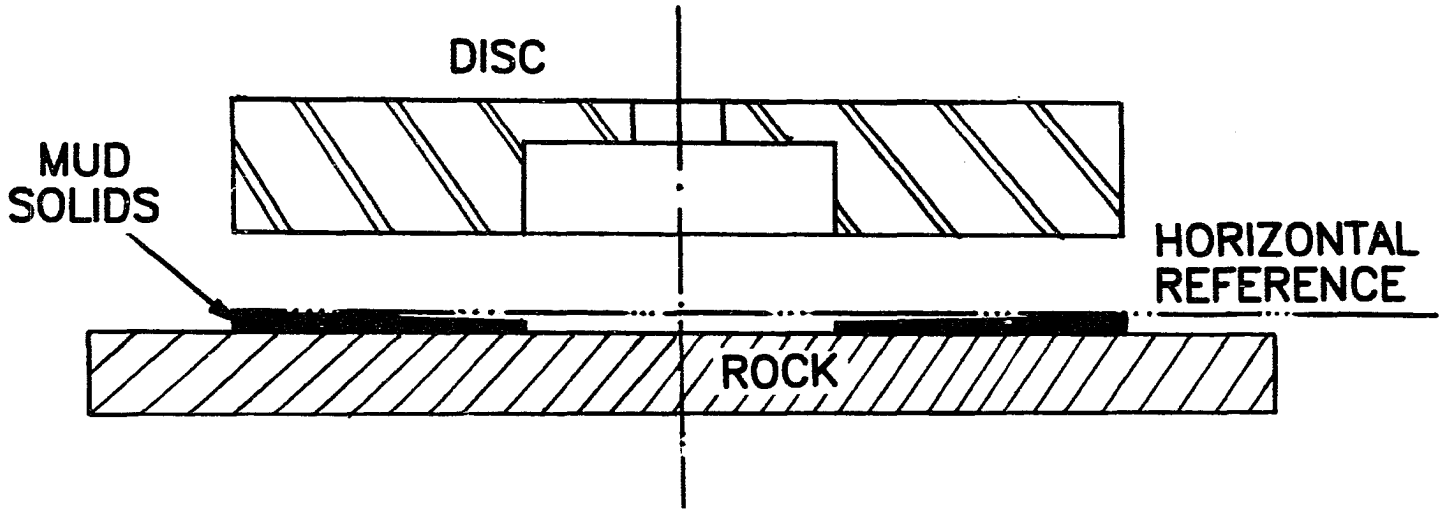

Fig. 11 - Schematics of solids deposition using oil base muds and the disc.

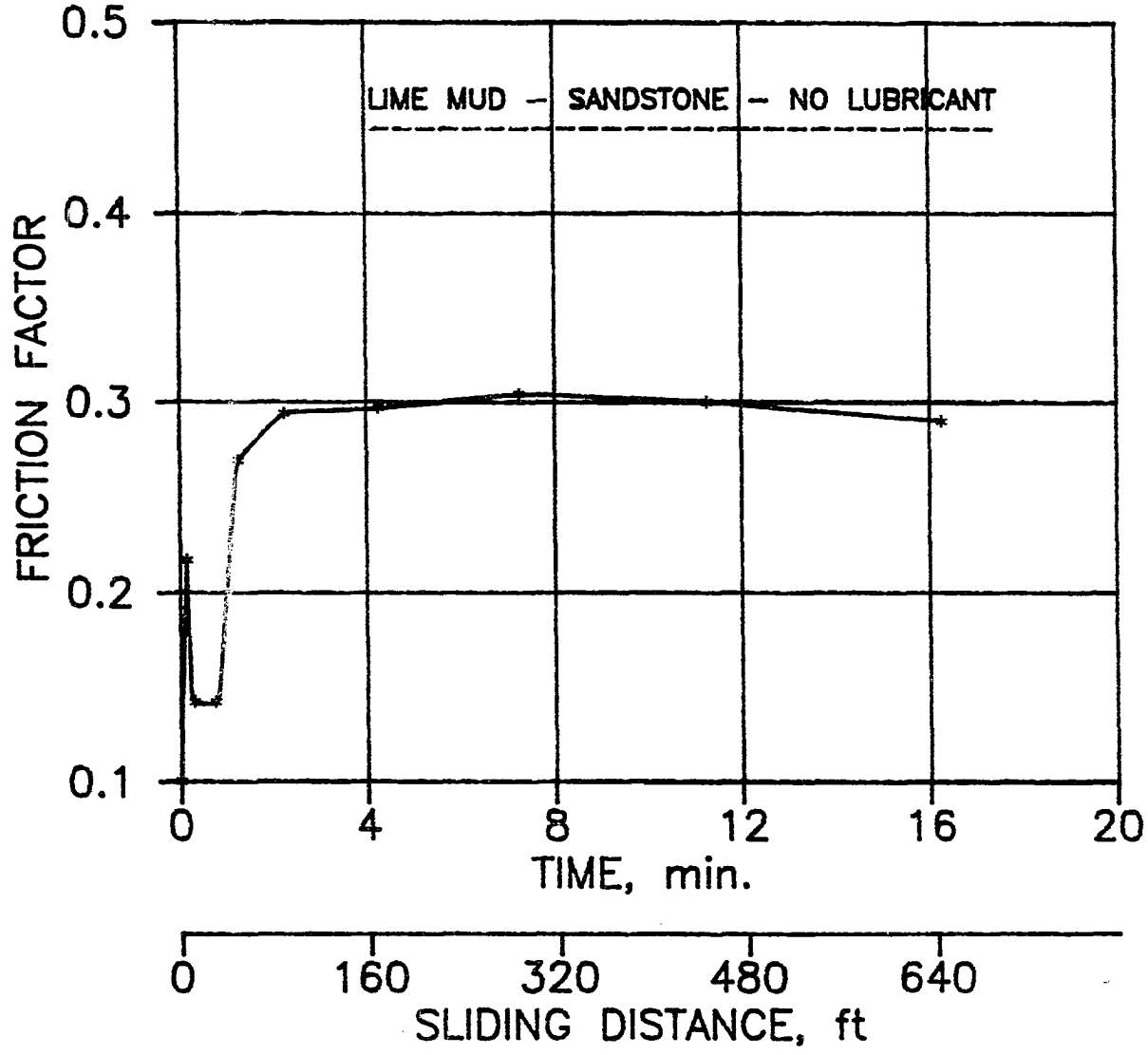

Fig. 12 - Typical frictional response for the lime mud, on sandstone with no lubricant addition.

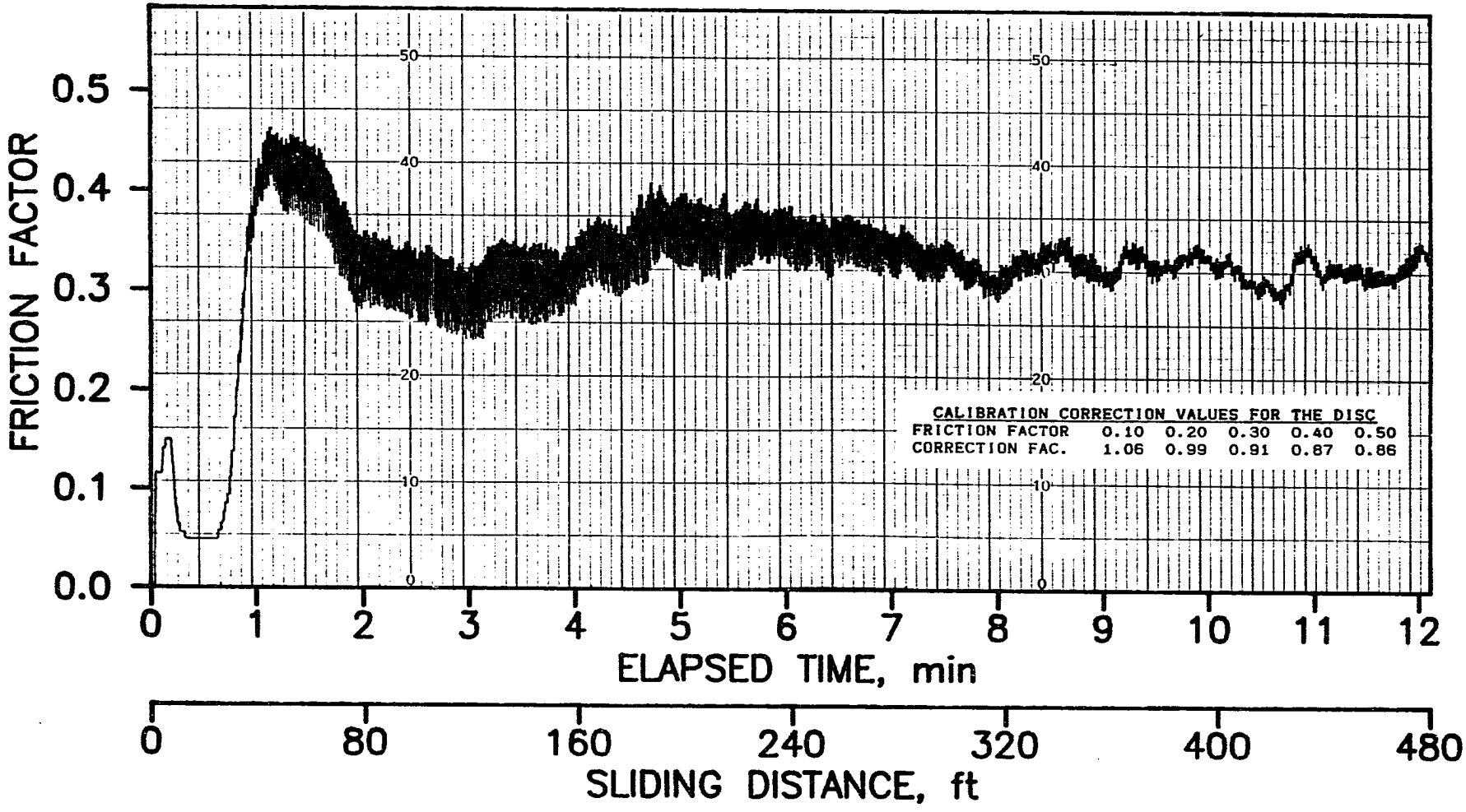

Fig. 13 - Experiment record for a lime mud, on sandstone, after a 30 min. filtration period, using the disc - D/W/S/MK/D/RT/30M/NL.

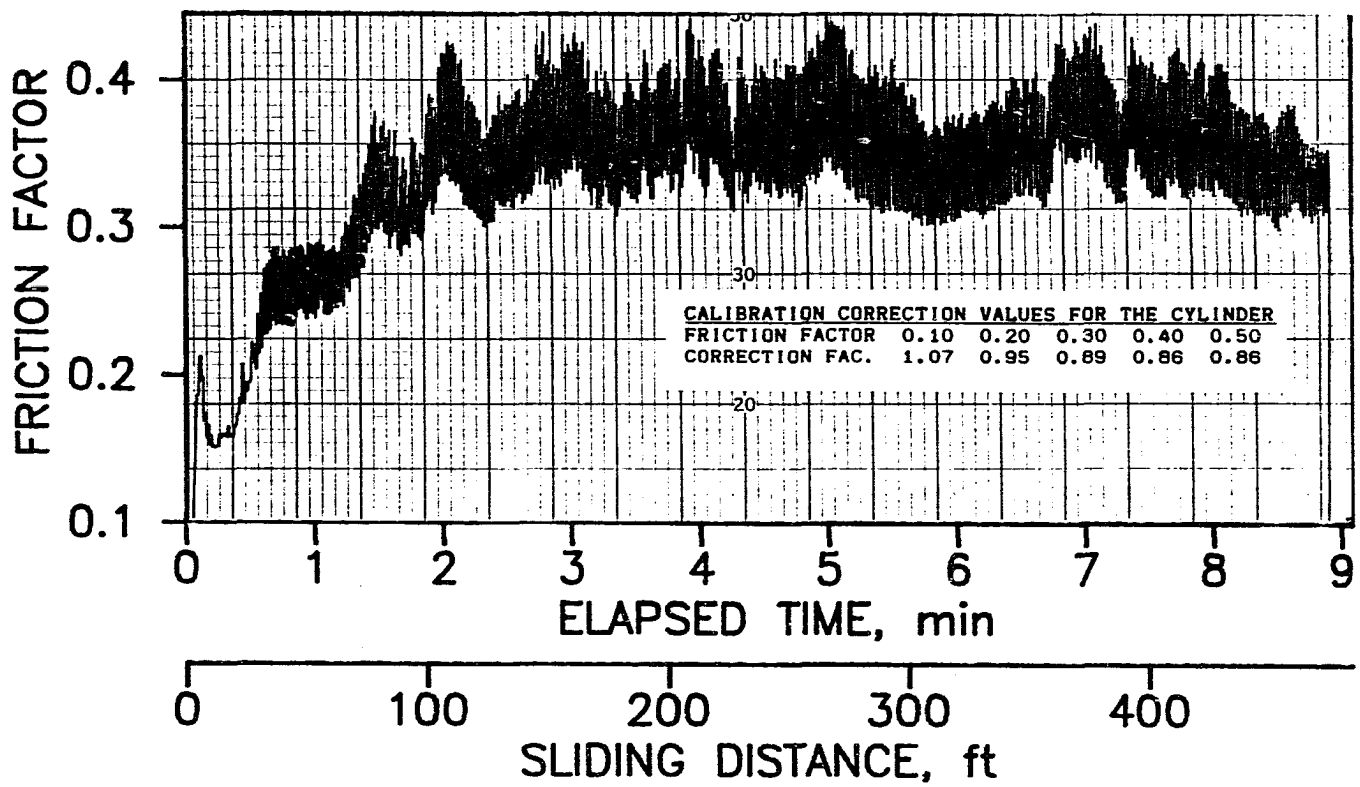

Fig. 14 - Experiment record for a lime mud, on sandstone, after a 30 min. filtration period, using the cylinder - D/W/S/MK/C/RT/30M/NL.

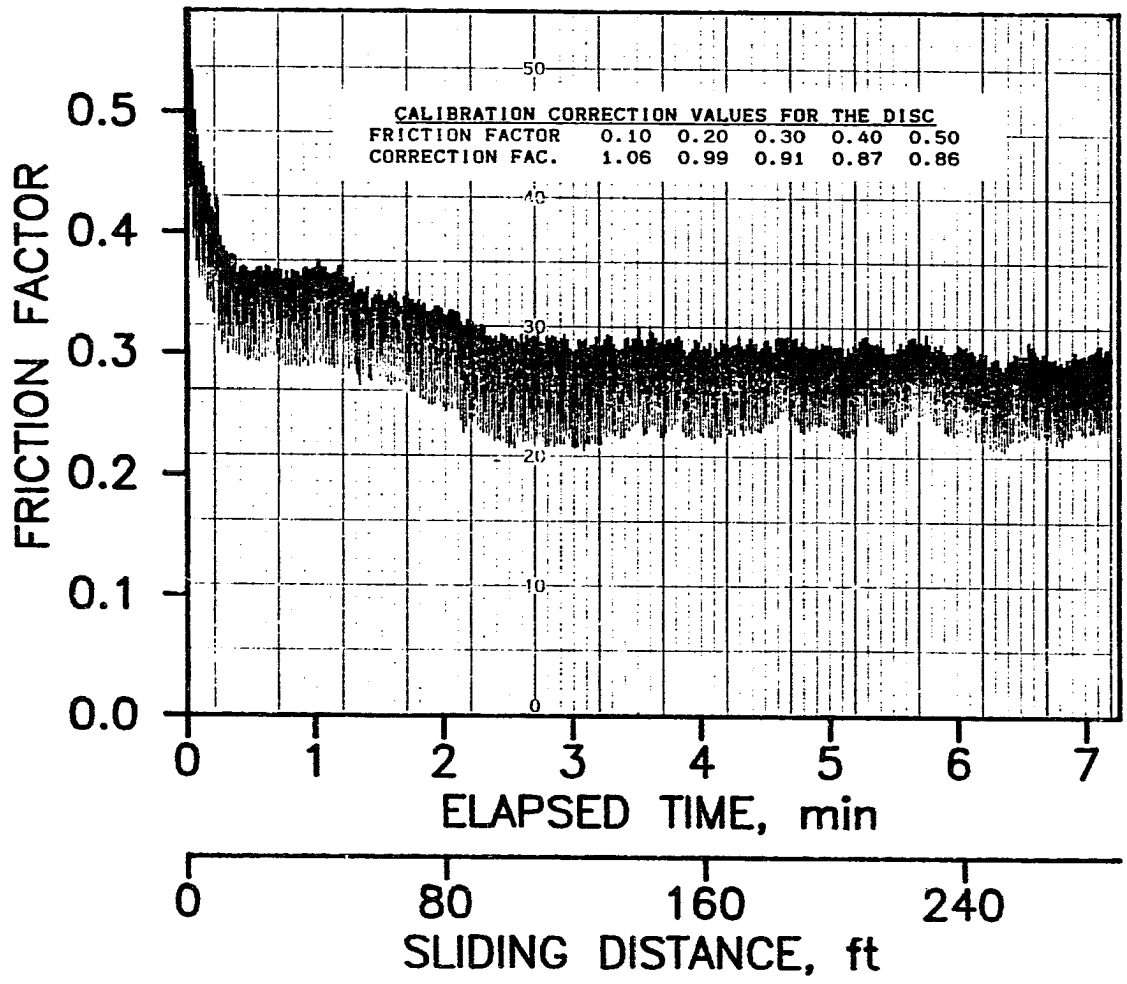

Fig. 15 - Experiment record for a lime mud, on sandstone, using drilling fluid only and the disc - D/W/S/M/D/RT/NF/NL.

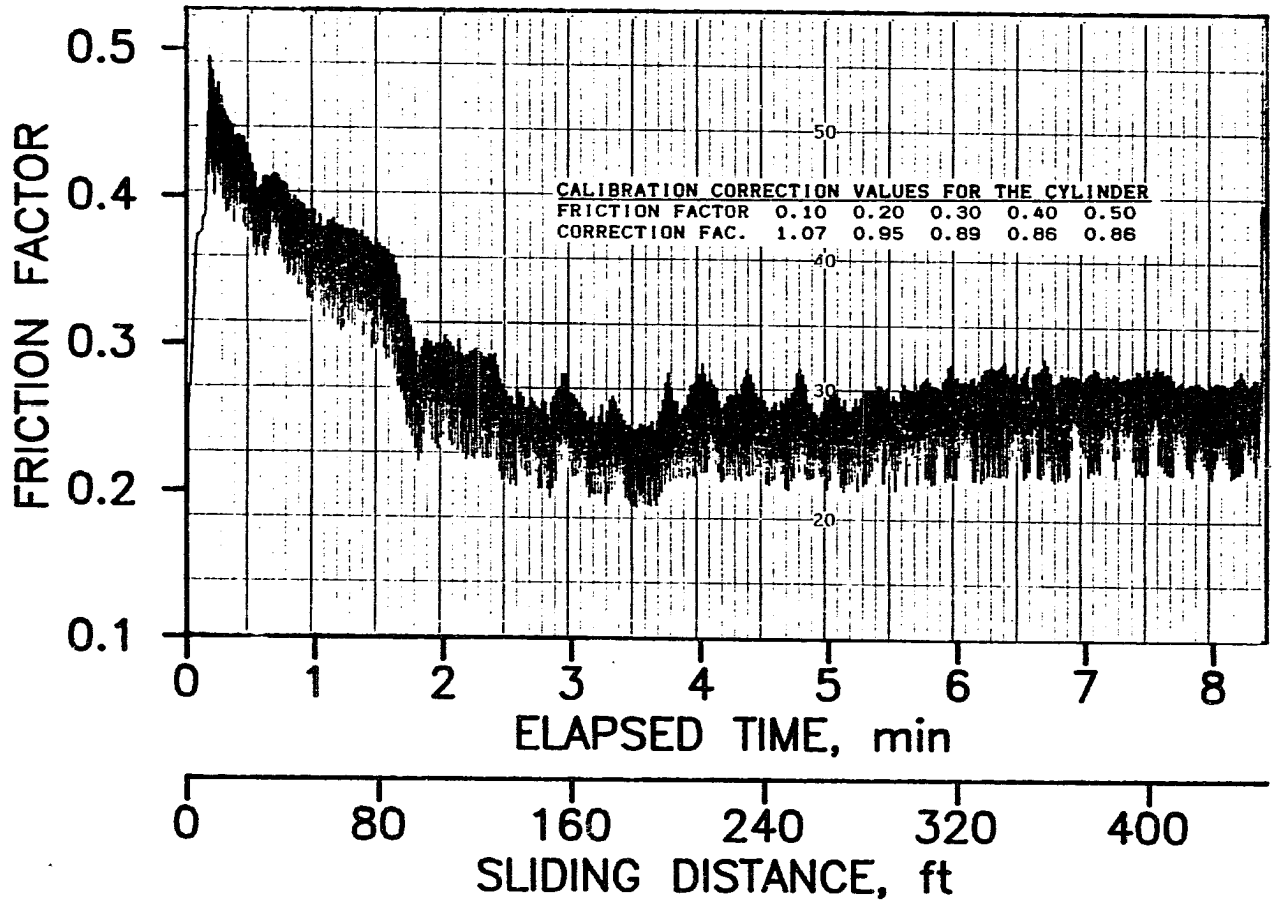

Fig. 16 - Experiment record for a lime mud, on sandstone, using drilling fluid only and the cylinder - D/W/S/M/C/RT/NF/NL.

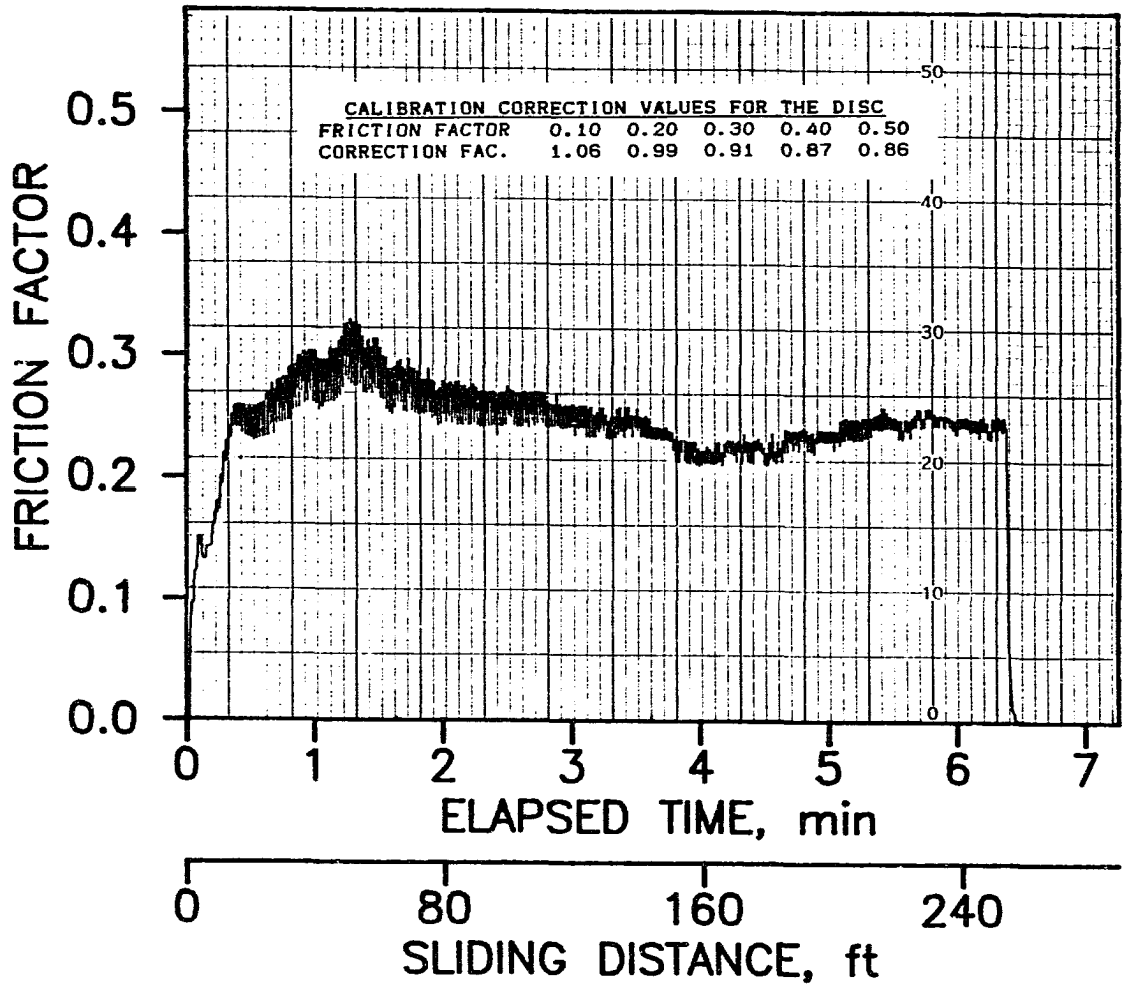

Fig. 17 - Experiment record for a lime mud, on sandstone, after a 2 min. filtration period, using the disc - D/W/S/MK/D/RT/2M/NL.

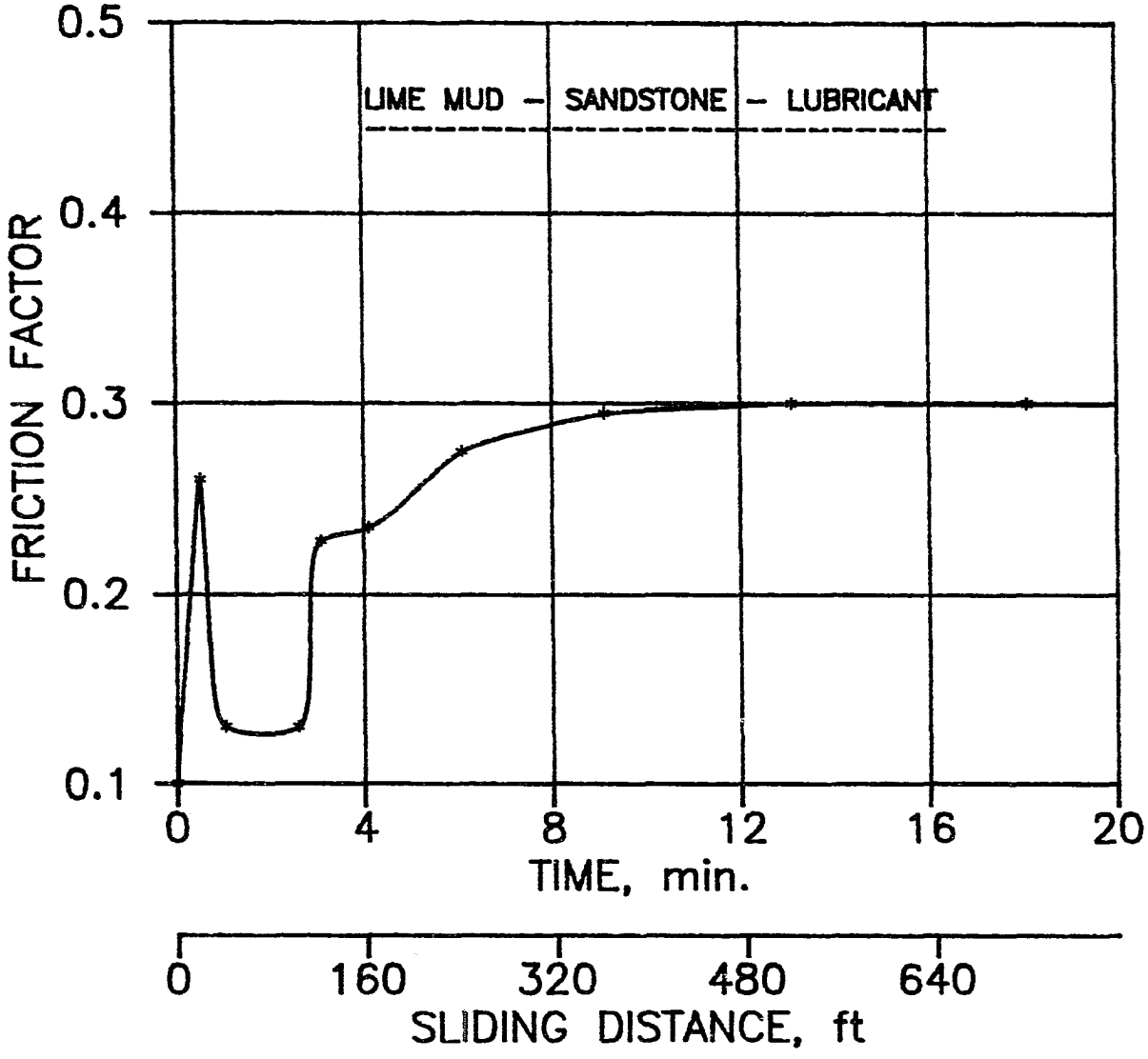

Fig. 18 - Typical frictional response for the lime mud and lubricant, on sandstone.

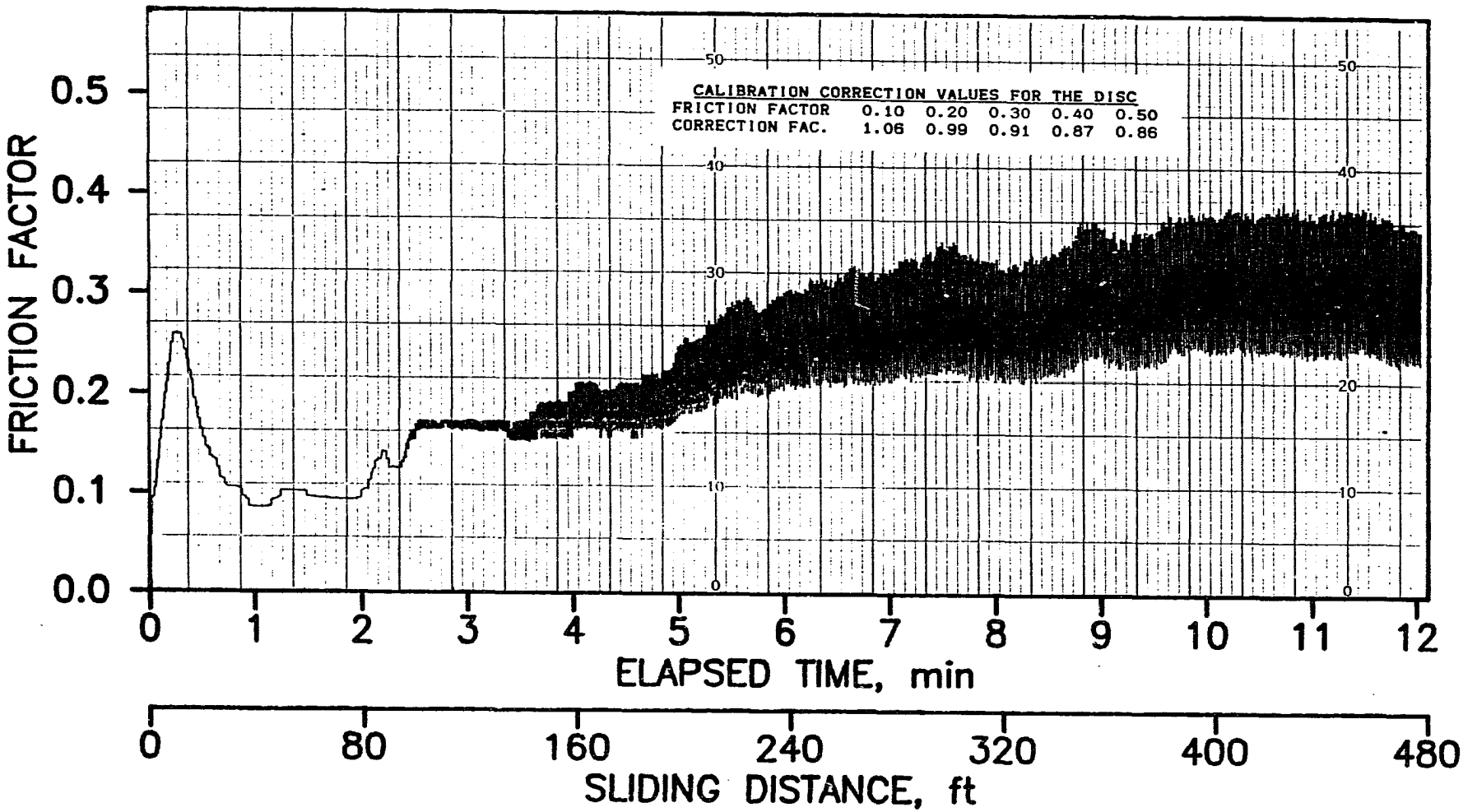

Fig. 19 - Experiment record for a lime mud and lubricant, on sandstone, after a 30 min. filtration period, using the disc - D/W/S/MK/D/RT/30M/L.

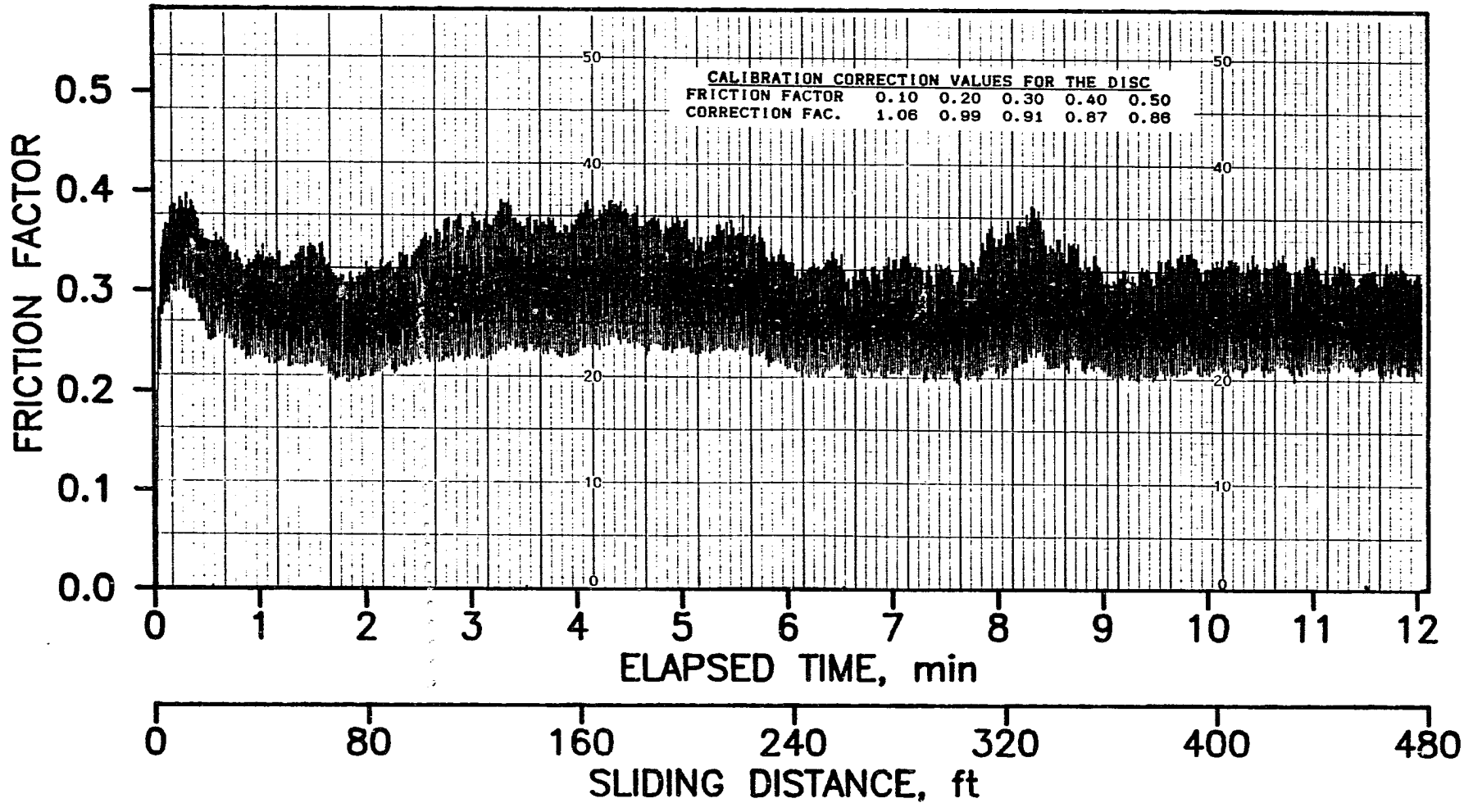

Fig. 20 - Experiment record for a lime mud and lubricant, on sandstone, using drilling fluid only and the disc - D/W/S/M/D/RT/NF/NL.

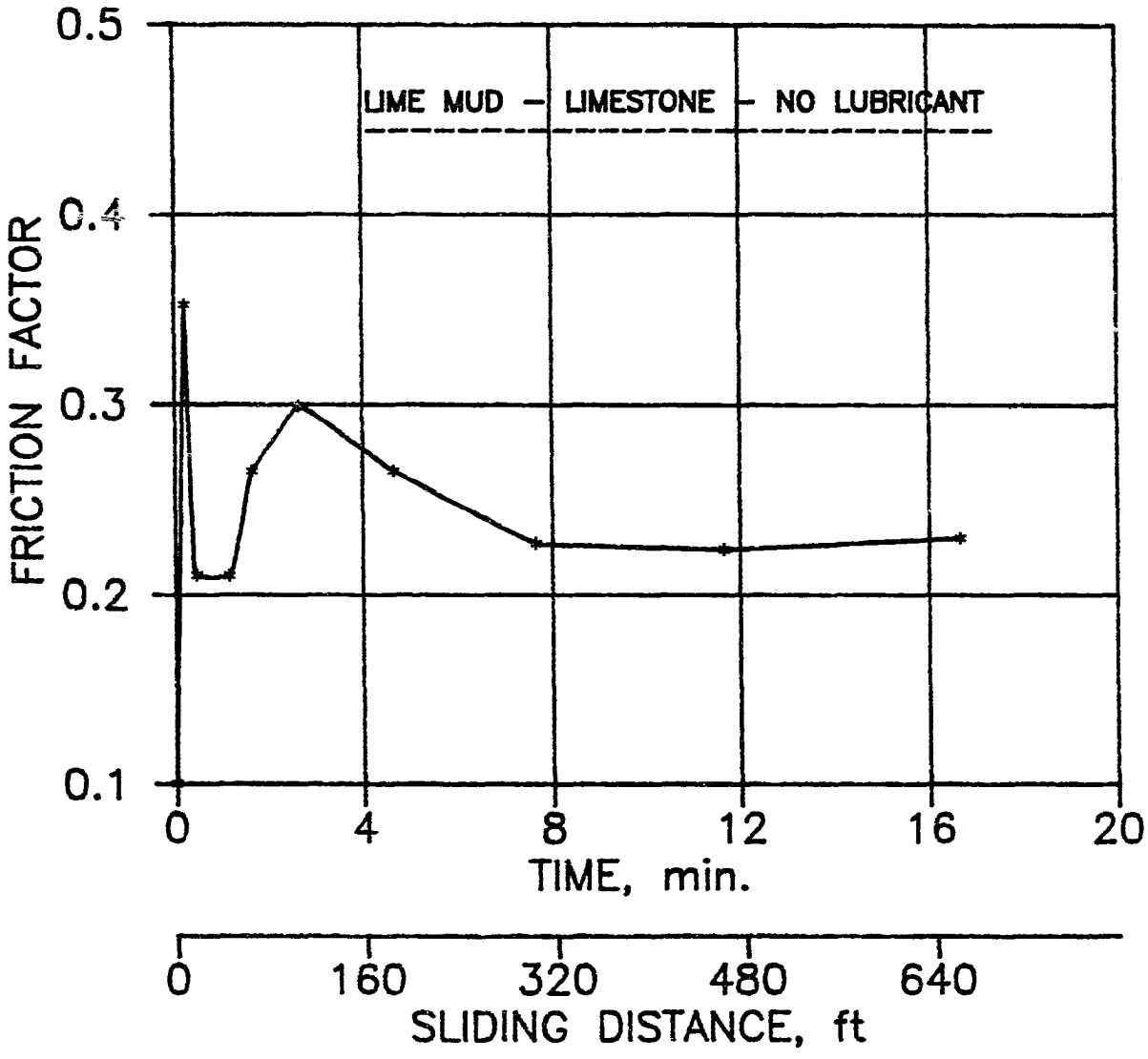

Fig. 21 - Typical frictional response for lime mud, on limestone with no lubricant addition.

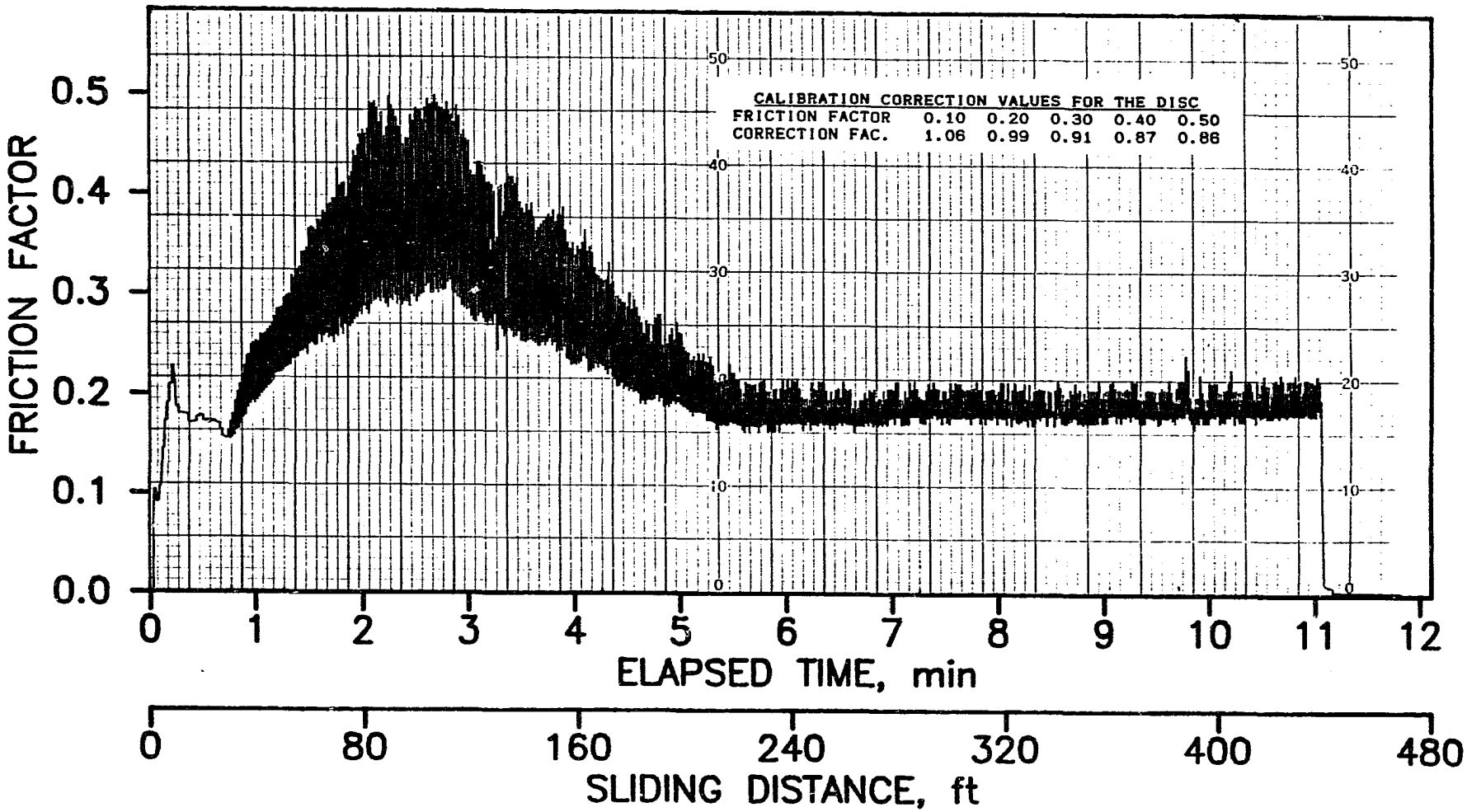

Fig. 22 - Experiment record for a lime mud, on limestone, after a 2 min. filtration period, using the disc - D/W/L/MK/D/RT/2M/NL.

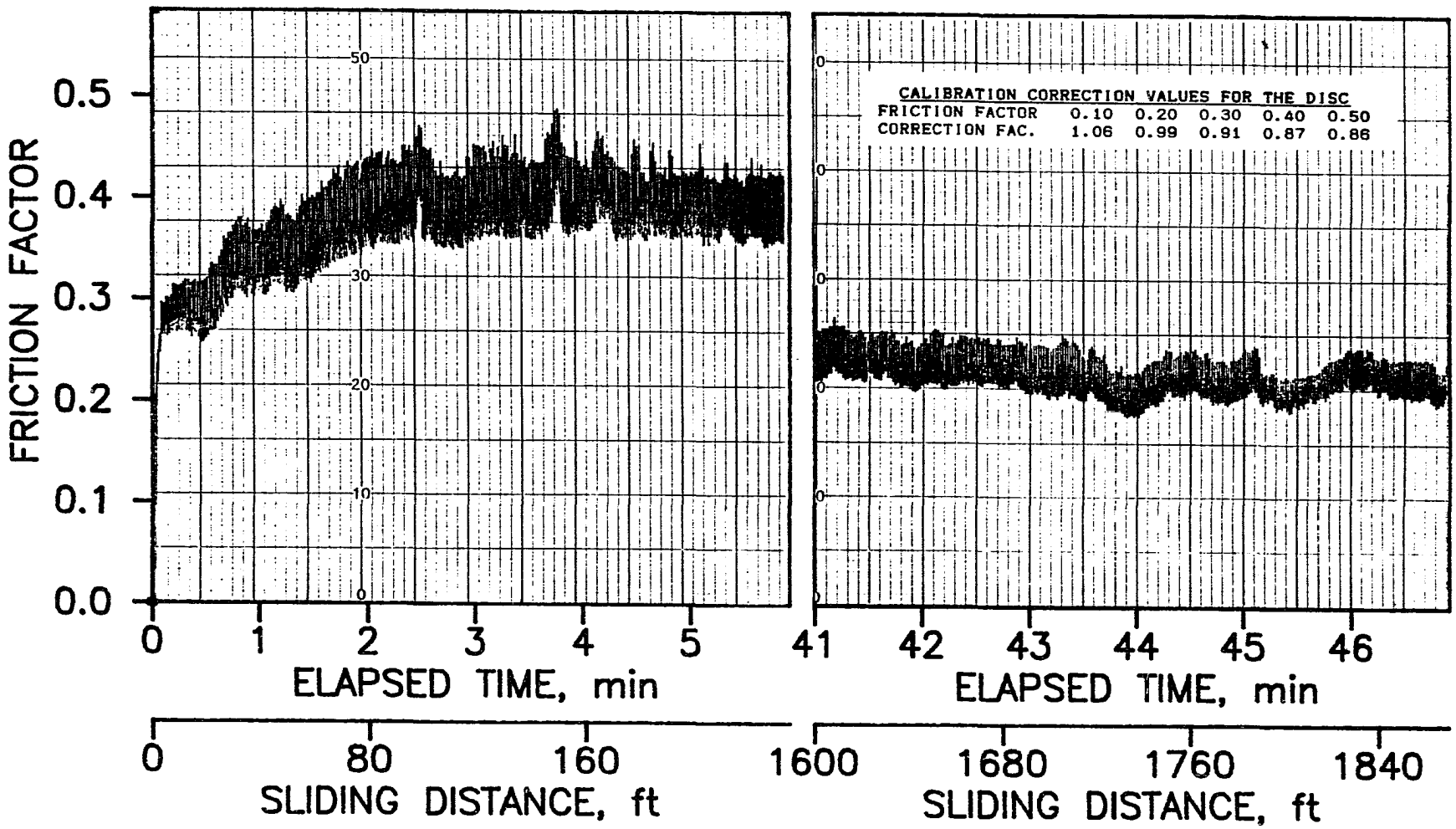

Fig. 23 - Experiment record for a lightly treated lignos. fresh. mud, on sandstone, after a 30 min. filtration period, using the disc - C/W/S/MK/D/RT/30M/NL.

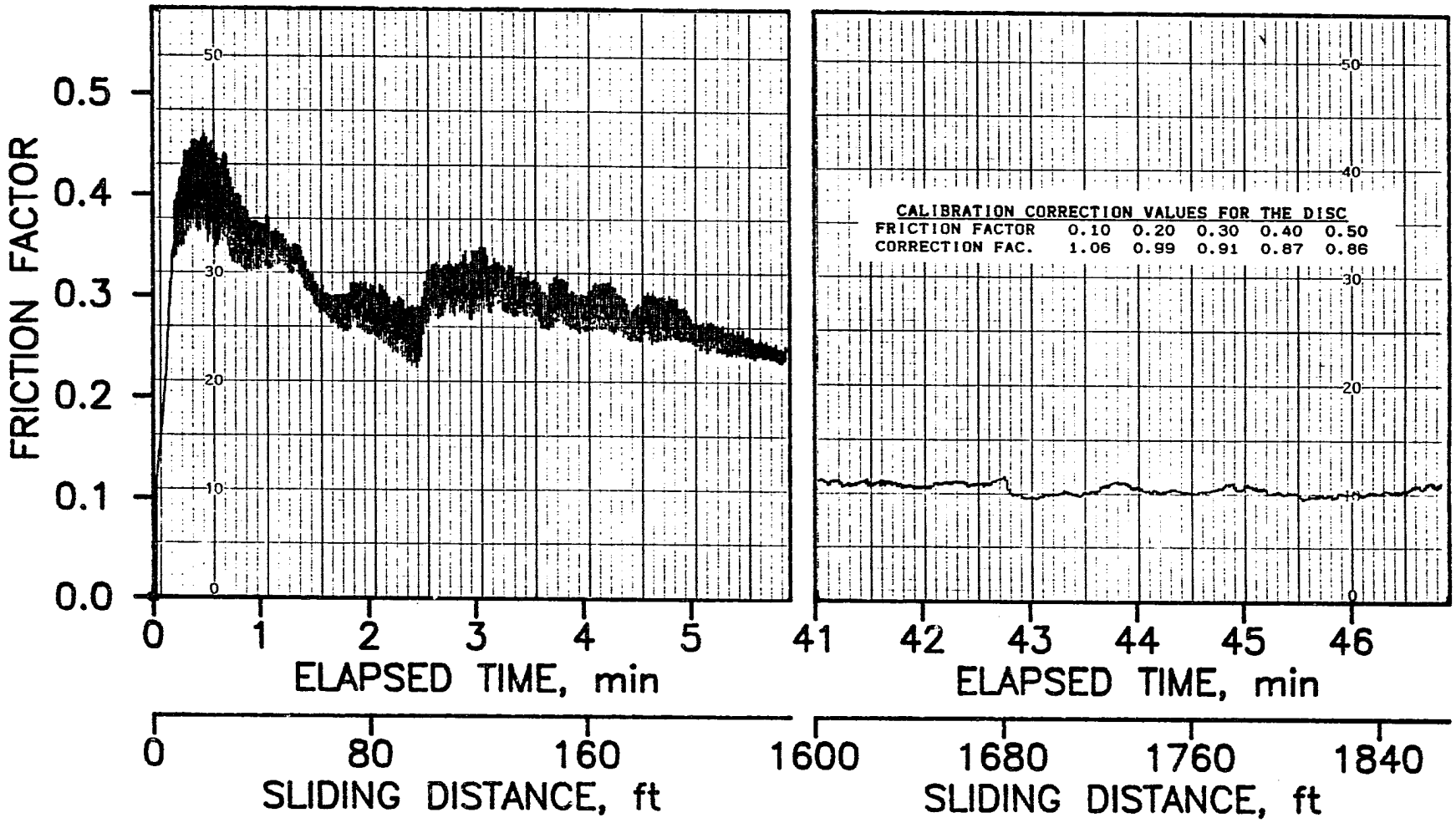

Fig. 24 - Experiment record for a lightly treated lignos. fresh. mud with lubricant, on sandstone, using the disc - C/W/S/MK/D/RT/NF/L.

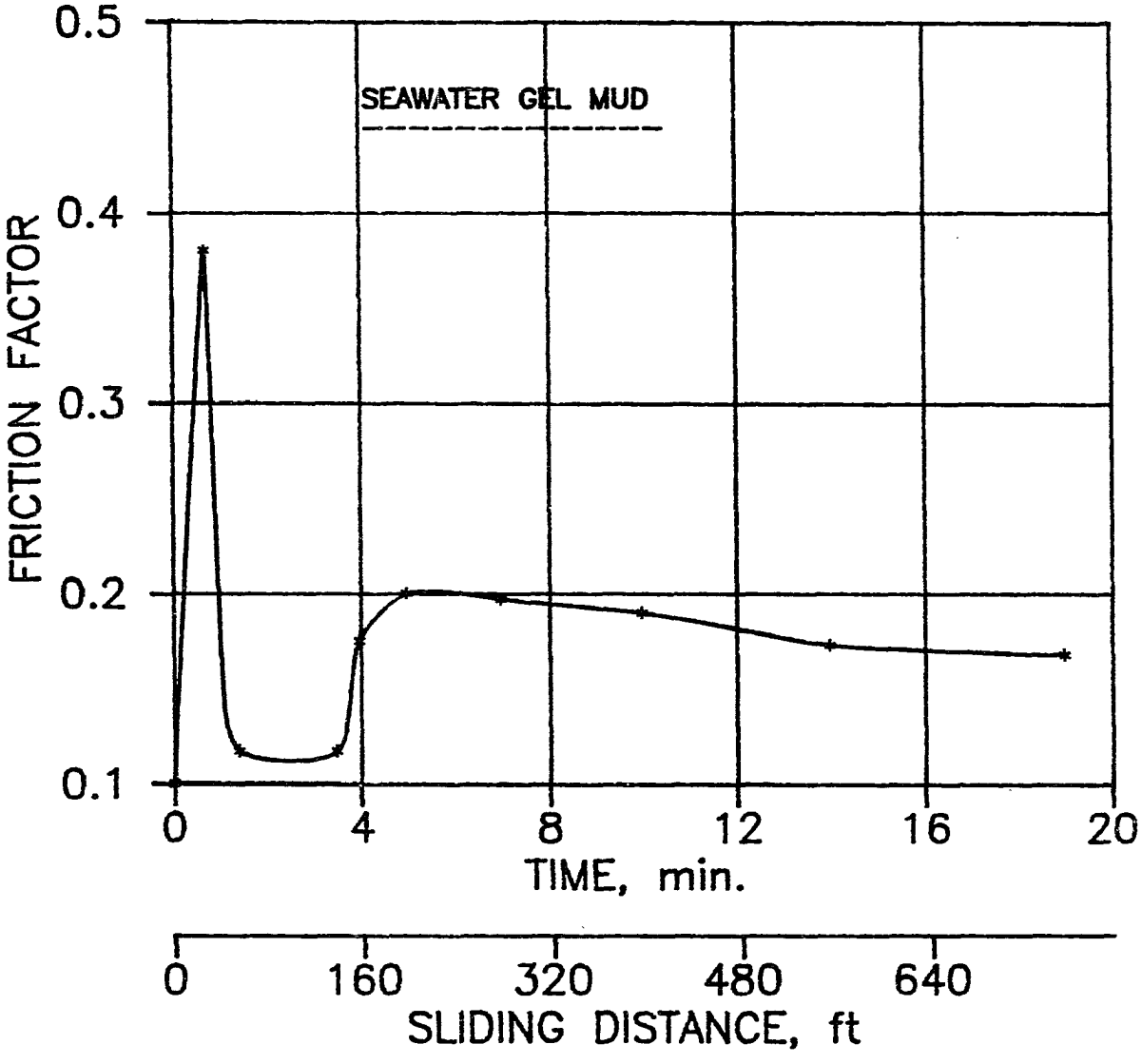

Fig. 25 - Typical frictional response for seawater gel mud.

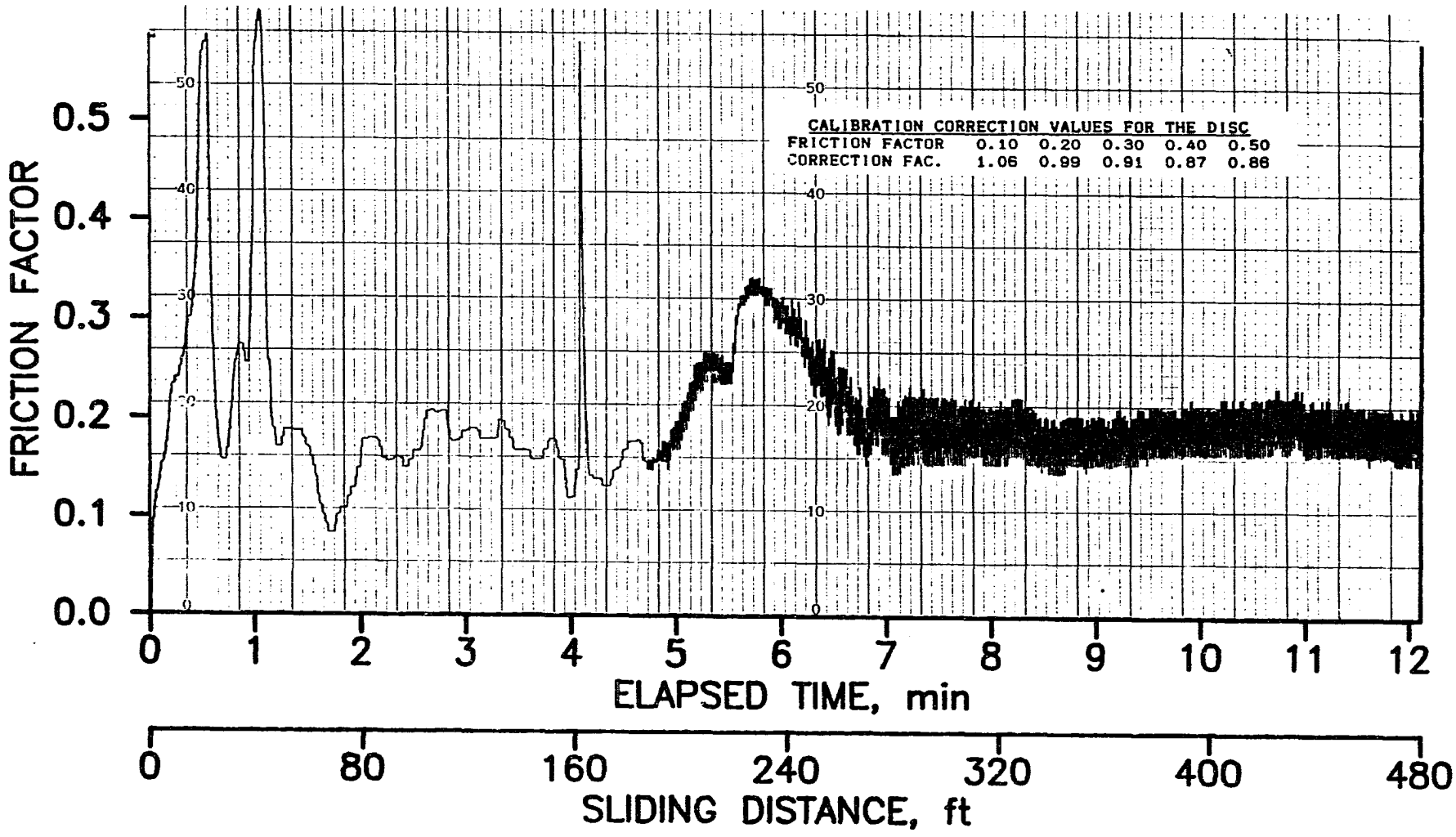

Fig. 26 - Experiment record for a seawater gel mud, on sandstone, after a 30 min. filtration period, using the disc - B/W/S/MK/D/RT/30M/NL.

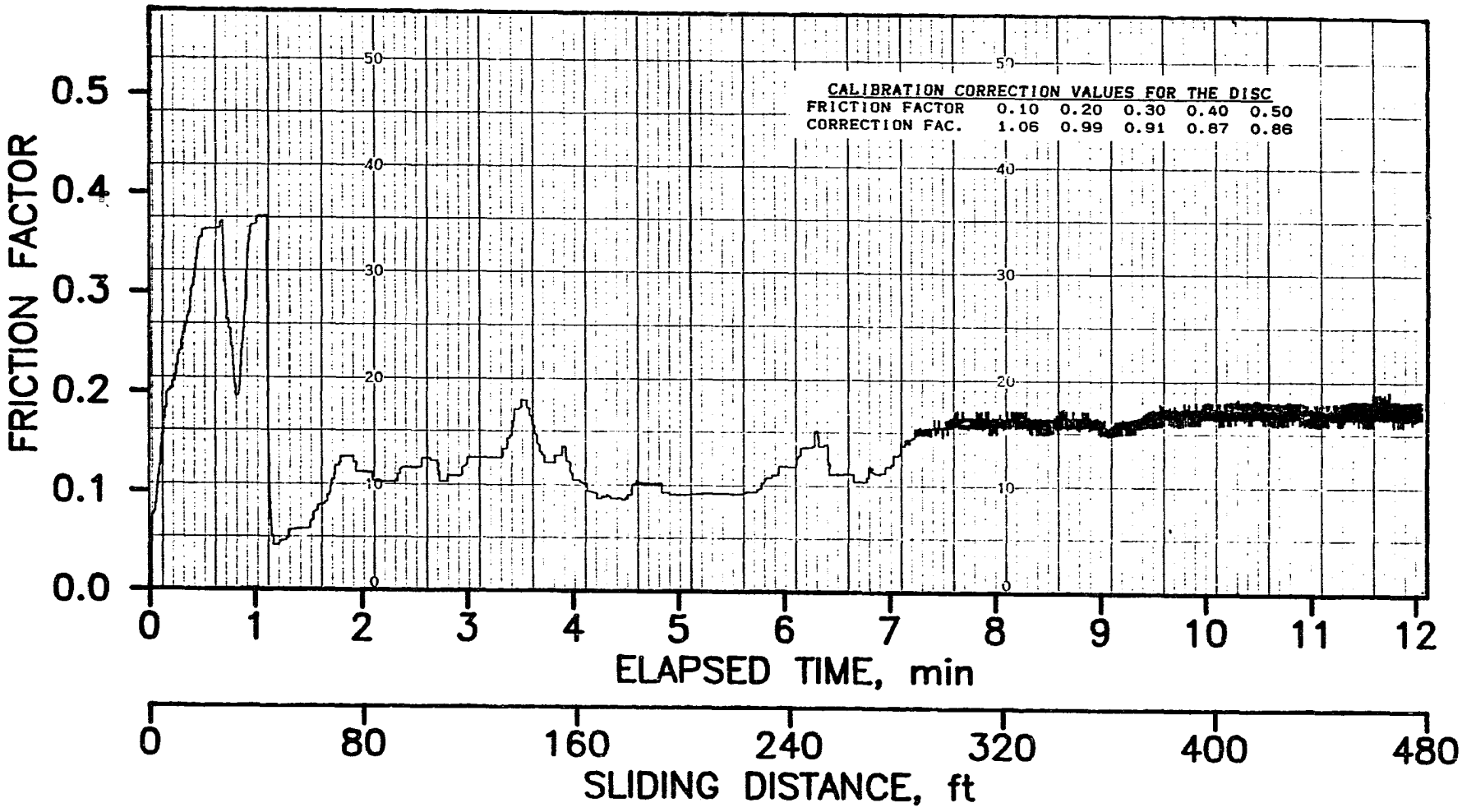

Fig. 27 - Experiment record for a seawater gel mud with lubricant, on sandstone, after a 30 min. filtration period, using the disc - B/W/S/MK/D/RT/30M/L.

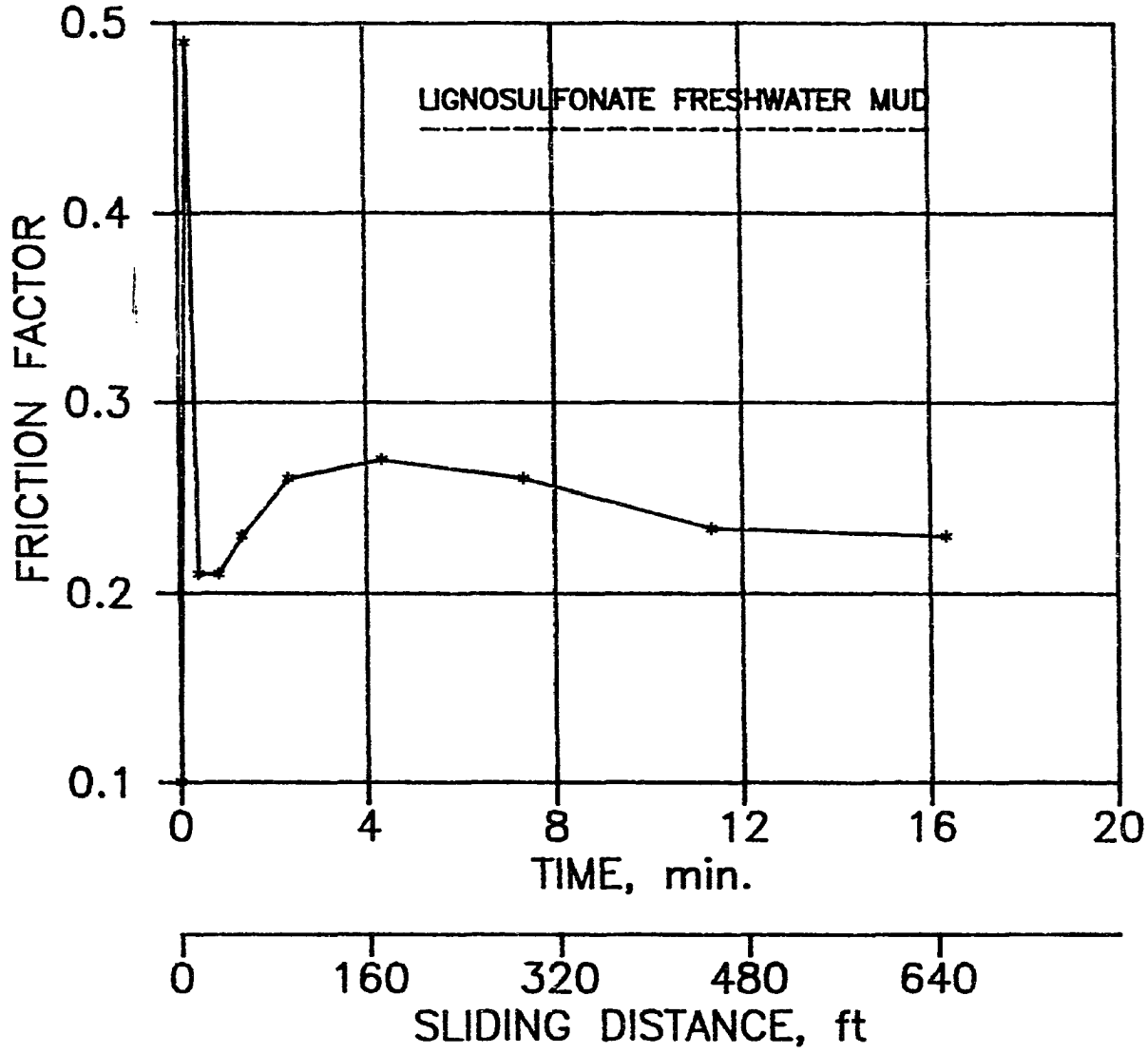

Fig. 28 - Typical frictional response for lignosulfonate freshwater muds.

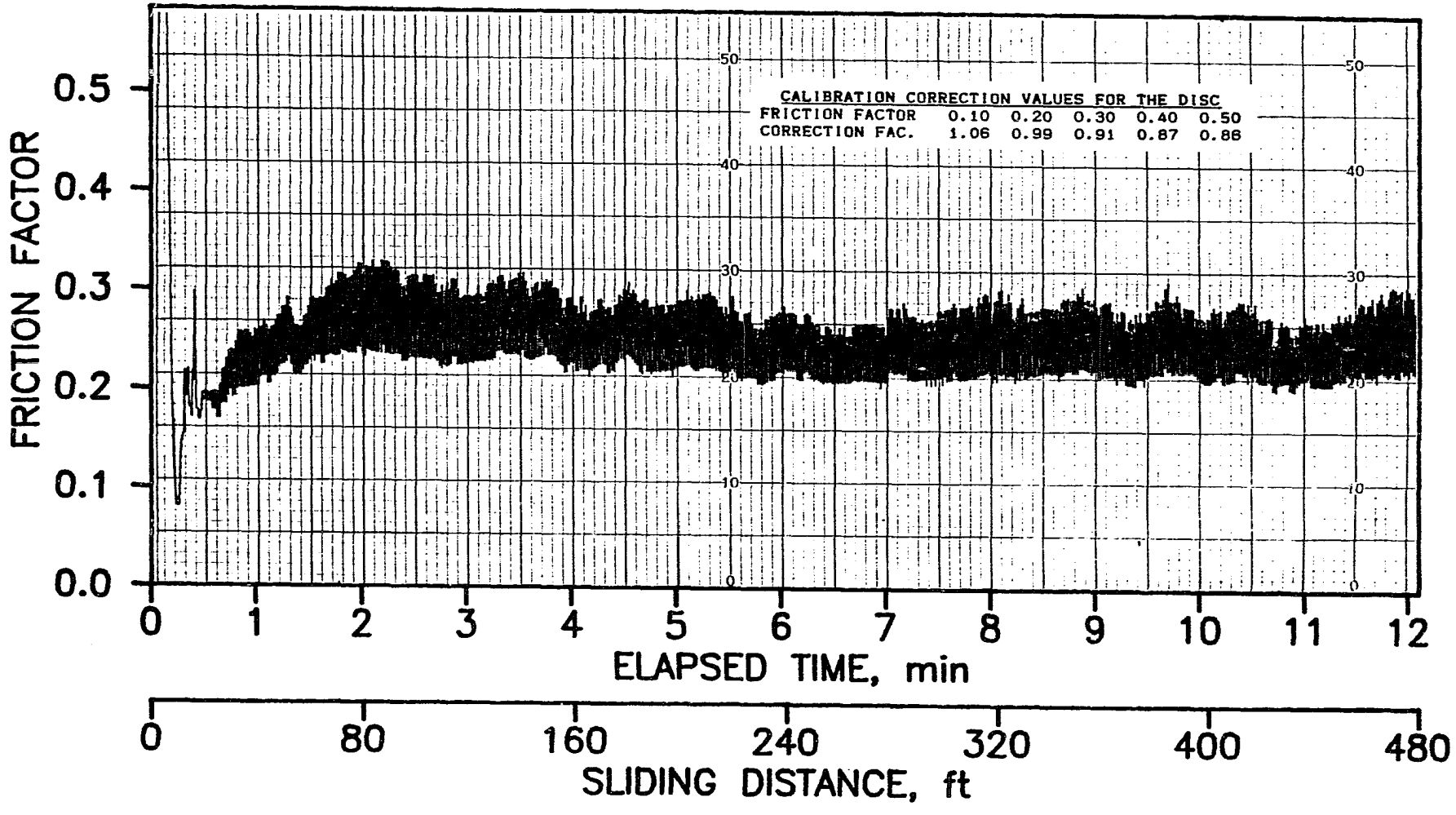

Fig. 29 - Experiment record for a lignosulfonate freshwater mud, on sandstone, after a 30 min. filtration period, using the disc - A4/W/S/MK/D/RT/30M/NL.

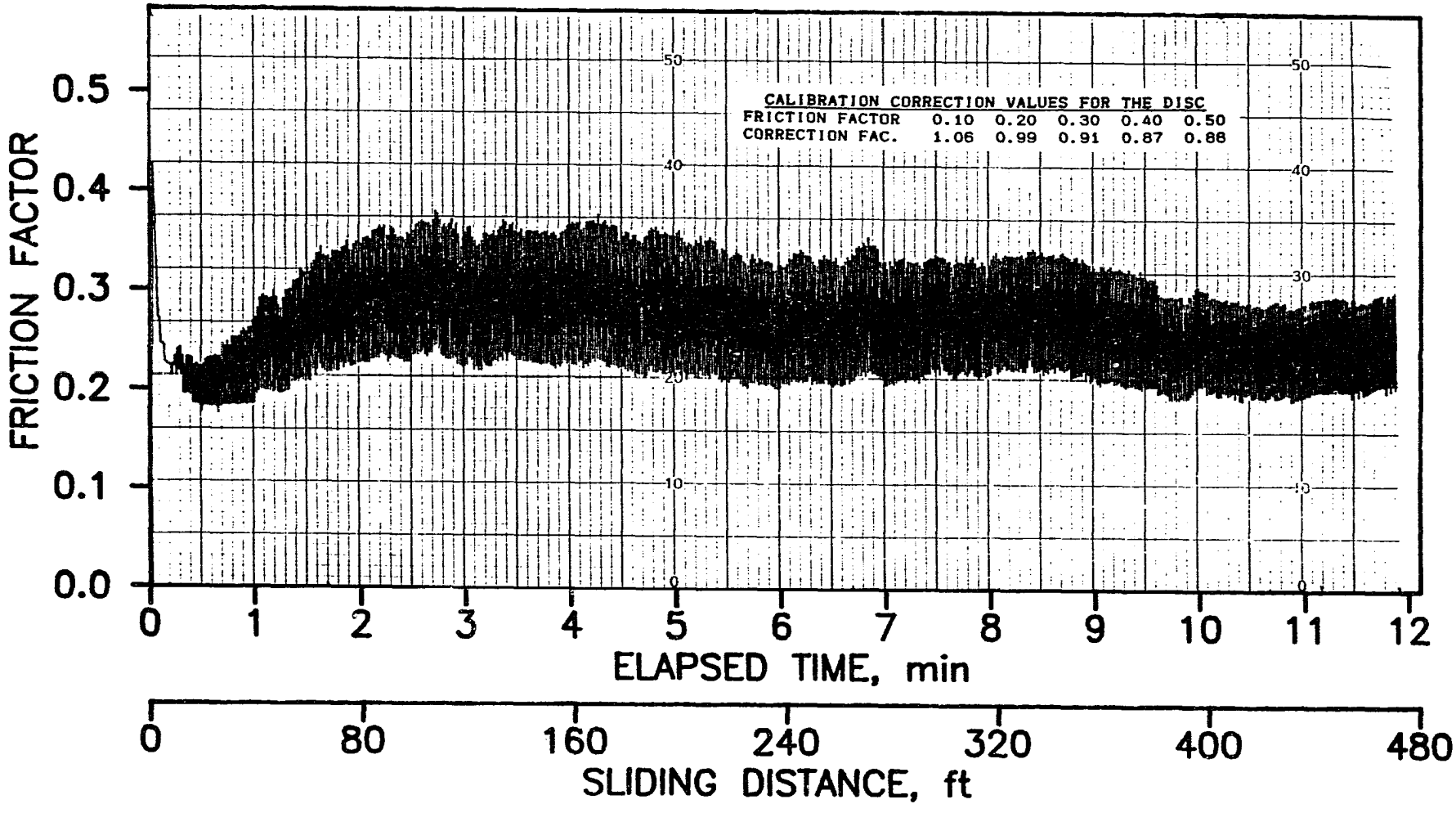

Fig. 30 - Experiment record for a lignosulfonate freshwater mud, on sandstone, after a 2 min. filtration period, using the disc - A4/W/S/MK/D/RT/2M/NL.

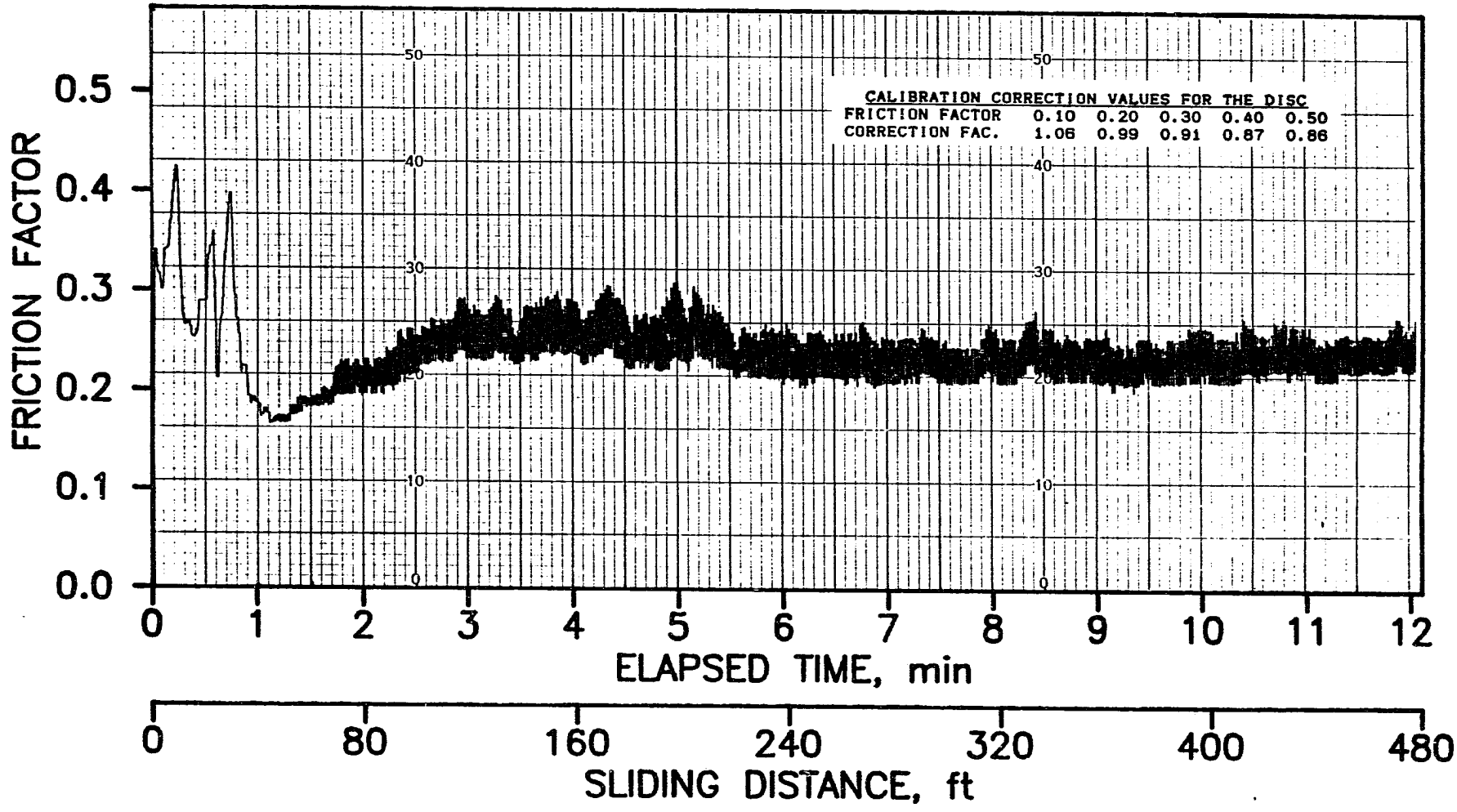

Fig. 31 - Experiment record for a lignos. freshw. mud with lubricant, on sandstone, after a 30 min filtration period, using the disc - A4/W/S/MK/D/RT/30M/L.

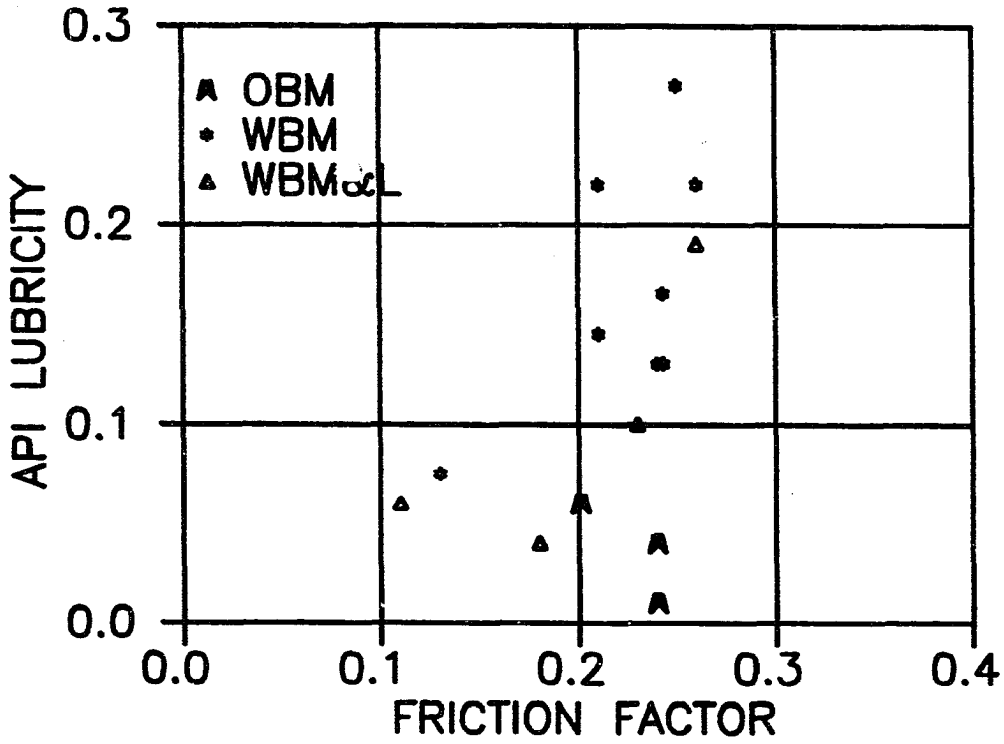

Fig. 32 - Insensitivity of the large-scale laboratory tester friction factor values to the API lubricity ones.

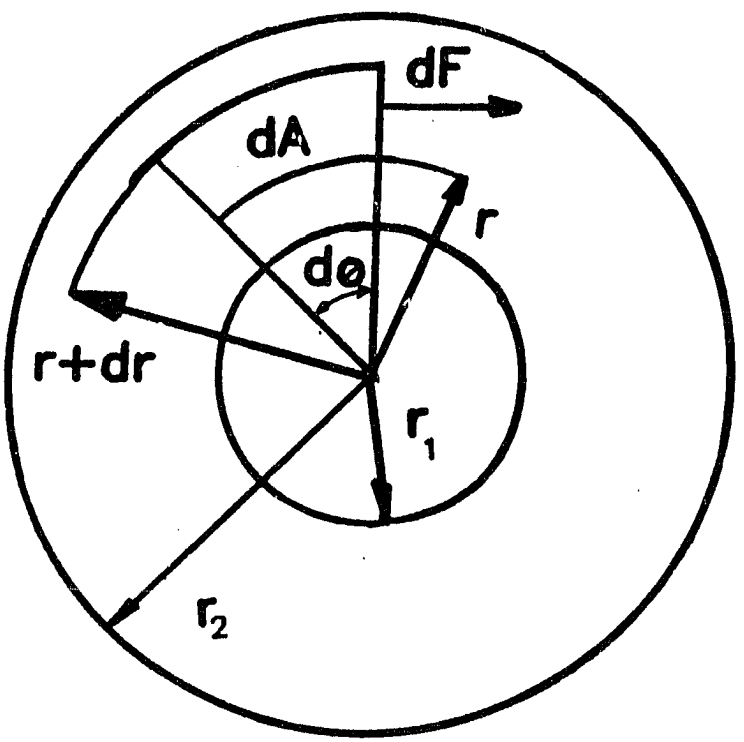

Fig. 33 - Analysis of the force acting on a small element on the disc or cylinder rock interface.

CHAPTER V

MINIMUM COST CASING DESIGN FOR VERTICAL AND DIRECTIONAL WELLS

INTRODUCTION

The tubular program of most oil wells represents the greatest single item of expense in well cost. It can be as much as 18% of the completed well cost. Therefore, even a small reduction in casing cost can save a considerable amount of money. This objective has been traditionally achieved by initially minimizing the number of strings and the length of each string and by then designing a combination casing string.

In vertical wells an optimum combination casing string has been a challenge for casing designers. Its principle is based on considering several combinations of the grade-weight-length sections of casing string. Each combination satisfies some predetermined external load condition. Eventually this combination casing string is selected, which allows the minimum total cost. Because of the very large number of combinations there is no currently existing method for the minimum-cost casing calculations. Instead, several step-wise procedures have been

developed[1,2,3,4] for casing grade-weight selection without explicit cost expressions. In these procedures the general observation is used that the casing price increases with increasing casing grade, weight, burst strength and joint strength. Therefore the lowest grade and weight casing having the lowest possible values of mechanical strength is supposed to give the lowest cost. Unfortunately this "minimum grade-minimum weight" approach cannot always yield the minimum cost simply because casing grade, weight and cost cannot be simultaneously minimized. Moreover, usually only a small selection of casings can be considered due to the computational problems. Another approach to the problem is presented by the set of graphs known as the Casing Quick Design Charts.[5,6] The charts are based on some computer calculations of the minimum cost. Though easy to use, the charts have limited applications due to the simplifying assumptions regarding external loads, borehole conditions and prices. Hence they can be only recommended as a general guidance in casing design. There are also a few theoretical investigations of the minimum-cost casing problem,[7,8] which are based on the mathematical theory of optimization and provide interesting concepts with very little practical use.

In directional wells, the effort of designers has been focused on the mechanical aspects of casing design. The most popular is the method of the vertical projected depth. In this method, the directional well is assumed to be vertical and the effect of wall support on casing weight is ignored. The unfavorable effect of the wall friction on the tensional load is sometimes considered as a constant value of tension drag. This approach is oversimplified. It disregards a geometrical

profile of the directional well. Besides, the cost factor is not included in directional well casing design.

In summary, a systematic analysis is needed of a potential cost reduction through casing optimization in vertical and directional wells. Also, there is a lack of a simple computational procedure for minimum-cost casing. This research addresses several basic problems related to the impact of casing cost on casing design.

1. How to calculate the absolute minimum cost of casing, given external loads, design factors and casing supply?

2. What is the quantitative effect of certain decisions made by the casing designer (value of the design factors, number of sections) on cost of casing?

3. How significant, given specific loads, is the conflict between minimum weight - minimum grade and minimum price of casing?

4. How do the external casing loads in directional wells affect casing cost?

5. What is the correlation between the directional well profile and its minimum casing cost?

6. What is the effect of the borehole friction on casing design in directional wells?

OPTIMIZATION MODEL OF CASING COST

The development of the model has been based both on the casing design theory[1,2] and the theory of optimization.[9,10] The theory of casing design for vertical wells is commonly known. The assumptions used in this research are as follows:

1. The maximum load casing method[1] is applied. At each depth, the maximum external and internal pressure values can be predetermined based on the casing-run-in mud density, maximum anticipated density of mud that will be in contact with the casing, fracture gradient at the casing seat, pore pressure at the bottom of the next casing and the type of casing (surface, intermediate or production).

2. For tension consideration, maximum surface running loads are considered.

3. Buoyancy is considered.

Calculations for directional wells are explained later in this paper.

The optimization model was first formulated in the general way, then it was simplified. The casing string is arbitrarily divided into N unit sections of equal length $\Delta\ell$ (Fig. 1). The casing design procedure starts at the bottom of the casing string and proceeds, in the step-wise manner, to the casing top. The minimum-cost problem is formulated as follows:

Find the minimum total cost of the casing string (objective function)

$$C_T = \min \sum_{n=1}^{N} C_n \tag{1}$$

that satisfies the following mechanical requirements (constraints):

$$\begin{aligned} (p_{cc})_n &\geq R_c \cdot (\Delta p_c)_n \\ (p_{bc})_n &\geq R_b \cdot (\Delta p_b)_n \\ (F_t)_n &\geq R_t \cdot F_{A_n} \end{aligned} \tag{2}$$

where

$$F_{A_n} = F_{A_{n-1}} + \Delta \ell \, q_n \cos \alpha_n + \sum_{j=1}^{N_a} F_j \tag{3}$$

and $n = 1, 2, \ldots, N$

The summation term in Eq. (3) represents all axial forces other than casing weight. These include: buoyant force, linear and belt friction, bending force, viscous drag, and stabbing effect, as well as some other phenomena. In case of a vertical welbore, the axial load is

$$F_{A_n} = F_{A_{n-1}} + \Delta \ell \, q_n - 0.052 \, \rho \, \ell_n \, (S_n - S_{n-1}) \tag{4}$$

and

$$F_{A_o} \equiv 0$$

$$S_o \equiv 0$$

At each casing unit section n, the set of the best casings is selected from all available casings. The best casings include the cheapest and the lightest casings. The best casing choice for any unit section depends on all previous decisions (n-1, n-2, ... 1) due to the additive

nature of the axial loads. Such a problem, from the standpoint of the optimization theory, is classified as the multistage decision process. It is solved using a computer and the recurrent technique of dynamic programming. Definitions and recurrent formulas are shown in Appendix A.

The general solution described above is impractical. It requires a relatively large amount computer memory and time-consuming calculations. A large number of variants may be generated as recursions progress. The only practical solution to this problem is to reduce number of casing variants.

Weight - Price Conflict in Casing Design

The analysis of the iterative procedure for casing design shows that the only source of the multitude of casing variants is the dilemma between casing weight and casing price. This dilemma has been observed by many casing designers. It can be called "weight - price conflict" and it has been also reported in the literature.[4] The conflict arises from the observation that the decision made in favor of the cheapest casing for any bottom section of casing string may yield eventually more expensive total casing string. On the other hand the casing string with a lighter (yet more expensive) lower part may be finally cheaper due to the reduction in axial load supported by the upper part of the casing. The concept of the weight-price conflict is visualized in Fig. 2. Since the conflict cannot be resolved before the casing design is completed, every casing lighter than the cheapest one has to be memorized at each step of the casing design - hence new variants are generated.

However, in the course of the large number of calculations it was noticed that the weight-price conflict could be simply ignored. In all cases the optimization model responded as if there was no significant number of variants. This observation was verified further by comparing the two modified versions of the casing optimization program:

1. Program for calculation of an unconditional minimum-cost casing at each step of the recurrent procedure. Its principle can be written as:

$$C_{T_{min}} = \Delta\ell \sum_{n=1}^{N} \min_{(r)} (P_n^r) \tag{3}$$

and the load requirements (2), (3) must be satisfied for n=1, 2, ..., N.

2. Program for calculating the absolute minimum-weight casing string. Its principle was based on selecting the cheapest casing within the lightest ones. In this program, the first priority was given to the weight, and the second priority to the price. The total cost of the minimum-weight casing string is

$$C_{T_N}(Q_{T_{min}}) = \Delta\ell \sum_{n=1}^{N} \min_{(r)} P_n^r [q_n^r = \min_{(m)} (q_n^{mr})] \tag{6}$$

and the requirements (Eqs. 2 and 3) must be satisfied for n=1, 2, ..., N.

The two programs were used to design a variety of casing strings with different sizes and lengths for the same external loads and geological conditions. In all cases the final casings designed by both programs were almost identical. The example of these calculations is shown in Table 1. The 9 5/8" intermediate casing string was designed. The casing setting depth was varied from 5000 ft to 11000 ft. The other design data - e.g., two mud densities, fracture gradient at the casing seat and the pore pressure at the next casing seat - were evaluated using the Profile #1 data in Table 2.

The analysis of the optimal design path was performed to explain why there is no weight/price conflict in casing design. The complete selections of the 7", 9 5/8" and 13 3/8" casing were analyzed together with their current price list (Lone Star Steel Co.). The plots of the optimal design paths were made for both the minimum-cost and the minimum-weight casing design. Each design path follows an increasing in casing load (burst pressure, collapse pressure, axial load). The examples of the plots are presented in Figs. 3, 4, 5. A very good convergence between the two optimum design patterns can be observed, and small discrepancies can be noticed. These discrepancies are probably completely nullified when all three loads are applied simultaneously and the minimum section length requirement is set.

Based upon the above analysis, the substantial simplification in the optimization procedure can be made (Appendix A). The simple version of the minimum-cost computer program can be developed.

ANALYSIS OF THE MINIMUM-COST CASING IN VERTICAL WELLS

The minimum-cost computer program was developed by using the recurrent equation (Eq. A-9) and the mathematical conditions of Eqs. A-3a through a-3c. The structure of the program is such that the casing load calculations can be modified without changing the optimization procedure. This provides the necessary flexibility for using different patterns of loads for the surface, intermediate, and production casing. Also, the files with casing size, properties and updated price lists are prepared. The file reference number is specified in the input of the program. Fig. 6 shows the computer input and the output summary.

Casing Cost Reduction

In order to estimate casing cost reduction, the minimum-cost casing computer program calculations are compared to the traditional method of casing design. In the traditional method the casing designer gives preference to lower grades and stronger casing joints. He also considers casing weights trying to achieve the necessary minimum of casing performance. This approach depends very much upon professional experience.

Combination casing strings designed by using the traditional approach can be from 7% up to 30% more expensive than the minimum-cost design. As an example, the 9 5/8" intermediate casing string is designed to 11400 ft. Other data are taken from Table 2 (profile #1) and presented in the input data of Fig. 6. The traditional casing design,

with the strongest preference given to casing grade, consists of the two sections of 53.5 lb/ft, C-75 casing (long thread and buttress) with a total cost of $428,215. The minimum-cost casing design, on the other hand, consists of five sections of N-80 and S-95 casing, and its cost is $326,491 which indicates a 24% cost reduction.

Furthermore, the minimum-cost casing design was compared to the Casing Quick Design Charts.[5] In the example presented here, the 7" intermediate and the 7" production casings are designed using the pore pressure and fracture gradient data given in Table 2 (profile #2). The setting depths of the casings vary from 6000 to 16000 ft. The resultant casing cost is shown in Table 3. It can be noticed that, for production casing, cost reduction increases with increasing setting depth from zero to 12.5%. In case of the intermediate casing design, there is a significant cost reduction of about 30% regardless of casing setting depth. A comparison of the Casing Quick Design Charts and the minimum-cost casing program cannot be done over the wide range of drilling conditions due to the limited mud weights in the Charts (max. 15 ppg) and unspecified loading patterns. Also, the Quick Design Charts casings do not always meet the mechanical requirements, particularly in the central part of the casing string. Moreover, the Casing Quick Design Charts generate the over-rated, intermediate casing as a result of using only one pattern of casing loads.

Optimization of the Liner Design

The economic advantage of a drilling liner is easy to calculate. Its relative cost reduction can be estimated as the ratio of liner length to the total length of the single intermediate casing string installed from the surface. The economics of production liners are more complex.[3,4] Two concepts of production liner are studied below: the production liner with tie-back casing and the liner without tie-back casing.

Production liners with tie-back casing are usually designed to protect the production string from excessive wear when exploratory drilling below the productive interval is planned. Their cost is higher than the cost of a single production string due to the cost of a liner hanger. In deep production wells, however, where the top of the casing string is solely controlled by tension, the liner with tie-back casing might be less expensive than the single casing string.[2,3] This is the case when the increased liner hanger cost is offset by the reduced pipe cost. Thus, the evaluation of the pipe cost should be performed prior to liner design. It can be noticed that the total pipe cost of the liner and tie-back casing is strictly a function of the liner length. This function has one distinctive minimum: the optimal position of a liner hanger can be calculated at which the minimum of the pipe cost is obtained can be calculated.

As an example, the optimization of the liner hanger setting depth is performed by using minimum-cost casing program. The 7" production

casing is to be set at 16500 ft in the 14 ppg mud. The minimum cost of the single production string is $394,428. This cost can be further reduced by using liner and tie-back casing system. The plot of the total cost of this system vs. setting depth of the liner hanger is shown in Fig. 7. Each point on the plot results from one run of the minimum-cost casing program, and it indicates the absolute minimum of pipe cost, given depth of liner hanger. The overall minimum cost is $338,808 for the liner hanger set at 6000 ft. At this point the maximum cost reduction is $55,620 or 14.1% of the minimum cost of the single string.

In case a production liner is installed inside intermediate casing without the tie-back casing, some significant cost reduction can be expected.[4] However, the small cost of an abbreviated production casing string has to be considered, together with the increased cost of the intermediate casing which must be designed for production loads. The example problem is to evaluate two variants of casing design for the 15000 ft production well. Profile #1 in Table 2 is used for the pressure data. Variant 1 consists of the 7" intermediate casing and the 15000 ft long 4½" production string. Variant 2 is the 7" intermediate production casing and the 4½" production liner with 200 ft overlap. The comparison of the minimum costs of variant 1 and variant 2 is shown in Fig. 8. The total cost reduction for the liner design (variant 2) shows a flat maximum value of 21% over the wide range of the intermediate casing setting depths. This total pipe cost reduction should be weighted against the cost of liner hanger and against the risk of using a casing that has been exposed to drilling operations.

Effect of Design Factors and Section Length

One of the most important problems in casing design is the assumed value of the design factors. The design factors are equal to the ratio of the casing minimum performance properties to the casing loads. Their values usually vary from designer to designer. The ranges of the design factors reported in the API study in 1955 were as follows: for burst considerations R_b = 1.0 to 1.75; for collapse consideration R_c = 1.0 to 1.5; for tension R_t = 1.5 to 2.0.

The values of currently applied design factors range from 1.0 to 1.25 for burst, from 1.0 to 1.125 for collapse, and from 1.55 to 1.9 for tension. The particular value of the design factor selected is based either on personal experience or it is just the most typical value used in drilling practices.[3,11]

The effect of the design factors for burst, collapse and tension on the minimum casing cost is presented in Fig. 9. The input data used for the design are shown in Fig. 6. The relative cost increase is calculated with respect to the minimum value of casing cost for the design factor equals unity. Because the casing string design is entirely controlled by burst and collapse, the design factor for tension does not affect the casing cost. It can be noticed that the most cost effective factor is that for the burst, which is quite common for the intermediate casing. A 0.1 value increase of the design factor for burst results in a 2% increase in casing cost -- information that can help the designer to compromise between casing cost and the risk of casing failure. This

example also shows that some decisions in the particular casing design are of no importance. In this case, the high value of the design factor for tension will not improve safety of the design.

The problem regarding number of sections for the combination casing string is logistical. This is particularly important in off-shore drilling. Casing must be loaded, shipped, unloaded and racked in the proper sequence. In mixed weight, grade or joint strength casing strings, the lower-most section must be racked first. This alone determines the sequence of loading and unloading for off-shore shipment. Rearrangement of pipe on location is difficult and may produce casing damage. Even in land operations a small number of pipe sections is desirable in order to avoid a complex inventory. Current experience shows that 3-4 sections for a 10000 ft combination casing string is an acceptable maximum. In off-shore operations the allowable number of sections is even smaller than that for land operations. Usually an operator specifies the number of sections (or minimum length of a section) for the casing designer. Also, there is an economic aspect related to the length of casing section: most casing distributors offer a discount for orders in excess of 100 joints.

The minimum-cost casing program is used to analyze the impact of the minimum section length on the minimum casing cost. The 9 5/8" intermediate casing string design is used as shown in Fig. 6. The assumed length of one section varies from 40 ft (maximum of 285 sections) to 10000 ft (one section only). The effect of the minimum section length on casing cost is shown in Fig. 10. It is interesting to

note that the minimum-cost casing with a minimum section length of 2000 ft is only 3.6% more expensive than the design with unlimited section length. Furthermore, the one-section design gives an ultimate cost increase of only 8%. The fact that over 50% reduction in the number of pipe sections causes less than 4% increase in minimum casing cost provides important information on how to minimize logistical problems and maintain close to minimum cost. In this case the 4-section string is the solution.

MODEL OF CASING DESIGN IN DIRECTIONAL WELLS

The minimum-cost casing procedure for vertical wells was expanded to directional wells. This was possible because the flexible structure of the model allows independent calculations of casing loads and the cost minimization. The following assumptions are used:

- Two-dimensional profile of the well is assumed.
- Elastic properties of casing are considered in bending calculations.
- Bending contribution to the axial stress is expressed as an equivalent axial force.
- Bending contribution to the normal force is neglected.
- Buoyancy is considered as the pressure-area axial force corrected for the variation in casing wall thickness.

- Effect of deviation angle on axial load is considered by using the axial component of casing weight.

- Favorable effect of friction on axial load during downward pipe movement is ignored.

- Unfavorable effect of friction on axial load during upward pipe movement is considered as linear drag and belt drag.

- Axial load is calculated as maximum pulling load.

- Burst and collapse corrections for the biaxial state of stress are calculated by using axial load (static) when casing is set.

The general flowchart of the program is shown in Fig. 11. The input of the program contains the following type of data:

1. Casing data: size of casing, casing performance and price data (all available casing).

2. Drilling data: vertical depths of this and the next casing, fracture gradient at the casing seat, minimum pore pressure expected, density of mud in which the casing is run, the heaviest mud density expected.

3. Directional well data: measured depths data (D_{KOP}, ℓ_{S1}, ℓ_{S2}, and ℓ_{DOF}) well inclination data (buildup rate, drop-off rate), depths of the preselected points in the well at which the highest tensional loads are expected (commonly: surface, kick-off point, doglegs).

4. Design data: type of the casing string (surface, intermediate, production), design factors for burst, collapse and tension, borehole friction factor, allowable minimum length of each section of the casing string, maximum surface pressure allowed (commonly BOP working pressure rating).

Depth conversion is made by projecting the actual well profile on the vertical. Vertical depths and inclination angles are calculated for all casing unit-sections. As a result, the complete directional well profile is generated from the directional well data. The profile is shown in Fig. 12. It simplifies the actual well trajectory for the purpose of casing design. It requires very few input data as opposed to the input based on the detailed directional survey. Formulas used in the depth conversion procedure are listed in Appendix B. Based on the conversion, the hydrostatic loads for burst and collapse consideration are assigned to the unit-sections of casing string as:

$$\Delta p_b\ (\ell_i) = \Delta p_b\ (D_i) = \Delta p_{b_n}$$

$$\Delta p_c\ (\ell_i) = \Delta p_c\ (D_i) = \Delta p_{c_n} \qquad (7)$$

Note that subscript "i" indicates position in the well, subscript "n" indicates the unit section of the casing string (Fig. 13). When the casing is set at the bottom: i = n.

Axial Load Calculations

Calculation of the axial load is the most challenging part of directional well casing design. Based on the maximum load principle, the concept of the maximum pulling load is applied. The concept is derived from the fact that the greatest value of the tensional stress in directional well casing is associated with the casing running operation when the casing sticks while passing a tight spot. Working the string up and down creates the highest tensile loading on the upstroke due to the wall friction. Calculation of the maximum pulling load for each unit section of casing string is the most cumbersome part of the program because it is related to the temporary position of this section in the hole. Such a situation is depicted in Fig. 13. The casing is accidently pulled on when the unit-section "n" is temporarily located at the position "i". The value of the axial pulling load supported by the unit section n is calculated as

$$F_{A_n}^{i} = F_{L_n} + F_{BN} \tag{8}$$

where the equivalent axial force due to bending, F_{BN}, is

$$F_{BN} = \frac{84.7194\ \Delta\ell\ \dot{\alpha}_i\ d_e \sqrt{F_{L_n}(d_e^2 - d_i^2)}}{\sqrt{d_e^2 - d_i^2}\ \tanh \dfrac{0.49443 \sqrt{F_{L_n}}}{\sqrt{d_e^2 - d_i^2}}} \tag{9}$$

and the axial force F_L is calculated using recurrent formula

$$F_{L_n} = F_{L_s}, \text{ for } s = n$$

where

$$F_{L_s} = F_{L_{s-1}} + \Delta\ell\, q_s \cos \alpha_{i-n+s} + F_{LD} + F_{BD} - F_{BO} \tag{10}$$

and the linear friction drag, F_{LF}, is

$$F_{LD} = 2\mu_B F_{L_{s-1}} \sin (0.5\, \dot{\alpha}_s \Delta\ell) \tag{11}$$

the belt friction drag, F_{BD}, is

$$F_{BD} = (-1)^a \left(1 - \frac{\rho}{65.5}\right) \Delta\ell\, q_s \sin \alpha_{i-n+s} \tag{12}$$

and the buoyancy effect is

$$F_{BO} = 0.052\, \rho\, D_{i-n+s}\, (S_k - S_{k-1} \tag{13}$$

In addition

$S_o \equiv 0$

$F_{L_o} \equiv 0$

$a = 1$; buildup portion

$a = 2$; drop off portion and slant hole

$s = 1, 2, \ldots\ldots n.$

Thus the value of the axial pulling load at the n-th unit section of the casing string is a function of a position "i" of this section in the borehole. There is one position at which the maximum value of the axial load is achieved. This value is selected for the maximum axial pulling load of the unit-section "n" as

$$F_{A_n} = \max_{(i)} (F^i_{A_n}) \tag{14}$$

where

$$i = n, n + 1, \ldots, N$$

DIRECTIONAL WELL ANALYSIS

Based on the casing design model for directional wells, the casing optimization computer program was developed. The program calculates the minimum-cost casing that satisfies static and running pulling loads. The example of the program input and output is shown in Fig. 14.

Preliminary applications of the program reveal that computing time is greatly dependant upon the iterations associated with the calculations of maximum axial loads. Moreover, it has been found that, it most cases, the highest axial pulling loads are at the surface and at the point that is situated one casing joint below the kick-off point. As a result, the program was modified so that the only three borehole points considered are the surface, the KOP, and the top of the drop-off portion. However, any other points at which the highest axial stresses are expected (dog-legs) can be input to the program. The program is also capable of calculating the minimum-cost casing for a vertical well. The results obtained are identical to those of the minimum-cost casing program for vertical wells. Also, part of the computer output is processed by a plotter.

Effect of the Borehole Friction Factor

The borehole friction factor represents the drag between the pipe and the wall of a borehole. This drag depends upon several factors such

as: type of rock in the wall, type of drilling mud and its properties (solids content, oil content, filtration cake quality), borehole conditions (key-seats, washouts) and number of centrilizers installed on the casing string. Therefore the borehole friction factor has a broader physical meaning than that of the simple coefficient of friction between steel and a rock surface. The most typical value of the friction coefficient in the borehole reported[12] is from 0.02 to 0.15. Also reported is the effect of the drag that represents the interaction between the casing and the borehole wall that can increase the value of the borehole friction factor to more than 1.0. Moreover, the incidental increase in axial tension has been observed when the casing was stuck in directional wells. All these facts contribute to uncertainty in the value of the axial drag component. As a result, in some directional well casing design procedures[13] the deviated well support is entirely ignored and the oversimplified model of the equivalent vertical well (ℓ = D) is applied.

In the authors' opinion, the proper approach is to provide for accidental loads by using an adequate design factor value for tension, yet to use the borehole friction factor. The latter should be evaluated in the field for similar borehole conditions. The main advantage of this factor is that it enables calculation of the axial stress distribution along the casing string with respect to well deviation and curvature; hence, it correlates casing design with directional well parameters.

The minimum-cost casing program has been used to estimate the effect of the borehole friction factor on the optimum casing design. As an example, the calculations for the 7" intermediate casing string set at 16000 ft are presented. The program input data are as in Fig. 14. The plot of the 7" casing cost versus the borehole friction factor is shown in Fig. 15. Note that for values of the borehole friction factor smaller than 0.3, the frictional drag component can be ignored. Above this value, however, the optimum casing design is considerably affected by the drag; the cost increase rate for this example is from 2.4% to 7.2% per 0.1 increase in the value of the borehole friction factor.

Effect of the Directional Well Profile

With the initialization of the proposed directional well, a lot of preplanning information is required in order to deduce the well geometrical pattern. Part of this information concerns casing sizes, number of strings and setting depth. The design and cost of any particular casing string is dependent upon the well deviation pattern. This interaction between casing design and directional well pattern should be considered with all the other factors affecting the total cost of the well. There are three types of directional well patterns:

- Type 1. This has a deflection point at the shallow depth, short buildup portion and long slant hole portion extended to the target zone.

- Type 2. This includes deflection point at the shallow depth, large inclination angle of the first slant hole portion to achieve the total horizontal displacement, and vertical second portion of the slant hole.

- Type 3. This type has a deeper position of the KOP and long buildup portion extended to the target zone.

The following aspects of directional well geometry are selected for the minimum-cost analysis: location of the kick-off point and the type of well pattern.

The effect of the kick-off point is calculated by using the example of the 7" deep intermediate casing design with the target zone located at 10000 ft and the lateral target displacement of 9000 ft. The casing data, drilling data and design data are identical to those presented in Fig. 14. The directional data are the result of the fixed values of the buildup rate (3°/100 ft), drop-off rate (2°/100 ft) and the various assumed values of D_{KOP} = 40 ft, 1040 ft, 2040 ft, 3040 ft, 4040 ft, 5040 ft and 6040 ft. The copy of the computer-generated plot of well trajectories is shown in Fig. 16. It is interesting to notice that the minimum casing cost decreases with increasing depth of the kick-off point disregarding a simultaneous increase in casing length. Position of the kick-off point at 4000 ft gives a casing cost reduction of $36,000. At the planning stage, this cost reduction can be compared with the technical difficulties associated with the deflection operation performed deep in the hole.

The analysis of the effect of the directional well pattern on the minimum casing cost is performed by using the example design of the 7" production casing string. Three types of directional well pattern are considered for the same vertical depth of 10000 ft and the 9000 ft horizontal departure of the target zone with 6000 psi formation pressure. The 0.5 value of the borehole friction factor, the buildup rate of 3°/100 ft and the drop-off rate of 2°/100 ft are assumed. The computer plot of well profiles and corresponding output data are presented in Fig. 17. Two factors are considered in the analysis: 1. degree of well deflection and curvilinearity as they affect casing cost due to the drag; 2. length of a casing string. The cheapest casing design is that for the Type 1 directional well in which both factors are minimized. However, a comparison of casing designs for the Type 2 and Type 3 directional wells shows that the shorter casing string might be more expensive. In the Type 2 directional well the casing cost increase due to the wellbore drag generated by the additional drop-off portion overshadows the cost reduction due to shorter casings. Thus the resultant casing cost is greater than that for the Type 3 well.

CONCLUSIONS

A new approach to casing design in directional wells is presented. By determining axial loads summarized in Eqs. (8) through (13) many new effects are considered. These effects have been traditionally disregarded in casing design.

Two computer programs for the minimum-cost casing design were developed to generate data necessary for this research. However, the final conclusions are independent from any computer program and can be useful for casing designers.

1 It has been found that the application of the optimization theory to casing design can be significantly simplified for the minimum cost casing design. A simple step-wise procedure was developed, which calculates the absolute minimum of casing cost, given loads. The procedure can yield up to 24% cost reduction over conventional design methods. Also, this procedure can be applied to any casing load configuration.

2 There is no need for more than 3 different types of casing for every 10,000 ft of well, as the impact on cost is, for most cases, less than 4% of the absolute minimum cost.

3 The setting depth for liner hangers in deep vertical wells completed by using production liner and the tie-back casing string will be above the mid-depth point in order to obtain a cheaper casing. The minimum-cost casing procedure can be used to calculate this depth.

4 For vertical-well casing, the optimization procedure can be easily programmed on microcomputer. It can be also adapted to the long-hand calculations. For directional wells casing, however, the nature of Eq. (7) suggests using computer due to larger number of iterations.

5 There are two aspects of the minimum-cost casing in directional wells which can improve the quality of the design: development of the procedure for field evaluation of the borehole friction factor better understanding of running and pulling loads in order to reduce the number of iterations in maximum pulling load calculations.

NOMENCLATURE

C_n = cost of unit section of casing string, Dollars

C_T = total cost of the combination casing string, Dollars

C_{Tmin} = absolute minimum cost of the combination casing string, Dollars

C_{Tmin_n} = minimum cost of n unit sections of casing string, Dollars

C_{Tn} = total cost of n unit sections of casing string, Dollars

d_e = nominal casing diameter, in.

d_i = internal casing diameter, in.

D = vertical depth, ft

D_{DOF} = Vertical depth at the top of drop-off section, ft

D_{KOP} = depth of the kick-off point, ft

D_T = total vertical depth of the well, ft

F_{A_n} = axial load supported by the top of casing unit section, lbf

F_{BD} = belt friction (capstan) drag, lbf

F_{BN} = equivalent axial force due to bending, lbf

F_{BO} = pressure-area (buoyant)

F_L = longitudinal force, lbf

F_{LD} = linear friction drag, lbf

F_n = mechanical loads supported by the n-th casing unit section, lbf

F_t = casing axial load rating (body yield or joint strength whichever is smaller), lbf

ℓ = measured depth in the borehole, ft

ℓ_{DOF} = measured depth at the top of the drop-off portion, ft

ℓ_{S1}, ℓ_{S2} = measured depths of the tops of the first and second slant hole portions respectively, ft

ℓ_T = total measured depth, ft

$\Delta\ell$ = length of casing unit section, ft

N = number of unit sections in the casing string

N_A = number of axial forces considered in the mathematical model of axial load

N_C = number of all casings available

N_{L_n} = number of casings lighter than the minimum-cost casing $P_n^{(km)}{}_{min}$

N_P = number of all casing prices available.

N_R = number of casings that satisfy requirements (12)

N_{S_n} = number of all possible optimum combinations of casing string below the n-th casing unit section

N_W = number of all casing weights available

p_b = casing burst resistance rating (psi)

p_{bc} = burst resistance rating corrected for biaxial stress, psi

p_c = casing collapse resistance rating, psi

p_{cc} = collapse resistance rating corrected for biaxial stress, psi

Δp_b = burst pressure differential (psi)

Δp_c = collapse pressure differential, psi

$P_n^{(km)}{}_{min}$ = unit price of the n-th casing unit-section that gives the minimum cost of n unit sections of casing string, Dollars/ft

$q_{n_{min}}^{(km)}$ = unit weight of n-th casing, which indicates minimum-cost casing string, lb/ft

Q = weight of the unit section of casing string, lbf

Q_T = total weight of the casing string, lbf

Q_{Tmin} = total weight of the minimum-weight casing string, lbf

q = unit weight of casing, lbf/ft

R_b, R_c, R_t = design factors for burst, collapse, tension, respectively

S = casing crossectional area, $in.^2$

α = inclination angle, deg.

$\dot{\alpha}$ = buildup rate or drop-off rate (always positive number) (deg./ft)

$\bar{\alpha}_i$ = average inclination angle at i-th position in directional borehole, deg.

$\alpha 1$, $\alpha 2$ = inclination angle of the first and second slant hole portion, respectively (deg.)

ρ = drilling mud density, lb/gal.

μ_B = borehole friction factor

Subscripts

i = borehole position index

j = summation index

n = casing section position index

s = casing position iterating index

Superscripts

a = sign exponent in Eq. 12

k = casing string variant index

k_{min} = index of casing string variant which indicates minimum-cost casing string

m = casing weight index

m_{min} = index of casing weight which indicates minimum-cost casing string

r = index of casings which satisfy load requirements (12)

t = index of casing lighter than the minimum-cost casing $q_n^{(km)}{}_{min}$

REFERENCES

1. Prentice, C. M. "Maximum Load Casing Design," J. Pet. Tech. p. 805-811 (July 1971).

2. Bourgoyne, A. T. "Applied Drilling Engineering," Chapter 7, pre9 print.

3. Greenip, T. F. "Optimum Casing Program Design Stresses Economy," Oil and Gas J. pp. 76-88 (Oct. 16, 1978).

4. Goins, W. C., Jr., Collings, B. J., O'Brien, T. B. "A New Approach to Tubular String Design," World Oil, pp. 136-140 (Nov. 1965), pp. 83-88 (Dec. 1965), pp. 51-56 (Jan. 1966).

5. "Casing Quick Design Charts," Lone Star Steel Co. (1981).

6. "Specification for Armco Oil Country Seamless Tubulars. Quick Design Charts for Computer Calculated Combination Casing Strings," Armco Tubular Division, Bull. #664 p. 14-57.

7. Jegier, J. "An Application of Dynamic Programming to Casing String Design," SPE paper, unsolicited manuscript #12348 (1983).

8. Phillips, Don T., Ravidran, A., Solberg, J. J. "Operations Research: Principles and Practice," John Wiley & Sons, New York, p. 419-472 (1976).

9. Roberts, Sanford M. "Dynamic Programming in Chemical Engineering and Process Control," Academic Press, New York, p. 23-32 (1964).

10. Mid-Continent District Study Committee of Casing Programs "Survey Report on Casing String Design Factors," Drilling Production Practice, API pp. 154-164 (1955).

11. Mitchell, B. J. "Applied Drilling Concepts," SPE short course, Houston, (Sept. 1984).

12. Woodlan, B., Powell, G. E. "Casing Design in Directionally Drilled Wells," Transactions of ASME, pp. 426-433 (May 1975).

APPENDIX A

General Theory of Casing Optimization

The combination casing string design is considered a multistage decision procedure in which the next-step decision depends upon the previous decisions. The general concept of the discrete version of dynamic programming is applied.[8,9] Dynamic programming terminology is defined as follows

1. Stage: a unit section of the casing string (length $\Delta\ell$) or a step in the recurrent design procedure. At each stage the set of the optimal casing variants is selected (Fig. 1).

2. State variables, F_n: loads supported by the n-th casing unit section.

$$F_n^{km}[\Delta p_b, \Delta p_c, (F_A)_n^{km}] \tag{A-1}$$

In general, there are $(N_{S_{n-1}} \cdot N_W)$ combinations of the loads at stage n, where:

$k = 1, 2, \ldots, N_{S_{n-1}}$

$N_{S_{n-1}}$ = number of possible different variants of casing string below section n,

$m = 1, 2, \ldots, N_W$, and

N_W = number of different casing unit weights.

The axial loads F_{An}^{km} for the n-th section are calculated from Eq. (3). For vertical wells, they can be computed using Eq. (4), while for the directional wells Eqs. (8) through (13) have to be used.

3. Decision variables, P_n: type of casing. In the computer program each type of casing is represented by one number, i.e. unit price of casing. For n-th unit section the available casings are expressed as.

$$P_n^{kr}\ [(p_c)_n, (p_b)_n, (F_t)_n] \tag{A-2}$$

The conversion from casing price to the grade, weight and the type of casing joint is made prior to the printout. The total number of casings available for unit-section n is selected by the computer by using the following requirements.

$$(p_{cc})_n \geq \Delta p_c \cdot R_c \tag{A-3a}$$

$$(p_{bc})_n \geq \Delta p_b \cdot R_b \tag{A-3b}$$

$$(F_t)_n^{kmr} \geq (F_A)_n^{km} \cdot R_t \tag{A-3c}$$

where:

$r = 1, 2, \ldots, N_{R_n}^{km}$

$N_{R_n}^{km}$ = number of casing that satisfy requirements of Eq. A-3, given value of the load F_n^{km}

4. Return Function, C_{T_n} : total cost of n unit-sections of casing.

$$C_{T_n}^{kmr}(F_n^{km}, P_n^{kmr})$$

$$= \Delta\ell \cdot P_n^{kmr} + \Delta\ell\ (P_{n-1}^{k} + \ldots + P_1^{k})$$

$$= \Delta\ell \cdot P^{kmr} + C_{T_{n-1}}^{k} \tag{A-4}$$

5. Accumulated Total Return, C_{Tmin_n} : minimal cost of n sections of casing for each load F_n^{km}.

$$C_{Tmin_n}^{km}\ (F_n^{km}, P_n^{kmr})$$

$$= \min_{(r)}\ (\Delta\ell \cdot P_n^{kmr} + C_{T_{n-1}}^{k}) \tag{A-5}$$

Because the transition of the cost and transition of the axial load from step (n-1) to step n is achieved by simple addition, the principle of optimality can be applied and equation (A-5) becomes:

$$C_{Tmin_n}^{km}\ (F_n^{km}, P_n^{kmr})$$

$$= \min_{(r)}\ (\Delta\ell \cdot P_n^{kmr}) + C_{Tmin_{n-1}}^{k} \tag{A-6}$$

where:

$C^{k}_{Tmin_{n-1}}$ = minimal cost of k variant of casing string supported by the (n-1)-th unit section.

The result of the procedure depicted by Eq. (A-1) a matrix of $(N_{S_n} \cdot N_{C_n})$ values is generated which includes all minimum-cost casings for each load F^{km}_n.

6. Minimum total return, C_{Tmin_n}, is the absolute minimum of the cost of n unit-sections of casing string.

$$C^{km}_{Tmin_n} [F^{(km)}_{n\,min}, P^{(km)}_{n\,min}] = \min_{(km)} (C^{km}_{Tmin_n}) \qquad \text{(A-7)}$$

For n = N, Eq. (A-7) gives the minimal cost of the total casing string. This cost corresponds to the optimum configuration of casing string stored in computer memory.

7. Modification of the number of variants is made by searching the matrix $C^{km}_{Tmin_n}$ generated by the procedure of Eq. A-6 and selection of all the variants indicated by

$t = m < m_{min}$, or $q^{kt}_n < q^{(km)}_{n\,min}$

where

$$t = 1, 2, \ldots, N_{L_n}$$

This procedure selects N_{L_n} casings lighter than that associated with the absolute minimum-cost casing (weight/price conflict). The new variants must be added and the next value of N_{S_n} becomes

$$N_{S_n} = N_{L_n} + N_{S_{n-1}}$$

Simplification of Theory

In practical computations the lack of the price/weight conflict has been observed. Mathematically, it means that $N_L = 0$. Moreover, it is obvious that for $N_L \equiv 0$, $N_C \equiv 1$ for all steps of the recurrent procedure. This fact gives rise to the significant simplification. At any unit-section of the casing string

1 There is only one set of loads supported by the (n-1)-casing section, F_{n-1}

2 Instead of $(N_S \cdot N_W \cdot N_R)$, there is $(N_{R_n} \cdot N_W)$ number of casings that satisfy requirements of Eq. A-3,

$$P_n^{mr}[(p_b)_n, (p_c)_n, (F_t)_n^{mr}) \tag{A-8}$$

3 The total number of the Accumulated Total Return values reduces from $(N_S \cdot N_W)$ to N_W, from which the value of the Minimum Total Return is selected and carried over to the next step of the iterative procedure. Thus the iterative formula of the dynamic programming procedure simplifies to

$$C_{Tmin_n} = \Delta\ell\{\min_{(mr)} (P^{mr}) + \sum_{j=1}^{n-1} [\min_{(mr)}(P^{mr})]_j\} \tag{A-9}$$

APPENDIX B

Depth Conversion Formulas

1. Vertical depth is calculated

   - for the vertical portion

$$D_i = \ell_i \tag{B-1}$$

   - for the buildup portion:

$$\ell_i = D_{KOP} + \frac{180}{\pi\dot{\alpha}} \sin (\dot{\alpha}\, \ell_i - D_{KOP}) \tag{B-2}$$

   - for the slant portions:

$$D_i = D_{i+1} + (\ell_i - \ell_{i+1}) \cos \alpha_{i+1} \tag{B-3}$$

   - for the drop-off portions:

$$D_i = D_{DOF} + \frac{180}{\pi\dot{\alpha}} \{\sin \alpha 1 - \sin [\dot{\alpha}(\ell_{S1} - \ell_i) + \alpha 2]\} \tag{B-4}$$

2. Inclination angle is computed

   - for the vertical portion:

$$\alpha_i = 0 \tag{B-5}$$

   - for the buildup portion:

$$\alpha_i = \dot{\alpha}(0.5 + \ell_i - D_{KOP}) \tag{B-6}$$

   - for the slant portions:

$$\alpha_i = \alpha_{i+1} \tag{B-7}$$

   - for the drop-off portion:

$$\alpha_i = \alpha 1 - \dot{\alpha}\, (0.5 + \ell_i - \ell_{DOF}) \tag{B-8}$$

   where

$$\alpha 1 = \dot{\alpha}(\ell_{S1} - \ell_{KOP}) \tag{B-9}$$

$$\alpha 2 = \alpha 1 - \dot{\alpha}(\ell_{S2} - \ell_{DOP}) \tag{B-10}$$

TABLE 1—EXAMPLE DESIGN OF THE 9⅝-in. INTERMEDIATE CASING

Casing Setting Depth (ft)	Minimum Weight Design			Minimum Cost Design		
	Number of Sections	Total Cost ($)	Total Weight (lbf)	Number of Sections	Total Cost ($)	Total Weight (lbf)
5,000	3	101,014	193,440	3	101,014	193,440
6,000	1	153,934	240,000	1	153,934	240,000
7,000	2	183,770	280,000	2	183,770	280,000
8,000	3	182,800	314,880	3	182,800	314,880
9,000	1	230,900	360,000	1	230,900	360,000
10,000	3	260,911	400,000	3	260,911	400,000
11,000	5	304,091	440,000	5	304,091	440,000

TABLE 2—EXAMPLE PRESSURE PROFILES: LOUISIANA GULF COAST

Depth (ft)	Profile 1		Profile 2	
	Pore Pressure (lbm/gal)*	Fracture Gradient (lbm/gal)*	Pore Pressure (lbm/gal)*	Fracture Gradient (lbm/gal)*
2,000	9.0	12.9	9.0	13
4,000	9.0	14.15	9.0	14.4
6,000	9.0	15.15	9.0	15.4
8,000	9.0	16.0	10.0	16.2
10,000	9.5	16.7	11.2	17.5
12,000	14.4	18.0	12.8	18.3
14,000	16.3	18.5	14.1	19.0
16,000	17.4	18.7	15.0	19.2

*Equivalent mud density

TABLE 3—7-in. CASING COST COMPARISON

Casing Setting Depth (ft)	Casing Cost, dollars		
	Quick Design Charts	Minimum Cost Design	
		Production	Intermediate*
6,000	85,287	82,579	78,636
8,000	138,095	141,033	93,145
10,000	196,027	187,916	135,321
12,000	259,579	243,411	188,018
14,000	334,330	311,441	—
16,000	441,099	386,417	—

*Equivalent mud density at the next casing seat assumed 15 lbm/gal (Refer to Profile 2 in Table 2)

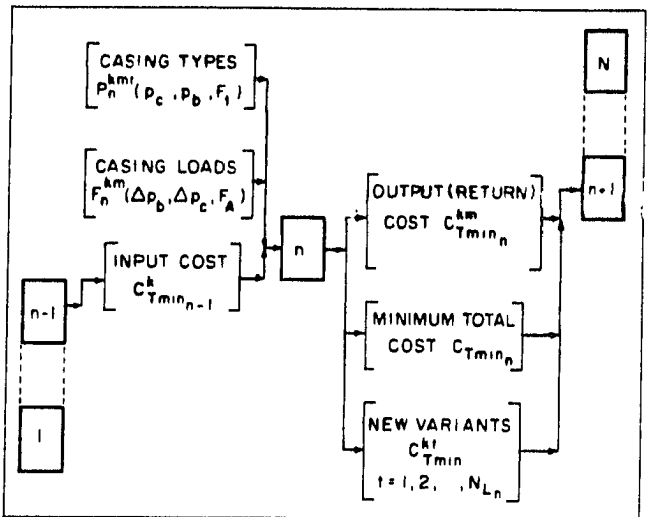

Fig. 1—Recursion of the optimum casing design procedure.

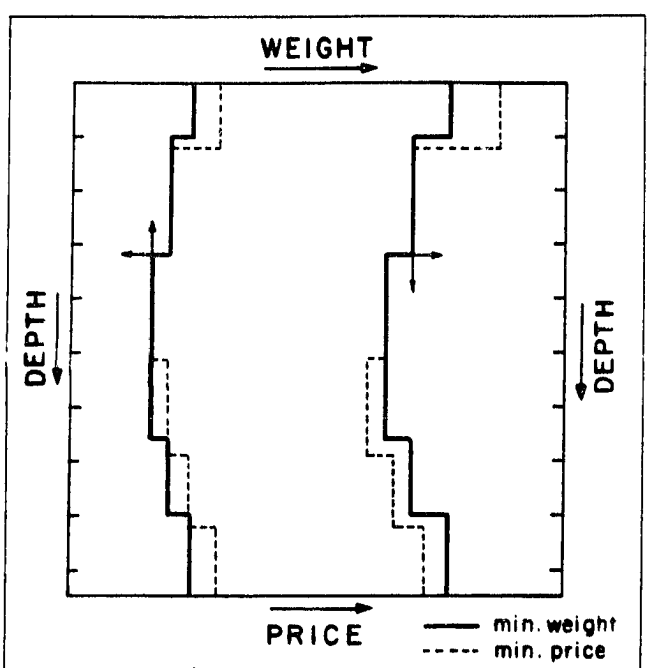

Fig. 2—Hypothetical conflict between minimum-weight and minimum-price design.

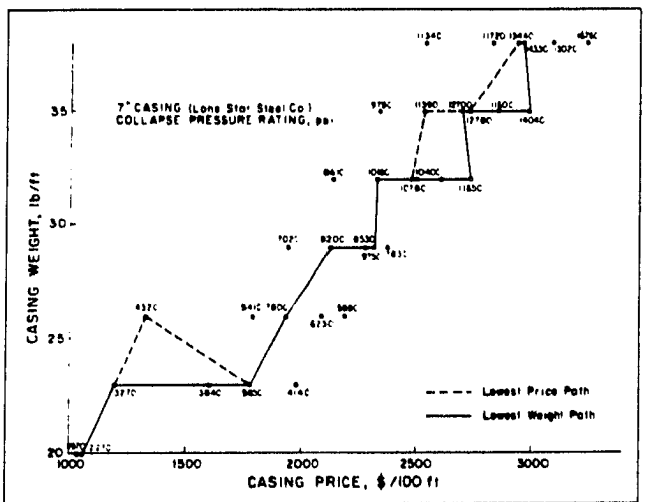

Fig. 3—Proximity of the minimum-price and minimum-weight casing design paths; progressive collapse pressure rating.

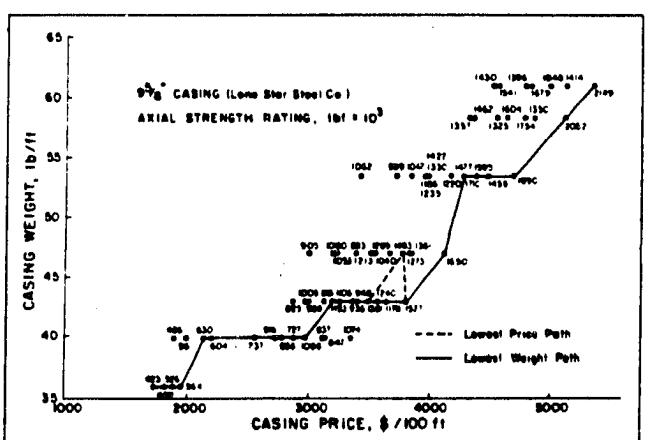

Fig. 4—Proximity of the minimum-price and minimum-weight casing design paths; progressive axial load rating.

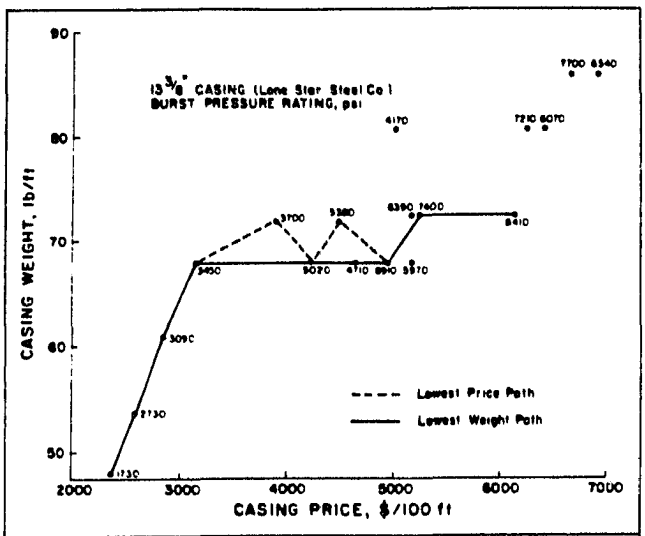

Fig. 5—Proximity of the minimum-price and minimum-weight casing design paths; progressive burst pressure rating.

```
                    INTERMEDIATE CASING DESIGN

THE WELL DATA USED IN THIS PROGRAM WAS:
      *EQUIVALENT FRACTURE GRADIENT AT CASING SEAT=17.4 PPG
      *TRUE VERTICAL DEPTH AT CASING SEAT=11400. FEET
      *BLOW OUT PREVENTOR RESISTANCE=5000. PSI
      *DENSITY OF THE MUD THE CASING IS SET IN=13.7 PPG
      *DENSITY OF HEAVIEST MUD IN CONTACT WITH THIS CASING=16.9 PPG
      *TVD OF NEXT CASING SEAT=15000. FEET
      *PORE PRES. AT NEXT CASING SEAT DEPTH=16.4 PPG
      *MINIMUM CASING STRING LENGTH=1000.

9 5/8" CASING LONE STAR PRICE LIST.  FILE REF.:PR962LS
MAIN PROGRAM:  CSG6

TOTAL PRICE=367400. DOLLARS
TOTAL STRING WEIGHT=518020. LBS

D.I=11400.-9120. L=2280. NN=13 W=43.50 M=2 MDFB=1.40 MDFC=1.65 MDFBY=9.67 $/100FT=3007.88
D.I= 9120.-6360. L=2760. NN=14 W=47.00 M=2 MDFB=1.40 MDFC=1.69 MDFBY=4.60 $/100FT=3240.61
D.I= 6360.-3800. L=2560. NN=18 W=47.00 M=2 MDFB=1.52 MDFC=1.20 MDFBY=3.47 $/100FT=3524.04
D.I= 3800.-2800. L=1000. NN=18 W=43.50 M=2 MDFB=1.48 MDFC=1.31 MDFBY=2.82 $/100FT=3261.62
D.I= 2800.-1800. L=1000. NN=14 W=47.00 M=2 MDFB=1.50 MDFC=2.70 MDFBY=2.39 $/100FT=3240.61
D.I= 1800.-   0. L=1800. NN=13 W=43.50 M=2 MDFB=1.50 MDFC=3.00 MDFBY=1.85 $/100FT=3007.88

THE MEANING OF SYMBOLS ARE:
      *D.I, DEPTH INTERVAL IN FEET
      *L, LENGTH (FEET)
      *NN, TYPE OF GRADE (SEE THE CODING BELOW)
      *W, WEIGHT/FOOT
      *M IS THE TYPE OF THREAD REQUIRED: M=1, SHORT THREAD
                                         M=2, LONG THREAD
                                         M=3, BUTTRESS
      *MDFB, MINIMUM DESIGN FACTOR FOR BURST
      *MDFC, MINIMUM DESIGN FACTOR FOR COLLAPSE
      *MDFBY,MINIMUM DESIGN FACTOR FOR BODY YIELD

GRADE CODE:
NN 1= ...H40 NN 2= ...J55 NN 3= ...K55 NN 4= ...C75 NN 5= ...L80
NN 6= ...N80 NN 7= ...C95 NN 8= ..P110 NN 9= ..V150 NN13= ...S95
NN14= .CYS95 NN15= ..S105 NN16= ...S80 NN17= ..S95 NN18= .LS110
NN19= .LS125
```

Fig. 6—Output of the minimum-cost casing computer program for vertical wells.

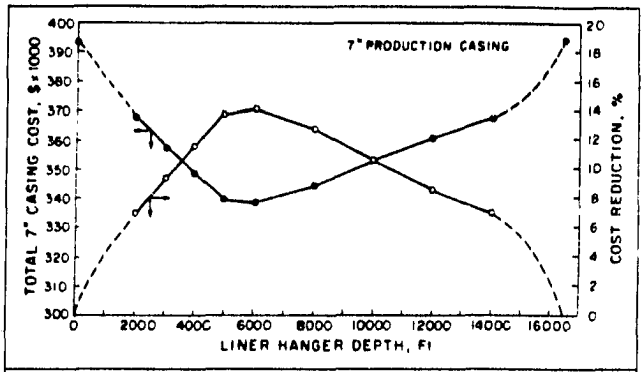

Fig. 7—Optimization of the 7-in. liner setting depth.

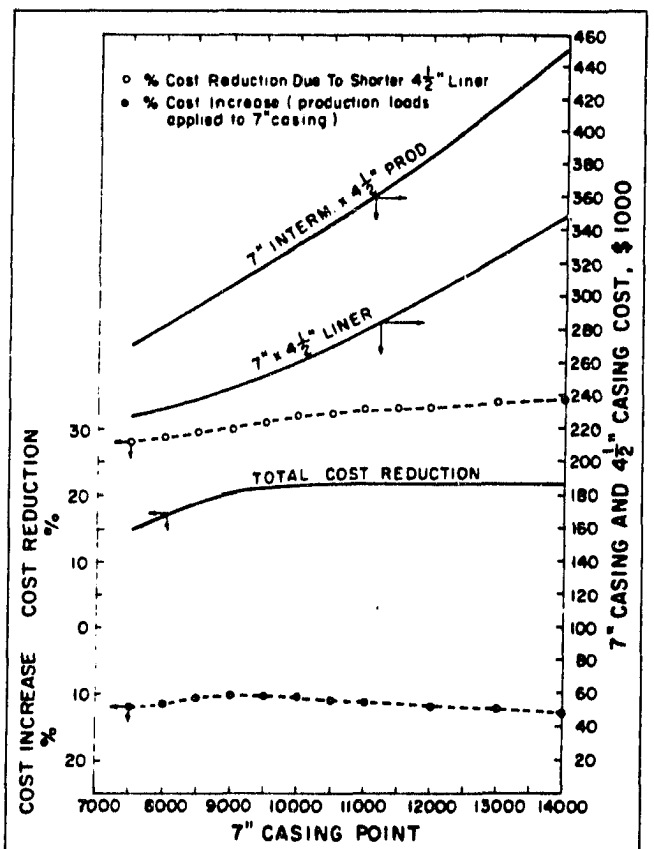

Fig. 8—Comparison of the two minimum-cost casing alternatives for a 15,000-ft well; production liner (no tieback) vs. full-length production string.

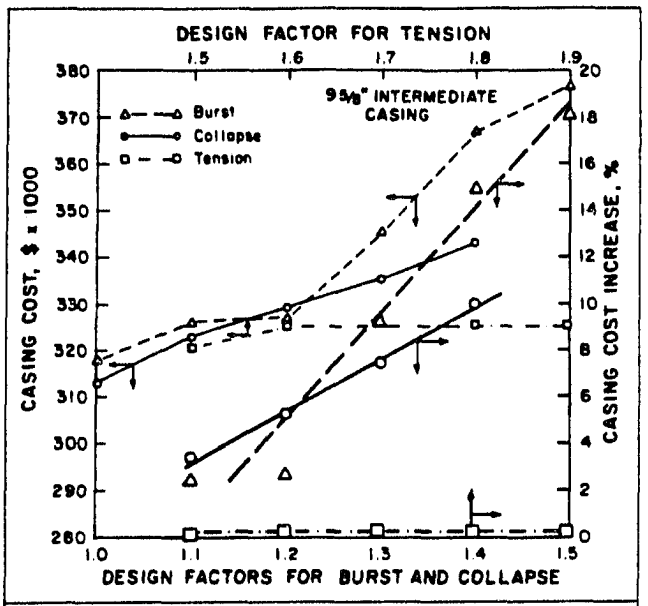

Fig. 9—Effect of design factors on the minimum cost of 9⅝-in. casing string.

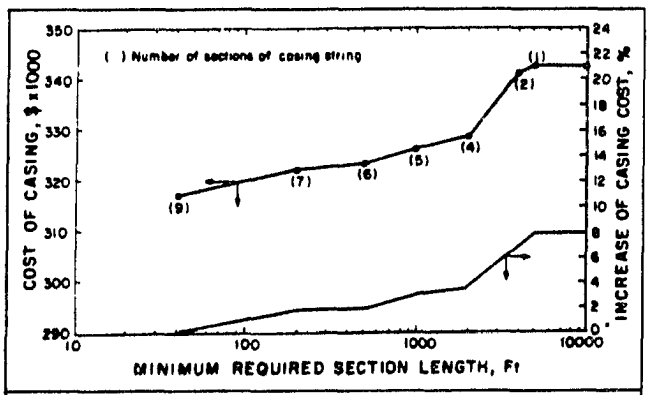

Fig. 10—Minimum-cost combination casing string with varying number of sections.

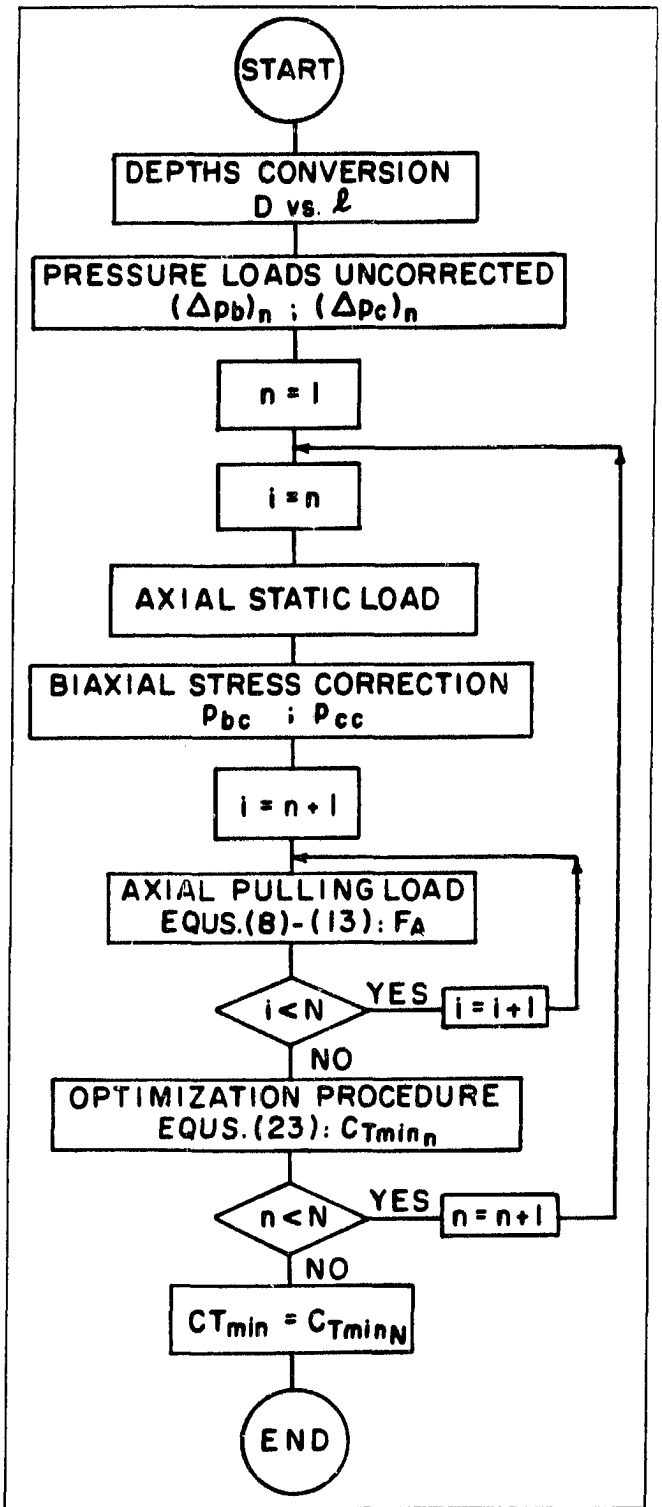

Fig. 11—Flow diagram of the minimum-cost casing design program for directional wells.

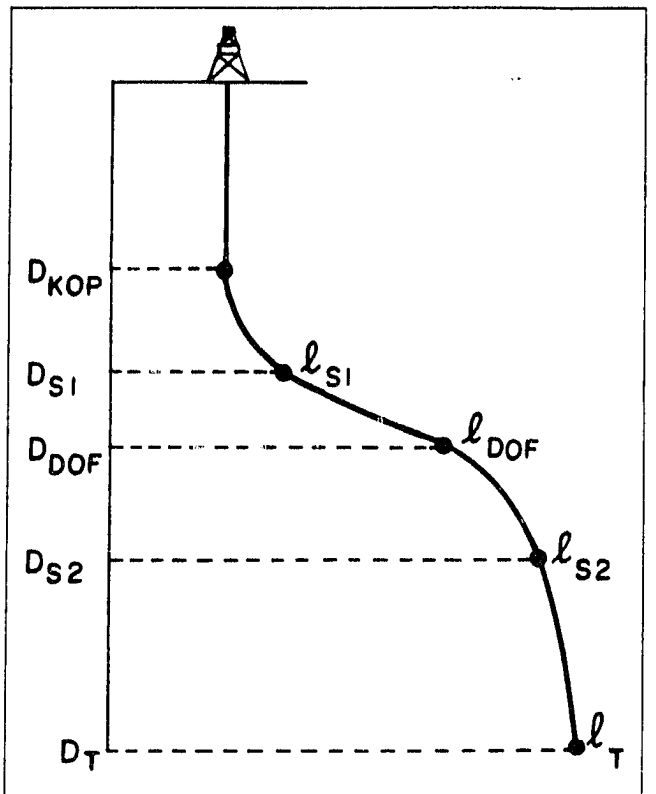

Fig. 12—Generalized vertical projection of a directional well.

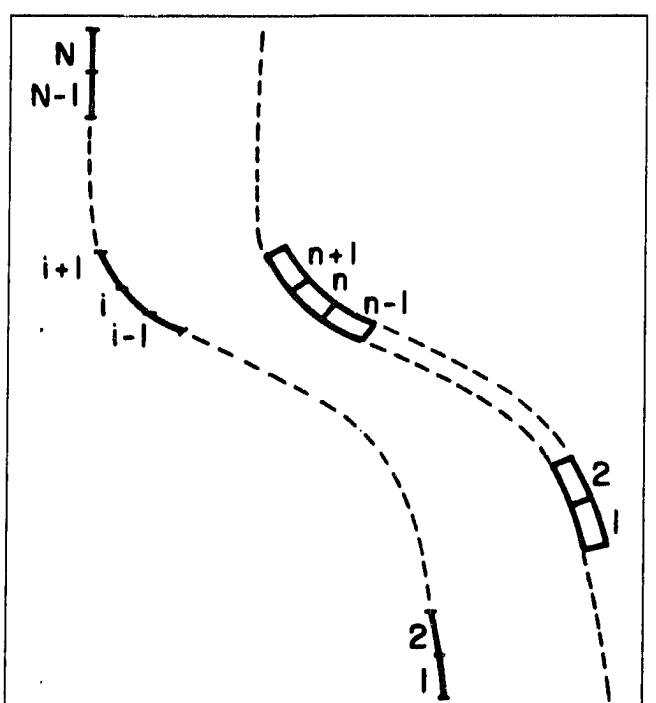

Fig. 13—Instantaneous *i*th position of the *n*th unit section of casing in a directional well.

```
                    DIRECTIONAL WELL INTERMEDIATE CASING DESIGN

THE WELL DATA USED IN THIS PROGRAM WAS:
     EQUIVALENT FRACTURE GRADIENT AT CASING SEAT=17.4 PPG
     BLOW OUT PREVENTER RESISTANCE=5000. PSI
     DENSITY OF THE MUD THE CASING IS SET IN=13.0PPG
     DENSITY OF HEAVIEST MUD IN CONTACT WITH THIS CASING=16.9 PPG
     TVD OF NEXT CASING SEAT=15000.FEET
     PORE PRES. AT NEXT CASING SEAT DEPTH=16.4 PPG
     MINIMUM CASING STRING LENGTH=1000.
     DSGN FAC:  BUR=1.100; COL=1.125; B.YIELD=1.000
     DESIGN FACTOR FOR RUNNING LOADS=1.500
     KICK OFF POINT=2000. FEET
     MEASURED DEPTH AT END OF BUILD UP=5600.FEET
     MEASURED DEPTH AT DROP OFF POINT= 9200.FEET
     MEASURED DEPTH AT END OF DROP OFF = 12000. FEET
     TOTAL MEASURED DEPTH=16000. FEET
     BUILD UP RATE= 3.0 DEG/100FT
     DROP OFF RATE= 2.0 DEG/100FT
     PSEUDO FRICTION FACTOR=0.500 D-LESS
     BOYANCY CONSIDERED ON STATIC LOADS

7" CASING LONE STAR PRICE LIST.  FILE REF.:PR700LS
MAIN PROGRAM:  CSGD3

TOTAL PRICE=293101. DOLLARS
TOTAL STRING WEIGHT=288977.LBS

D.I=16000.-10240. L= 5760. NN= 6 W= 23.00 M=2 MSFB= 1.17 MSFC= 1.13 MSFBY= 6.18 $/100FT= 1608.00
D.I=10240.- 5080. L= 4360. NN=13 W= 23.00 M=2 MSFB= 1.30 MSFC= 1.42 MSFBY= 3.20 $/100FT= 1782.58
D.I= 5080.- 4600. L= 1280. NN=13 W= 23.00 M=3 MSFB= 1.38 MSFC= 1.50 MSFBY= 3.40 $/100FT= 1906.56
D.I= 4600.- 2800. L= 1800. NN=18 W= 26.00 M=3 MSFB= 1.73 MSFC= 1.85 MSFBY= 3.69 $/100FT= 2241.50
D.I= 2800.-    0. L= 2800. NN=13 W= 26.00 M=3 MSFB= 1.56 MSFC= 3.32 MSFBY= 2.48 $/100FT= 2071.75

THE MEANING OF SYMBOLS ARE:
     D.I, DEPTH INTERVAL IN FEET
     L, LENGTH (FEET)
     NN, TYPE OF GRADE (SEE THE CODING BELOW)
     W, WEIGHT/FOOT
     M IS THE TYPE OF THREAD REQUIRED: M=1, SHORT THREAD
                                       M=2, LONG THREAD
                                       M=3, BUTTRESS
MSFB, MINIMUM SAFETY FACTOR FOR BURST
MSFC, MINIMUM SAFETY FACTOR FOR COLLAPSE
MSFBY,MINIMUM SAFETY FACTOR FOR BODY YIELD

GRADE CODE:
NN 1= ...H40 NN 2= ...J55 NN 3= ...K55 NN 4= ...C75 NN 5= ...L80
NN 6= ...N80 NN 7= ...C95 NN 8= ..P110 NN 9= ..V150 NN13= ...S95
NN14= .CYS95 NN15= ..S105 NN16= ...S80 NN17= ..SS95 NN18= .LS110
NN19= .LS125
```

Fig. 14—Output of the minimum-cost casing computer program for directional wells.

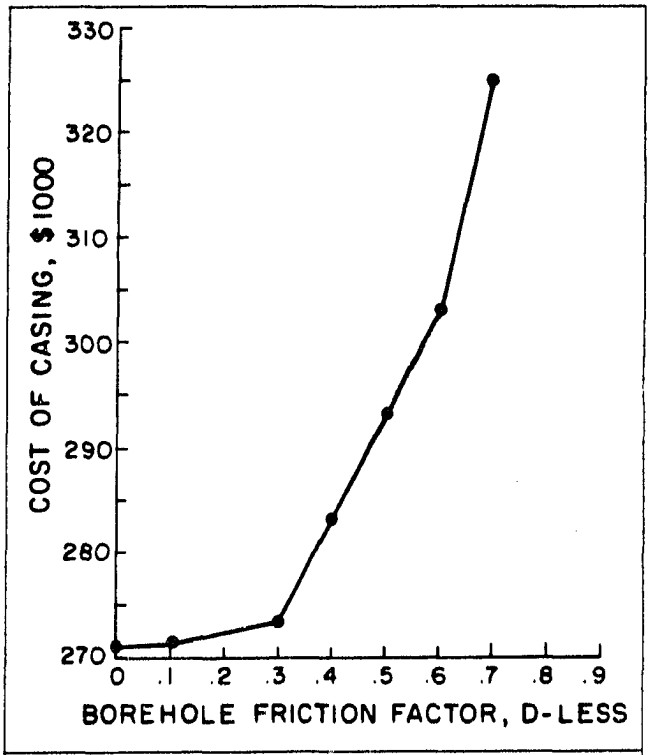

Fig. 15—Effect of the borehole friction factor on the minimum cost of 7-in. intermediate casing in a directional well.

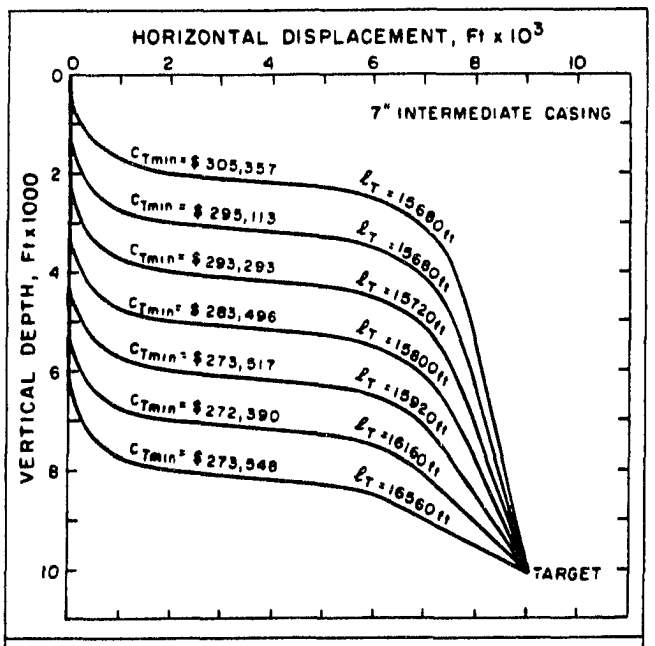

Fig. 16—Minimum cost and total length of casing string for various depths of the kickoff point.

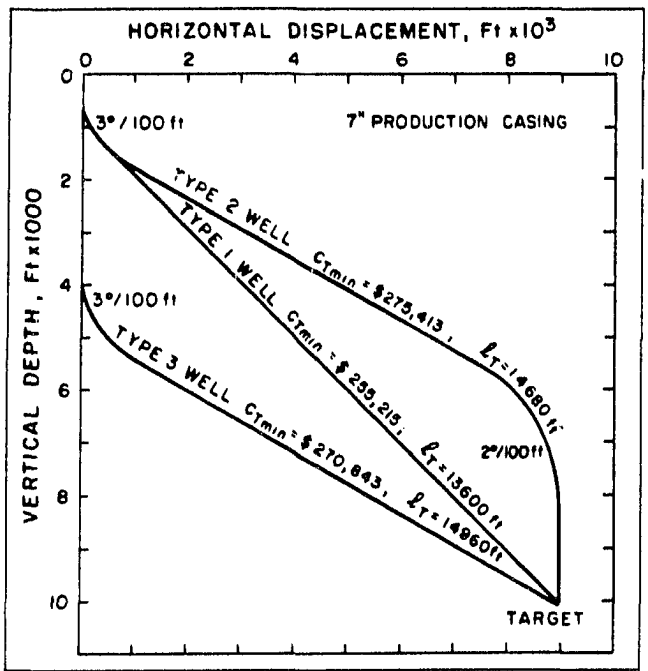

Fig. 17—Effect of directional well profile on the minimum casing cost.

CHAPTER VI

SUMMARY AND RECOMMENDATIONS

The main contributions of this research can be summarized as:

1. A field method for the borehole friction evaluation was presented that includes the hydrodynamic viscous drag contribution to hook loads while running a string of pipe in the well. The numerical simulation studies revealed that if viscous drag is disregarded, the borehole friction factor could be overestimated by as much as 26% (for a slant well inclination of 30 deg. and a casing running velocity of 2 ft/sec).

2. Field studies also revealed that not every directional well, or section of one, qualified for borehole friction factor assessment. The accuracy of this parameter's estimation was best for drag-weight ratios above 25%.

3. The laboratory experiments showed that 80% of the stabilized friction factor values were between 0.20 and 0.30.

4. The inclusion of drag to casing design reduces the pulling-out load prediction as compared to the conventional method. This occurs since the conventional method ignores the well trajectory, thus compensating by using for every well the same overpull design factor to account for both drag and borehole problems.

5. The general theory for casing design optimization for minimum cost was developed. A simplification of the optimization procedure was possible based on the price structure of three casing manufactures here in the U.S. that showed that the minimum-weight casing string was equivalent to the minimum-cost casing string.

Further investigations, concerning this research, could include:

o The study of differential sticking that could cause some drag increase before the casing string is initiated to reciprocate for cementing. This could be done by upgrading the existing laboratory equipment to accommodate simultaneously dynamic filtration under high pressure, temperature, and torque measurements (friction factor measurements).

o The existing laboratory equipment can be used to evaluate the effectiveness of several commercial lubricants on the final stabilized friction factor values.

o Some of the effects disconsidered by the 3-D model, such as torsion and spring effects, could be studied. They might contribute to increase the hook loads, specially in areas of shallow doglegs, and could also be significant at the very end of the pipe string.

APPENDIX 1

Permission of Copyright Holder

Department of Petroleum Engineering
LOUISIANA STATE UNIVERSITY AND AGRICULTURAL AND MECHANICAL COLLEGE
BATON ROUGE · LOUISIANA · 70803-6417
504/388-5215

June 16, 1987.

SOCIETY OF PETROLEUM ENGINEERS
Publications - c.o. Mrs Frances Morton
P. O. Box 833836
Richardson, Tx 75083-3836

Ref.: SPE papers 14499, 15696, 16663.

Dear Sirs:

I wish to use reprints of my papers published and copies of manuscripts accepted for publication as the major part of doctoral dissertation. Since the bound dissertation will be microfilmed, I am writing to request written permission to remicrofilm the articles as required by Louisiana State University. (A copy of Instructions for preparation of dissertations using reprints is enclosed).

The papers for which remicrofilming is requested are:

1. A. Wojtanowicz, E. E. Maidla, "Minimum Cost Casing Design for Vertical and Directional Wells". SPE 14499, 1985.

2. E. E. Maidla, A. Wojtanowicz, " Field Method of Assessing Borehole Friction For Directional Well Casing", SPE 15696, 1987.

3. E. E. Maidla, A. Wojtanowicz, "Field Comparison of 2-D and 3-D Methods for the Borehole Friction Evaluation in Directional Wells", SPE 16663, 1987.

Sincerely
Eric E. Maidla

SPE
Society of Petroleum Engineers
P O BOX 833836 • RICHARDSON TX 75083 3836 USA • (214) 669 3377 • TELEX 730989 SPEDAL • FACSIMILE (214) 669 0135

GEORGEANN BILICH
Technical Publications Manager

July 22, 1987

Eric E. Maidla
Louisiana State U.
Dept. of Petroleum Eng.
Baton Rouge, LA 70803-6417

Re: Your Copyright Inquiry of June 16, 1987

Thank you for your recent request to use material copyrighted to the Society of Petroleum Engineers. This is to grant one-time permission to use the material identified on the enclosed form for the purpose specified, provided that you include full and proper notice of SPE copyright ownership and acknowledgment of the source.

Proper copyright ownership acknowledgment and source attribution for the item(s) SPE can give you permission to use appear in the right-hand column of the enclosed form. Permission to use this is subject to your proper identification of SPE as the copyright holder and source. Please see the SPE Copyright Notice at the bottom of the enclosed form.

The Society's copyright position encourages the broadest possible distribution of technical material to which it holds copyright, as is consistent with our copyright agreements with authors. Thank you for your cooperation in this matter, which is essential to protect the rights of the many authors who make technical material generally available through the Society.

Sincerely yours,

Georgeann Bilich

Georgeann Bilich

Enclosures

SOCIETY OF PETROLEUM ENGINEERS

Use of Material Copyrighted to SPE-AIME

Date: 7/21/87

I request permission to use material from the following SPE publication(s).

And agree to include the following notice of SPE Copyright Ownership on each item used:

Check One: ☐ JPT ☐ SPEJ ☐ SPEDE ☐ SPEFE ☐ SPEPE ☐ SPERE
☐ SPE Book ☒ Paper Number SPE 14499

Title of Paper or Book: Minimum Cost Casing Design for Vertical and Directional Wells

Date Published: _____ 19 ___ The specific material requested is:

Page	Figure Number	Table Number	Text or Other (Describe)
___	___	___	whole article
___	___	___	
___	___	___	

OFFICE USE ONLY

☒ Copyright © 19 85 SPE-AIME
☒ Paper first presented at the Eastern Regional Meeting
held November 6-8 19 85 in Morgantown WV
☐ First published in the ☐ JPT ☐ SPEJ ☐ SPEDE ☐ SPEFE ☐ SPEPE ☐ SPERE
_____ 19 ___

Check One: ☐ JPT ☐ SPEJ ☐ SPEDE ☐ SPEFE ☐ SPEPE ☐ SPERE
☐ SPE Book ☒ Paper Number SPE 15696

Title of Paper or Book: Field Method of Assessing Borehole Friction for Directional Well Casing

Date Published: _____ 19 ___ The specific material requested is:

Page	Figure Number	Table Number	Text or Other (Describe)
___	___	___	whole article
___	___	___	
___	___	___	

OFFICE USE ONLY

☒ Copyright © 19 87 SPE-AIME
☒ Paper first presented at the Middle East Oil Show
held March 7-10 19 87 in Manama, Bahrain
☐ First published in the ☐ JPT ☐ SPEJ ☐ SPEDE ☐ SPEFE ☐ SPEPE ☐ SPERE
_____ 19 ___

Check One: ☐ JPT ☐ SPEJ ☐ SPEDE ☐ SPEFE ☐ SPEPE ☐ SPERE
☐ SPE Book ☒ Paper Number SPE 16663

Title of Paper or Book: Field Comparison of 2-D and 3-D Methods for the Borehole Friction ...

Date Published: _____ 19 ___ The specific material requested is:

Page	Figure Number	Table Number	Text or Other (Describe)
___	___	___	whole article
___	___	___	
___	___	___	

OFFICE USE ONLY

☒ Copyright © 19 87 SPE-AIME
☒ Paper first presented at the Annual Fall Technical Conference & Exhibition
held September 27-30 19 87 in Dallas, TX
☐ First published in the ☐ JPT ☐ SPEJ ☐ SPEDE ☐ SPEFE ☐ SPEPE ☐ SPERE
_____ 19 ___

I request permission to use this material one time in:

Title: Borehole Friction Assessment and application to oilfield Casing Design in Directional Wells
Author(s): Eric E. Maidla
Publisher: _____ Publication Date: DEC/1987
Form of Publication: dissertation Number of Copies: _____
Signature: Eric E. Maidla Name: Eric E. Maidla
Organization: Louisiana State U.
Address: Dept. of Petroleum Eng.
Baton Rouge, La
70803-6417
Phone: _____ Telex: _____

RETURN THIS FORM TO:
SPE Publications Dept.
P.O. Box 833836
Richardson, TX 75083-3836

1/87 Retain for Your Files

SPE Copyright Notice

Proper notice of SPE copyright ownership is required on (1) any copy or substantial portion of an SPE paper or other SPE publication and (2) any figure, table, or other portion of any publication to which SPE holds copyright.

As noted above, proper notice of SPE copyright ownership consists of the word "Copyright" or the symbol ©, the year of first publication by SPE and the words "Society of Petroleum Engineers of AIME" or "SPE-AIME." This acknowledgment must appear legibly on each copy of the work or portion thereof.

In addition, SPE requests that each acknowledgment include either (1) the date of publication and the book or journal in which published or (2) the name, location, and dates of the meeting where first presented. This information appears above in this column for each item for which permission is granted.

APPENDIX 2

Reprint:

Maidla, Eric E., Wojtanowicz, Andrew K.,

"Field Method of Assessing Borehole

Friction for Directional Well Casing",

SPE 15696, 1987.

SPE
Society of Petroleum Engineers

SPE 15696

Field Method of Assessing Borehole Friction for Directional Well Casing

by E.E. Maidla and A.K. Wojtanowicz, Louisiana State U.
SPE Members

This paper was prepared for presentation at the Fifth SPE Middle East Oil Show held in Manama, Bahrain March 7-10, 1987

ABSTRACT

This paper presents a method to evaluate an overall friction coefficient between borehole and casing. The computation is done by matching hook load data, recorded in the field, with the calculated hook load obtained by assuming a friction factor coefficient. The equations for predicting surface hook loads are derived from the respective governing differential equations. The iterative nature of the calculations are handled by a computer program. One case history from a rig offshore Louisiana State, confirmed the possibility of evaluating this friction coefficient, while also describing the equipment and necessary care used to record the data.

INTRODUCTION

A new method for casing design in directional wells was presented in Nov'1985[1]. It introduced a new constraint to the casing design process by imposing the need of upward pipe movement, whether for reciprocation while cementing, whether for pulling out part of the (or the entire) casing string from the hole, due to any technical problem while running it in. This design method requires, among other data, the knowledge of an overall friction coefficient.

Other design methods have simply ignored the effect of wall support on casing, and simple don't design for the possibility of any upward pipe movement. The method of the vertical projected depth is an example of this. In this situation, when reciprocation for cementing purposes is required, a reciprocation trial takes place when the casing shoe reaches the bottom of the hole, that isn't always successful.

In this research work, friction between the borehole and casing is looked at in a macroscopic scenario, where its overall average value is relatively constant along a borehole. This approach is similar to that undertaken in previous research[2,3] on the drillstring borehole friction. The overall friction coefficient is a simplification of what is believed to be a complex mechanism of mechanical interaction between a tubular string and a borehole. Though it basically ignores the effects of lithology stratification, the compressive and shear strength of the rocks, rock and casing hardness, and the everchanging borehole diameter. It provides an attractive simplification useful in directional casing string design for a given location.

The overall friction coefficient equation can be summarized as:

$$FF = \frac{HL - VPBW}{NF} \qquad (1)$$

Unfortunately equation (1) is of no practical importance for this situation due to the dependence of the normal force (while on a curved path), on the axial load immediately below. Thus a computer is necessary to calculate the friction coefficient having a recursive procedure and an iterative search procedure built in it.

DESCRIPTION OF THE MODEL:

The calculations proceed from the lower

References and illustrations at end of paper.

end of the casing string upwards. This procedure is the same regardless the casing being pulled out or run in. Calculations are performed at each survey point. If the casing end is in between two survey points, linear interpolation is used to assign survey values to that point. The simplified program flowchart is shown in Fig. 1.

The stepwise procedure was used for calculating tensional loads when going from one survey station to the next. Before proceeding to the next step, there are three possible situations to consider:

CASE I, the inclination can increase with increasing depth (build-up section);

CASE II, the inclination can decrease with increasing depth (drop-off section);

CASE III, the inclination can remain unaltered with increasing depth (slant hole portion).

CASE I:

For CASE I, the borehole friction is controlled by the direction and the value of the normal force. The forces acting on a small casing element in the well are shown in Fig. 2. Here, three positions of casing in the borehole are possible - Fig. 3. For the upmost position, while pulling-out casing, at survey station "i" (i = 1, ... , K), the tensional load at the top (station "i+1") is:

$$T_{i+1} = T_i \times A1 + B \times [C \times D1 - E \times F1] \quad ...(2)$$

where $T_1 = 0$

$$A1 = e^{[FF \times (I_i - I_{i+1})]}$$

$$B = \frac{R \times W \times BF}{1 + FF}$$

$$C = FF - 1$$

$$D1 = SIN(I_{i+1}) - SIN(I_i) \times A1$$

$$E = 2 \times FF$$

$$F1 = COS(I_{i+1}) - COS(I_i) \times A1$$

$$R = \frac{MD_i - MD_{i+1}}{I_i - I_{i+1}} \quad .....(3)$$

For the intermediate position, while pulling-out casing:

$$T_{i+1} = T_i + R \times W \times BF \times [SIN(I_i) - SIN(I_{i+1})] \quad (4)$$

For the bottom position, while pulling-out casing, the tensional load equation is:

$$T_{i+1} = T_i \times A2 + B \times [C \times D2 + E \times F2] \quad ...(5)$$

where: $A2 = e^{-FF \times (I_i - I_{i+1})}$

$$D2 = SIN(I_{i+1}) - SIN(I_i) \times A2$$

$$F2 = COS(I_{i+1}) - COS(I_i) \times A2$$

The equations for the situation of running-in casing are similar to the ones derived while pulling-out, due to the sign convention used (see Fig. 2 , 4 , and 5). Therefore for the upmost position, eq(5) is obtained, for the bottom position eq. (2) is obtained, and for the intermediate position the equation remains unaltered.

CASE II:

For the drop-off interval of a borehole, tensional load is controlled only by the type of operation. The forces acting on a small casing element in the well are shown in Fig. 4.

For pulling-out scenario, the tensional load is:

$$T_{i+1} = T_i \times A2 - B \times [C \times D2 + E \times F2] \quad ...(6)$$

For the running-in scenario:

$$T_{i+1} = T_i \times A1 - B \times [C \times D1 - E \times F1] \quad ...(7)$$

CASE III:

For the slant hole portion, the forces acting on a small casing element in the well are shown in Fig. 5. The tensional load for pulling-out is:

$$T_{i+1} = T_i + (MD_i - MD_{i+1}) \times W \times BF \times G1 \quad ..(8)$$

where: $G1 = FF \times SIN(I_{i+1}) + COS(I_i)$

and for running in:

$$T_{i+1} = T_i + (MD_i - MD_{i+1}) \times W \times BF \times G2 \quad ..(9)$$

where: $G2 = COS(I_i) - FF \times SIN(I_i)$

Using equations (2) through (9) it is possible to calculate hook load for a given friction factor value, as:

$$HL = T_K \quad .....(10)$$

The basic assumptions used in the model are:

- .Inclination changes (doglegs) with measured depth is of major significance and is accounted for.
- .Direction changes are not considered. This can be visualized by considering a succession of vertical planes, each one limited between two survey points.
- .Bending contribution to normal force is not considered.
- .Buoyancy is considered.
- .One single value of an overall friction factor represents all possible mechanisms working against pipe movement in the open hole.
- .The effect of different lithologies is implicit in the overall friction factor.
- .Differential sticking is not considered.
- .Fluid pressure changes (while moving pipe) are not considered.
- .The inclination angle remains below 90 degrees.

FIELD PROCEDURE TO RECORD HOOK LOAD:

Limited experimental experience from the preliminary field tests gave rise to establishing a field procedure for collecting hook load data. An electronic tensiometer proved to be a reliable way to measure hook load. It was attached to the dead line so that the tension was picked up by a load cell containing a strain gauge. The electric signal produced was further digitized and stored by a computer. A schematic diagram illustrating an installation for the measurement is shown in Fig. 6.

An alternative field procedure is to install a hydraulic sensor on the hydraulic line that connects the dead line anchor signal to the driller's console. Such equipment is available to us here at LSU, but was not the equipment used to record the data described in the field case study in this paper. Normally the dead line is attached to an anchor device. The anchor can rotate a certain amount but its movement is stopped by a hydraulic sensor. The hydraulic signal produced by this sensor is proportional to the hook load for a given number of strings through the blocks, a given diameter of the dead line anchor, and a given area of the sensor device.

The parameters recorded during the casing run were hook load, time, and depth. The necessary resolution was around 1000 lbf. The sampling rate was selected so that at least 15 values of hook load were recorded for one casing pipe run. Our experience showed that one sample per second was adequate.

It was found advisable to check upon the accuracy obtained with each different equipment that depended upon the calibration of the components involved in measuring the different signals and also their correct maintenance. Specific calibration details will not be addressed here because different type of equipment will have its own peculiarities, but one "point checkup" for the whole system is necessary. Its procedure is as follows: while circulating on bottom (before running casing), stop the pump, rotate for a while and then measure the hook load with the same equipment that will be used to record the casing hook load. The load measured then should equal the calculated vertical projected buoyant weight of the pipe.

Preliminary experience gained in this research indicated that the hook load recording should begin when the casing shoe is below the buildup portion of the well, as will be shown later on in this paper.

If the hole conditions are good the possibility of picking up the casing string should be studied at predetermined depths. The picking-up procedure used in this research was as follows: casing was slowly picked up until hook load stabilized - normally between 10 to 30 ft above slips. These points were used to calculate friction factor while pulling casing out. The values of the borehole friction factor calculated from pulling tests, provided an ultimate verification of the procedure. Ideally, of course, they should be equal to those calculated from running-in data. The discrepancy between the two was a measure of the effect of some other factors such as incorrect measurements or additional component of borehole friction disregarded in the model.

In order to avoid an overload on the casing while pulling out, it is recommended that hook load not exceed 70% of the weakest joint strength in the casing string or 70% of the weakest pipe strength which ever is smaller.

CASE HISTORY:

Field record of casing installation was performed in March 1986 at a jackup rig, offshore Louisiana. The horizontal departure and the vertical section of this well are shown in Fig. 7 and Fig. 8 respectively. A 7 5/8" production casing string was run to 11,538 ft. Surface 10 3/4" casing was set at 3,820 ft. Then, the 9 1/2" bit was used to reach the target of 11538 ft. The drilling fluid was a water base mud of 9.3 lbf/gal density, 41 sec/quart viscosity, 9.5 pH, and and the API filtration of 6.5 cc/30 sec.

The operator's equipment was used to record the data. An electronic tensiometer provided the hook load readings that were

further digitized and stored. Before running in casing, during the last circulation on bottom, the pumps were stopped, the drill pipe was rotated, and hook load was measured. This reading equalled the calculated vertical projected buoyant weight of the drill string, as expected, providing a good check up on the equipment. All the maintenance of the tensiometer and intermediate equipment, was handled by a subcontractor that was constantly monitoring the system. At the time of recording the weather was good.

The raw experimental data included 60 hook load vs time graphs obtained during the entire casing run, out of which 3 also included picking up the casing string. An example of one of these three graphs is shown in Fig. 9: this graph was recorded when the casing shoe was at 9741 ft; first the casing string was picked up from the slips and held for about 24 sec; then 35ft of casing were run in, taking about 17 sec.; about 5 ft before hitting the slips, the elevator was stopped and the string was held there for another 17 sec.; after that the pipe was picked up 40 ft slowly (about .5 ft/sec); the string was then run in again and placed in slips. The sampling time was 1 sec. For each of the graphs, with only running in hook load data, one hook load value was selected by fitting manually the best horizontal straight line representing its average value for that particular run. From the other 3 graphs two values of average hook load were obtained (one for running in, and one for pulling out).

For each hook load and depth, a respective friction factor was calculated using the computer program. The sample output of the computer program is shown in Table 1. Note that it includes the average friction factor while running in casing. The program also plotted the measured hook load versus depth as shown by the symbols on Fig. 10 (running in situation) and Fig. 11 (pulling out situation), and the predicted hook load as shown by the solid line. A good match between calculated and measured data is evident in Fig. 10. This is to be expected since the value of the friction factor originated from this data. Furthermore, Fig. 11 shows an actual verification of the model. The pulling hook load profile (continuous curve), was calculated using the borehole friction values calculated from running in data. The comparison shows the similar trend and the constant difference of about 32000 lbf. This difference can be attributed to many factors such as: an initial estimation error of the weight of the travelling block, slip elevator with bell guide and hook; stabbing effect; spring effect, etc. As for now it seems that there was a slight prediction difference between hook load calculation while running in and pulling out casing. The explanation follows.

The plot of friction factor versus measured depth was made (Fig. 12 and 13). It can be seen that the very shallow data yields quite different results than the deepest ones. There was some uncertainty of the weight of the casing hanging equipment. In the calculating procedure this weight was subtracted from the hook load reading. Since this weight was measured with the rig weight indicator, by lying the travelling block and everything beneath it on the rig floor, the error involved equalled the resolution of the rig system that was of ± 5000 lbf. A +4000 lbf error in this case results in the scenario depicted in Fig. 13, 14, 15 and 16. An average value of 1.31 was obtained for the friction factor coefficient while running casing in. In addition, the average value of the borehole friction factor was calculated from regression analysis using the original data (Fig. 12) with no provisions made for casing hanging equipment weight error. In this approach, the data regarding the top of the build-up portion were simply ignored as being biased by stabbing effect and the spring effect.

One important conclusion from this analysis was that unlike the kick off portion, the bottom portion of the data was not sensitive to the small hook load changes caused by various external factors. The relative error in the borehole friction factor associated with the unit change in hook load decreases as the total casing length in the hole increases.

By ignoring the data from the kick-off section and from the build up section, or by performing the sensitivity analysis of the hook load, the results obtained were similar.

Based on the average borehole friction factor value of 1.3 the prediction was made for running load - Fig. 15, and pulling loads - Fig 16. This time, the verification of the model indicated a 13000 lbf maximum error between the predicted curve and actual pulling data or 4.3 percent.

This particular casing run was scheduled to be reciprocated after reaching bottom, however, the casing was pulled on several times, with no success of any pipe movement on bottom. These trials were recorded and are shown in Fig. 17. Finally the well was cemented without reciprocating. Analyzing the pickup loads we see that the greatest value the casing was pulled on was 356000 lbf (382000 lbf read of the graph minus 26000 lbf of the casing hanging equipment). On bottom, the predicted value (Fig. 16) is 396000 lbf. This means that only considering friction, it would be necessary at least another 40000 lbf to be able to start to reciprocate that particular string of casing.

CONCLUSIONS:

First analysis indicates that the

overall average friction coefficient is possible to be obtained from field experiments in a practical manner.

By analyzing the forces acting on a small casing element several differential equations were developed. The solution to these equations yield a practical and easy way to calculate the axial force from one survey point to the next.

A field procedure to record hook load should be verified by using "point checkup" for calibration insuring that the equipment was operating correctly.

The relative error in the friction factor coefficient is smaller for deeper depths.

The values of the overall friction coefficient may be expected to be higher than one. In the field case presented here, an average value of 1.3 was found.

Further field experiments are necessary before more conclusions are drawn.

NOMENCLATURE

A	=	Casing crossectional area (sq. in.)
BF	=	1-(RO/65.5); boyancy factor (d-less)
FF	=	Borehole friction factor (d-less)
HL	=	Hook load (lbf)
I	=	Inclination angle in the directional borehole (rad)
K	=	Number of survey stations for a given measured hook load
MD	=	Measured depth in the borehole (ft)
MDMHL	=	Measured depth for a given measured hook load
MHL	=	Measured hook load
N	=	Number of casing sections in the well for a given measured hook load
NF	=	Normal force (lbf)
R	=	Radius of curvature (ft)
RO	=	Drilling mud density (lbf/gal)
T	=	Axial force (lbf)
VD	=	Vertical depth in the borehole (ft)
VPBW	=	Vertical projected boyant weight (lbf)
W	=	Unit weight of casing (lbf/ft)

ACKNOWLEDGEMENTS

The authors thank the Mobil Oil Exploration and Production Southeast Inc. for help in recording field data.

Grateful appreciation is given to TOTCO, Shell Offshore Inc. and Tenneco Oil Company for their assistance and equipment support.

REFERENCES

1. Wojtanowicz, A., Maidla, E., "Minimum Cost Casing Design for Vertical and Directional Wells", SPE#14499, 1985.

2. Johancsik, C. A., Friesen, D. B., Dawson, R., "Torque and Drag in Directional Wells - Prediction and Measurement", JPT, pp. 987-992, June 1984.

3. Mitchell, B. J., "Applied Drilling Concepts", SPE short course, Dallas, Feb. 1986.

APPENDIX

Derivation of the Main Formulas

1. Build-up section

1.1 Pulling-out casing:

The forces acting on a small casing element in the build-up section are shown in Fig. 2. At equilibrium, the following differential equation results:

$$\frac{dT}{dl} = -FF \times Q \times SIN(I) - T - Q \times COS(I) \qquad (A1)$$

where: $Q = R \times W \times BF$

boundary conditions:

$$T(l_i) = T_i$$

$$T(l_{i+1}) = T_{i+1} \qquad (A2)$$

Solving eq. (A1) using boundary conditions (A2), and also considering the situations depicted in Fig. 3, results in equations (2), (4) and (5).

1.2 Running-in situation:

In a similar way (Fig. 2), at equilibrium:

$$\frac{dT}{dl} = FF \times Q \times SIN(I) - T - Q \times COS(I) \qquad (A3)$$

Equations (A3) and (A1) yield the same results but for different scenarios (Fig. 3). This is due to the sign convention used. The main text clearly explains which situation each equation pertains.

2. Drop-off section

2.1 Pulling-out casing:

The forces acting on a small casing element in the drop-off section is shown in Fig. 4. At equilibrium:

$$\frac{dT}{dl} = FF \times Q \times SIN(\theta) + T \times FF + Q \times COS(\theta) \quad \text{(A4)}$$

Using boundary conditions (A2), the solution is equation (6).

2.2 Running-in casing:

In a similar way (Fig. 4), at equilibrium:

$$\frac{dT}{dl} = -FF \times Q \times SIN(\theta) - T \times FF + Q \times COS(\theta) \quad \text{(A5)}$$

Using boundary conditions (A2), the solution is equation (7).

3. Slant section

3.1 Pulling-out casing:

The forces acting on a small casing element in the slant hole portion are shown in Fig. 5. At equilibrium:

$$\frac{dT}{dMD} = W \times BF \times FF \times SIN(\theta) + W \times BF \times COS(\theta) \quad \text{(A6)}$$

boundary conditions: $T\,MD_i = T_i$

$$T\,MD_{i+1} = T_{i+1} \quad \text{(A7)}$$

Using these boundary conditions, the solution is equation (8).

3.2 Running-in casing:

In a similar way (Fig. 5), at equilibrium:

$$\frac{dT}{dMD} = -W \times BF \times FF \times SIN(\theta) + W \times BF \times COS(\theta) \quad \text{(A8)}$$

Using boundary conditions (A7) the solution is equation (9).

TABLE 1

INPUT AND OUTPUT OF THE FRICTION FACTOR COMPUTER PROGRAM

MAIN PROGRAM NAME: (FF)
DATA FILE NAME: D1 N80/S95 5 5/8"; RECOR. DATE: MAR86
WELL IDENT.: XXXX PLAT.ID:XXXXX SLOT#: XXX HOLE PROF: # XX

FRICTION FACTOR WHILE RUNNING CASING

DATA USED: MUD DENSITY: 9.3 LBF/GAL
CORRECTION VALUE = 4000 LBF (SENSIT. ANAL.
FROM 3820. FT UPWARDS 0.10 WAS USED AS "FF"

CASING STRING BREAK DOWN

DEPTH (FT)	OD (IN)	ID (IN)	WEIGHT (LBF/FT)	THREAD
11538.	7.625	6.875	29.70	LONG

RESULTS

INPUT DATA			OUTPUT DATA	
MEASURED DEPTH (FEET)	MEASURED HOOK LOAD (LBF)	MODE	FRICTION FACTOR (D-LESS)	CALCUL. HOOK LOAD LBF)
11317.	213000.	IN	1.444	213220.
11274.	218000.	IN	1.312	217755.
11230.	213000.	IN	1.425	212972.
11189.	220000.	IN	1.228	219980.
11145.	209000.	IN	1.500	209266.
11101.	216000.	IN	1.303	216018.
11018.	220000.	IN	1.172	219937.
10974.	218000.	IN	1.209	217966.
10888.	214000.	IN	1.294	213808.
10845.	213000.	IN	1.294	213280.
10803.	216000.	IN	1.200	216120.
10861.	213000.	IN	1.275	212893.
10718.	213000.	IN	1.256	213022.
10674.	210000.	IN	1.331	209870.
10634.	210000.	IN	1.312	210027.
10593.	210000.	IN	1.294	210182.
10551.	210000.	IN	1.275	210286.
10508.	210000.	IN	1.275	209755.
10465.	207000.	IN	1.350	206758.
10380.	205000.	IN	1.369	205133.
10336.	203000.	IN	1.425	202836.
10293.	203000.	IN	1.406	202901.
10209.	201000.	IN	1.444	200797.
10079.	201000.	IN	1.387	200977.
10039.	202000.	IN	1.331	202169.
10039.	309000.	UP	1.050	308975.
9954.	199000.	IN	1.406	198929.
9911.	199000.	IN	1.387	198955.
9868.	199000.	IN	1.369	198868.
9828.	199000.	IN	1.350	198999.
9781.	198000.	IN	1.369	197893.
9741.	202000.	IN	1.200	202079.
9741.	301000.	UP	1.125	300839.
9656.	199000.	IN	1.275	198854.
9614.	200000.	IN	1.219	199820.
9571.	194000.	IN	1.425	193771.
9442.	199000.	IN	1.162	198929.
9400.	199000.	IN	1.144	198807.
9400.	284000.	UP	1.059	283933.
7927.	181000.	IN	0.862	181253.
7839.	174000.	IN	1.200	174176.
7799.	173000.	IN	1.237	172943.
7755.	174000.	IN	1.125	174017.
7630.	172000.	IN	1.125	171977.
7083.	161000.	IN	1.275	161028.
6842.	161000.	IN	0.900	160717.
6717.	155000.	IN	1.275	154750.
6384.	148000.	IN	1.425	147854.
6341.	146000.	IN	1.575	145963.
6300.	146000.	IN	1.500	145827.
6257.	147000.	IN	1.200	147249.
6215.	147000.	IN	1.125	146999.
6174.	144000.	IN	1.425	144174.
6090.	144000.	IN	1.200	144135.
6047.	142000.	IN	1.425	141935.
6004.	142000.	IN	1.275	142072.
5962.	142000.	IN	1.200	141738.
5922.	139000.	IN	1.575	138893.
5879.	139000.	IN	1.425	138970.
5837.	140000.	IN	1.050	140187.
5795.	139000.	IN	1.125	138989.
5753.	134000.	IN	1.950	134281.
5710.	134000.	IN	1.800	134283.

AVERAGE FRIC. FACTOR = 1.312
(WHILE RUNNING IN CASING ONLY)

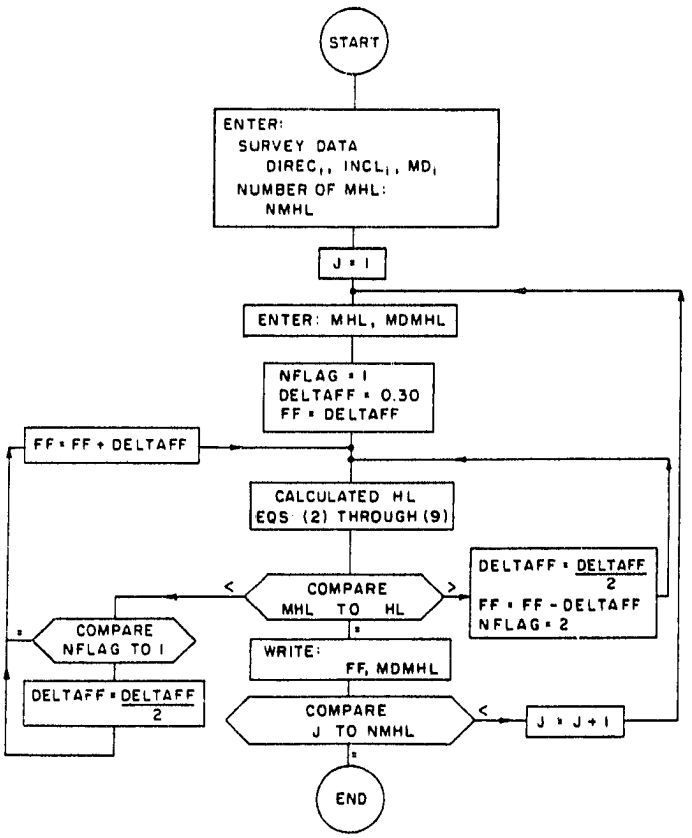

Fig. 1—Flow diagram of the friction factor computation procedure.

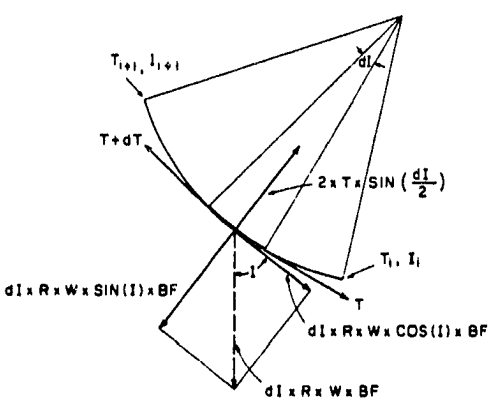

Fig. 2—Forces acting on a small casing element within buildup section.

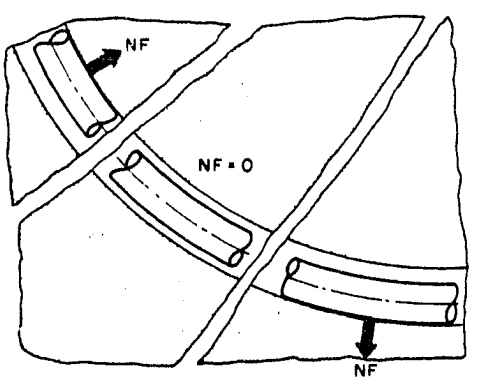

Fig. 3—Possible directions of the normal force in a buildup section.

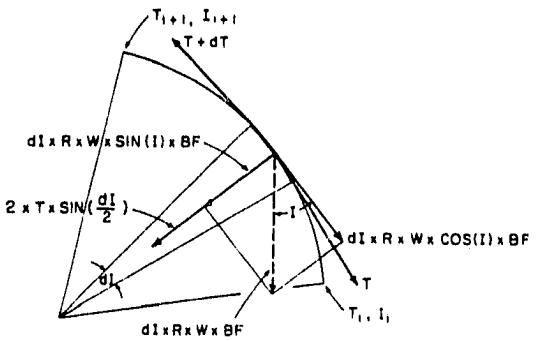

Fig. 4—Forces acting on a small casing element within drop-off section.

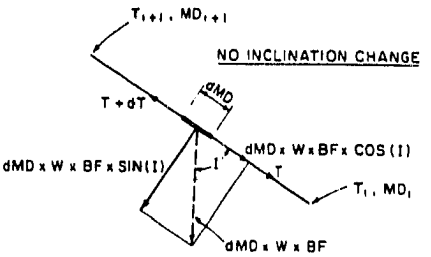

Fig. 5—Forces acting on a small casing element within slant section.

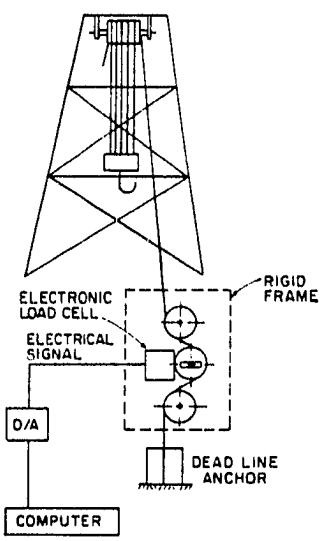

Fig. 6—Schematics of the hook load recording process.

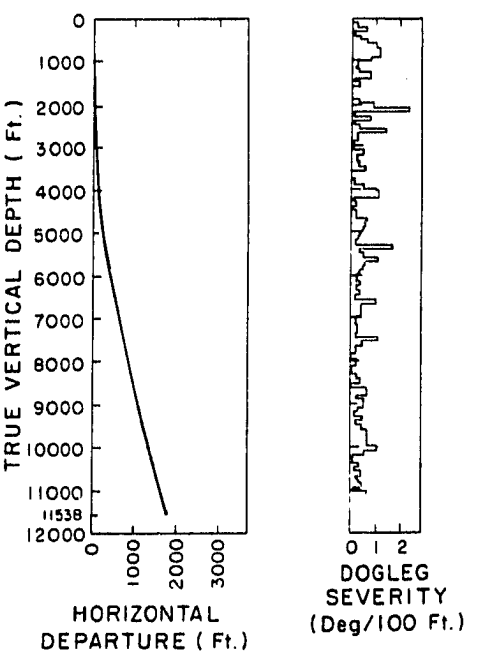

Fig. 7—Vertical projection of Well D-1.

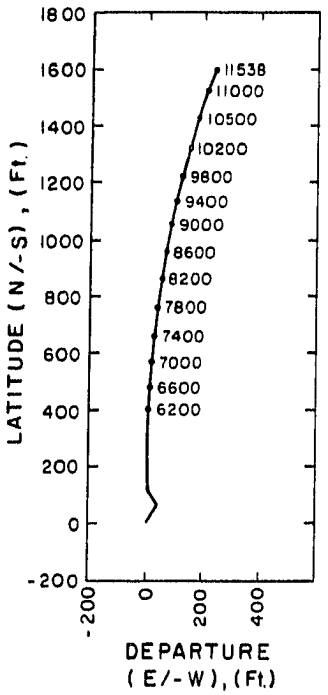

Fig. 8—Horizontal projection of Well D-1.

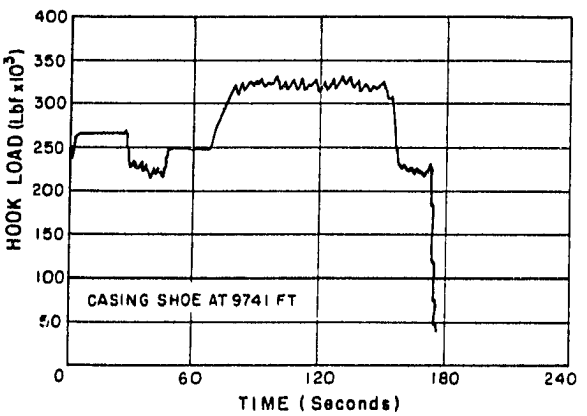

Fig. 9—Casing running-in and pulling-out hook loads.

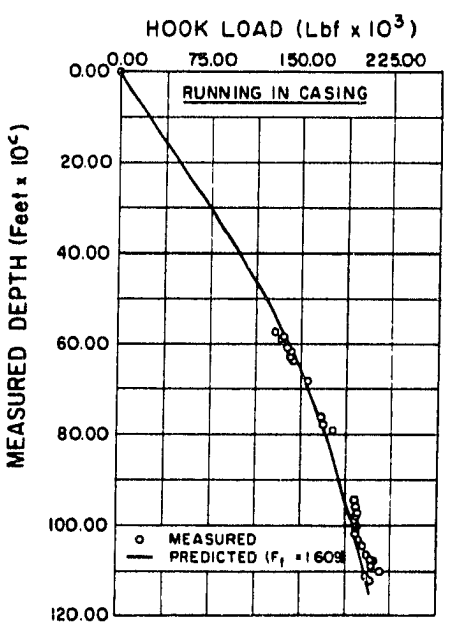

Fig. 10—Measured and predicted hook load vs. depth while running-in casing.

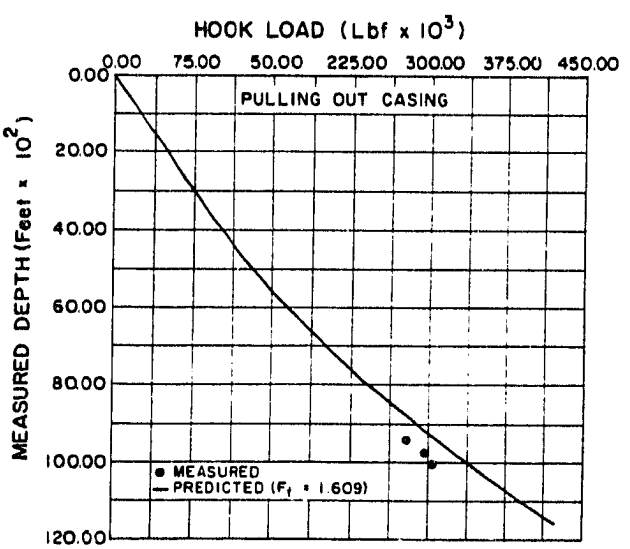

Fig. 11—Hook load vs. depth while pulling-out casing.

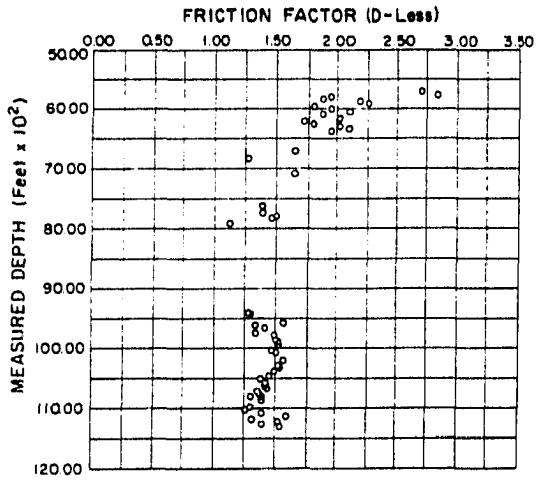

Fig. 12—Friction factor vs. depth.

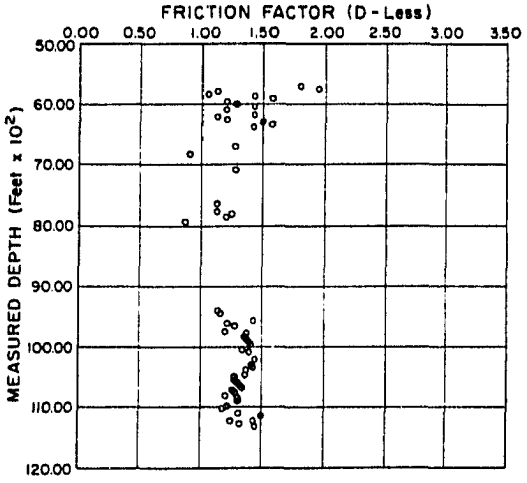

Fig. 13—Friction factor vs. depth—after performing sensitivity analysis

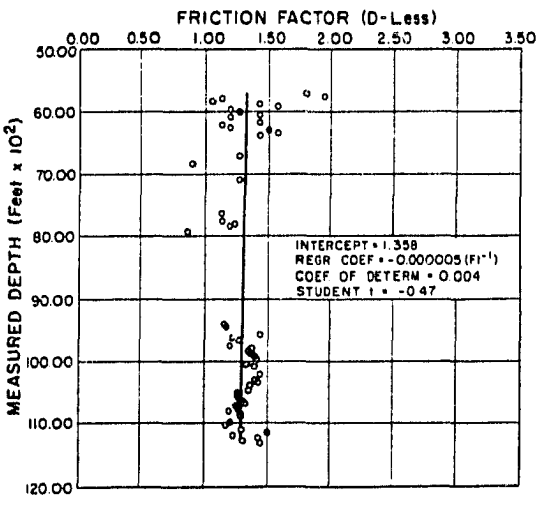

Fig. 14—Stabilization of friction factor

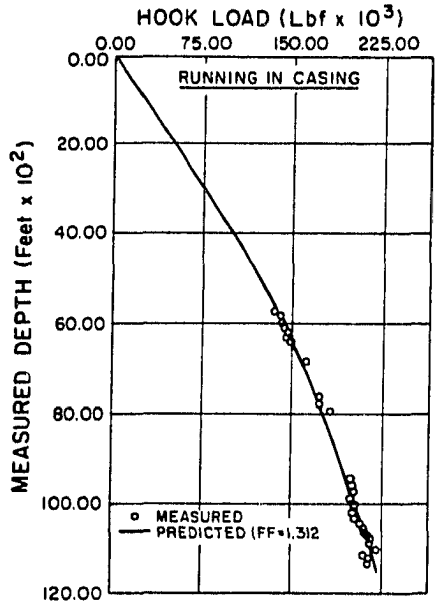

Fig. 15—Measured and predicted hook load vs. depth while running-in casing.

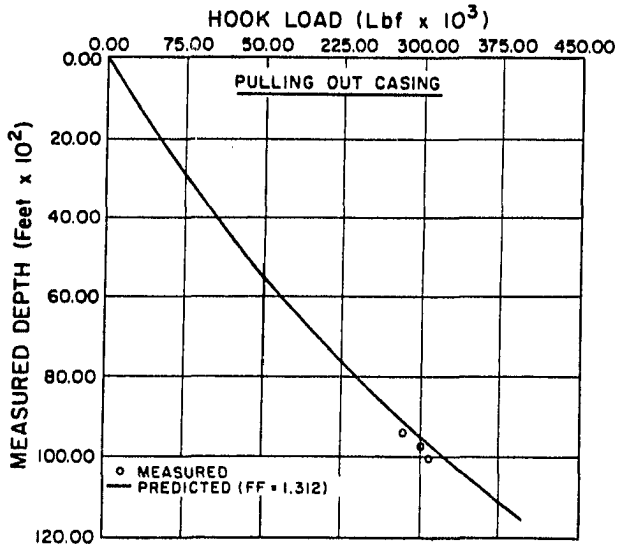

Fig. 16—Hook load vs. depth while pulling-out casing.

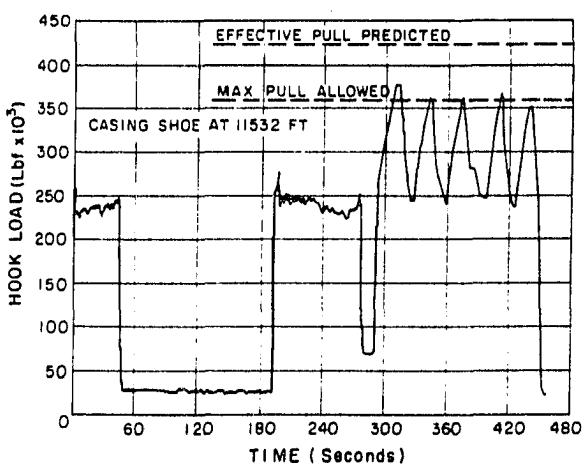

Fig. 17—Unsuccessful pulling on casing string, set at the total depth.

VITA

Eric Edgar Maidla was born in Sao Paulo City, Sao Paulo State, Brazil on November 30, 1958. He received a B.S. degree in Mechanical Engineering from Escola de Engenharia Maua in Brazil on December 1981, and an M.S. degree in Petroleum Engineering from LSU in 1985.

As far as his professional experience, he has worked at: Banco Lar e Brasileiro/Chase Manhattan Bank (Jan/83-Aug/83) where he acquired knowledge of international trading finance and Chase's credit policy; ASEA Electrica Ltda (a Swedish firm that manufactures current rectifier valves of high voltage and transformers - Jan/82-Jan/83) as a mechanical project engineer; Ford Brazil (Feb/81-Dec/81)as an engineer in training in the tractor plant in the engineering department, having worked with projects, equipment maintenance and material handling.

DOCTORAL EXAMINATION AND DISSERTATION REPORT

Candidate: Eric Edgar Maidla

Major Field: Petroleum Engineering

Title of Dissertation: Borehole Friction Assessment and Application to Oilfield Casing Design in Directional Wells

Approved:

A. Wojtanowicz
Major Professor and Chairman

Dean of the Graduate School

EXAMINING COMMITTEE:

Adam T. Bourgoyne Jr

Julius Langlinais

Robert Desbrandes

John A. Greenwood III

Date of Examination:

November 23, 1987